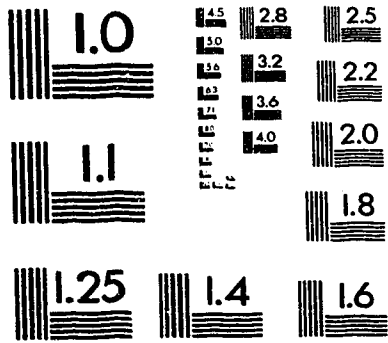


1



MADE IN MEXICO No. 10 19700 0000 100

VERED

CONSTRUCIONES VERED S.A. S. DE C.V.



National Library
of Canada

Acquisitions and
Bibliographic Services Branch

395 Wellington Street
Ottawa, Ontario
K1A 0N4

Bibliothèque nationale
du Canada

Direction des acquisitions et
des services bibliographiques

395, rue Wellington
Ottawa (Ontario)
K1A 0N4

Your file / Votre référence

Cher file / Votre référence

NOTICE

The quality of this microform is heavily dependent upon the quality of the original thesis submitted for microfilming. Every effort has been made to ensure the highest quality of reproduction possible.

If pages are missing, contact the university which granted the degree.

Some pages may have indistinct print especially if the original pages were typed with a poor typewriter ribbon or if the university sent us an inferior photocopy.

Reproduction in full or in part of this microform is governed by the Canadian Copyright Act, R.S.C. 1970, c. C-30, and subsequent amendments.

AVIS

La qualité de cette microforme dépend grandement de la qualité de la thèse soumise au microfilmage. Nous avons tout fait pour assurer une qualité supérieure de reproduction.

S'il manque des pages, veuillez communiquer avec l'université qui a conféré le grade.

La qualité d'impression de certaines pages peut laisser à désirer, surtout si les pages originales ont été dactylographiées à l'aide d'un ruban usé ou si l'université nous a fait parvenir une photocopie de qualité inférieure.

La reproduction, même partielle, de cette microforme est soumise à la Loi canadienne sur le droit d'auteur, SRC 1970, c. C-30, et ses amendements subséquents.

University of Alberta

**Development and Testing of a
Composite Ice-Resisting Wall**

by



Thomas J.E. Zimmerman

**A Thesis Submitted to
the Faculty of Graduate Studies and Research
in Partial Fulfillment of the Requirements for the
Degree of Doctor of Philosophy
in Civil Engineering**

Department of Civil Engineering

**Spring, 1993
Edmonton, Alberta**



National Library
of Canada

Acquisitions and
Bibliographic Services Branch

395 Wellington Street
Ottawa, Ontario
K1A 0N4

Bibliothèque nationale
du Canada

Direction des acquisitions et
des services bibliographiques

395, rue Wellington
Ottawa (Ontario)
K1A 0N4

Vous êtes un auteur canadien ?

Vous êtes un auteur étranger ?

The author has granted an irrevocable non-exclusive licence allowing the National Library of Canada to reproduce, loan, distribute or sell copies of his/her thesis by any means and in any form or format, making this thesis available to interested persons.

L'auteur a accordé une licence irrévocable et non exclusive permettant à la Bibliothèque nationale du Canada de reproduire, prêter, distribuer ou vendre des copies de sa thèse de quelque manière et sous quelque forme que ce soit pour mettre des exemplaires de cette thèse à la disposition des personnes intéressées.

The author retains ownership of the copyright in his/her thesis. Neither the thesis nor substantial extracts from it may be printed or otherwise reproduced without his/her permission.

L'auteur conserve la propriété du droit d'auteur qui protège sa thèse. Ni la thèse ni des extraits substantiels de celle-ci ne doivent être imprimés ou autrement reproduits sans son autorisation.

ISBN 0-315-82041-1

Canada

APR-12-1993 12:45 FROM GULF CDA PUB AFF 2335520

14-12-88 12:00

TO

C-FER EDMONTON-

3815 P.01

408 330 6520:0 1/ 1

RECEIVED BY RAPIFAX LOCAL 3815

Telefax

Bob Henderson
Apr 12 12:45 PM '93

RECEIVED BY RAPIFAX LOCAL 3815



To: John Sparks
Public Affairs
Gulf Canada Resources Ltd.

Date: April 12, 1993

Project: personal

Fax No: 213-5520

Total Pages: 1

Subject: Permission for use of photo in Ph.D. Thesis

From: Thomas J.E. Zimmerman, P.Eng.
Manager, Structures & Pipelines Technology

Centre for Frontier Engineering Research
200 Karl Clark Road
Edmonton, Alberta
T6N 1R2

Telephone: (403) 450-3300
Telefax: (403) 450-3700

Message

As I mentioned to you on the telephone today, I would like to include a copy of a Gulf photo in my Ph.D. thesis which is being submitted to the University of Alberta next week. The thesis deals with the design of ice-resisting walls for offshore Arctic structures. The photo I would like to include on the inside cover is the one of the Ted Harrison painting which appears on the cover of Gulf's Amauligak Development Study report. I will, of course, acknowledge Gulf's permission to use the photo.

Please advise me by fax if this is possible. Let me know if there are any special requirements as far as acknowledgments are concerned (i.e. stated any particular way).

Thank you for your help.

To THOMAS ZIMMERMANN
Re your request to use photos
in your thesis as per fax April 12,
Please proceed with our permission

Bob Henderson
233-5417

Telefax



To: John Sparks
Public Affairs
Gulf Canada Resources Ltd.

Date: **FAK**
April 12, 1993

Project: personal

Fax No: 233-5520

Total Pages: 1

Subject: Permission for use of photo in Ph.D. Thesis

From: Thomas J.E. Zimmerman, P.Eng.
Manager, Structures & Pipelines Technology

Centre for Frontier Engineering Research
200 Karl Clark Road
Edmonton, Alberta
T6N 1E2

Telephone: (403) 450-3300
Telefax: (403) 450-3700

Message

As I mentioned to you on the telephone today, I would like to include a copy of a Gulf photo in my Ph.D. thesis which is being submitted to the University of Alberta next week. The thesis deals with the design of ice-resisting walls for offshore Arctic structures. The photo I would like to include on the inside cover is the one of the Ted Harrison painting which appears on the cover of Gulf's Amauligak Development Study reports. I will, of course, acknowledge Gulf's permission to use the photo.

Please advise me by fax if this is possible. Let me know if there are any special requirements as far as acknowledgments are concerned (i.e. stated any particular way).

Thank you for your help.

Telefax



To: John Sparks
Public Affairs
Gulf Canada Resources Ltd.

Date: April 12, 1993

Project: personal

Fax No: 233-5520

Total Pages: 1

Subject: Permission for use of photo in Ph.D. Thesis

From: Thomas J.E. Zimmerman, P.Eng.
Manager, Structures & Pipelines Technology

Centre for Frontier Engineering Research
200 Karl Clark Road
Edmonton, Alberta
T6N 1E2

Telephone: (403) 450-3300
Telefax: (403) 450-3700

Message

Further to my fax of earlier today, there is also a second photo which I would like to use in the thesis if possible. It is the drawing of the proposed Amauligak production structure. I believe it was done in-house by Gulf.

Please let me know.

Thank you again for your help.

University of Alberta

Release Form

Name of Author: Thomas J.E. Zimmerman
Title of Thesis: Development and Testing of a Composite Ice-Resisting Wall
Degree: Doctor of Philosophy in Civil Engineering
Year Granted: 1993

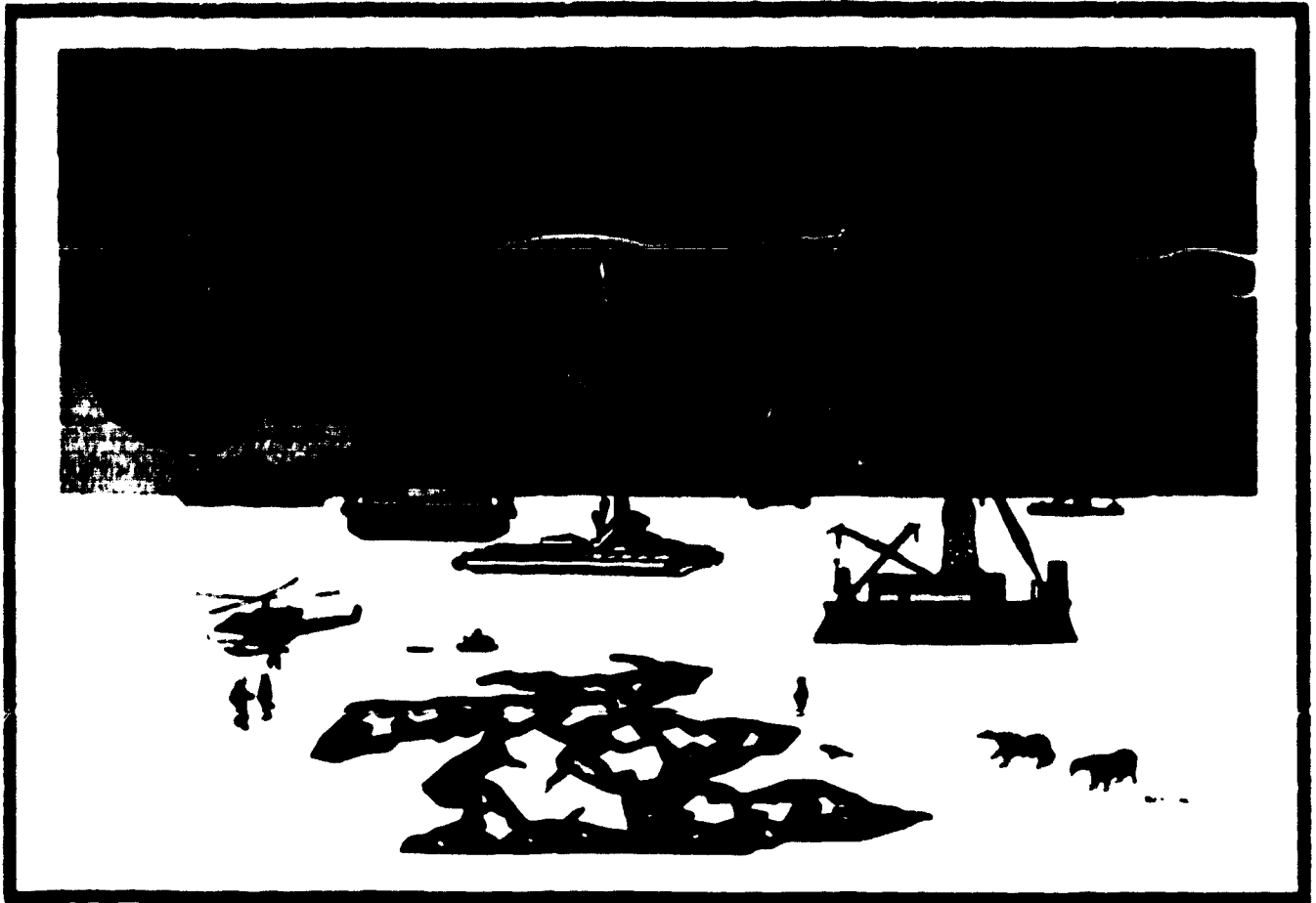
Permission is hereby granted to the University of Alberta Library to reproduce single copies of this thesis and to lend or sell such copies for private, scholarly or scientific research purposes only.

The author reserves all other publication and other rights in association with the copyright in the thesis, and except as hereinbefore provided neither the thesis nor any substantial portion thereof may be printed or otherwise reproduced in any material form whatever without the author's prior written permission.



**Thomas J.E. Zimmerman
Centre for Frontier Engineering Research
200 Karl Clark Road
Edmonton, Alberta
Canada
T6N 1E2**

April 20, 1993



(photo courtesy of Gulf Canada Resources Ltd.)

"There are strange things done in the midnight sun ..."

**"The Cremation of Sam McGee",
Robert W. Service**

University of Alberta

Faculty of Graduate Studies and Research

The undersigned certify that they have read, and recommend to the Faculty of Graduate Studies and Research for acceptance, a thesis entitled "Development and Testing of a Composite Ice-resisting Wall" submitted by Thomas J.E. Zimmerman in partial fulfillment of the requirements for the degree of Doctor of Philosophy in Civil Engineering.


James G. MacGregor (Supervisor)


J.J. Roger Cheng


John R. Colbourne


Alaa E. Elwi


Sami H. Rizkalla


Sidney H. Simmonds

February 23, 1993

**To my boys
Dylan and Daniel**

ABSTRACT

The research presented in this thesis has investigated the use of composite construction (a steel-concrete sandwich system) for the exterior, ice-resisting walls of an Arctic, offshore drilling/production structure. The composite system developed consists of two steel plates enclosing a concrete core. The system can be visualized as a reinforced concrete wall with the reinforcing steel (in the form of steel plates) on the outside.

The proposed composite ice-resisting wall configuration is simple from a fabrication and construction point of view. The outer and inner steel plates are fastened together with continuous, vertical steel diaphragms which are at a relatively wide spacing. No other welded details in the wall are required. This results in a significant reduction in labour-intensive welding, compared to a conventional, all-steel wall. The steel frame is self-supporting and therefore requires no additional formwork when concrete is poured. No additional reinforcing steel is required beyond that provided by the external steel plates and the diaphragm plates.

The testing program which was part of the research work consisted of sixteen quarter-scale beam specimen tests and three quarter-scale slab specimen tests. The tests showed the wall to possess high strength in both flexure and shear and to exhibit ductile modes of failure when the ultimate capacity is exceeded.

An analysis and design approach is presented which is consistent with the same generally accepted engineering principles used in reinforced concrete design; empirical equations, lower bound plasticity methods and upper bound energy methods. The methods showed good agreement with the test results and are also consistent with the limit states philosophy and provisions contained in the new CSA Standard for the Design, Construction and Installation of Fixed Offshore Structures.

Cost analyses were conducted which compared the cost of composite wall construction with those of reinforced concrete and all-steel construction. The comparison showed the composite wall concept to be cost competitive.

This work has demonstrated that a steel-concrete composite sandwich wall is a viable concept, both technically and economically, for constructing the peripheral, ice-resisting wall of an Arctic offshore structure.

Acknowledgments

This research was developed out of the core research program at the Centre for Frontier Engineering Research (C-FER) in Edmonton, Alberta, Canada. The author wishes to thank C-FER and its funding members, in particular Gulf Canada Resources Ltd., for their support in developing this project and for their permission to release the results for inclusion in this thesis.

The author would also like to thank his project advisor, Dr. J.G. MacGregor, without whom this would not have been possible, and Dr. P.F. Adams for suggesting the work in the first place.

TABLE OF CONTENTS

1.0	Introduction	1
2.0	Scope and Objectives	6
3.0	Code Requirements and Design Criteria	8
3.1	Existing Code Requirements for Composite Walls	8
3.1.1	List of Codes Reviewed	8
3.1.2	Composite Wall Requirements in S473	10
3.1.3	Composite Wall Requirements in Other Codes	10
3.1.3.1	API Bul 2N	12
3.1.3.2	API RP 2N	12
3.1.3.3	ABS.....	13
3.1.3.4	DnV.....	13
3.1.3.5	FIP.....	14
3.2	Ice Loading	14
3.3	Design Assumptions	15
4.0	Testing Program	19
4.1	Testing Procedure and Specimen Details	19
4.1.1	Beam Specimens	19
4.1.2	Slab Specimens	20
4.1.3	Material Properties	21
4.1.3.1	Structural Steel Plate	21
4.1.3.2	Concrete	21
4.2	Boundary Conditions	22
4.3	Instrumentation	23
4.4	Test Results	23
4.4.1	Beam Specimens	24
4.4.1.1	Specimens CF-1 to CF-3	24
4.4.1.2	Specimens CF-4 to CF-9	26
4.4.1.3	Specimens CF-10 to CF-13.....	27
4.4.1.4	Specimens B-1 and B-2	28
4.4.2	Slab Specimens	29
4.4.2.1	Specimen SP-1	30
4.4.2.2	Specimen S-1	31
4.4.2.3	Specimen S-2	31
4.5	Discussion of Test Results	33
4.5.1	Beam Specimens	33
4.5.2	Slab Specimens	35

5.0	Ultimate Strength Calculation Methods	64
5.1	Traditional Methods	65
5.1.1	Plane Section Method for Flexure	65
5.1.1.1	Case 1, $t' > t$	67
5.1.1.2	Case 2, $t' < t$	68
5.1.1.2	Case 3, $t' = t$	69
5.1.2	Empirical Method for Shear	70
5.1.2.1	ACI and CSA Equations for Reinforced Concrete	70
5.1.2.2	Empirical Equations for Composite Walls	72
5.2	Plasticity Methods	74
5.2.1	Lower Bound Plasticity Method	75
5.2.1.1	Previous Experience	75
5.2.1.2	Strut and Tie Truss Model for Flexure	77
5.2.1.3	Compression Field Method for Shear	78
5.2.2	Upper Bound Plasticity Method	80
5.2.2.1	Shear Failure Mechanism	81
5.2.2.2	Flexural Failure Mechanism	85
5.3	Recommended Ultimate Strength Calculation Methods.....	87
6.0	Design Method	103
6.1	Recommended Design Method	103
6.1.1	Determine Ultimate Limit State Loads	103
6.1.2	Trial Sections: General Requirements.....	104
6.1.3	Design for Flexure	105
6.1.4	Design for Shear	106
6.1.5	Additional Considerations	106
6.2	Design Example	106
7.0	Comparative Cost Analysis.....	112
7.1	Isolated Peripheral Wall Elements.....	112
7.1.1	Composite Wall.....	112
7.1.2	Open-faced Composite Wall	113
7.1.3	Reinforced Concrete Wall	113
7.1.4	All-steel Wall.....	114
7.2	Cost Comparison.....	114
7.3	Total Structural Cost	116
8.0	Other Considerations.....	124
8.1	Finite Element Analysis.....	124
8.2	Concrete Fatigue Due to Cyclic Ice Loads.....	125
8.2.1	Low-intensity, Long-term Fatigue	125
8.2.2	High-intensity, Single-event Fatigue.....	125
8.2.3	Summary of Fatigue Tests	126

9.0	Conclusions	131
10.0	References	133
Appendices		
Appendix A	Detailed Results	137
Appendix B	Compression Field Method for Shear	157
Appendix C	Upper Bound Plasticity Method for Shear	164
Appendix D	Offshore Structure Conceptual Design.....	177

LIST OF TABLES

Table 4.1	Specimen Details and Summary of Results	37
Table 4.2	Loading Patterns for Beam Specimens CF-1 to CF-14.....	38
Table 4.3	Cracking Patterns for Beam Specimens CF-1 to CF-14.....	39
Table 5.1	Linear Regression Analysis, Eqn. 5.12a	88
Table 5.2	Linear Regression Analysis, Eqn. 5.13a	89
Table 5.3	Summary of Results and Failure Load Predictions.....	90

LIST OF FIGURES

Figure 1.1	General Configuration of a Composite Ice-Resisting Wall.....	3
Figure 1.2	Composite Wall Type Developed by Zimmerman.....	4
Figure 1.3	Composite Wall Type Tested by O'Flynn.....	4
Figure 1.4	Composite Wall Type Suggested by Berner and Gerwick	5
Figure 1.5	Composite Wall Type Tested by Matsuishi and Iwata	5
Figure 1.6	Composite Wall Type Tested Ohno.....	5
Figure 3.1	Croasdale's Ice Pressure Curve	17
Figure 3.2	Sanderson's Ice Pressure Curve.....	17
Figure 3.3	Proposed Structure for the Amauligak Field in the Beaufort Sea.....	18
Figure 4.1	Specimen in Beam Testing Frame.....	40
Figure 4.2	Schematic of Beam Testing Frame	40
Figure 4.3	Slab Specimen in MTS Universal Testing Machine.....	41
Figure 4.4	Specimen Configuration for B-1 and B-2	41
Figure 4.5	Slab Specimen Configurations.....	42
Figure 4.6	Concrete Strength Data	43
Figure 4.7	Support Boundary Conditions.....	44
Figure 4.8	Typical Instrumentation for Beam Specimens	44
Figure 4.9	Typical Instrumentation for Slab Specimens.....	45
Figure 4.10	Load vs. Deflection Curves for CF- ¹ CF-2 and CF-3.....	46
Figure 4.11	Sketches of Specimen CF-3 Test.....	47
Figure 4.12	Photographs of Specimen Test CF-3	48
Figure 4.13	Photographs of Specimen Test CF-2	51
Figure 4.14	Load vs. Deflection Curves for CF-4 to CF-9.....	52

Figure 4.15	Load vs. Deflection Curves for CF-10 to CF-14.....	54
Figure 4.16	Specimen CF-11 Near End of Test.....	56
Figure 4.17	Specimen CF-12 Near End of Test.....	56
Figure 4.18	Load vs. Deflection, Specimens B-1 and B-2	57
Figure 4.19	Load vs. Deflection, Specimens SP-1, S-1 and S-2	58
Figure 4.20	Specimen S-1 After Test.....	59
Figure 4.21	Specimen S-1: Close-up of "Punched" Area of Plate.....	59
Figure 4.22	Underside of Specimen S-1.....	60
Figure 4.23	Specimen S-2 After Test.....	61
Figure 4.24	Specimen S-2: Close-up of Failed Region	61
Figure 4.25	Specimen S-2: Close-up of Dented Area of Plate.....	62
Figure 4.26	Correlation Between Post-Failure Strength and (a/d) Ratio	63
Figure 5.1	Plane Sections Method for Flexure in a Composite Wall.....	91
Figure 5.2	Applicability of Plane Sections Method.....	92
Figure 5.3	Empirical Equation for Shear Strength of a Composite Wall.....	93
Figure 5.4	Accuracy of Empirical Equation for Shear Strength.....	94
Figure 5.5	Comparison of Empirical Equations for Shear Strength.....	95
Figure 5.6	Empirical Shear Strength Equation Including Concrete Material Resistance Factor.....	96
Figure 5.7	Lower Bound Truss Model for a Simply Supported R.C. Deep Beam	97
Figure 5.8	Lower Bound Truss Model for a Continuous R.C. Deep Beam.....	97
Figure 5.9	Lower Bound Truss Model for a R.C. Corbel.....	97
Figure 5.10	Lower Bound Plastic Truss Model for Specimen CF-2	98
Figure 5.11	Truss Model Analysis for Specimen CF-8.....	99
Figure 5.12	Compression Field Method for Predicting Shear Capacity of Specimen CF-10.....	100

Figure 5.13	Upper Bound Failure Mechanism for a Reinforced Concrete Beam	101
Figure 5.14	Upper Bound Failure Mechanism for a Composite Beam.....	101
Figure 5.15	Accuracy of Upper Bound Shear Strength Equation.....	102
Figure 6.1	Composite Wall Design Flow Chart	108
Figure 6.2	Summary of Composite Wall Design Equations.....	109
Figure 6.3	Composite Wall Design Example.....	110
Figure 7.1	Composite Wall Alternative	118
Figure 7.2	Hybrid Wall Alternative	119
Figure 7.3	Reinforced Concrete Wall Alternative.....	120
Figure 7.4	Structural Steel Wall Alternative.....	121
Figure 7.5	Vessel Schematic	122
Figure 7.6	Cost Comparison for Peripheral Wall Alternatives.....	123
Figure 8.1	Composite Beam Finite Element Model	127
Figure 8.2	Load-deflection Plot for Specimen CF-2	128
Figure 8.3	Load-deflection Plot for Specimen CF-4	128
Figure 8.4	High-cycle Low-amplitude Fatigue Specimen	129
Figure 8.5	Load-deflection Plot for High-cycle Low-amplitude Fatigue Specimen.....	129
Figure 8.6	Low-cycle High-amplitude Fatigue Specimen	130
Figure 8.7	Load-deflection Plot for Low-cycle High-amplitude Fatigue Specimen.....	130

1.0 INTRODUCTION

Offshore oil and gas production structures, which operate year round in the harsh environments of the Arctic and off the Canadian east coast, must be designed to resist very large, concentrated ice loads in a safe and efficient manner.

In an effort to find cost-effective solutions to the design of ice-resisting walls for these structures, composite steel-concrete walls have been proposed. The general structure of a composite ice-resisting wall is shown in Figure 1.1. It consists of outside and inside steel plates, fastened together with diaphragm plates or some other means, and a structural concrete fill in between. The basic idea is to replace the large amounts of congested reinforcing steel contained in a reinforced concrete wall with an exterior shell of welded steel plate. The system is more efficient than a concrete wall, since the steel plates act as reinforcing in both directions simultaneously, the concrete cover is eliminated and the steel shell effectively confines the concrete leading to enhanced strength and ductility properties.

In 1977, the Hitachi Shipbuilding and Engineering Company introduced the idea of using a composite steel/concrete sandwich system for the exterior walls of offshore structures. In several papers published that year, Hitachi presented the results of a test program on sandwich composite wall elements consisting of two steel plates enclosing a concrete core (Matsuishi et. al., 1977a, 1977b).

During the next decade the sandwich system caught the attention of structural engineers engaged in the planning and construction of offshore structures and several research programs were initiated in various locations throughout the world (Gerwick and Berner, 1987; Matsuishi, et. al., 1977a, 1977b, 1978, 1980a, 1980b, 1987; Smith and McLeish, 1987; O'Flynn and MacGregor, 1987; Ohno, et. al., 1987; Hattori, et.al, 1985; Shioya, et.al., 1986; Adams, et.al., 1987, 1988) These programs focussed on particular arrangements of the wall elements and utilized different means for achieving composite action and for transferring load through the thickness of the wall.

All of the composite wall types considered by the various researchers are similar in that they are composed of two steel plates enclosing a concrete core. The differences are in the internal details; the methods used to fasten the plates together and to the concrete. Figure 1.2 shows a typical composite wall specimen of the type developed by the author in

the research work discussed herein. Figures 1.2 to 1.6 show the wall specimen types tested by some of other researchers referenced in the previous paragraph. In addition, a variety of other specimen types can be found in Nojiri and Koseki [1986].

As a result of this research, several advantages of composite ice-resisting walls have been recognized: simplified construction, reduced material and stiffening requirements for the steel plates, and improved load distribution (Gerwick 1985; Zinserling and Cichanski, 1986; Rojansky and Hsu, 1985; Bruce and Roggensack, 1984). In addition, the research shows that composite walls can exhibit very high shear and flexural strength, as well as the post-failure ductility required to prevent a progressive collapse failure in the event of a local overload (Nojiri and Koseki, 1986; Shioya, et al., 1986; Hattori, et al., 1985).

The composite system developed by the author and presented in this thesis, stresses simplicity. The system is simpler than most other composite schemes which have been studied; the number of internal welded details being kept to a minimum.

The research presented here shows the effectiveness of this simple system, presents results from a physical testing program and outlines a design approach which should be applicable to many types of composite wall members. The design approach is consistent with the generally accepted engineering principles used in reinforced concrete design. It has been used as the basis for developing code clauses for Part III of the new CSA Code for the Design, Construction and Installation of Fixed Offshore Structures (Clause 13, Composite Walls, CSA Preliminary Standard S473, Steel Structures, 1990).

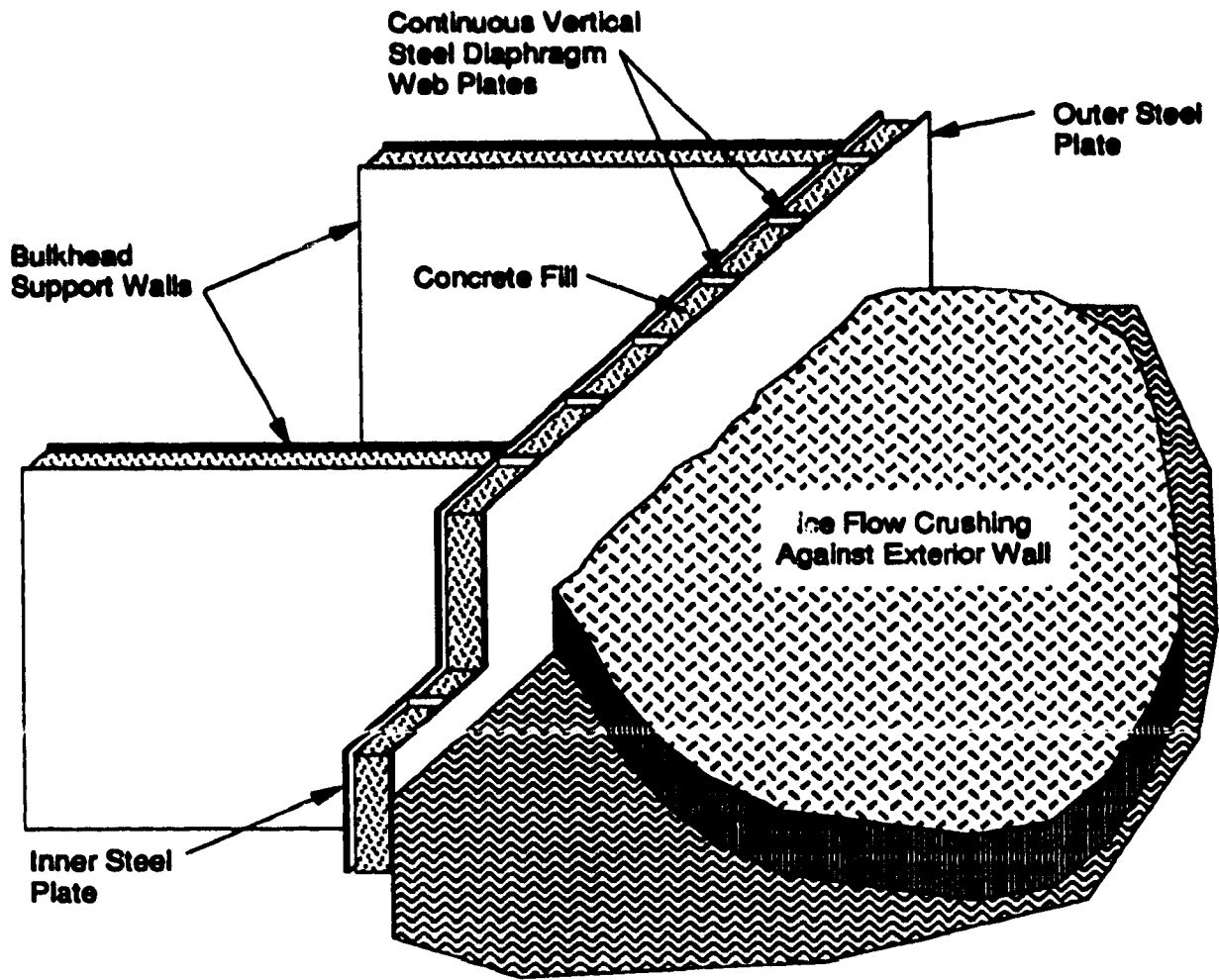


Figure 1.1 General Configuration of a Composite Ice-Resisting Wall

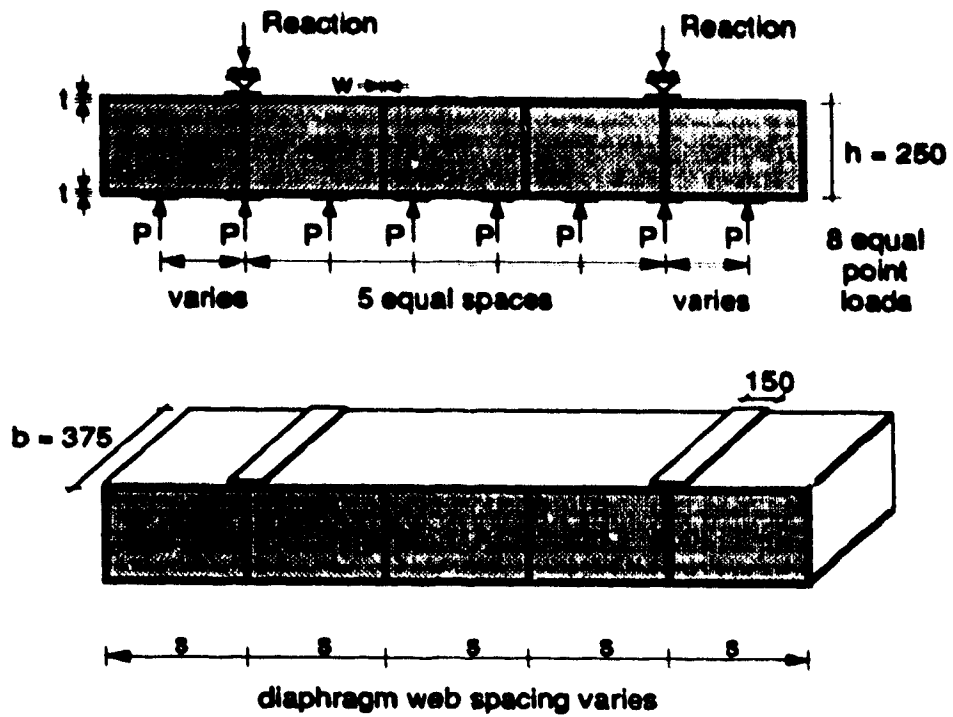


Figure 1.2 Composite Wall Type Developed by Zimmerman

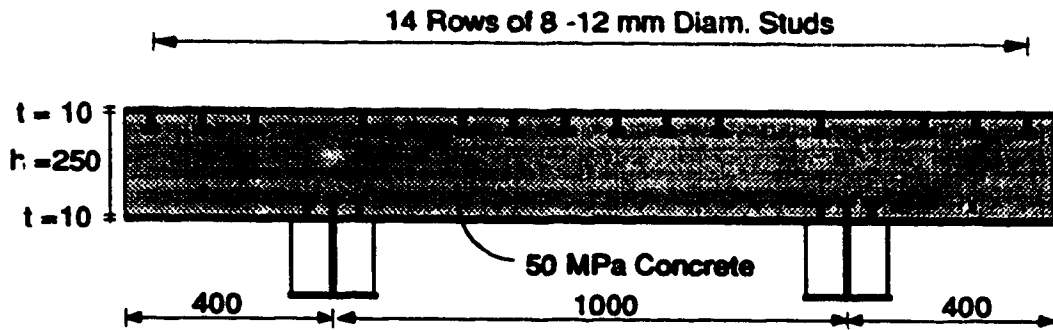


Figure 1.3 Composite Wall Type Tested by O'Flynn

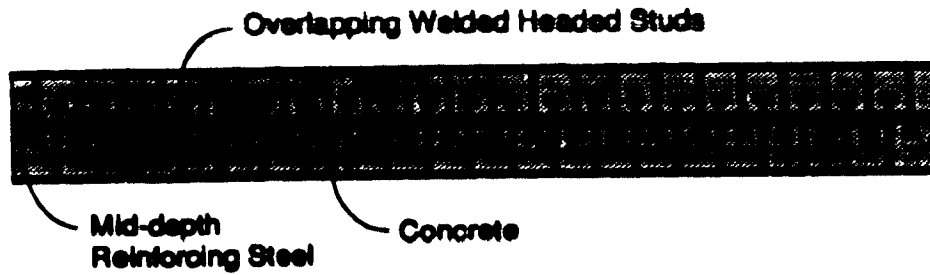


Figure 1.4 Composite Wall Type Suggested by Berner and Gerwick

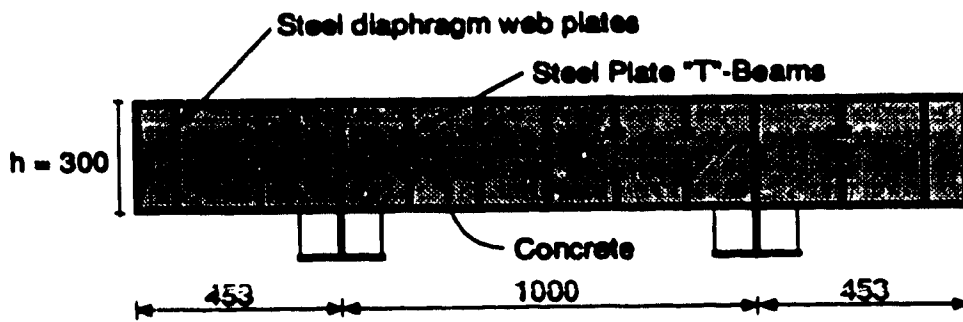


Figure 1.5 Composite Wall Type Tested by Matsuishi and Iwata

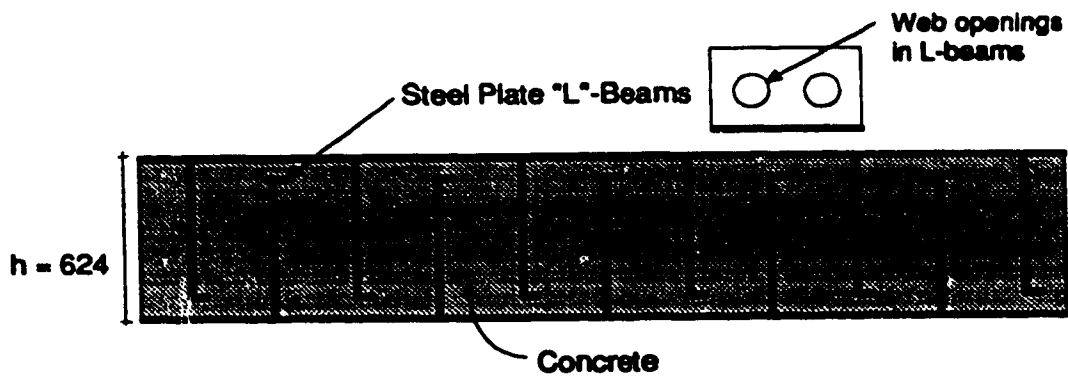


Figure 1.6 Composite Wall Type Tested by Ohno

2.0 SCOPE AND OBJECTIVES

For a composite wall design to be considered for use in an offshore structure, it must satisfy three basic requirements:

- 1. Strength** - the wall must possess sufficient capacity in both flexure and shear to resist very high ice loads.
- 2. Ductility** - following a local failure, the wall must possess sufficient strength through large deformations to ensure that structural damage which would cause environmental damage or loss of life will not occur.
- 3. Economy** - details of the wall must be sufficiently simple so that the cost of fabrication and construction is competitive with conventional steel or reinforced concrete wall designs.

In developing composite wall details, the last of these requirements must be kept in mind. If a composite wall design satisfies the first two criteria, but not the last, there may not be sufficient incentive to pursue a new type of design.

Conventional, all-steel ice-resisting walls are composed of heavily stiffened plate panels, with the skin plate spanning between closely spaced T-ribs and the T-ribs spanning between closely spaced bulkhead frames. An extensive amount of labour intensive welding is required. Conventional, reinforced concrete ice-resisting walls are composed of thick sections containing high percentages of reinforcing steel in all directions (Gerwick, 1985). This construction method is also labour intensive, requiring the difficult placing of highly congested reinforcing bars.

The philosophy adopted for this research work then, was to develop a composite wall scheme which would avoid the high cost items associated with the two conventional wall types, and to show through a physical testing program, that the chosen scheme could also satisfy the appropriate high strength and high ductility requirements.

In order to evaluate the large number of composite schemes that are possible (see for example Nojiri and Koseki, 1986), and to choose those simple schemes with a reasonable chance of success, it was important to develop a preliminary analysis and design

method to estimate the capacity of these walls. An initial assessment showed that a limit analysis approach, which utilizes lower bound plastic theory, appeared appropriate for members of this type.

With all of the foregoing in mind, the objectives of the research program were set out as follows:

- 1. Develop a basic, simple composite wall configuration which avoids, as much as possible, welded stiffening details and complicated reinforcing schemes.**
- 2. Test a series of 1/4 scale beam and slab specimens subject to transverse loads.**
- 3. Develop limit analysis methods, which use concrete plasticity concepts and incorporate these methods into an overall design approach.**
- 4. Evaluate existing finite element computer programs to determine their applicability in modeling a problem of this type, and develop appropriate modeling techniques within an existing program.**
- 5. Prepare recommendations concerning optimum structural configurations, as well as analysis and design methods.**

While all of these objectives have been met, the work presented in this thesis essentially discusses objectives 1,2,3, and 5. The finite element work (objective 4) has been conducted by others and is only briefly commented on. Additional recent work by the author, dealing with concrete fatigue due to cyclic ice loads, is also mentioned briefly.

3.0 CODE REQUIREMENTS AND DESIGN CRITERIA

The purpose of this section is to review existing code requirements for the design of composite walls for fixed offshore structures and to discuss the criteria for the design of such walls. It gives a complete list of the codes which were reviewed in this regard, as well as the abbreviations used to refer to them. It also contains a brief discussion of those clauses which were felt to relate directly to each of these areas, as well as summary statements and conclusions made from this review.

The section provides sufficient documentation to show that composite walls can be designed to meet the same general code requirements used to design more traditional forms of construction. This provides a rationale for regulatory acceptance of a composite design.

3.1 Existing Code Requirements for Composite Walls

3.1.1 List of Codes Reviewed

The codes and guidelines which have been reviewed are shown below, along with the abbreviations used in this report to make reference to them.

- ABS** **Rules for Building and Classing Offshore Installations: Part 1 - Structures, American Bureau of Shipping, 1983.**

- ACI 357** **Guide for the Design and Construction of Fixed Offshore Concrete Structures, ACI Committee 357 Report 357R-84, American Concrete Institute, 1984.**

- ACI 357.1** **State-of-the-Art Report on Offshore Concrete Structures for the Arctic, ACI Committee 357 Report 357.1R-85, American Concrete Institute, 1985.**

- API Bul 2N** **API Bulletin on Planning, Design and Constructing Fixed Offshore Platforms in Ice Environments, API Bul. 2N, First Edition, American Petroleum Institute, Washington, D.C., 1982.**

- API RP 2A** **API Recommended Practice for Planning, Design and Constructing Fixed Offshore Platforms, API Recommended Practice 2A**

- (RP 2A), Seventeenth Edition, American Petroleum Institute, Washington, D.C., 1987.
- API RP 2N** **API Recommended Practice for Planning, Design and Constructing Fixed Offshore Platforms in Ice Environments, API Recommended Practice 2N (RP 2N), First Edition, American Petroleum Institute, Washington, D.C., 1988.**
- BSI** **Code of Practice for Fixed Offshore Structures, BS6235, British Standards Institute, 1982.**
- CSA S471** **Canadian Standards Association, Preliminary Standard S471, General Requirements, Design Criteria, Environment, and Loads; Part I-CSA Code for the Design, Construction and Installation of Fixed Offshore Production Structures, Ninth Draft, 1988.**
- CSA S473** **Canadian Standards Association, Preliminary Standard S473, Steel Structures; Part III-CSA Code for the Design, Construction and Installation of Fixed Offshore Production Structures, Seventh Draft, 1988.**
- CSA S474** **Canadian Standards Association, Preliminary Standard S474, Concrete Structures; Part IV-CSA Code for the Design, Construction and Installation of Fixed Offshore Production Structures, Eighth Draft, 1988.**
- DnV** **Rules for the Design, Construction and Inspection of Offshore Structures, Det norske Veritas, Oslo, Norway, 1977.**
- FIP** **Recommendations for the Design and Construction of Concrete Sea Structures, Fourth Edition, Federation Internationale de la Precontrainte (FIP), 1985.**
- NPD** **Regulations for Structural Design of Load-Bearing Structures Intended for Exploitation of Petroleum Resources, Norwegian**

Petroleum Directorate, Regulations and Provisions for the Petroleum Activity, Volume 2 of Acts, January 1986.

3.1.2 Composite Wall Requirements in S473

CAN/CSA Standard S473-92, part of the Code for the Design, Construction and Installation of Fixed Offshore Structures, is virtually the only offshore structures code which currently addresses the design of sandwich composite walls in detail. Clause 13 of this Standard, titled Composite Walls, was initially written by the author and made extensive use of the information generated by the research presented in this thesis. There has also significant input from an ad hoc CSA Working Group (chaired by the author); Working Group 5, Composite Walls. The Working Group included representatives from industry (Charles Yu, Gulf; John Fitzpatrick, Amoco), government (Ray Smith, COGLA), consultants (Ben Gerwick, BCG Inc., Bob Mast, ABAM) and universities (J.G. MacGregor, University of Alberta). If CSA Standard S473 is adopted by the regulatory authorities prior to design and construction of an offshore structure, regulatory approval of a composite design would not be a problem. The composite wall design itself should also be straight forward, as the design method given in this document is completely consistent with the requirements of Clause 13 in S473.

3.1.3 Composite Wall Requirements in Other Codes

In order to cover the possibility that S473 is not in-force when a structure is built, it was deemed advisable to look at the requirements of other offshore codes which could be used to justify a composite wall design. The code review revealed the following:

- (a) Three other codes (API Bul 2N, API RP 2N and ABS) contain references to composite or hybrid structures, but do not contain any specific guidance or recommendations for design.**
- (b) In the absence of any specific requirements, approval of a composite design may best be achieved as follows:**
 - Demonstrate, by submission of information such as that contained in this thesis, that the composite design method is based on sound engineering principles, and is founded on the same limit states design concepts, as are**

the accepted design criteria used for reinforced concrete and structural steel designs.

- Cite the offshore structures codes that allow novel structural concepts (DnV and FIP) such as composite walls to be used provided that they are verified by model tests.
- Provide details of testing programs to substantiate the composite design method and the capacity of the resulting structure.

The three codes, other than CSA S473, that mention composite or hybrid structures, API Bul 2N, API RP 2N, and ABS Part 1, generally refer to various types of mixed systems. In fact, Clause 5.6, Hybrid Structures, in API Bul 2N, refers to any structure incorporating at least two different construction materials (e.g. steel-earthfilled structures, concrete structures with protective ice berms, etc.). API RP 2N does make a brief mention of steel-concrete composite walls. Other codes make no reference to composite walls, but do discuss the use of model tests to justify a novel design concept. The particular Clauses from these codes are given below.

As mentioned, very little design guidance is actually given in these Clauses. However, the API codes do state that "both elastic and plastic analysis methods may be used" where appropriate. They also state that there is "no generally accepted procedure for hybrid structures" and that it is "essential to adopt a consistent approach throughout the hybrid structure design, such as is offered by the limit state procedure". Both these comments indicate recognition of composite designs as a possibility for offshore structures.

Several references are given specifically for designing hybrid steel-concrete structures (AISC, BS5400, Knowles and several AOGA project reports), but most of these references deal with traditional composite elements, such as beams or columns, which are significantly different from composite wall elements. The AOGA projects mentioned are proprietary research efforts that deal with composite walls; however, the reports are not available to those outside of the joint industry group which funded them and significant research work, such as that presented here, has been completed since then.

3.1.3.1 API Bul 2N

Clause 5.6.1 "A hybrid structure is defined as one incorporating at least two different construction materials in major parts of the structure. Examples of this are mixed steel and concrete structures, earthfilled concrete or steel caissons, and steel or concrete structures surrounded by earthfill or ice berms."

Clause 5.6.6 "There is no generally accepted design procedure for hybrid structures. As explained in Section 2, different materials frequently imply different design codes. However, it is essential to adopt a consistent approach throughout the hybrid structure design such as is offered by the limit state procedure."

"Procedures for the design of hybrid steel-concrete structures may be found in Knowles (1969), BS 5400 (1978), AISC (1978, 1986) and AOGA Projects #265 (1984), #296 (1985), and #324 (1985)."

The information in all of these references, except the AOGA Projects, relates to more traditional types of composite beam and column members commonly used in building and bridge structures. They are not appropriate references for composite wall behaviour or design.

3.1.3.2 API RP 2N

Clause 5.6.1 "General. Examples of hybrid structures are mixed steel and concrete structures such as CIDS (Wetmore 1984a and 1984b) and SSCD (Berlie, 1984), earthfilled concrete or steel caissons such as Tarsiut (Fitzpatrick, 1983) and Molikpaq (Bruce, 1982) and steel and/or concrete structures surrounded by earthfill or ice berms such as the Prudhoe Bay Waterflood Facility. An example of a hybrid structural component is a composite (steel and concrete) ice resisting wall."

"Procedures for the design of hybrid steel-concrete structures may be found in Knowles (1969), BS 5400 (1978), AISC (1978, 1986) and AOGA Projects #265 (1984), #296 (1985), and #324 (1985). Procedures for the design of hybrid earthfilled structures may be found in NAV-FAC DM-70.2 (1982)."

Clause 5.6.2 “Design Considerations. The designer should consider the effects from the interaction of different materials based on their individual physical and mechanical properties. Design inconsistencies that can develop when using more than one design procedure should be avoided. The analysis method must ensure deformation compatibility at interfaces between component materials.”

3.1.3.3 ABS

There is a brief mention of concrete-steel hybrid structures in this code, but no guidance or methods are provided.

Clause 5.7.4 “Concrete-Steel Hybrid Structures - Special attention is to be paid to the design of the connections between steel and concrete components.”

Clause 6.1.4 “Steel-Concrete Hybrid Structures - The steel portions of a steel-concrete hybrid structure are to be designed in accordance with the requirements of this section, and the concrete portions are to be designed as specified in Section 7.”

Clause 7.1.4 “Steel-Concrete Hybrid Structures - The concrete portions of a steel-concrete hybrid structure are to be designed in accordance with the requirements of this section, and the steel portions are to be designed as specified in Section 6.”

3.1.3.4 DnV

No mention is made of composite walls, but this code does refer to using model tests in place of theoretical calculations for novel systems.

Clause 4.6 Design by Testing - “Model tests may, when adequate, be used in combination with or instead of theoretical calculations. In cases of structures or details for which adequate analytical methods of analysis do not exist, tests may be required for verification of acceptable structural resistance. When it is obvious by judgment that acceptable resistance or performance exists, such model tests may be dispensed with.”

3.1.3.5 FIP

No mention is made of composite walls, but this code does refer to using model tests in conjunction with model analysis for novel systems.

Clause 4.6.6 Model analysis and testing - "A design may be deemed satisfactory on the basis of results from an appropriate model test, coupled with the use of model analysis to predict the behaviour of the actual structure, provided that the work is carried out by engineers with relevant experience using suitable equipment."

Clause 4.6.7 Experimental development of analytical procedures - "A design may be deemed satisfactory if the analytical or empirical basis of the design has been justified by development testing of prototype units and structures relevant to the particular design under consideration."

3.2 Ice Loading

Initially, it is important to know approximately the type and magnitude of load to which an ice-resisting wall of an offshore structure will be subjected. The ice load to be used in design is still the subject of much debate and research. Although it is not possible to discuss ice loads in any detail here, it is necessary to give them some consideration.

It is known that local ice pressures are primarily a function of ice type, temperature and salinity, the geometry of the ice feature, the geometry of the structure and the rate of loading (Allyn 1986). In addition, it is well recognized that the effective ice pressure decreases as the loaded area increases. Croasdale (1984) discusses the decrease in failure pressure with an increase in interaction area. His graph, shown in Figure 3.1, does not indicate specific ice pressures or loaded areas, but does show the general trend. It also attempts to explain why the ice failure pressure decreases as the loaded area increases. Sanderson (1986) proposed a pressure-area curve which is shown in Figure 3.2. Also shown on this plot are data points from lab tests and full scale field tests, which Sanderson gathered from a number of different sources. Many others have treated this problem. One good source of additional information is contained in two publications by Public Works Canada (Marcellus, et. al., 1988 and Morrison, et. al., 1988).

At the time of the initiation of this project, a reasonable consensus of available information was that ice pressures appropriate for the design of ice-resisting walls are between 10 MPa and 15 MPa for concentrated loads on areas of approximately 1 m² and between 3 MPa and 5 MPa for loads on areas of 5-10 m². For the purposes of this research work, these values are considered appropriate.

3.3 Design Assumptions

In establishing the design approach, a number of assumptions need to be made concerning the structural layout and the serviceability and ultimate strength requirements for a typical structure. Figure 3.3 shows the structure used as a "target" structure in this work. This structure consists of a series of barges, which fit together and enclose a sand core to make an island. The exterior walls of this structure could be constructed using steel-concrete composite walls. The design assumptions were made with this structure in mind, however, these assumptions are not limited to this structure alone and indeed are also valid for a large number of different structural layouts. The design assumptions are as follows:

1. The composite wall spans horizontally between vertical bulkhead supports, resulting in a one-way slab system.
2. Limitations on bulkhead capacity will likely require a bulkhead spacing of not greater than 5 or 6 metres.
3. The overall thickness of the wall should be large enough to allow a worker access to the inside of the wall during fabrication; i.e. not less than approximately 800 mm to 1000 mm.
4. Preference should be given to steel plate thicknesses of 25 mm or less, to avoid, as much as possible, difficult welding procedures.
5. Although in-plane restraining forces in a wall may increase its capacity, the magnitude of these forces is not easily determined and will conservatively be neglected for the initial work. The possible detrimental effects of in-plane restraint must still be considered.

- 6. Under normal ice loads, the wall should have sufficient stiffness so that cracking of the concrete core is not excessive and deflections remain small, in the elastic range.**

- 7. The ultimate capacity of the wall is considered to have been reached when a mechanism is formed due to yielding of the steel tension plate, a shear/compression failure in the concrete or a bearing failure at the support. Following this failure, the catenary action of the steel plates may provide additional capacity which will be available to help prevent a progressive collapse failure.**

It is believed that these assumptions will lead to a practical design which will be feasible to build and will exhibit satisfactory performance.

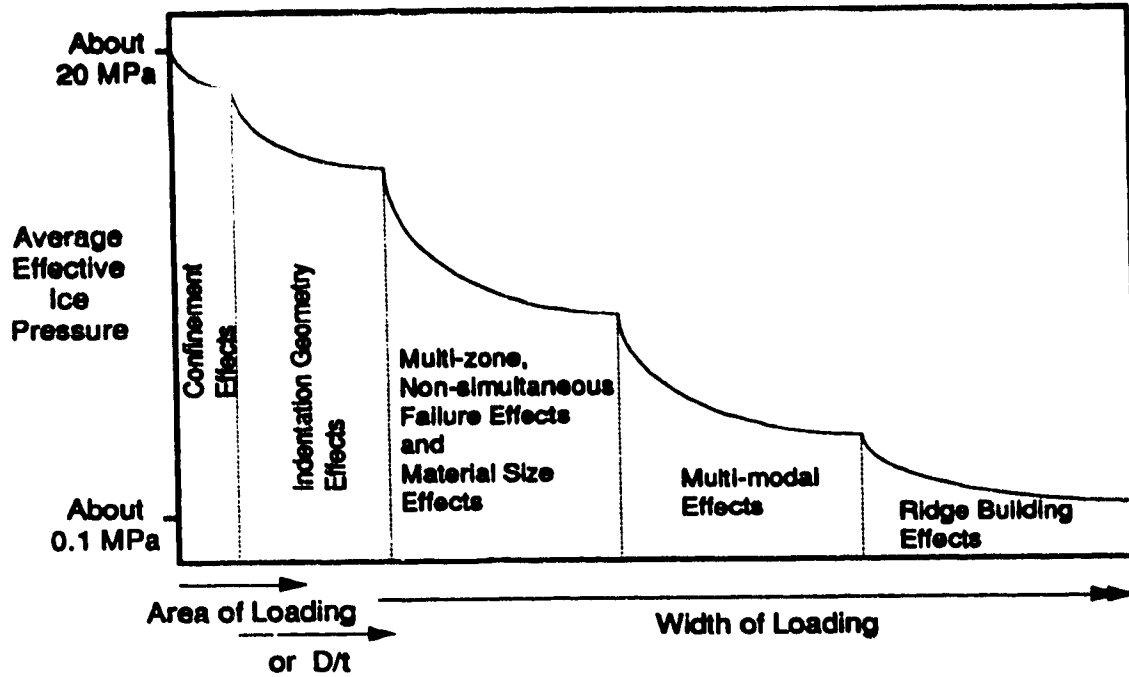


Figure 3.1 Croasdale's Ice Pressure Curve (1984)

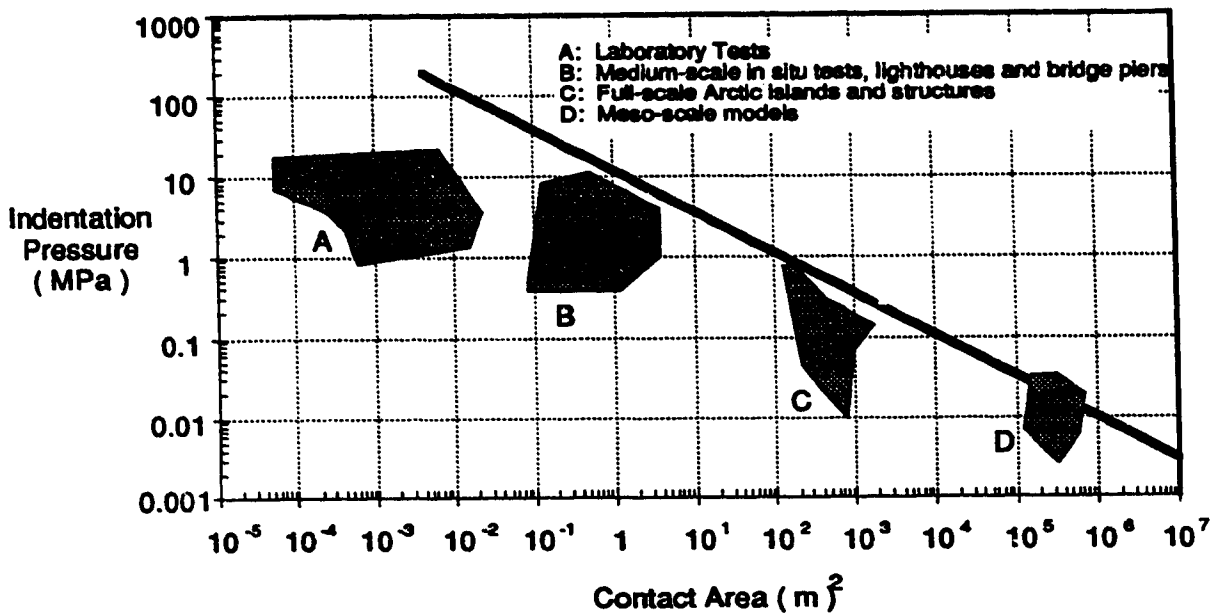


Figure 3.2 Sanderson's Ice Pressure Curve (1986)

Code Requirements and Design Criteria



4.0 TESTING PROGRAM

A total of 16 beam specimens and 3 slab specimens made up the test program. Fourteen of the beam specimens were tested in the test frame shown in Figures 4.1 and 4.2. The other two beam specimens and the three slab specimens were tested using the University of Alberta's 6600 kN Universal Testing Machine (see Figures 4.3 and 4.5).

The two ice load cases that may govern the design of an ice-resisting wall are a concentrated load giving a high pressure on a small area, or a lower pressure acting on a larger area. In the concentrated load case, three dimensional effects are important, since, as the load is transferred to the bulkhead supports, it will distribute laterally. As a result, a larger "tributary area" of the wall will be available to resist the load. For the lower pressure case, the problem is essentially two dimensional, with the effect of the third dimension being limited to the imposition of a condition of plane strain.

The beam specimen tests described in this thesis are intended to consider the latter load case (ignoring the effects of plane strain), while the slab specimen tests are intended to consider the high concentrated "punching" load case (where three dimensional effects are more important).

4.1 Testing Procedure and Specimen Details

The wall configuration which the preliminary work selected for study is the simple configuration shown in Figure 1.1. The outer and inner steel plates are connected together with continuous, vertical diaphragm plates (also referred to as transverse web plates; i.e. transverse to the span). The diaphragm plates are welded to both the outer and inner plates with continuous fillet welds. Only vertical diaphragms are used to facilitate concrete placing and worker access. The prototype wall would contain no other welded details. Most test specimens also used only vertical diaphragm plates.

4.1.1 Beam Specimens

The test frame constructed for the first fourteen beam specimen tests is shown in Figures 4.1 and 4.2, and the dimensions of a typical beam specimen are shown in Figure 1.2. The specimen is inverted in the test frame, with the load being applied from the bottom, with a total of sixteen, 45 tonne hydraulic jacks (in pairs of two, at eight load

points). The total load that can be applied to a specimen in this frame is 7120 kN, distributed along the length of the member, or 890 kN applied at any one location. The first fourteen beam specimens (CF-1 to CF-14) were all single span, with cantilevered ends providing flexural continuity over the supports. The majority of these specimens were tested with all the load points acting, intending to simulate a uniform load on both the main span and on the cantilevered ends of the beam. The last two beam specimens (B-1 and B-2) were three-span continuous beams with two concentrated loads applied near the centre of the middle span (Figure 4.4). These two specimens were tested in the U of A's MTS machine.

The variables considered for the beam specimens were:

- plate thickness;
- diaphragm spacing;
- concrete strength;
- boundary conditions;
- amount of additional shear reinforcing;
- span-to-depth ratio.

Details for the beam specimens and loading configurations are shown in Tables 4.1 and 4.2. Where specimen loads are shown in kilonewtons (kN), the load refers to the concentrated load, P, applied at each load point. Where specimen loads are shown in megapascals (MPa), the load refers to the pressure exert by a single load point over its tributary area. The appropriate tributary areas are: 375 mm x 200 mm for CF-1 to CF-3; 381 mm x 300 mm for CF-4 to CF-9; and 375 mm x 250 mm for CF-10 to CF-14.

4.1.2 Slab Specimens

In order to properly determine the capacity of this composite wall configuration to a high local "punching" load, two composite slab specimen tests were conducted (Specimens S-1 and S-2). In addition, a preliminary slab specimen (Specimen SP-1) was tested in order to determine the approximate failure load and failure mode of Specimens S-1 and S-2. Details of the three slab specimens are also given in Table 4.1.

All three specimens were loaded with a single point load. A photograph of the overall test set-up is shown in Figure 4.3 and schematic diagrams the individual set-ups are shown in Figure 4.5. Specimen SP-1 was a simple span, 1/5 th scale specimen, while Specimens S-1 and S-2 were three-span continuous, 1/4 scale specimens.

4.1.3 Material Properties

4.1.3.1 Structural Steel Plate

All specimens were specified to be fabricated with structural steel plate conforming to CSA Standard G40.21-M, "Structural Quality Steels", grade 300W, which has a nominal minimum tensile yield strength of 300 MPa. This material is normal grade structural steel plate common in the building construction industry and was used because it is readily available and has properties at room temperature similar to Arctic grade plate. The type of plate common for Arctic offshore structures is ABS grade EH36, which has a slightly higher minimum yield strength (350 MPa), as well as low temperature notch toughness properties. Welding was specified to be done with E480 electrodes. The yield strength (f_y) and the tensile strength (f_u) for each specimen are shown in Table 4.1. All specimens conformed to the specified minimum yield strength, with the exception of Specimens CF-1, CF-2 and CF-3, which were under-strength by approximately 12 percent. It is likely that the plate material used for these three specimens was grade 265W.

4.1.3.2 Concrete

The concrete used for all specimens was a normal density (2395 kg/m³), high-early strength mix design with a low water/cement ratio (0.28), a high cement content (471 kg/m³) and a superplasticizer added for workability. Both the mix design and concrete were obtained from Alberta Concrete Products, a local ready-mix supplier. The superplasticizer was added to the concrete transit vehicle on site and the concrete was then placed either directly from the vehicle or using a bottom-dumping concrete bucket. Little vibration was required during placing because the specimens were virtually free of congested reinforcing steel and because of the very high slump (not measurable) resulting from use of the superplasticizer.

Concrete compressive test cylinders were field cured by being placed adjacent to the representative beam or slab specimen. Four separate batches of concrete were used to construct the specimens. Specimens CF-1 to CF-3 were cast from the first batch on January 21, 1986; Specimens CF-4 to CF-9 were cast from the second batch on May 2, 1986; Specimens CF-10 to CF-14 were cast from the

third batch on August 21, 1986; and Specimens B-1, B-2, S-1 and S-2 were cast from the fourth batch on January 30, 1987. Sets of three field-cured cylinders were tested at regular intervals after casting, with the average being assumed as the concrete strength on that date. For the first fourteen beam specimens, the cylinder testing dates did not generally match the dates on which the specimens were tested; therefore for any particular test, f'_c was determined from the equation of a best-fit curve through the average test results. It was felt that this would give a better prediction of the actual compressive strength of the concrete in a particular specimen. The concrete strength curves as well as the actual average cylinder strength data are shown in Figure 4.6. The concrete strength of each of the last four specimens was determined by testing the field-cured cylinders on the same day as the specimen test.

4.2 Boundary Conditions

The test set-ups included load and reaction point details which were intended to simulate three different boundary conditions, as shown in Figure 4.7. Steel half-round rocker plates and roller bearings were used so that the applied load either remained normal to the surface of the specimen (as in the beam tests) or normal to the horizontal (as in the slab tests). Reaction points used the same system so that the reactions were always in a vertical direction. No in-plane restraining forces were applied to any of the specimens for the reasons indicated in Section 3.2, Item 5.

The vertical force applied to the overhanging (cantilevered) ends of the beam specimens was generated in one of two ways (see Table 4.2). Either an active force, P , was applied (Specimens C-1 to C-9) or a passive restraint was used to provide flexural continuity (Specimens C-10 to C-14). The use of passive restraint on the cantilevers for the last five specimens resulted in the set-up being statically indeterminate. This change was made in an effort to provide a test set-up that would remain stable as the member failed so that more information could be gathered concerning the post-peak response. Failures were typically unsymmetrical shear failures, which produced an unbalanced load which the testing frame could not easily handle.

The end conditions used on beam specimens B-1 and B-2, and slab specimens S-1 and S-2, provided resistance to uplift by fastening the ends of the specimens directly to the

strong floor on which the specimens were supported for testing. This was achieved by welding each vertical end plate to a thick (50 mm) horizontal plate which was bolted to the strong floor. Specimen SP-1 was the only specimen which was simply supported.

There were two notable exceptions to the elimination of horizontal, in-plane forces at the reaction points. Specimens CF-1 and CF-3 both used "low-friction" teflon pads under the support points and reaction points, rather than steel roller bearings. The teflon had a coefficient of friction of about 0.02 which led to horizontal friction forces of sufficient magnitude to affect the test results (as discussed in Section 4.4.1.1). Thus for Specimen CF-1 the horizontal reaction at ultimate load was in the order of 50 kN, approximately 8% of the yield strength of the tension plate. This implies an 8% increase in effective flexural capacity of the specimen. This actually turned out to be a fortuitous event, as it allowed the observation that even a very moderate in-plane restraining force can change the mode of failure in a structure; in this case from one of flexure to one of shear. As this type of in-plane restraint is also present in any real structure, its effects must be assessed.

4.3 Instrumentation

All specimens were instrumented with electrical resistance strain gauges, in order to determine the stresses and strains in the steel plates. The general location of the strain gauges is shown in Figures 4.8 and 4.9.

Loads were measured by monitoring the pressure in the hydraulic system used to operate the hydraulic loading jacks (all jacks were hydraulically linked in parallel). Reactions were checked (i.e. compared to the load going in) by monitoring electric resistance gauges placed on the steel reaction frame.

Displacements were measured with LVDT's (linear variable displacement transducers).

4.4 Test Results

To provide a logical sequence for presenting the thesis, test results are given next. It may, however, be preferable to first read Section 4.5, Discussion of Test Results, so that the significance of the results given in this section will be clear.

The test results (observations, strain gauge measurements, displacement measurements, etc.) given in this section are only those which are considered of immediate relevance to the conclusions and recommendations. A laboratory test summary sheet for each test is given in Appendix A. This summary sheet shows the cracking pattern for each specimen and gives material properties, dimensions, mid-span deflections and tension plate strains. It also provides observations and comments concerning the specimen's behaviour during the test.

4.4.1 Beam Specimens

Test results for all of the beam specimens are presented here; however, results for Specimens CF-2 and CF-3 are given in more detail than the other specimens, as they best illustrate some of the features of this type of composite system. Table 4.1 summarizes test results for all the specimens. Table 4.2 gives loading patterns for the first fourteen beam specimens and Table 4.3 shows cracking patterns for the same specimens just prior to failure.

4.4.1.1 Specimens CF-1 to CF-3

Specimens CF-1, CF-2 and CF-3 were identical in all respects, except for: 1) a slight variation in concrete strength; 2) the presence of wire reinforcing cages in Specimens CF-2 and CF-3; and 3) the boundary conditions at the supports. The first two of these differences are considered to have had very little effect on the strength or behaviour of the specimens, while the third, the support boundary conditions, will be shown to have had a considerable effect.

The load vs. deflection curves for the three tests are shown in Figure 4.10. Specimens CF-1 and CF-3, which had the same support boundary conditions (moderate horizontal restraint due to friction), had the same shear failure mode and approximately the same failure load (9.1 and 9.6) MPa. Specimen CF-2, however, failed in a flexural rather than a shear mode, and at a slightly lower load (8.2 MPa). This specimen had roller supports which offered virtually no horizontal restraint at the supports.

It should be noted that the CF-1 test was stopped after the first shear failure occurred, due to instability in the test frame caused by the unbalanced type of failure. This prevented the "ductile" part of the curve from being obtained. This unsymmetrical, unbalanced type of shear failure caused this same difficulty in a number of the other tests as well. The ultimate failure load was always obtained, however, and post-failure curves were obtained for a sufficient number of specimens to allow valid conclusions to be drawn.

Strains were measured in the steel plates at a number of locations in each of the specimens (Figure 4.8). Refer to the load-strain diagrams shown on the summary sheets in Appendix A.

4.4.1.1.1 Specimen CF-3 - Shear Failure

The sketches in Figure 4.11 and the pictures in Figure 4.12 show specimen CF-3 at various different stages of loading. Loads are given in MPa and represent a uniform pressure over the tributary area of each load point (200 mm x 375 mm). At an applied load of 4.5 MPa (Figures 4.11a and 4.12a) the member was uncracked; very slight separations had opened at particular locations between the concrete and the diaphragms. These separations closed again if the load was removed. The deflection at this point was approximately 3 mm. By the time a load of 6 MPa had been reached (Figures 4.11b and 4.12b), diagonal shear cracks had formed adjacent to each support. A flexural tension crack had also formed in the concrete at mid-span. Load cycling (five load cycles) at this load level caused no further progression of these cracks. At a load of 9.5 MPa (Figure 4.12c), numerous diagonal cracks had formed and concrete crushing was evident adjacent to the supports. At a load of 9.6 MPa (Figure 4.12d), shear failures occurred in the cracked regions at each end of the beam. These involved crushing of the concrete at either end of the diagonal shear cracks, with coincident diagonal tensile failures along the length of the shear cracks. The load subsequently dropped to approximately 7.5 MPa, where it remained reasonably constant as the specimen was pushed through significant deformations. As deformations became large, the specimen began to take more load. At the conclusion of the test (the specimen could be pushed no further in the test frame), the load was nearly back to what it had been at first failure. When the test was terminated, the specimen, in the

damaged condition shown in Figures 4.11c and 4.12e, was still able to carry a load of almost 9.5 MPa. Both inside and outside steel plates had yielded extensively, but were not fractured at any locations.

4.4.1.1.2 Specimen CF-2 - Flexural Failure

Up to a load of approximately 6 MPa, specimen CF-2 behaved identically to CF-3, including the formation of diagonal shear cracks. At this load, however, a flexural failure began to occur as the tension plate yielded in the centre third of the specimen. Both the mid-span flexural crack and the gaps at the diaphragms opened up, as deflections became large. Failure of the specimen occurred at a load of 8.2 MPa, when the tension plate fractured in the heat affected zone (or adjacent to it) at the diaphragm/tension plate weld. Following this failure, the specimen had no further load capacity. The failed specimen is shown in the pictures in Figure 4.13. No crushed concrete was observed.

4.4.1.2 Specimens CF-4 to CF-9

The variables for these six specimens were: concrete strength (36 MPa to 61 MPa); plate thickness (5.4 mm, 10.0 and 12.6 mm); diaphragm spacing; and, loading arrangement (uniform load or patch load). Refer to Table 4.1 for details. Load-deflection curves for each of these test specimens are shown in Figure 4.14.

The following items are especially worthy of note for these six specimens:

1. All of the members eventually failed in shear: Specimens CF-4,5,7 and 9, without significant yielding of the longitudinal steel; Specimen CF-6, after some flexural yielding; and, Specimen CF-8, after significant flexural yielding.
2. Specimen CF-8 reached its full flexural capacity at a load very close to that theoretically calculated from a truss analogy (see Figure 5.11). The capacity corresponding to a plastic hinge mechanism for this specimen is shown as a dashed line in Figure 4.14(e).

3. The lower concrete strength of Specimen CF-5 (36 MPa; other specimens had concrete strengths between 50-60 MPa) reduced its shear capacity.
4. All of the specimens had a post-failure capacity of approximately 50% of the full capacity (except CF-8 which had an additional diaphragm plate in the critical shear span, thus reducing by half the a/d ratio). This post-failure capacity should be compared to that of Specimens CF-3 at 79% and CF-8 at 87%.

4.4.1.3 Specimens CF-10 to CF-14

The variables for these five specimens, shown in Table 4.1, were: diaphragm spacing, shear reinforcing, and, end restraint. All of the specimens in this group were tested with the free ends restrained against vertical deflection. Refer to Table 4.1 for details. Load-deflection curves for these specimens are shown in Figure 4.15. Pictures of Specimens CF-11 and CF-12, near the end of each test, are shown in Figures 4.16 and 4.17.

The following items are especially worthy of note:

1. All of the specimens eventually failed in shear: Specimens CF-13 and 14, without significant yielding of the longitudinal steel plates; Specimen CF-12, after some flexural yielding; and, Specimens CF-10 and 11, after significant yielding.
2. The additional shear reinforcing in Specimen CF-10 (headed studs and rebar; see Figure 5.12) significantly increased the shear capacity.
3. The closer diaphragm spacing of Specimens CF-11 and CF-12 significantly increased the shear capacity.
4. Prior to the shear failure, Specimen CF-11 became fully yielded in flexure, with a plastic hinge forming at mid-span. It ultimately

failed in shear at a load very close to the theoretical capacity calculated from an upper bound plastic solution (see Table 5.3).

5. Specimen CF-11 showed remarkable redundancy while failing in shear. One at a time, shear failures occurred in the concrete in two cells at one end of the specimen and in one cell at the other end, and one diaphragm web plate at each end of the specimen fractured. Each time a failure occurred, the load found a new path to the support, finally being transferred via membrane tension in the upper steel plate (Figure 4.16).
6. As a percentage of full capacity, the post-failure capacities of the specimens were:

CF-10 and 11	98% ;
CF-12	70% ;
CF-13	53% ;
and, CF-14	66%

4.4.1.4 Specimens B-1 and B-2

These two three-span, continuous beam specimens were companion specimens for the three-span, continuous slab specimen, Specimen S-1 (see Section 4.4.2.2). The purpose of the tests was to determine the effect of specimen width on the failure load (by comparing B-1 with S-1), and to determine the effect of a 30% reduction in the diaphragm plate thickness. Specimen B-1 had a diaphragm plate thickness of 6.80 mm, compared to a thickness of 4.90 for Specimen B-2. Load deflection curves for these two tests are shown in Figure 4.18.

The following items are especially worthy of note:

1. Both specimens B-1 and B-2 behaved almost identically, until the later stages of the tests.

2. Both specimens failed in shear prior to yielding of the longitudinal steel plates. In each case, at a load slightly above 1000 kN, shear cracking at one end of the centre span was closely followed by shear cracking at the other end, closely followed by a shear failure at one end and a reduction in load to approximately 800 kN. After some continued deformation, a second shear failure occurred and the load dropped to between 400 and 500 kN. Further loading achieved a post-failure load near 600 kN (60% of ultimate).
3. After considerable deformation, Specimen B-1 finally failed by fracturing of the upper plate in a region of high plastic deformation over one of the interior diaphragms. Specimen B-2 did not fracture in this way, but maintained the post-failure load level throughout the test.
4. The reduction in diaphragm plate thickness of 30% between Specimens B-1 and B-2 had no discernible effect on the failure load or post-failure response, as in both cases the diaphragm plates were not stressed to their ultimate capacities.

4.4.2 Slab Specimens

Three slab specimens were tested: Preliminary Specimen SP-1, a single span slab specimen shown in Figure 4.5(b); and Specimens S-1 and S-2, three-span, continuous slab specimens.

Specimens S-1 and S-2 are shown in Figure 4.5 (a). These specimens were intended to determine the resistance of a composite wall to a high local “punching” load. The only difference in the two specimens was the thickness of the exterior steel plates. Specimen S-1 had a plate thickness of 5.35 mm, compared to a thickness of 9.35 mm for S-2.

4.4.2.1 Specimen SP-1

The only purpose of Specimen SP-1 was to determine the approximate failure load and failure mode of Specimens S-1 and S-2, which were designed and tested following testing of SP-1. The results are also being reported however, since this specimen illustrates some typical features of composite wall behaviour. A load-deflection curve for this specimen is shown in Figure 4.19 (a).

The following items are especially worthy of note:

1. This 1/5th scale simple-span specimen had oversized exterior steel plates (12.5 mm) in order to prevent a premature flexural failure.
2. Indenting of the specimen at the load point, bulging of the tension plate under the load point, and a leveling off of the load-deflection curve at approximately 3000 kN indicated the initiation of a punching-shear failure.
3. Punching-shear was not the ultimate cause of failure. Local membrane action of the steel plate around the load point arrested the punching failure and allowed the full shear capacity of the section to develop.
4. At a load of 3270 kN the specimen began failing in shear as a wide beam, almost identically to the shear failures observed in the beam specimen tests.
5. A post-failure load of approximately 2500 kN (76% of ultimate) was sustained through large deformations, until termination of the test.
6. The pressure on the centrally loaded area was 165 MPa at the initiation of the punching-shear failure.

4.4.2.2 Specimen S-1

A load-deflection curve for Specimen S-1 is shown in Figure 4.19 (b). Pictures of the specimen following the test are shown in Figures 4.20, 4.21 and 4.22.

The following items are especially worthy of note:

1. The initiation of a punching shear failure in the concrete core of Specimen S-1 was indicated by the indenting of the top plate (loaded plate) and the bulging of the bottom plate at a load of 2500 kN. A conical piece of concrete was pushed down, bearing on the bottom plate of the specimen.
2. Following considerable deformation of this type, the bottom plate began to fracture. Two fractures started on the bottom plate, on the longitudinal mid-line of the specimen in the heat affected zone of the welds connecting the bottom plate to the two interior transverse diaphragm plates. As loading continued, the fractures slowly propagated transversely toward the edges of the specimen (Figure 4.22).
3. The specimen lost all its load carrying capacity, when a sudden shear failure occurred in the steel in the top plate around the perimeter of the loaded area (Figure 4.21).
4. The load magnitude required for the initiation of the punching-shear failure in the concrete was very high; a pressure of 90 MPa on the centrally loaded area.

4.4.2.3 Specimen S-2

A load-deflection curve for this specimen is also shown in Figure 4.19 (b). Pictures of the specimen following the test are shown in Figures 4.23, 4.24 and 4.25.

The following items are worth noting:

1. The initial response of the specimen was somewhat stiffer than Specimen S-1 due to the increase in the exterior plate thickness.
2. The strains measured in the tension plates of the specimen were close to those predicted by the results of an elastic truss-model analysis.
3. A punching shear failure began at a load of approximately 3660 kN at the first peak in the load-deflection curve; however, the membrane action of the top and bottom steel plates arrested the punching failure allowing the full shear capacity of the specimen to be developed (Figure 4.25).
4. The specimen failed in one-way shear as a "wide beam" at a load of 4170 kN in the same manner as Preliminary Specimen SP-1 (Figure 4.24).
5. The member was very efficient in laterally spreading the concentrated load. The diaphragm web plates welded to the outer plates acted as "I-beams" to laterally distribute load (in Figures 4.23 and 4.24 it appears as if the entire centre third of the centre span was loaded, rather than just the 188 mm diameter load point).
6. The specimen maintained a post-failure load capacity of approximately 2500 kN (60% of ultimate) through large deformations until termination of the test.
7. The magnitude of the load required to initiate the punching-shear failure mode was very high; 132 MPa on the centrally loaded area.

4.5 Discussion of Test Results

The basic idea when the test program began, was to start with very simple wall details and gradually increase their complexity until the necessary strength and ductility were achieved. It was quickly realized that the very simple details worked well and were capable of providing high strength in flexure and shear, as well as providing ductile failure modes in both flexure and shear. For this reason, the simple configuration, utilizing transverse diaphragm plates (Figures 1.1 and 1.2), was adopted as the "basic" design configuration. All of the other specimens were variations of this basic design.

This design uses transverse diaphragm plates as the only means of tying the exterior plates together, providing interfacial shear transfer between the exterior plates and the concrete core and providing shear reinforcing for the wall (at discrete locations, rather than distributed as in a conventional reinforced concrete member).

As will be shown, the most important variables, in determining the strength and ductility of the wall, are: plate thickness; concrete strength; and "a/d" ratio of the unreinforced cell between diaphragm plates (Figure 5.14). The horizontal dimension "a" is equivalent to the effective shear-span, as this is the maximum distance over which the shear force must be transferred before being intercepted by a diaphragm plate or support.

4.5.1 Beam Specimens

The behaviour of the beam specimens was similar in some respects to that of a reinforced concrete beam with tension and compression reinforcement. Flexure involved the development of a force couple with tension being generated in the bottom steel plate and compression being generated in the top plate and the adjacent concrete at the top of the beam. Shear was transferred through the beam via diagonal compression struts which were anchored at the intersections of the tension steel and the diaphragm plates.

The post-failure response of those specimens which were taken far past the point at which the first shear failure occurred usually involved large deformations and the development of catenary action in the steel plates. This is depicted well in Figures 4.12, 4.16 and 4.17 which show Specimens CF-3, CF-11 and CF-12 at the termination of each test.

The following deductions can be made from the beam specimen test results:

1. Flexural strength is dependent on the maximum tensile force couple that can be generated by the exterior steel plates (Specimen CF-2); this implies that the important parameters are plate thickness, yield strength, tensile strength and section depth (i.e. wall thickness). Comparing the results of Specimens CF-2 and CF-3 also shows that the presence of in-plane boundary restraint can increase the flexural capacity.
2. Shear capacity is dependent on: concrete strength (CF-4 vs. CF-5); exterior steel plate thickness (CF-6 vs. CF-7); and a/d ratio (CF-4 vs. CF-8). It is also obvious that section depth is an important parameter.
3. A composite wall can be designed to provide a stiff response with few cracks in the service load range (as exhibited by all specimens).
4. The inclusion of additional shear reinforcing in the unreinforced cells between diaphragm plates (Specimen CF-10 vs. CF-12) increases shear capacity. However, it appears that such additional shear reinforcing will not be necessary in order to attain the required level of shear capacity; most specimens had shear capacities greater than the target ice load level (3 to 5 MPa; see Section 3.2).
5. The post-failure capacity as a percentage of ultimate, for specimens failing in shear, appears to be mainly a function of the a/d ratio and the presence of additional shear reinforcement, if any. The relationship between a/d ratio and post-failure strength is shown in Figure 4.26 for all beam specimens. It should be noted that CF-2 failed in flexure not shear. Basically, the lower the a/d ratio, the steeper the shear failure surface and the higher the post-failure strength. Additional shear reinforcing also increased the post-failure strength (Specimen CF-10), as would be expected.

6. When failing in flexure, a composite wall specimen of this type can develop its full flexural capacity (Specimen CF-8), provided that there is sufficient shear capacity to prevent an earlier shear failure. The load required to form a flexural mechanism can be accurately calculated from a plastic truss analysis. Whether or not this mechanism can be achieved in an actual structure, however, is dependent on the amount of in-plane boundary restraint which acts on a particular section of wall. In some cases in-plane restraint, due to the continuity of the wall beyond the section being considered, would reduce the flexural tensile stresses in the wall, thus increasing the flexural capacity of the wall to the point where a shear failure occurs before a flexural mechanism fully develops. This is discussed further in Section 5, Design Methods.
7. Inclined (diagonal) cracks were always contained within a single cell. In no case did a single inclined crack extend across two cells.

4.5.2 Slab Specimens

The following deductions can be made from the results of the slab specimen tests:

1. This composite wall design, which uses transverse diaphragm plates, has a great ability to laterally distribute local loads. This results in a one-way action in the slab, so that in the tests it behaved essentially as a wide-beam, even for local concentrated loads.
2. The slab specimens displayed a very high resistance to a punching-shear type of failure. The pressure on the loaded area required to initiate a punching failure was an order of magnitude higher than any anticipated local ice load (the minimum pressure recorded for punching initiation was 90 MPa on a centrally loaded area vs. a probable maximum local ice pressure of 12-15 MPa). However, this may be an important mode of failure to consider for loading events other than ice-loading (e.g. ship collision).

3. **The magnitude of the punching-shear failure load is dependent on exterior plate thickness (as shown by the tests). It is also intuitively obvious (although not considered in the tests) that loaded area perimeter, depth of section and concrete strength also have an effect on punching-shear capacity.**
4. **For an ice-load event, the ultimate shear failure mode of concern is wide-beam shear.**
5. **If the possibility of a punching-shear failure is discounted, a ductile, wide-beam shear failure mode can be achieved, with a high post-failure strength (60% and 76% of ultimate were achieved in two of these tests). Even for a punching-shear type of failure, ductility can be achieved, provided that a shear-fracture in the exterior steel plates can be prevented.**

Table 4.1 Specimen Details and Summary of Results

Spec. No.	Failure Load, P		Type of Failure	f _c (MPa)	f _y (MPa)	f _u (MPa)	t (mm)	w (mm)	h (mm)	L (mm)	b (mm)	s (mm)	a (mm)	d (mm)	a/d	V _u (kN)	Post-Failure Strength
	(kN)	(MPa)															
CF-1	684	9.12	shear	58.0	265.0	390.0	6.35	6.35	250	1000	375	333	235	244	0.96	684	77 %
CF-2	617	8.23	flexure	62.1	265.0	390.0	6.35	6.35	250	1000	375	333	235	244	0.96	617	100 %
CF-3	717	9.56	shear	58.8	265.0	390.0	6.35	6.35	250	1000	375	333	258	244	1.06	717	78 %
CF-4	560	4.90	shear	53.5	371.0	500.0	12.60	6.35	250	1500	381	500	425	238	1.79	551	50 %
CF-5	437	3.82	shear	36.3	371.0	500.0	12.40	6.25	250	1500	381	500	425	238	1.79	430	50 %
CF-6	561	4.91	shear	57.5	352.0	530.0	10.00	6.25	250	1500	381	500	425	243	1.75	552	50 %
CF-7	601	5.26	shear	58.4	347.0	477.0	16.10	6.45	250	1500	381	500	425	234	1.82	592	50 %
CF-8	761	6.66	shear	59.5	371.0	500.0	12.40	6.20	250	1500	381	250	175	238	0.74	1498	87 %
CF-9	754	6.60	shear	61.0	371.0	500.0	12.50	6.35	250	1500	381	500	375	238	1.58	691	50 %
CF-10	908	9.69	shear	54.5	401.0	n/a	9.54	6.35	250	1250	375	417	175	241	0.73	1816	98 %
CF-11	757	8.07	shear	58.2	388.0	490.0	9.54	6.35	250	1250	375	208	133	241	0.55	1514	98 %
CF-12	772	8.23	shear	56.6	398.0	495.0	9.54	6.35	250	1250	375	313	113	241	0.47	1544	70 %
CF-13	712	7.59	shear	56.0	398.0	500.0	9.54	6.35	250	1250	375	417	342	241	1.42	712	53 %
CF-14	745	7.95	shear	60.0	398.0	500.0	9.54	6.35	250	1250	375	417	342	241	1.42	745	66 %
SP-1	3270	N/A	shear	46.0	340.0	n/a	12.50	6.35	200	1000	1200	333	258	188	1.37	1635	76 %
S-1	2500	N/A	punching	58.5	340.0	510.0	6.65	6.35	250	1250	1200	417	342	243	1.41	1250	80 %
S-2	4170	N/A	shear	64.3	450.0	n/a	10.40	6.35	250	1250	1200	417	342	240	1.43	2085	60 %
B-1	1092	N/A	shear	66.5	340.0	510.0	6.91	6.80	250	1250	375	417	342	243	1.41	531	60 %
B-2	1050	N/A	shear	65.9	340.0	510.0	6.79	4.90	250	1250	375	417	342	243	1.41	525	60 %

Notation

- f_c - 28-day concrete strength
- f_y - yield strength of exterior plates
- f_u - tensile strength of exterior plates
- t - exterior plate thickness
- w - diaphragm plate thickness
- h - specimen height, out-to-out of exterior plates
- L - span
- b - specimen width
- s - diaphragm plate spacing
- a - clear shear span; horizontal projection of potential shear crack
- d - specimen height, centre-to-centre of exterior plates

V_u - shear force across critical shear crack, at ultimate load; calculated from statics, assuming that any loads between the shear crack and the support go directly to the support and are therefore not included.

Table 4.2 Loading Patterns for Beam Specimens CF-1 to CF-14

Specimen No.	Load Type	Span, L (mm)	Diaph. Spacing, s (mm)	Loading Pattern
CF-1 CF-2 CF-3	A	1000	333	
CF-4 CF-5 CF-6 CF-7	B	1500	500	
CF-8	B	1500	250	
CF-9	C	1500	500	
CF-10	D	1250	417	
CF-11	D	1250	208	
CF-12	D	1250	313	
CF-13 CF-14	E	1250	417	

Table 4.3 Cracking Patterns for Beam Specimen CF-1 to CF-14

Specimen No.	Load Type	Failure Load, P (kN)	Shear Span, a (mm)	Loading Pattern
CF-1 * CF-2 CF-3	A	684 617 717	235 235 258	
CF-4 CF-5 CF-6 CF-7 *	B	560 437 561 601	425	
CF-8	C	761	175	
CF-9	D	754	375	
CF-10	E	908	175	
CF-11	F	757	133	
CF-12	F	772	113	
CF-13 * CF-14	G	712 745	342	

* Indicates which specimen's cracking pattern is shown.

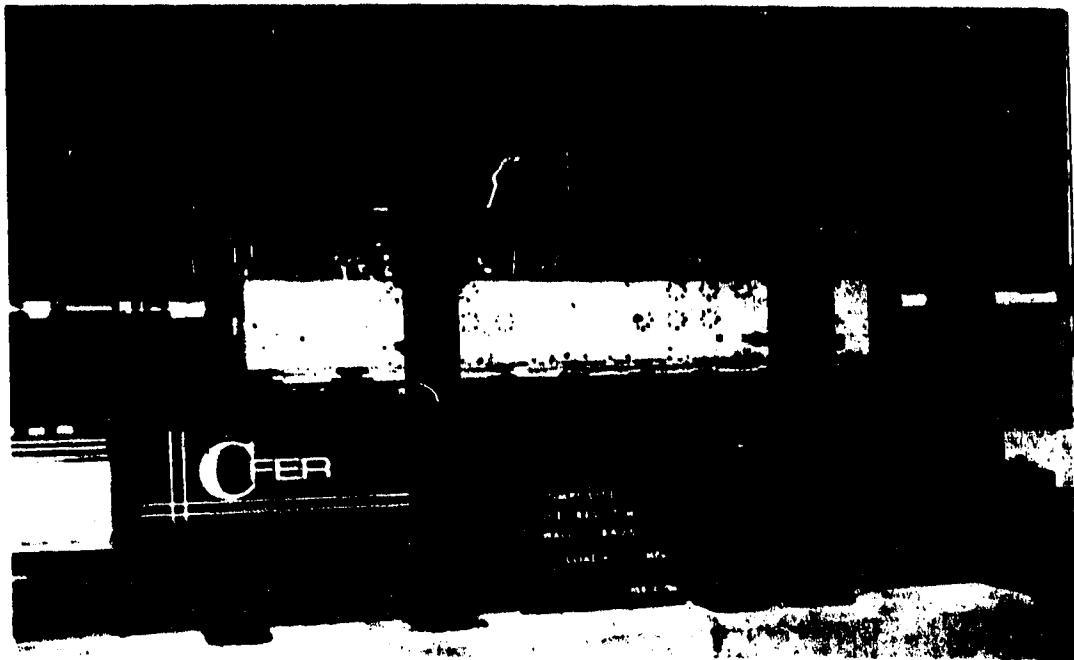


Figure 4.1 Specimen in Beam Testing Frame

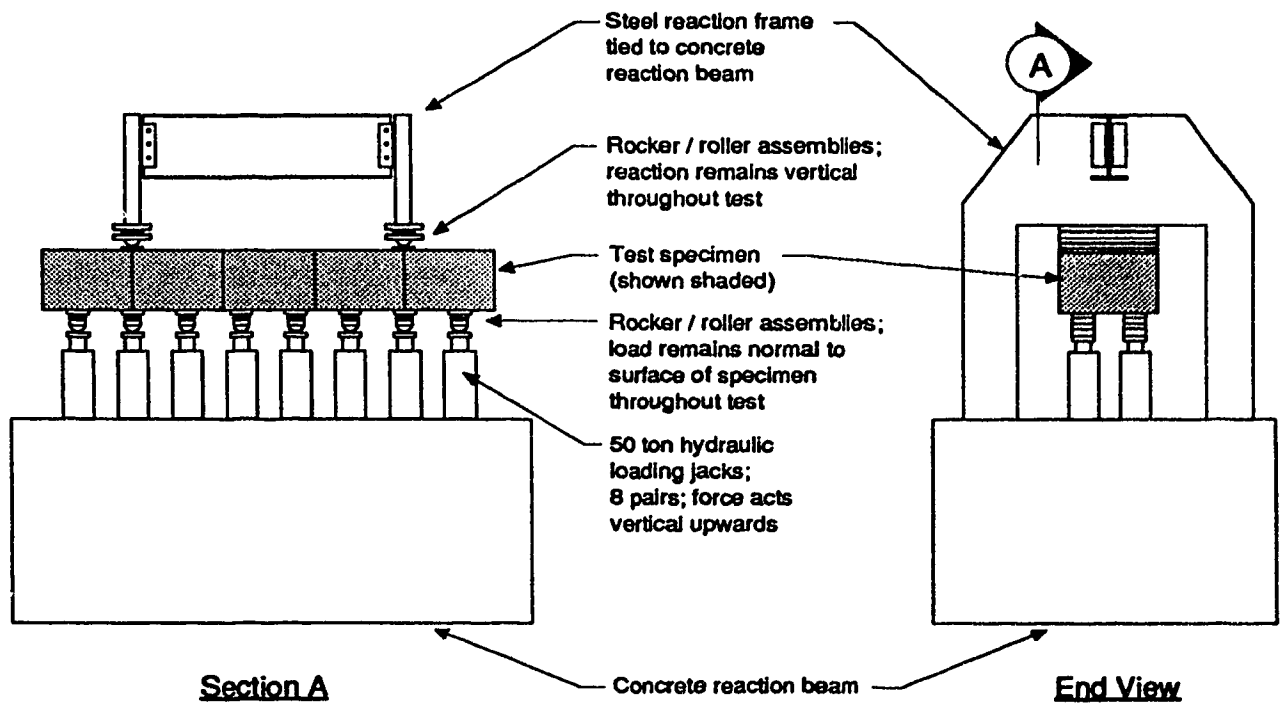


Figure 4.2 Schematic of Beam Testing Frame

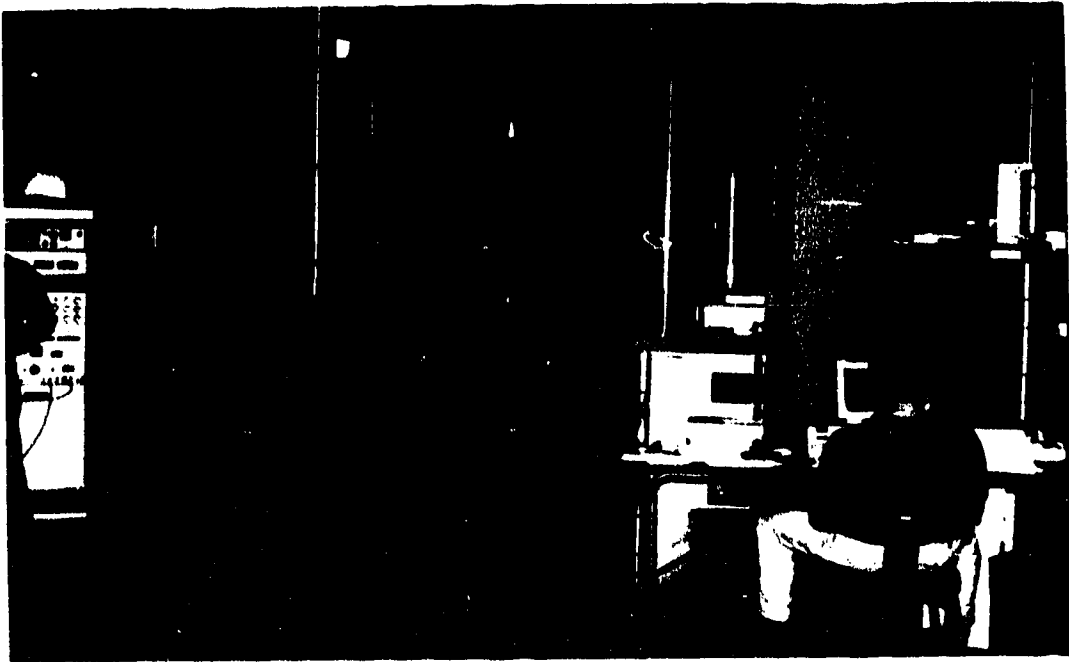


Figure 4.3 Slab Specimen in MTS Universal Testing Machine

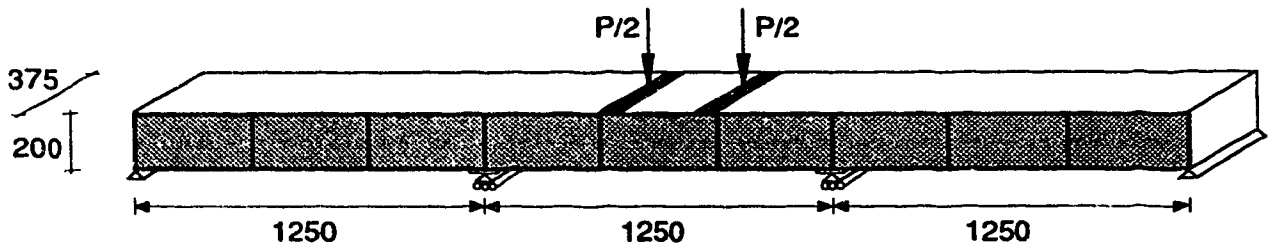
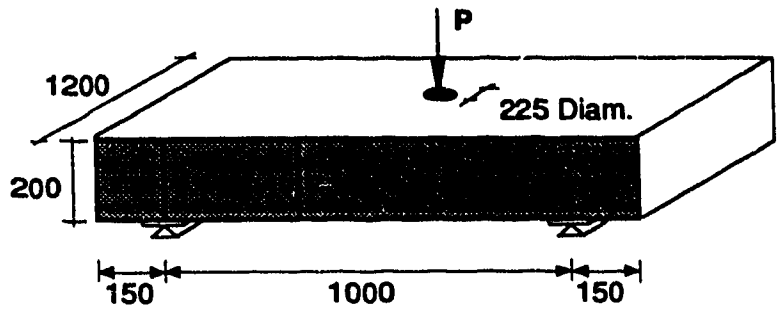
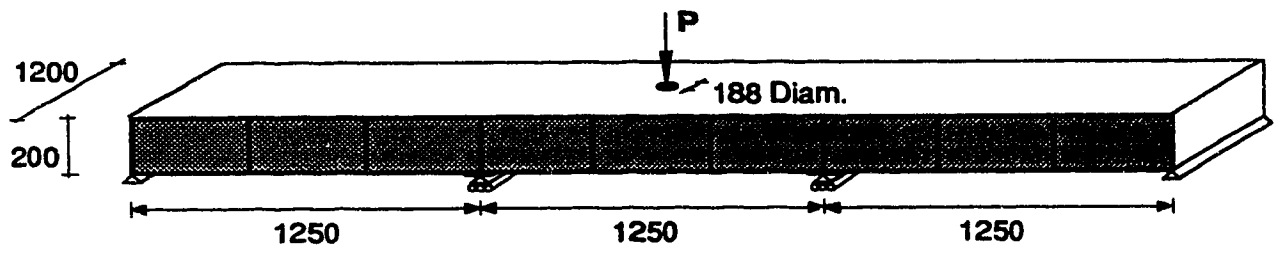


Figure 4.4 Specimen Configuration for B-1 and B-2

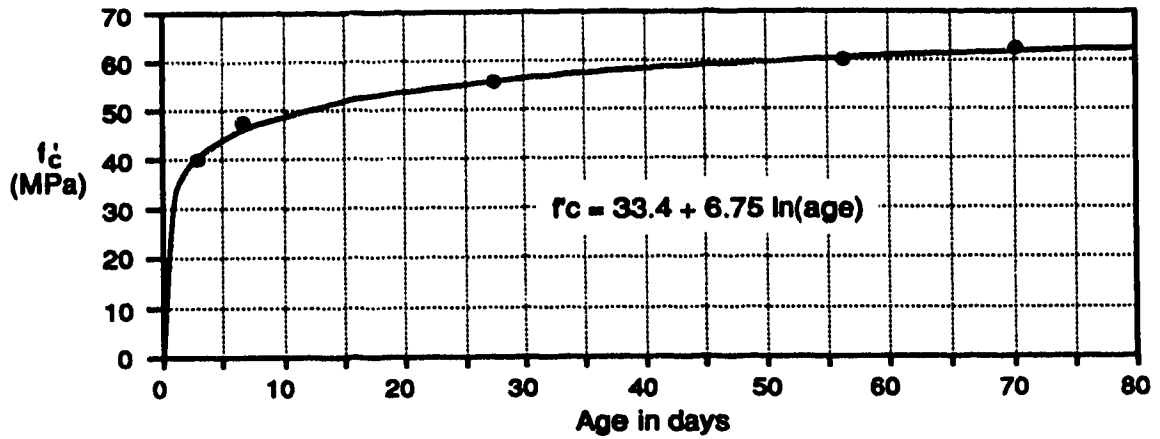


(b) Specimen SP-1

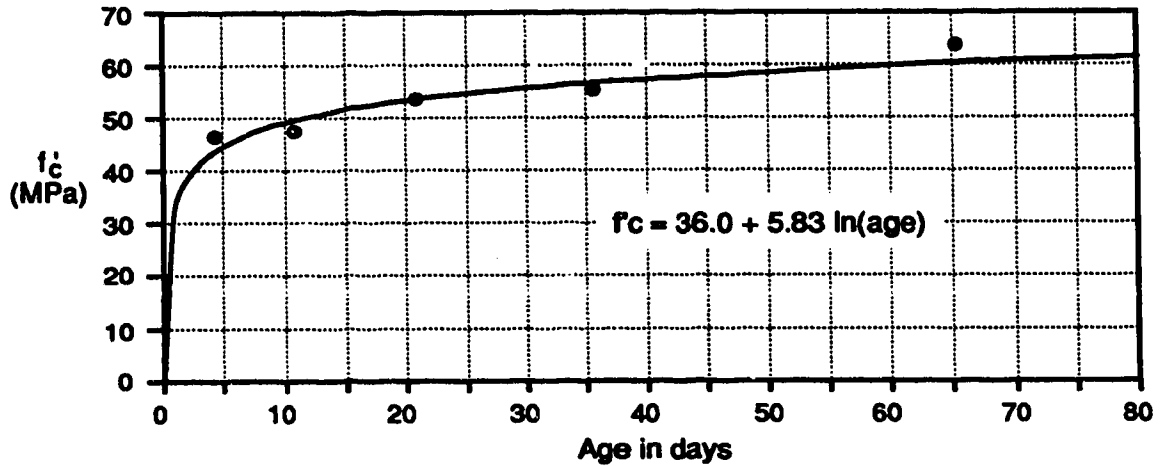


(a) Specimens S1 and S2

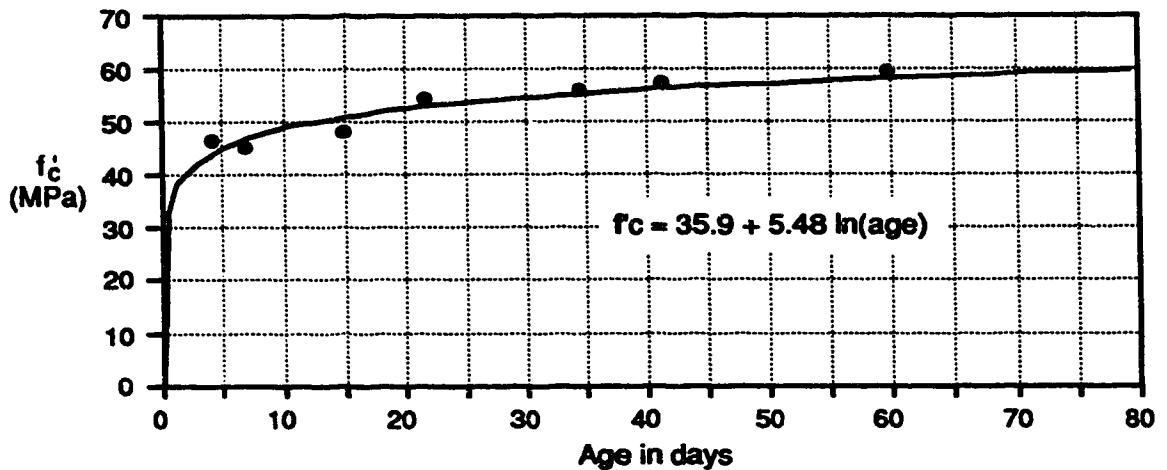
Figure 4.5 Slab Specimen Configurations



(a) Concrete Batch No. 1; Specimens CF-1 to CF-3



(b) Concrete Batch No. 2; Specimens CF-4 to CF-9



(c) Concrete Batch No. 3; Specimens CF-10 to CF-14

Figure 4.6 Concrete Strength Data

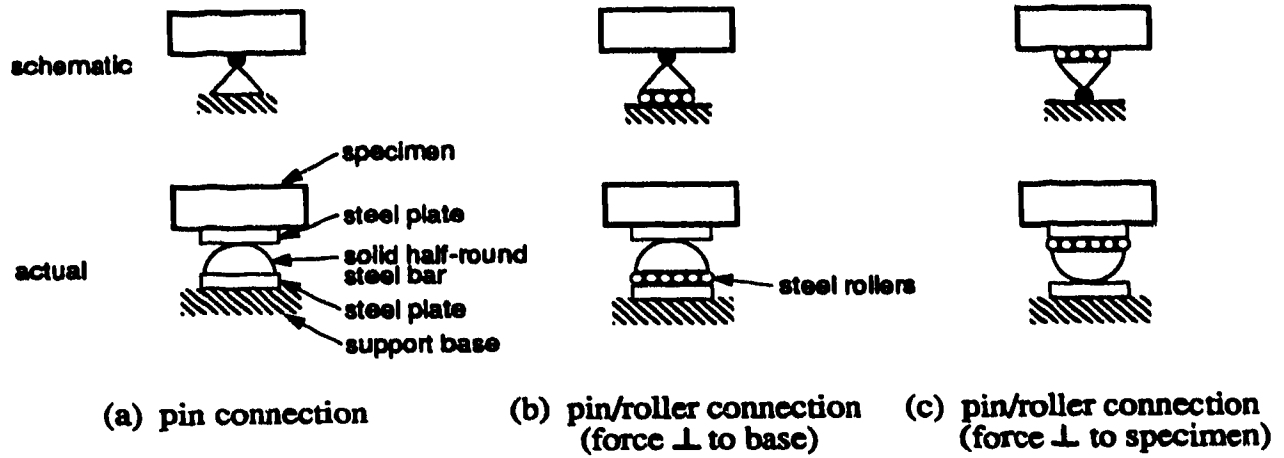


Figure 4.7 Support Boundary Conditions

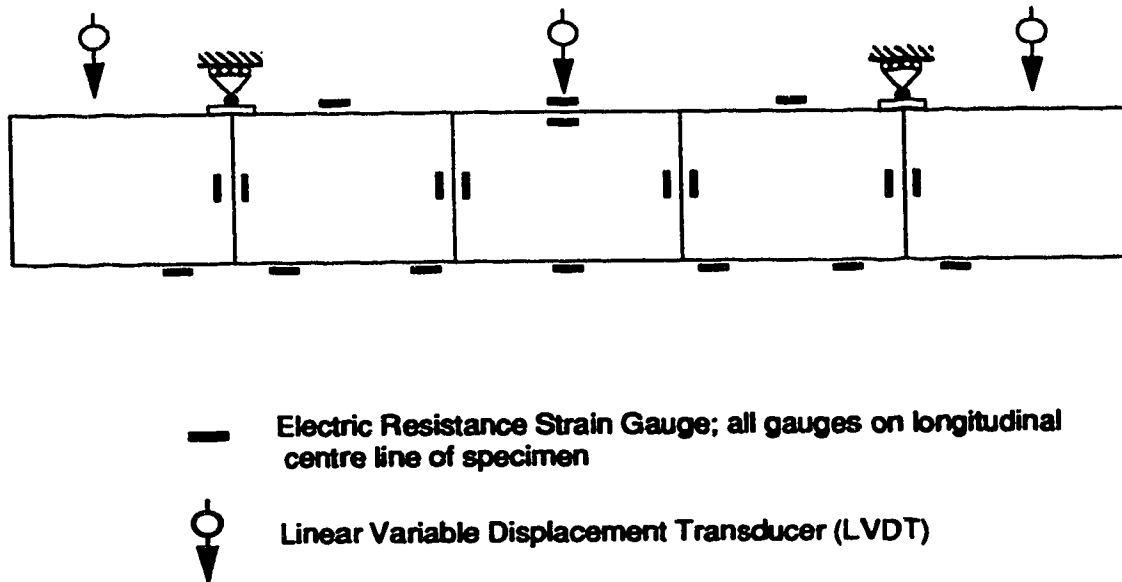


Figure 4.8 Typical Instrumentation for Beam Specimens

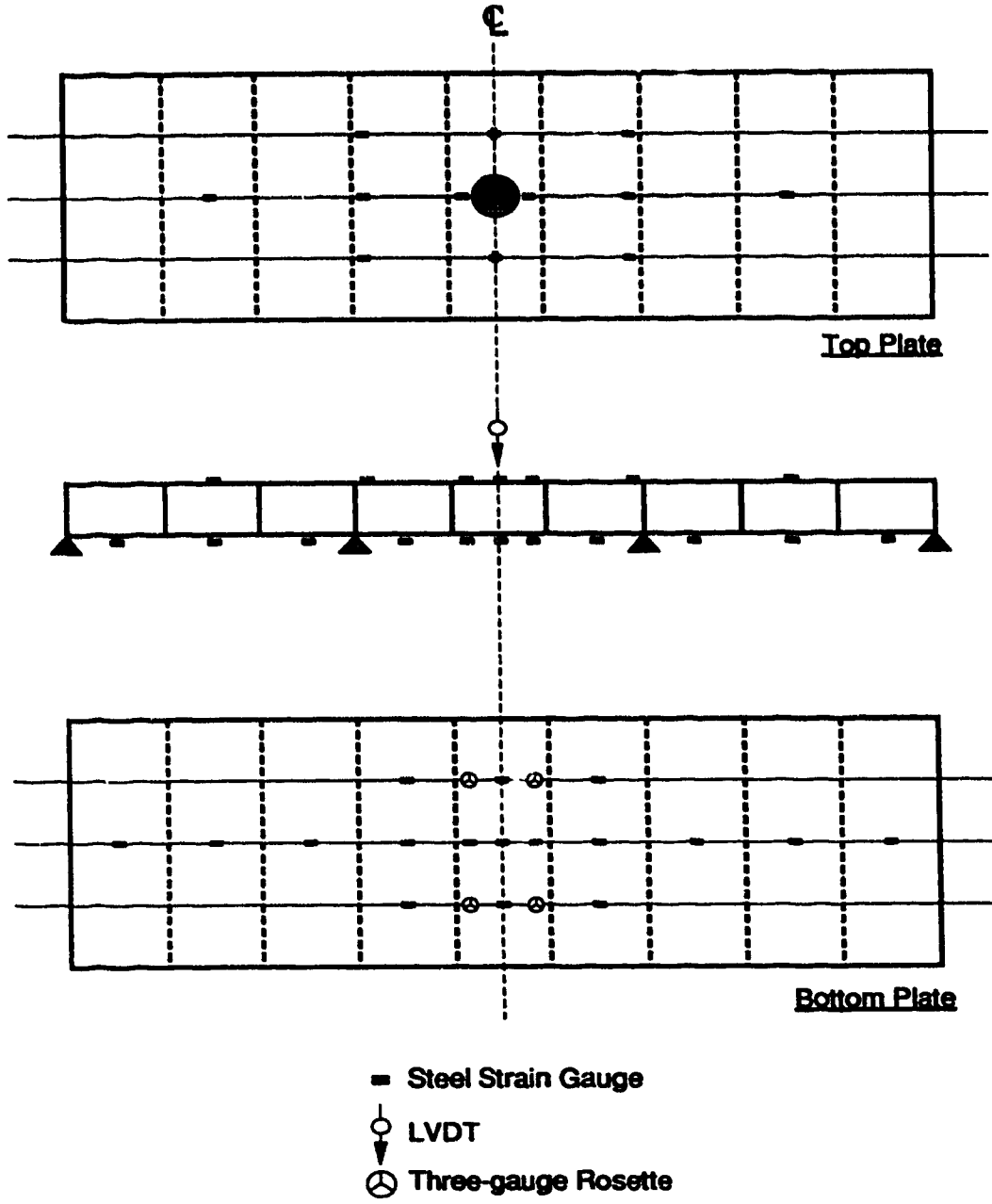
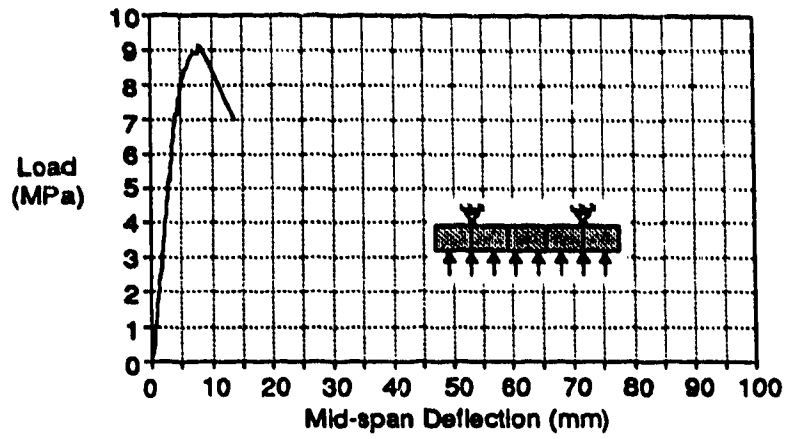
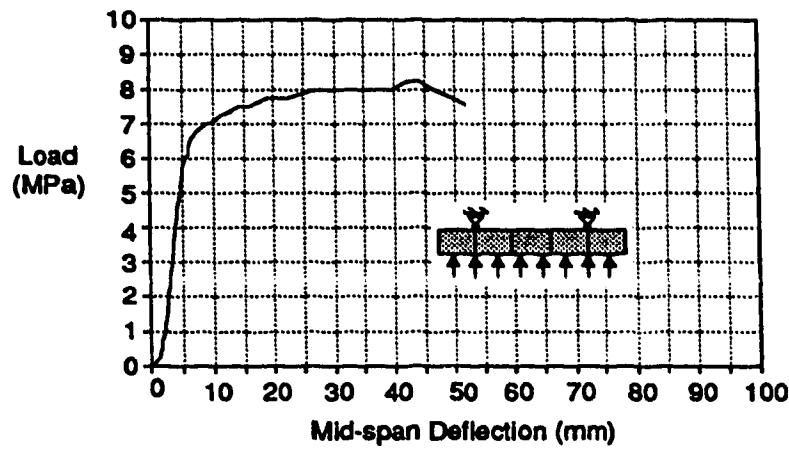


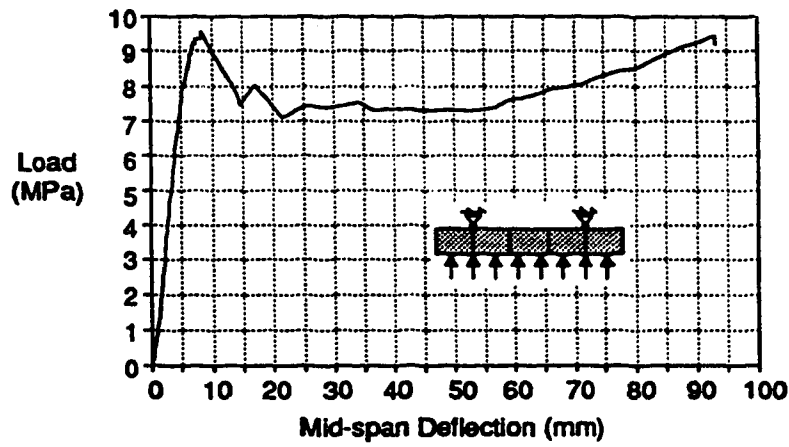
Figure 4.9 Typical Instrumentation for Slab Specimens



(a) Specimen CF-1

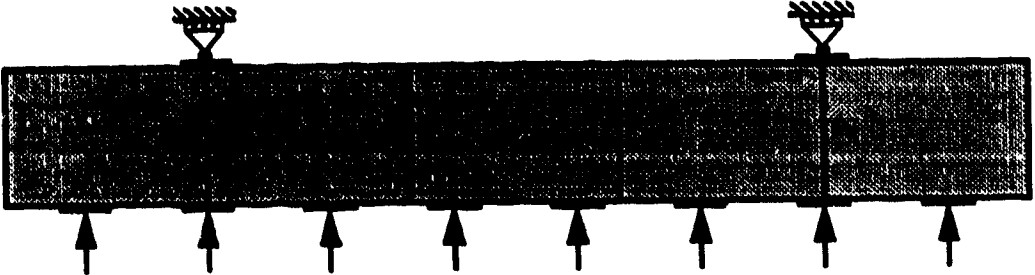


(b) Specimen CF-2

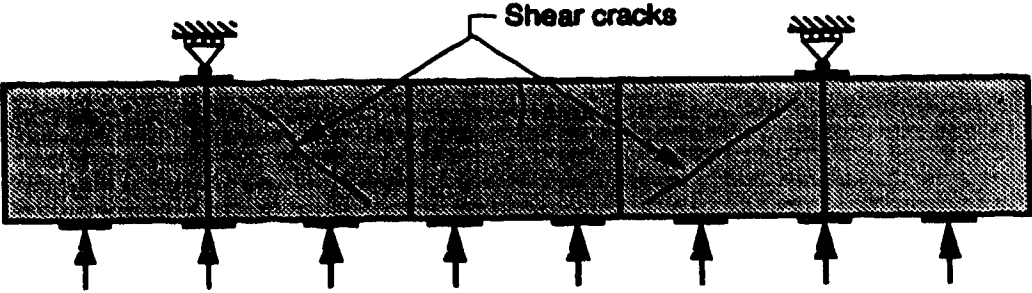


(c) Specimen CF-3

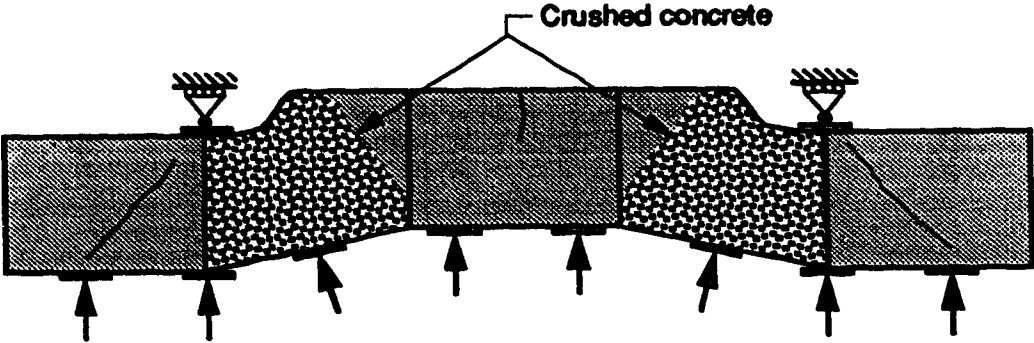
Figure 4.10 Load vs. Deflection Curves for CF-1, CF-2 and CF-3



(a) Load = 4.5 MPa



(b) Load = 6.0 MPa



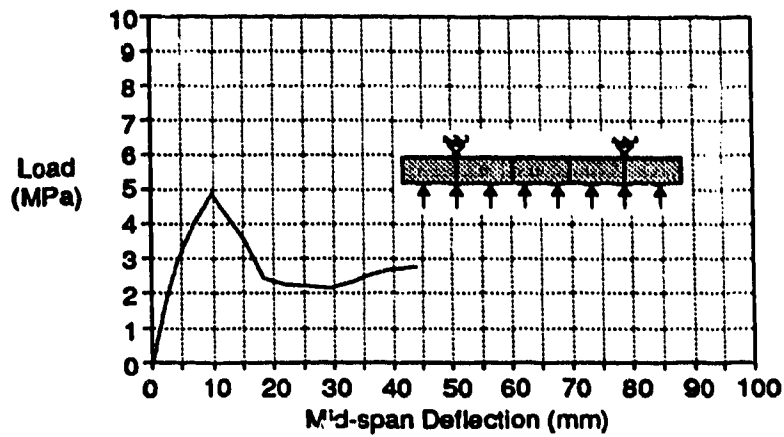
(c) Load = 9.4 MPa

Figure 4.11 Sketches of Specimen CF-3 Test

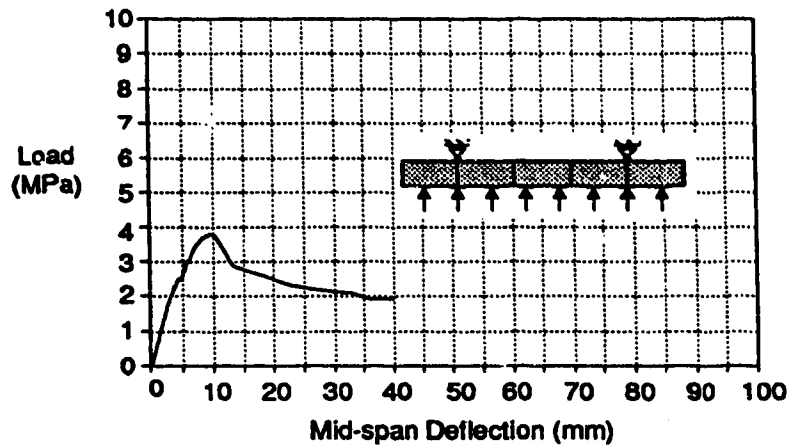


(e) After completion of test

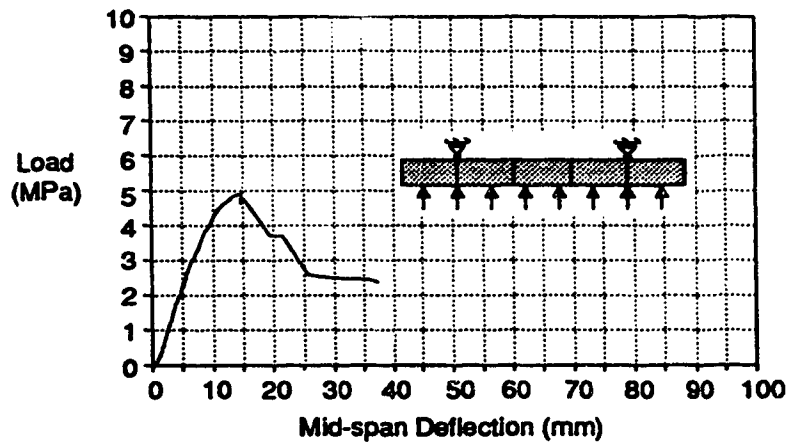
Figure 4.12 Photographs of Specimen Test CF-3



(a) Specimen CF-4

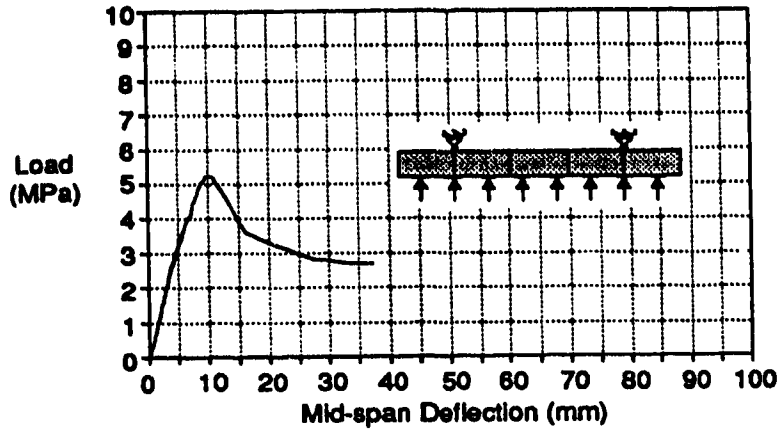


(b) Specimen CF-5

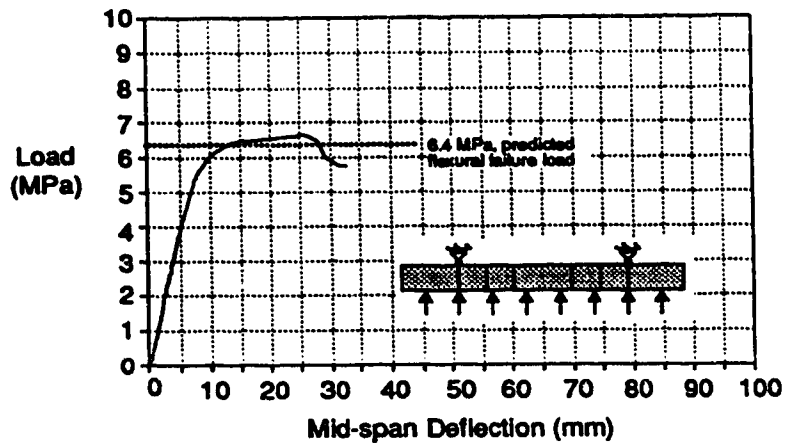


(c) Specimen CF-6

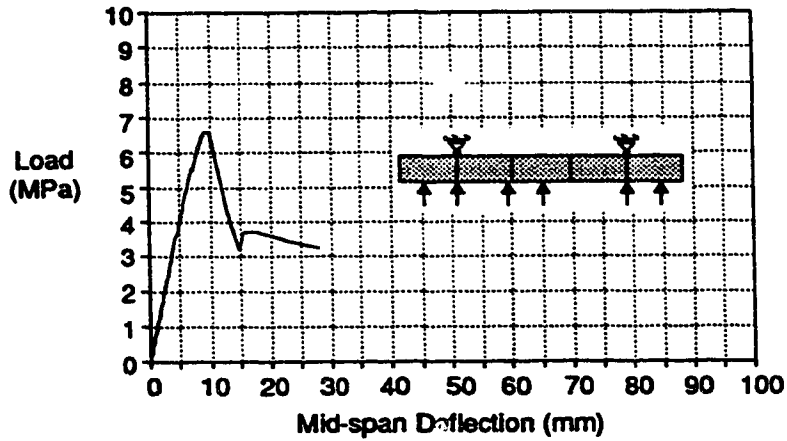
Figure 4.14 Load vs. Deflection Curves for CF-4 to CF-9



(d) Specimen CF-7

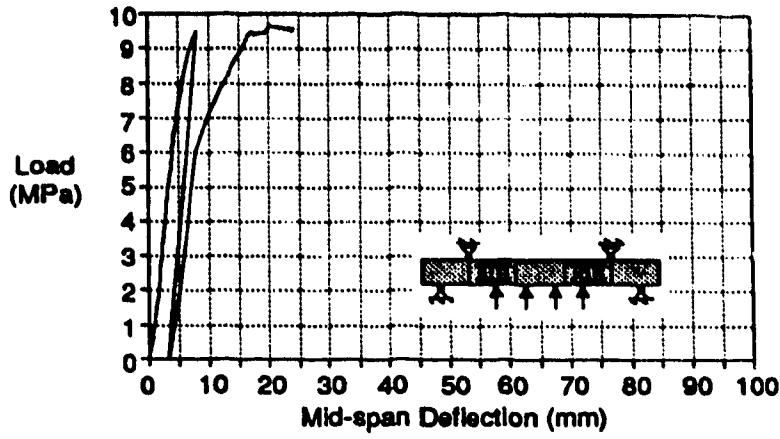


(e) Specimen CF-8

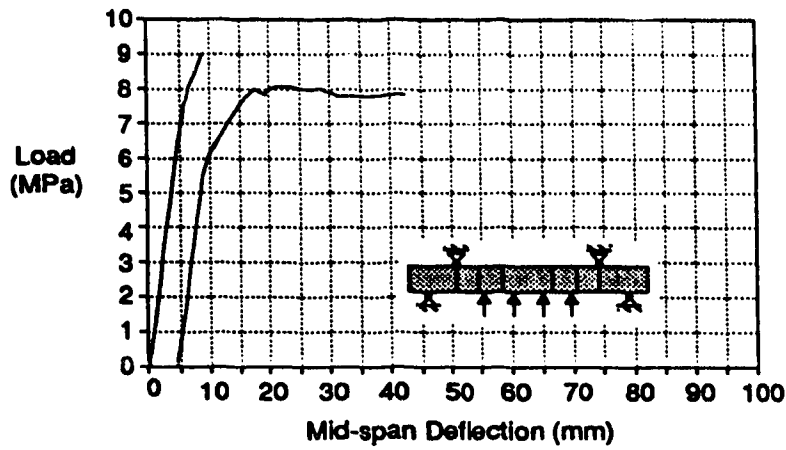


(f) Specimen CF-9

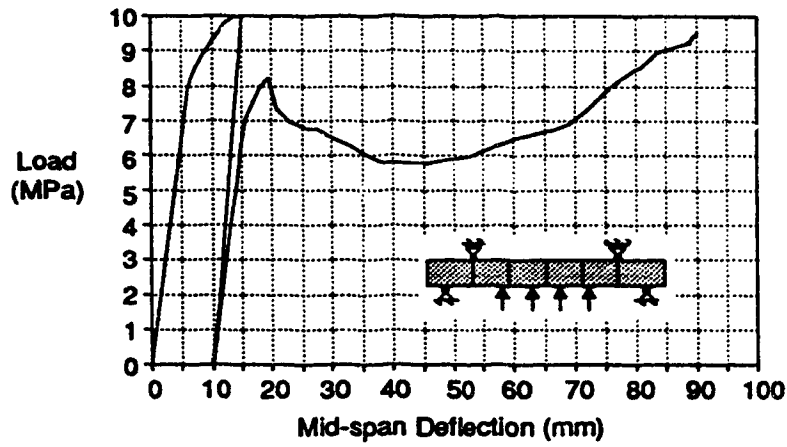
Figure 4.14 Load vs. Deflection Curves for CF-4 to CF-9



(a) Specimen CF-10



(b) Specimen CF-11



(c) Specimen CF-12

Figure 4.15 Load vs. Deflection Curves for CF-10 to CF-14

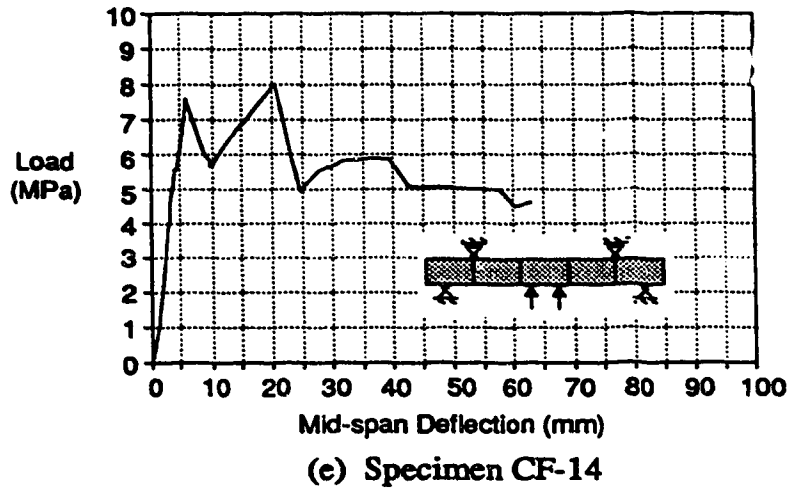
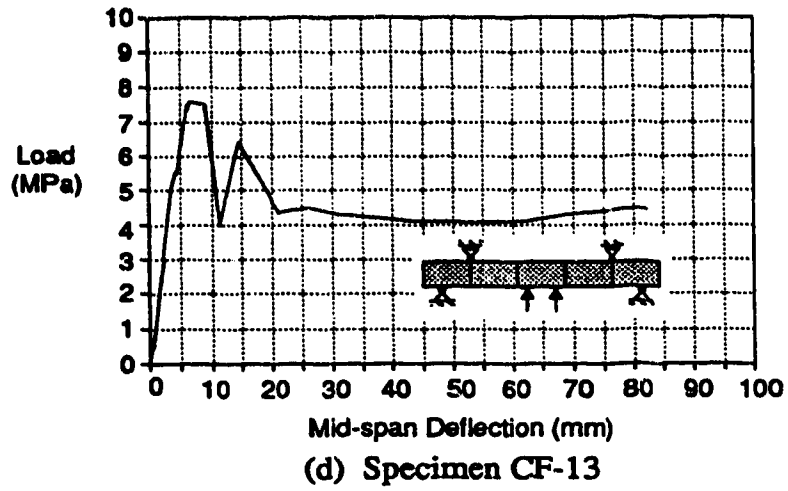
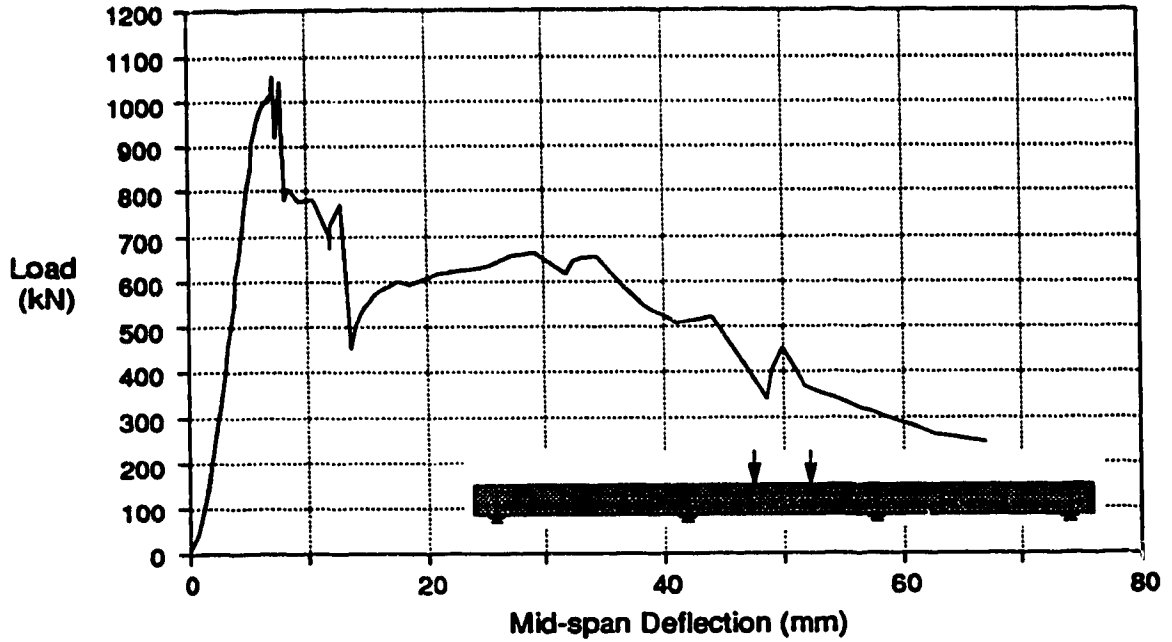
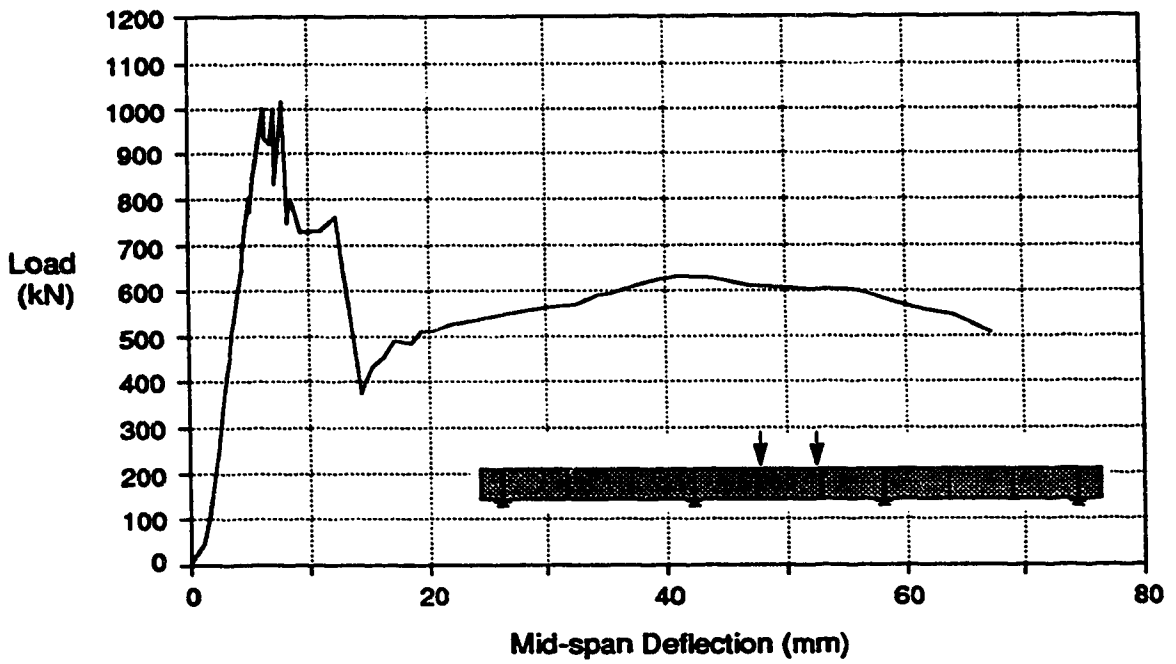


Figure 4.15 Load vs. Deflection Curves for CF-10 to CF-14

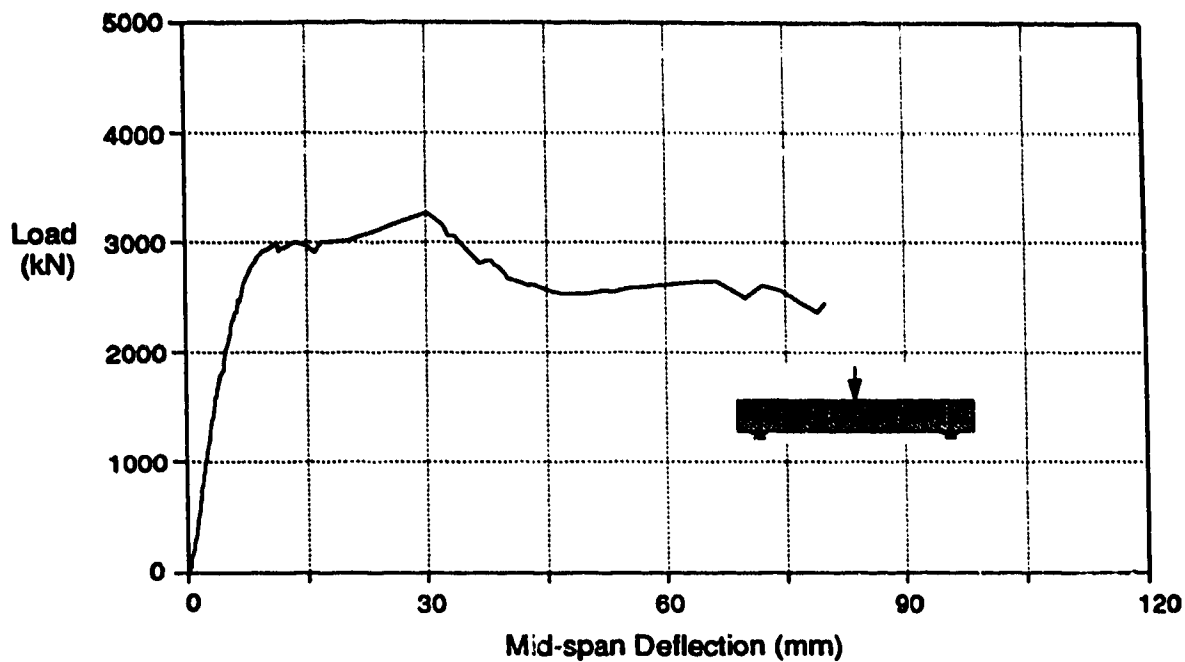


(a) Specimen B-1

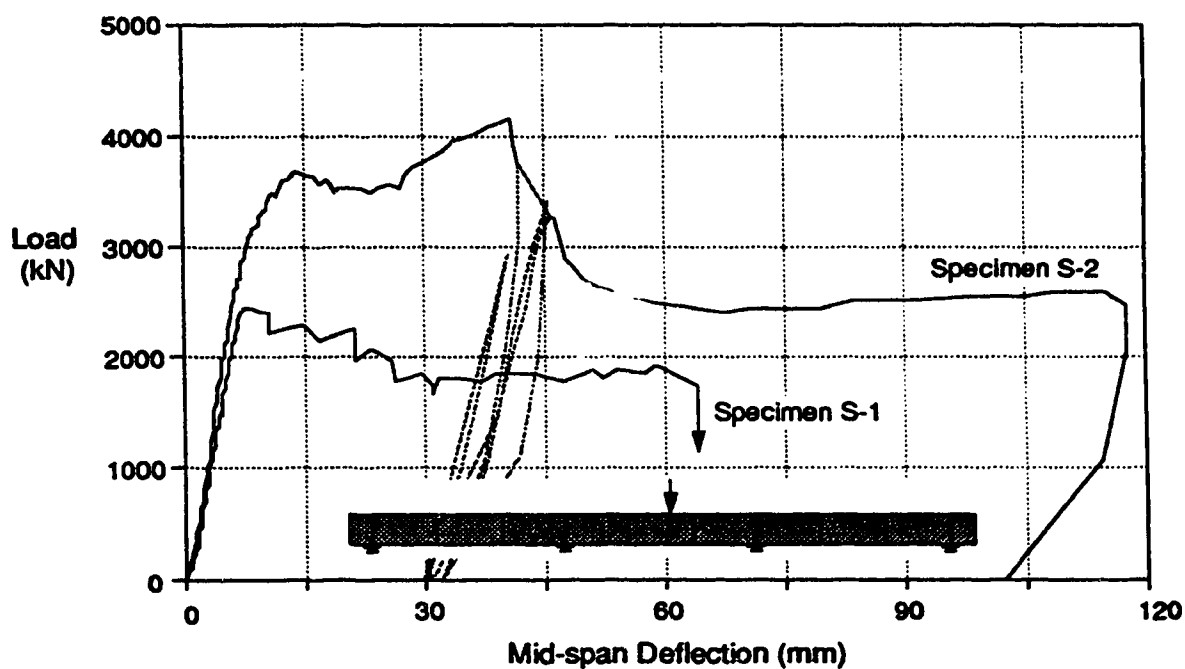


(b) Specimen B-2

Figure 4.18 Load vs. Deflection, Specimens B-1 and B-2



(a) Specimen SP-1



(b) Specimens S-1 and S-2

Figure 4.19 Load vs. Deflection, Specimens SP-1, S-1 and S-2

Testing Program

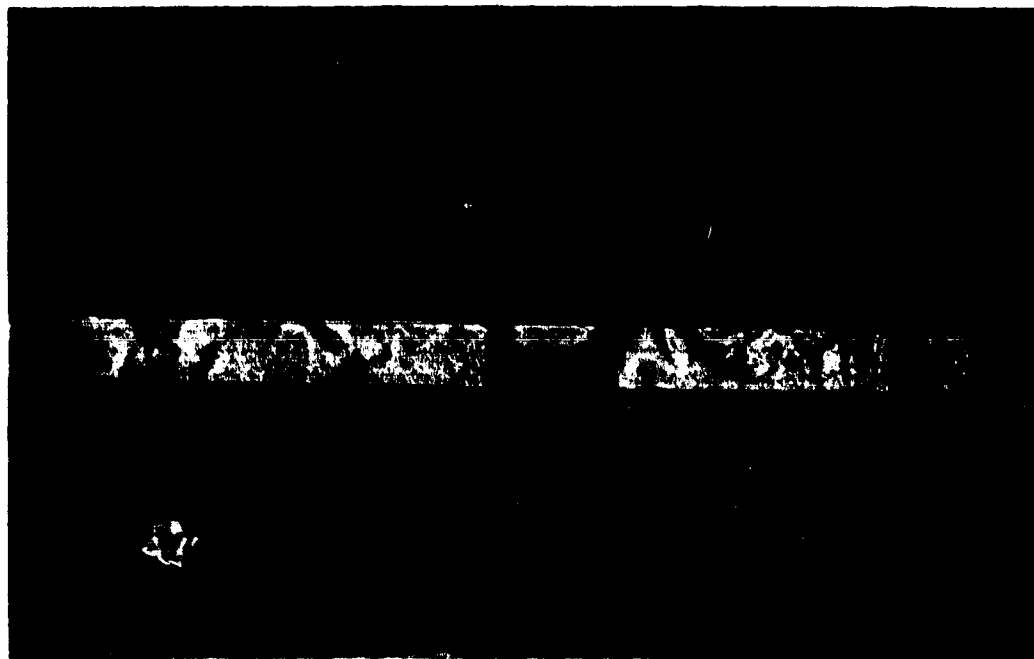


Figure 4.20 Specimen S-1 After Test

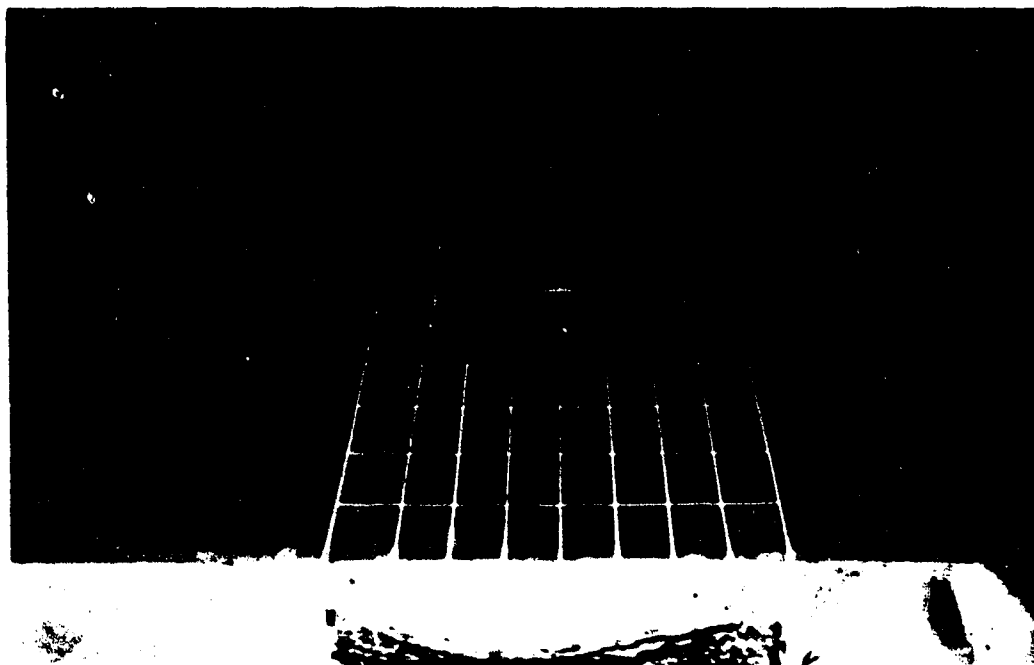


Figure 4.21 Specimen S-1: Close-up of "Punched" Area of Plate



Figure 4.22 Underside of Specimen S-1

(the painted "grid" indicates the centre third of the middle span, i.e. between the centre diaphragm web plates; the vertical white bands on either side, mark the inner two supports)



Figure 4.25 Specimen S-2: Close-up of Dented Area of Plate

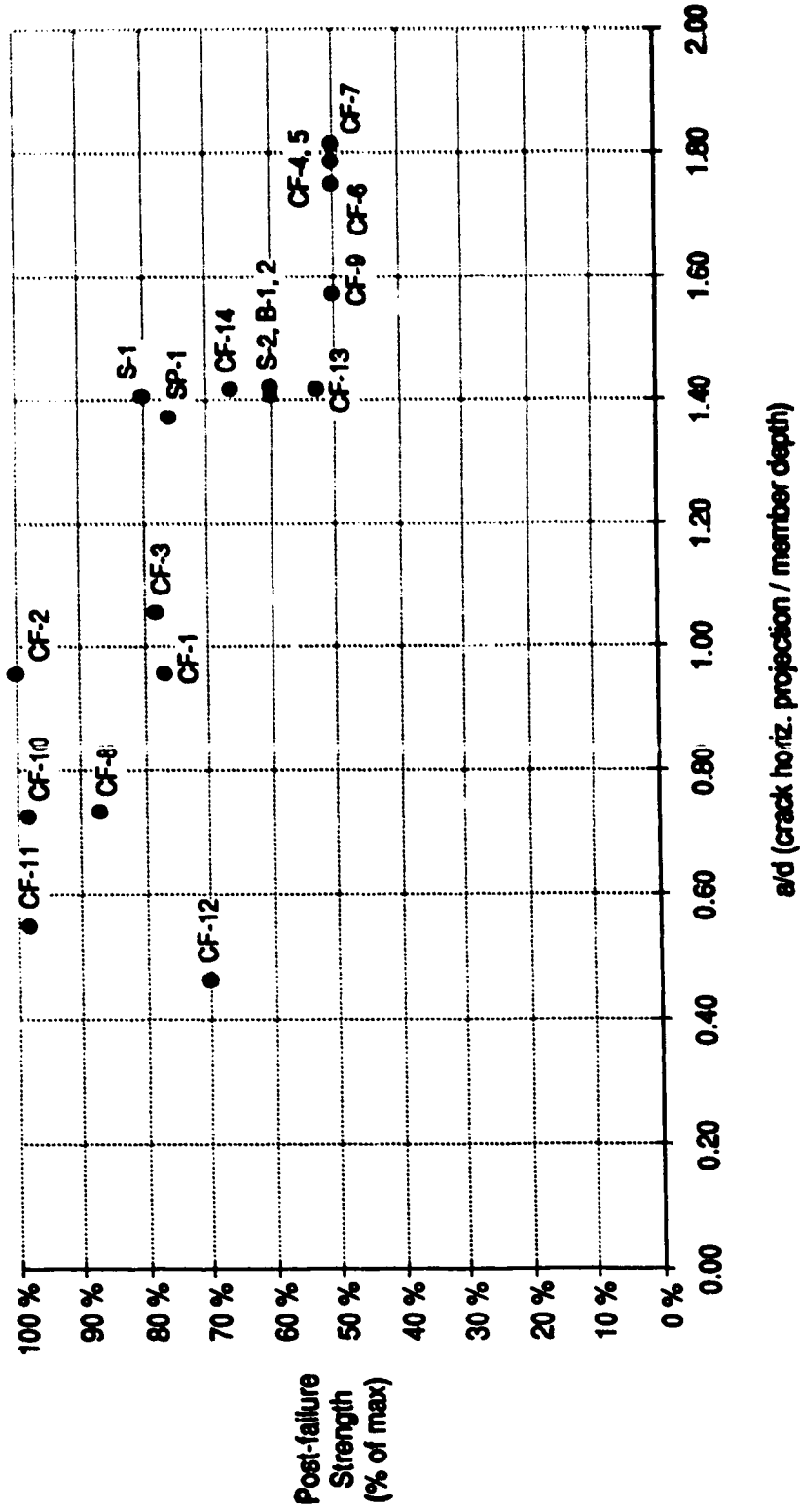


Figure 4.26 Correlation Between Post-Failure Strength and (a/d) Ratio

5.0 ULTIMATE STRENGTH CALCULATION METHODS

The rational methods used to determine the ultimate strength of composite walls are essentially the same as those used for reinforced concrete beams and slabs. This is not surprising since these methods are based on equilibrium and material strength concepts and should therefore be valid for members which are really not so very different from reinforced concrete members. On the other hand, the existing empirical methods of reinforced concrete design are generally not applicable for use with composite wall members. Again this is not surprising, since empirical methods are sensitive to member details and structural application. Any empirical methods which are considered for use must be developed experimentally for the particular member details being considered.

This chapter considers three basic methods for determining ultimate strength and makes recommendations advising where each should be used. The three basic methods are:

1. Traditional Methods:

Plane Section Method for Flexure - A method which assumes a linear strain distribution through the depth of the section, a non-linear stress-strain relation for concrete, an elastic perfectly plastic stress-strain relation for steel and requires the maintenance of equilibrium;

Empirical Method for Shear - A method which assumes the shear capacity is made up of a concrete contribution, which is computed by an empirical equation, and a shear reinforcement contribution;

2. Lower Bound Plasticity Methods:

Those plasticity methods which do not require strain compatibility, but which do require the maintenance of equilibrium by assuming some statically admissible stress distribution within the member which nowhere exceeds the strength of the material and which assumes sufficient material ductility such that the assumed stress field can be achieved; and

3. Upper Bound Plasticity Methods:

These are plasticity methods which do not require strain compatibility, but which do require the maintenance of equilibrium during failure by some kinematically admissible failure mechanism, and which assume that the external work done during failure equals the internal work expended, as calculated by a plastic failure theory.

The equations presented in this chapter will contain material performance factors ϕ_c and ϕ_s , in accordance with the limit states design method used by Canadian codes. The material performance factors deemed appropriate for use are as follows:

1. For comparing predictions with test results:

$$\phi_c = 1.0$$

$$\phi_s = 1.0$$

2. For use in design:

$$\phi_c = 0.60 \quad \text{for } f_c \leq 40 \text{ MPa}$$

$$\phi_c = 0.67 \quad \text{for } f_c > 40 \text{ MPa}$$

$$\phi_s = 0.90$$

These are the same values given in CSA Preliminary Standard S474.

5.1 Traditional Methods

5.1.1 Plane Section Method for Flexure

The plane section method is used in the design of reinforced concrete for flexure and axial loads (CSA Standard A23.3, 1984). It assumes the following:

1. The internal distribution of stress satisfies the applicable conditions of equilibrium.
2. The strain distribution through the depth of the member is linear and is directly proportional to the distance from the neutral axis; i.e. plane sections remain plane.

3. Strain compatibility is maintained between the concrete and the reinforcing steel.
4. The maximum usable strain at the extreme concrete compression fibre is equal to 0.003.
5. The compressive stress/strain curve of the concrete may be parabolic, trapezoidal or any other shape that results in correct strength predictions. It is normally assumed to take the shape of the familiar "equivalent rectangular stress distribution".
6. The tensile strength of concrete is neglected.
7. The stress/strain response for the reinforcement is based on the stress-strain curve and is normally assumed to be linear elastic, perfectly plastic.

Figure 5.1 shows the fully plastified internal stress and force distributions in a composite wall section which result from the plane section method assuming strains large enough to reach the full plastic moment capacity (theoretically this requires an infinite strain). The three cases shown are discussed in Sections 5.1.1.1 to 5.1.1.3.

In order for this method to be valid for composite walls, it must be demonstrated that all of the above assumptions are valid. There are two situations where some of these assumptions are not valid and the method can therefore not be used: 1) Deep flexural members, where significant arching action tends to produce non-linear variations in strain through the depth of the cross section; and 2) Members which allow slip between the steel plates and the concrete core and thereby render the assumption of compatibility invalid. For these two situations, one of the two plasticity design methods must be used. Figure 5.2(a) illustrates some composite wall types for which the plane section method is not valid; Figure 5.2(b) shows some where it may be valid. It should be noted that even for the wall types shown in Figure 5.2(a), at particular critical sections, the stress distributions shown in Figure 5.1 can be constructed using either the upper or the lower bound plasticity methods, as discussed in Section 5.2.

As noted in Figure 5.2(a), the span-to-depth ratios for which deep beam behaviour should be assumed are not well defined. It is likely, that for the extremely large ice forces that a composite ice-resisting wall must resist, member depth will always be such that deep beam behaviour should be assumed. Therefore it is recommended that one of the two plasticity methods should be used.

For flexural design using the plane section method, there are three cases that can be considered; the case where the top plate is thicker than the bottom plate ($t' > t$), the case where the top plate is thinner than the bottom plate ($t' < t$) and the case where the plate thicknesses are equal ($t' = t$). The experimental work in this research program only dealt with the last case, however, equations for all three cases are presented here. In each case the derivation is of the case of pure flexure (zero axial force).

5.1.1.1 Case 1, $t' > t$

This case is illustrated in Figure 5.1(a). Because the top plate is thicker than the bottom plate, and because the concrete is assumed to take no tension, the plastic neutral axis will be in the top plate. The depth of the compressive stress block in the upper steel plate, a , is found by summing horizontal forces, i.e. $\Sigma F_h = 0$. The flexural design equation can then be derived by summing moments about the centroid of the tension steel. The derivation is as follows:

$$\Sigma F_h = 0 \quad \therefore \quad C - T' = T$$

$$\left(\frac{a}{t'}\right)A'_s\phi_s f_y - \left(1 - \frac{a}{t'}\right)A'_s\phi_s f_y - A_s\phi_s f_y = 0$$

$$\therefore \quad a = (A'_s + A_s) \frac{t}{2A'_s}$$

$$\text{since } A'_s = t'b \text{ and } A_s = tb$$

$$\therefore \quad a = \frac{1}{2} \left[t + \frac{t^2}{t'} \right]$$

[5.1]

$$\begin{aligned}\Sigma M_T &= M_u \quad \therefore \quad M_u = C \frac{f'_c}{2} + T \left[h - \frac{1}{4t} (t^2 + 3tt' + 2t'^2) \right] \\ &= \phi_s f_y \left[\frac{a A'_s}{2} + A_s h - \frac{A_s}{4t} (t^2 + 3tt' + 2t'^2) \right]\end{aligned}$$

with further reduction the equations for M_u becomes

$$M_u = \phi_s f_y \left[\frac{a A'_s}{2} + A_s h - \frac{A_s}{4t} (t^2 + 3tt' + 2t'^2) \right] \quad [5.2]$$

$$\begin{aligned}\text{where} \quad A_s &= bt \\ A'_s &= bt'\end{aligned}$$

Substituting for a , A_s and A'_s results in the following equation for ultimate flexural capacity:

$$M_u = \phi_s f_y b \left[ht - t't - 2t^2 - \frac{t^3}{t'} \right] \quad [5.3]$$

5.1.1.2 Case 2, $t' < t$

This case is illustrated in Figure 5.1(b). Because the top plate is thinner than the bottom plate, and because the concrete is assumed to take compression, but no tension, the plastic neutral axis will be in the concrete. The depth of the compressive stress block, a , is found by summing horizontal forces, i.e. $\Sigma F_h = 0$. The flexural design equation can then be derived by summing moments about the centroid of the tension steel. The equations are derived in the same way as those above and are as follows:

$$a = \frac{\phi_s f_y}{0.85 \phi_c f'_c} (t - t') \quad [5.4]$$

$$M_u = 0.85 \phi_c f'_c a b \left(d - \frac{t + a}{2} \right) + A'_s \phi_s f_y d \quad [5.5]$$

$$\text{where} \quad d = h - \left[\frac{t + t'}{2} \right]$$

Substituting for a , A_s and A'_s , and defining a new variable, ϕ , results in the following equation for ultimate flexural capacity:

$$M_u = \phi_s f_y b \left[dt - \frac{1}{0.85} \frac{\phi(t-t')^2 + (t-t') t'}{2} \right] \quad [5.6]$$

$$\text{where} \quad \phi = \frac{\phi_s f_y}{\phi_c f_c}$$

As stated earlier, this solution requires that strain compatibility be maintained between the top plate and the concrete, both of which are in compression.

5.1.1.3 Case 3, $t' = t$

For the special case where $t = t'$, the flexural equations for both of the first two cases (equations 5.2, 5.3, 5.5 and 5.6) reduce to the following:

$$M_u = A_s \phi_s f_y d \quad [5.7]$$

$$\text{where} \quad A_s = bt = A'_s = bt'$$

$$d = h - t$$

Some measure of the accuracy of this equation can be determined by considering the peak load carried by Specimen CF-2 (the only specimen to ultimately fail in flexure) and using F_u (390 MPa) rather than F_y (265 MPa) in the calculation. This is justified since the ultimate load was reached for this specimen when the top (tension) plate fractured. In accordance with this, the predicted capacity is as follows:

$$\begin{aligned} M_u &= b t f_y d \\ &= \frac{375 \cdot 6.35 \cdot 390 \cdot 244}{1 \times 10^6} = 227 \text{ kN}\cdot\text{m} \end{aligned}$$

The actual ultimate moment at failure for this specimen as determined from simple statics was:

$$M_u = 224 \text{ kN}\cdot\text{m}$$

The agreement is within a few percent.

5.1.2 Empirical Method for Shear

5.1.2.1 ACI and CSA Equations for Reinforced Concrete

The current American concrete design code (ACI Standard 318-83) and the previous Canadian concrete design code (CSA Standard A23.3-M77) both handle design for shear in the same way. The method is essentially an empirical one, which assumes the following:

1. In members without shear reinforcement, the shear capacity, V_c , is provided by the concrete web.
2. In members with shear reinforcement, the shear capacity is provided by contributions from two parts: V_c , the capacity of the concrete web; and V_s , the capacity of the shear reinforcement.
3. In both the above cases, V_c is taken equal to the shear causing significant inclined cracking and is calculated from one of a number of semi-empirical equations. These equations are intended to include the effects of aggregate interlock, dowel action and shear carried by the concrete compression zone (ACI-ASCE Committee 425, 1973).
4. The shear capacity, V_s , is calculated assuming a shear crack through the depth of the member at an angle of 45° , and is taken equal to the vertical force required to yield the shear reinforcing which crosses this crack.

The empirical code equations for the shear capacity provided by the concrete are as follows:

$$V_c = 0.17\sqrt{f'_c}bd \quad [5.8]$$

or

$$V_c = (0.16\sqrt{f'_c} + 17\rho_w \frac{V_{ud}}{M_{uv}})bd \quad [5.9]$$

$$\leq 0.3\sqrt{f'_c}bd$$

where the ratio V_{ud}/M_{uv} shall not be greater than 1.0.

Special provisions are made for deep flexural members (defined for shear as members with span-to-depth ratios less than 5) as follows:

$$V_c = \text{Eqn. [5.8]} \quad [5.10]$$

or

$$V_c = (3.5 - 2.5 \frac{M_{uv}}{V_{ud}}) \times \text{Eqn. 5.9} \quad [5.11]$$

$$\leq 0.5\sqrt{f'_c}bd$$

where the first term in Eqn. 5.11 shall not exceed 2.5.

Other clauses dictate where the critical sections should be taken. This affects the calculations of both the shear capacity and the shear to be resisted.

These equations were based on research for reinforced concrete beams conducted prior to 1970. They have been used for many years in the design of reinforced concrete beam elements although they tend to be conservative, especially for deep members.

None of these empirical equations were found to be applicable for the types of composite members which have been considered to date, either in this research program or in the published Japanese papers.

5.1.2.2 Empirical Equations for Composite Walls

Since the empirical code equations for reinforced concrete appeared to be inappropriate for use with composite members, it was decided to develop an

empirical equation specifically for composite members of the type developed in this project. The empirical equations were derived applying the techniques of dimensional analysis and statistical regression analysis (Zsutty 1968) to the data from this research work. Following Zsutty's lead, the empirical equation is assumed to be of the form:

$$\frac{V_c}{bd} = \frac{(\text{Const.})(f_c)^x(\rho)^y}{\left(\frac{a}{d}\right)^z}$$

The purpose of the regression analysis is to determine the value of the constant and the exponents x , y and z . These values are determined by taking the natural logarithm of both sides of this equation

$$\ln\left(\frac{V_c}{bd}\right) = (\text{Const.}) + x\ln(f_c) + y\ln(\rho) - z\ln\left(\frac{a}{d}\right)$$

and conducting a multiple linear regression analysis.

Two sets of regression analyses were conducted using the computer software package Lotus 1-2-3, which has multiple linear regression capabilities. Only data from twelve of the first fourteen specimens (CF-1 to CF-14) were used. Specimens CF-2 and CF-10 were excluded, since CF-2 was a flexural failure and CF-10 contained shear reinforcing steel. Data and results from the two regression analyses are given in Tables 5.1 and 5.2.

In the first analysis, an empirical equation was derived using a value for "a", the shear span, defined as the horizontal distance from the centre of a reaction point to the centre of a load point, or the centre of the nearest diaphragm plate, whichever was closer. This centre-to-centre definition was used initially as it appeared to be consistent with that assumed by Zsutty. The resulting empirical equation, including now a material factor for concrete, is as follows:

$$V_c = \frac{3.39\phi_c f_c^{0.8} bd\rho^{0.54}}{(a/d)^{1.29}} \quad [5.12a]$$

The equation can be simplified, with a negligible loss in accuracy, as follows:

$$V_c = \frac{1.35\phi_c f_c b d \sqrt{\rho}}{(a/d)^{1.3}} \quad [5.12b]$$

where f_c is in MPa.

The second analysis used a definition for “a” as the clear distance from the edge of a reaction plate to the edge of a load plate, or the centre of the nearest diaphragm plate, whichever was closer. This definition is consistent with that used in the tables in Chapter 4, the plasticity solutions in Section 5.2, and throughout this thesis. In this case the resulting empirical equation is as follows:

$$V_c = \frac{1.20\phi_c f_c^{0.92} b d \rho^{0.50}}{(a/d)^{0.84}} \quad [5.13a]$$

The equation can be simplified, with a negligible loss in accuracy, as follows:

$$V_c = \frac{0.87\phi_c f_c b d \sqrt{\rho}}{(a/d)^{0.8}} \quad [5.13b]$$

This is the equation which is suggested for design purposes and is referenced throughout the rest of the thesis. A plot of this equation is shown in Figure 5.3 and the accuracy of this equation is shown in Figure 5.4, where it is compared to test results. It is also compared to test results in Table 5.3.

Equation 5.13b is used to calculate the concrete contribution to shear capacity of a member which fails along a diagonal crack with a horizontal projection, “a”. It can be used for design, but should not be used for members that differ significantly from those for which it was developed (composite members with transverse webs), nor should it be used outside the range of parameters studied in this work ($35 \text{ MPa} \leq f_c \leq 65 \text{ MPa}$; $0.5 \leq a/d \leq 2.0$).

It is interesting to note the similarity between this equation and those developed by Zsutty (1968, 1971). Zsutty's equations (metric form) are as follows:

$$V_c = \frac{2.17bd(f'_c\rho)^{0.33}}{(a/d)^{0.33}} \quad \text{for } a/d > 2.5 \quad [5.14]$$

$$V_c = \frac{5.43bd(f'_c\rho)^{0.33}}{(a/d)^{1.33}} \quad \text{for } a/d < 2.5 \quad [5.15]$$

A comparison between equation 5.13b and Zsutty's equations is shown in Figure 5.5 where they are compared to test results. In Zsutty's equations, "a", is the distance from the load to the support in a simple beam.

Although the equation itself is empirical, it can be used in a rational design process. Figure 5.6 shows this equation with a ϕ_c factor equal to 0.67 included. This value of ϕ_c is used in CSA Preliminary Standard S474 for high strength concrete.

5.2 Plasticity Methods

"Limit-analysis" techniques, based on the upper and lower bound theorems of plasticity, have been used successfully for a great number of years in the analysis and design of structural steel and reinforced concrete members. The basic tenets of plastic theory, including the upper and lower bound theorems, are given in detail in a number of references (Chen 1982, Nielsen 1984). The plasticity methods were described in simple terms at the beginning of Chapter 5.

Early applications of plasticity to reinforced concrete beams and slabs consisted of situations where the strength was governed by the yielding of the flexural reinforcement (e.g. yield-line and strip methods for slabs). In situations where failure in the concrete governs the strength, plastic theory is more difficult to apply, since concrete is not a perfectly plastic material, but exhibits significant strain softening. Even so, during the last decade plastic theory has been successfully used in such situations, most notably for

determining shear capacity in reinforced concrete beams (Nielsen and Braestrup, 1978; Collins and Mitchell, 1980; Chen 1982; and Nielsen 1984). Design codes have also recognized the validity of both upper and lower bound methods for reinforced concrete (CEB-FIP 1978, CSA A23.3-M84, 1984). In addition, the new Canadian offshore structures code, which contains the requirements for composite member design (CAN/CSA-S473-92, Clause 13), is being written so that either of the two plasticity methods will be acceptable provided they have been experimentally verified. The work contained in this thesis has contributed significantly to the development of the requirements contained in Clause 13 of S473. The standard is available from the Canadian Standards Association.

Figures 5.7 to 5.9 demonstrate a number of applications of plastic, limit-analysis solutions.

5.2.1 Lower Bound Plasticity Method

5.2.1.1 Previous Experience

Figure 5.7 shows plastic "truss" models for designing reinforced concrete beams. This is the method specified for use by the Canadian concrete building design code (CSA CAN3-A23.3-M84, 1984) and by the new Canadian offshore structures code (CSA Standard S474), for the design of "deep" reinforced concrete members. Such models have been suggested by a number of authors, including Rogowsky and MacGregor (1986), Marti (1985), and Schlaich et al. (1987), as well as those mentioned earlier.

The type of composite member being considered in this research is analogous to a reinforced concrete beam, with the reinforcing moved to the exterior, and with shear reinforcement at discrete locations, rather than distributed. While there is no bond per se between the steel and the concrete, the mechanical interlock of the steel walls and diaphragms with the concrete infill allows forces to be transferred from concrete to steel. It is therefore reasonable to apply this same plastic "truss" design approach to a composite wall. There are problems, however, in applying the truss model (or strut-and-tie model) methods given in CSA Standard A23.3, Clause 11.4.7. The main problems are as follows:

1. In determining the capacity of the diagonal struts (which is key to determining the shear capacity), it is assumed that the tensile strains in the concrete are compatible with the tensile strains in the reinforcing steel. This is a fair assumption for reinforced concrete, but not for the type of composite member being considered here. These composite members allow "slip" between the steel plates and the concrete infill, and thus the compatible strain assumption cannot be made.
2. "Nodal zones" in the strut-and-tie models are dimensioned by assuming that the centroid of the reinforcing steel and the centroid of the nodal zone coincide. This is not so for a composite wall, since the plates are exterior to the member and, therefore, cannot be at the centroid of the node. This is an important consideration, since the nodal zone dimensioning plays a large role in determining the capacity of a plastic truss.

A review of the strut and tie model methods, indicates that the lower bound solution procedure is an excellent method for visualizing the flow of forces and for determining the reinforcing requirements (i.e. for determining the steel areas required to keep the plastic truss in equilibrium). It is more difficult, however, to use this method to obtain an accurate prediction of shear capacity, unless the shear capacity is governed by yielding of reinforcement (e.g. stirrups yielding), or the results are modified by an empirical factor. Even so, success has been reported by others in this regard (O'Flynn and MacGregor, 1987).

Because of these considerations, this research work suggests the use of strut and tie models for determining the reinforcing steel requirements; both plate steel, and where appropriate, steel studs and additional steel in the form of deformed reinforcing bars. This covers both the reinforcing requirements for flexure and for shear. This work also suggest the use of lower bound compression field theory to determine the shear capacity of a composite wall which contains additional shear reinforcement and for which the shear stress can be assumed to be uniformly distributed over the depth of the member. It does not consider lower

bound plasticity methods for determining the shear capacity of composite walls with plain concrete cores, nor for situations where the assumption of uniform shear stress is obviously invalid.

The basic approach is to take the existing lower bound plasticity methods for reinforced concrete (both strut and tie models and compression field theory) and adapt them for use with the type of composite wall elements developed in this research project.

5.2.1.2 Strut and Tie Truss Model for Flexure

Figure 5.10 shows a strut and tie model for Specimen CF-2. The model is constructed by assuming that the applied loads must be carried to the supports through uniaxial truss members carrying either tension or compression. The steel plates are allowed to carry either tension or compression; the concrete is only allowed to function in compression. Engineering judgment is required in constructing the truss, since in most cases there are a number of plausible configurations. In this case, the truss has been constructed so that the model is statically determinate. This has the advantage of not requiring assumptions to be made concerning the relative stiffnesses of the truss members. The stiffness of a steel truss member is easily determined since the cross-sectional area and modulus of elasticity of each steel plate is known to a high degree of accuracy. To determine the stiffness of a concrete compression strut, however, requires an assumption concerning the width of the member. This becomes difficult since the geometry of the nodal zones is not easily determined, as explained previously.

Once the truss has been constructed, the force in each of the truss members is determined from statics. Figure 5.10 shows the forces and strains determined from the truss model for Specimen CF-2. Also shown are the measured strains for this specimen. The strain in the upper plate tension tie is in close agreement with the calculated values. Actual strains in the bottom compression plate are less than the calculated value since the concrete adjacent to this plate shares some of the load. Actual strains in the web diaphragm plates are considerably less than the calculated values, likely because part of the load from the two centre load points arches

directly to the support. In any case, the stresses and strains predicted by the truss model are conservative from a design point of view.

For design, steel plates thicknesses (and yield strengths) are chosen by ensuring that the factored ultimate tensile capacity of each plate is equal to or greater than the calculated factored force. Considering the truss geometry, and assuming equal plate thickness both top and bottom, produces a flexural design equation identical to equation 5.7.

A second truss model, this time for Specimen CF-8, is shown in Figure 5.11. As noted in Section 4.4.1.2, this specimen developed a full flexural mechanism prior to finally failing in shear. Also shown in Figure 5.11 is the actual crack pattern in the specimen, as well as the load-deflection curve with the predicted flexural failure load indicated. The cracking pattern is consistent with the flow of forces indicated by the truss model, and the strength predictions are certainly within acceptable accuracy limits. Again, the tension plate stresses measured agreed well with those predicted by the truss model.

5.2.1.3 Compression Field Method for Shear

The general method for shear design of reinforced concrete beams given in Clause 11.4 in CSA Standard A23.3-M84 (CSA 1984) is based on the lower bound theory of plasticity. This section proposes using this method for composite walls with distributed shear reinforcement, like that contained in Specimen CF-10.

This method of design determines the resistance of members in shear "by satisfying applicable conditions of equilibrium and compatibility of strains and by using appropriate stress-strain relations for reinforcement and for diagonally cracked concrete" (CSA A23.3-M84). For a given concrete strength, cross sectional dimensions are chosen to ensure that the diagonally cracked concrete has sufficient capacity to resist the inclined compressive stresses. Areas of longitudinal and transverse reinforcement are chosen which are capable of equilibrating this field of diagonal compression.

The method assumes that stresses are uniformly distributed over the cross-sectional area of the member and that the direction of the principal

compressive stresses remains constant over the member depth. For composite walls with diaphragm plates as the only form of shear reinforcement, it is inappropriate to make this assumption, since slip is allowed between the exterior steel plates and the concrete core, and since there is no distributed shear reinforcement to provide a vertical reaction for the uniformly distributed inclined struts. This method, therefore, is applicable to only one of the specimens tested in this program; Specimen CF-10.

A review of the general method for shear design in reinforced concrete beams is given in Appendix B, along with the development of an ultimate strength design equation for composite members based on this method. The equation for ultimate shear capacity given there is as follows:

$$\frac{V_r}{bh} \max = \rho_v \phi_s f_y \sqrt{\frac{\sqrt{0.22 + \frac{1}{\omega_v} (680 \epsilon_x + 1.36)} - (1.14 + 340 \epsilon_x)}{340(\epsilon_x + 0.002)}} \quad [5.16]$$

where $\rho_v = \frac{A_v}{sb}$ [5.17]

and $\omega_v = \frac{\rho_v \phi_s f_y}{\phi_c f'_c}$ [5.18]

Figure 5.12 shows how this method is applied to predict the shear capacity of Specimen CF-10. This specimen contained additional shear reinforcement in the deformed reinforcing bars which were anchored to the steel face plates by overlapping with short headed studs which were fastened to the face plates. The area of shear steel provided by the deformed bars was 600 mm², at a longitudinal spacing of 48 mm. Since no tensile coupons were tested for the deformed bars a yield strength of 477 MPa is assumed in the calculations. This is the mean value determined for Grade 400, 10 M bars (Nessim, et.al. 1992). Using equation 5.16, and assuming a mid-depth concrete tensile strain (ϵ_x) of zero (since slip between the

steel plate and concrete can occur), an ultimate shear capacity of 1798 kN is determined. This compares remarkably well with the experimental value of 1816 kN.

5.2.2 Upper Bound Plasticity (UBP) Method

The UBP method is an upper bound plasticity approach (an energy method) which considers the internal and external work expended when the member fails in accordance with some geometrically admissible displacement field. This method is well known for the flexural design of reinforced concrete slabs, where it is called the "yield line method". More recently, it has been applied to cases of shear in plain and reinforced concrete by Nielsen et al. (1978, 1984).

The philosophical problem with using upper bound plasticity methods for materials like concrete is that the kinematically admissible failure mechanism involves yielding, which is not a property exhibited by plain concrete. None-the-less, Nielsen's research group at The Technical University of Denmark has been successful in applying upper bound techniques to shear in plain and reinforced concrete. There has not yet been general acceptance of these methods, however, mainly because the theoretical results have to be modified in an empirical manner in order to make them work. In the author's opinion, this does not detract from their usefulness, for two reasons: firstly, the design methods are far less empirical in nature than those used to date; and secondly, they can increase one's understanding of structural behaviour by forcing the designer to focus on the actual modes of failure.

Appendix C provides an overview of the upper bound plasticity methods developed by Nielsen for shear in reinforced concrete members. In the section which follows, Nielsen's method is briefly reviewed; this same basic method is then adapted for use in determining the shear capacity of composite members. The section following that considers the upper bound method for flexure in composite members. Shear and flexural are considered separately, since they are distinctly different mechanisms of failure.

5.2.2.1 Shear Failure Mechanism

As discussed in Appendix C, Nielsen (1984) developed upper bound solutions for shear in plane and reinforced concrete by constructing work equations

which equate the external work being done by the load to the internal work being dissipated in the member. To achieve this, he had to derive expressions for energy dissipation in the constituent materials; concrete and steel. The equation given for the energy which is dissipated along a shear failure plane in plain concrete is:

$$W_L = \frac{1}{2} \nu f'_c u b (1 - \sin \alpha) \quad [5.19]$$

where

- W_{Ic} = internal work dissipated per unit length
- f'_c = uniaxial compressive strength of concrete
- u = displacement
- b = thickness of the element
- α = angle between the yield line and the displacement vector
- ν = efficiency factor used to modify concrete strength
($\nu f'_c$ is referred to as the effective, or plastic, concrete strength)

Energy dissipation in reinforcing steel is based on the assumptions that bars are straight, material is rigid-plastic and bars are capable of carrying only axial stress. In addition, the normal assumption is made that the material yields when the axial stress reaches the uniaxial yield stress, F_y . The equation for the energy dissipated in a reinforcing bar crossing a yield line is given as follows:

$$W_L = -A_s F_y u \cos(\alpha + \beta) \quad [5.20]$$

where

- W_{Is} = internal work dissipated in the reinforcing steel bar
- A_s = area of reinforcing steel bar
- F_y = uniaxial tensile strength of steel
- u = displacement of one side of the yield line with respect to the other
- α = angle between the yield line and the displacement vector
- β = angle between the yield line and the reinforcing bar
- θ = angle between the displacement vector and the reinforcing bar

Using these expressions, upper bound solutions are developed for shear in reinforced concrete beams, both with, and without, additional shear reinforcement. In keeping with current practice, the equations shown here have material resistance factors included.

5.1.2.1.1 Beams Without Shear Reinforcement

For beams without shear reinforcement, the work equation derived in Appendix C is:

$$V \sin(\alpha + \beta) = bh\phi_c f_c' \left[\frac{v(1 - \sin \alpha)}{2 \sin \beta} - \Phi \cos(\alpha + \beta) \right] \quad [5.21]$$

where Φ is the mechanical degree of longitudinal reinforcement

$$\Phi = \frac{(A_s + A_s')}{bh} \frac{\phi_s F_y}{\phi_c f_c'} \quad [5.22]$$

The left hand side of equation 5.21 is the external work done by the load; the right hand side is the internal work dissipated by the concrete (first term inside the square brackets) and the longitudinal reinforcing steel (second term inside the square brackets). The lowest upper bound gives the following equations for the shear capacity:

$$V_r = \frac{bhv\phi_c f_c'}{2} \left[\sqrt{\left(\frac{a}{h}\right)^2 + \frac{4\Phi(v - \Phi)}{v^2}} - \frac{a}{h} \right] \quad \text{for } \Phi \leq v/2 \quad [5.23]$$

$$V_r = \frac{bhv\phi_c f_c'}{2} \left[\sqrt{\left(\frac{a}{h}\right)^2 + 1} - \frac{a}{h} \right] \quad \text{for } \Phi > v/2 \quad [5.24]$$

Expressions for the concrete efficiency factor, v , have been suggested by several different authors for reinforced concrete beams (Nielsen 1984; Rogowsky 1983). O'Flynn (1987) developed an efficiency factor for composite beams of a type similar to those developed here. In Table 5.3 two different efficiency factors

are used with equations 5.23 and 5.24 to calculate shear capacities for the specimens tested in this work. The factors used are shown below.

$$v = 0.95 \tag{5.25}$$

and

$$v = \frac{0.029}{\sqrt{\phi_c f_c}} \left[\frac{(200,000)k}{a} \sqrt{1+(a/d)^2} \right]^{0.6} \leq 1.0 \tag{5.26}$$

The choice of efficiency factor in equation 5.25 was made because the number is less than and close to 1.0, which seems reasonable, and it provides an average test/predicted ratio for all specimens of exactly 1.0. The expression in equation 5.26 was adapted from O'Flynn's expression for composite beams, but with a cut-off at 1.0 included. This also seems reasonable and produces good results both in terms of the test/predicted ratio average (1.0) and standard deviation (0.10).

5.2.2.1.2 Beams With Shear Reinforcement

For reinforced concrete beams with shear reinforcement, and referring now to Figure 5.13, the following work equation is given:

$$V \cdot u = \rho_v f_y b h \cot \beta \cdot u + \frac{1}{2} v f_c b (1 - \cos \beta) \frac{h}{\sin \beta} \cdot u \tag{5.27}$$

where $\rho_v = A_v/sb =$ shear reinforcement ratio
 $f_y =$ yield strength of the shear reinforcement

The first term on the right-hand side of the equation is the dissipation in the stirrups which cross the yield line; the second term is the dissipation in the concrete. Since the movement is vertical, the longitudinal reinforcement is assumed to do no work (the reinforcing steel is assumed to have no bending or shear capacity).

The solution for this equation, for the special case of $\tan \beta = h/a$ and including material resistance factors, is:

$$V_r = \frac{bhv\phi_c f_c'}{2} \left[\sqrt{\left(\frac{a}{h}\right)^2 + 1} - \frac{a}{h} + 2\psi \frac{a}{h} \right] \quad [5.28]$$

where ψ is the degree of shear reinforcement:

$$\psi = \rho_v \frac{\phi_s f_y}{v\phi_c f_c'} \quad [5.29]$$

A kinematically admissible failure mechanism for a composite beam or one-way slab is shown in Figure 5.14. It consists of a yield line running from the edge of the support plate to the intersection point of the diaphragm plate and the upper, exterior plate. The relative displacement rate vector v , which describes the relative movement across the yield surface, is inclined at an angle α to the yield line. The similarity between this failure mechanism and that shown for a reinforced concrete beam (see Appendix C) is obvious, resulting in equations 5.23, 5.24 and 5.28 being valid for composite wall members as well.

Figure 5.15 compares the predictions given by these equations (see Table 5.3) to the composite wall test results. It shows an accuracy comparable to that of the C-FER empirical equation (Figure 5.4), as indicated by comparing the standard deviations.

Since this method is an upper bound solution procedure, it should give an upper bound to the load carrying capacity. It is therefore important for design to know the correct failure mechanism. If the correct failure mechanism is chosen, it theoretically gives the exact solution; the wrong failure mechanism will give an unconservative prediction. Since there are relatively few possible failure modes to check, however, the procedure can be considered a viable design tool.

5.2.2.2 Flexural Failure Mechanism

Energy solutions for flexure in reinforced concrete slabs are well known and can be most easily demonstrated by the simple case of a fixed-ended beam (or one-way slab) developing a three-hinge mechanism. This method is directly applicable to composite wall analysis, and is developed in the this section.

The validity of this method depends on the ability of the member to undergo sufficient plastic deformation at the hinge locations so that all three plastic hinges can develop before failure occurs. The ability of a composite wall of the type tested in this research work (i.e. with diaphragm web plates) to achieve such a three-hinged mechanism was demonstrated in an extension to the work discussed here. Most of the specimens which were tested in this work were shear critical and failed in shear below their flexural capacities. This is of no consequence, provided that the shear failure is recognized to be the governing failure mode and that it is also sufficiently ductile.

In designing reinforced concrete beams, it is often assumed that there is insufficient plastic deformation capacity to allow a full three-hinge mechanism to develop. This is due to crushing of the compression zone at the first hinge, before subsequent hinges form. This appears to be avoided in this type of composite member because large tensile strains, which occur in the yielding reinforcement at the first hinge, are not transmitted to the concrete core, since slip is allowed at the concrete-steel interface between the diaphragm plates.

(Note: This allowance of slip may also increases the shear capacity of the member, since the concrete is not being forced to undergo strains compatible with those of the longitudinal reinforcement, which would otherwise cause cracks. This phenomenon of increased shear capacity was noticed by Leonhardt and Walther (1964) when comparing reinforced concrete beams with deformed and smooth reinforcing bars.)

The energy method can be used to determine the required flexural capacity of a continuous composite wall spanning in one direction and subjected to a uniformly distributed load. For this situation the moment which the wall must sustain at each of the hinges while developing a three-hinge mechanism is:

$$M_u = \frac{wL^2}{16} \quad [5.22]$$

Equations for other loading situations are easily developed.

In order to determine the flexural capacity of a composite wall in resisting this moment, one of the equations given in Section 5.1.1 can be used.

If this design method is to be used, there are two other factors which must be considered: 1) The possibility of plastic deformations occurring at service loads; and, 2) the effect of in-plane restraint caused by the surrounding structure.

The first of these considerations depends upon the service/ultimate load ratio and upon the acceptability of some plastic deformations at service load levels. If the service/ultimate load ratio is smaller than the ratio of yield moment to fully-plastic moment, then yielding will not be expected to occur at service load levels. If the opposite is true, then the frequency of this occurrence will have to be considered, along with the implications for the rest of the structure of some permanent deformations. It is possible that permanent, local deformations may be acceptable on a more frequent basis than the frequency of the occurrence of the factored ultimate design load.

The second consideration is the effect of in-plane restraint. The effect is normally a beneficial one, with respect to flexural capacity, and ignoring it is conservative. It must be recognized, however, that the increase in flexural capacity, caused by the in-plane restraint, may change the mode of failure to one of shear, and it is therefore insufficient to determine the ductility of a system based only on a flexural failure mode; the shear failure mode must also be a ductile one. If a global analysis is used to determine the amount of in-plane restraint which can be counted

on in a particular structure, this can be used to decrease the size of the exterior steel plates, since they provide the flexural strength.

5.3 Recommended Ultimate Strength Calculation Methods

In the author's opinion, no one design approach is entirely suitable for all of the components in the wall; each of the methods discussed in the previous sections has its strengths and weaknesses.

The lower bound plasticity approach given in Section 5.2.1 is well suited for determining the design forces in all of the steel components of the wall. It is recommended for the design of exterior plates, diaphragm plates, welds, and additional reinforcing (if required). The lower bound truss models are an excellent method for visualizing the flow of forces in the structure.

The upper bound plasticity approach given in Section 5.2.2 is recommended for determining the shear capacity of the wall. This method is well suited for considering all of the important mechanisms of shear failure which can occur in the concrete core and allows the determination of the critical failure mechanism.

The empirical equation for shear capacity given in Section 5.1.2.2 is relatively simple, but is only recommended for a composite wall with details which match those of the specimens tested in this research program (i.e. a configuration which uses diaphragm plates and meets the dimensional and material requirements set out in Section 6.2.2). Care must be taken in extending this equation outside the range of parameters from which it was developed (subsequent work has shown that the empirical equation may be unconservative for members with reinforcement ratios lower than 0.025).

Table 5.1 Linear Regression Analysis, Eqn. 5.12a

Specimen No.	Vu (kN)	fc (MPa)	fy (MPa)	l (mm)	w (mm)	h (mm)	L (mm)	b (mm)	s (mm)	a (mm)	d (mm)	sd	ln(Vu/d)	ln(Au/d)	ln(fc)
CF-1	604	58.0	265.0	6.35	6.35	250	1000	375	333	333	244	1.36	2.01	-3.05	4.08
CF-3	717	59.8	265.0	6.35	6.35	250	1000	375	333	333	244	1.36	2.06	-3.05	4.07
CF-4	551	53.5	371.0	12.00	6.35	250	1500	301	500	500	238	2.10	1.80	-2.84	3.86
CF-5	430	36.3	371.0	12.40	6.25	250	1500	301	500	500	238	2.10	1.56	-2.85	3.59
CF-6	552	57.5	352.0	10.00	6.25	250	1500	301	500	500	243	2.06	1.79	-3.19	4.05
CF-7	582	58.4	347.0	16.10	6.45	250	1500	301	500	500	234	2.14	1.89	-2.88	4.07
CF-8	1498	59.5	371.0	12.40	6.20	250	1500	301	250	250	238	1.05	2.80	-2.95	4.09
CF-9	691	61.0	371.0	12.50	6.35	250	1500	301	500	450	238	1.89	2.29	-2.85	4.11
CF-11	1514	58.2	368.0	9.54	6.35	250	1280	375	208	208	241	0.86	2.82	-3.23	4.08
CF-12	1544	56.6	368.0	9.54	6.35	250	1250	375	313	250	241	1.04	2.84	-3.23	4.04
CF-13	712	56.0	368.0	9.54	6.35	250	1250	375	417	417	241	1.73	2.06	-3.23	4.02
CF-14	745	60.0	368.0	9.54	6.35	250	1250	375	417	417	241	1.73	2.11	-3.23	4.09

Regression Output:

Constant	1.22	variable constant
Std Err of Y Est	0.13	const. 2.39
R Squared	0.94	fc 0.80
No. of Observations	12	Au/d 0.54
Degrees of Freedom	8	sd 1.29

$$V_u = \frac{3.39 \rho^{0.54} f_c^{0.80} b d}{(s/d)^{1.29}}$$

X Coefficient(s)	-1.29	0.54	0.80
Std Err of Coef.	0.14	0.15	0.29

Table 5.2 Linear Regression Analysis, Eqn. 5.13a

Specimen No.	Vu (kN)	fc (MPa)	fy (MPa)	t (mm)	w (mm)	h (mm)	L (mm)	b (mm)	s (mm)	e (mm)	d (mm)	AV	ln(Vu/d)	ln(e/d)	ln(Ae/d)	ln(f _c)
CF-1	604	58.0	265.0	6.35	6.35	250	1000	375	333	235	244	0.96	2.01	-0.04	-3.05	4.06
CF-3	717	58.8	265.0	6.35	6.35	250	1000	375	333	258	244	1.06	2.09	0.09	-3.05	4.07
CF-4	561	53.5	271.0	12.60	6.35	250	1500	361	500	425	236	1.79	1.80	0.59	-2.94	3.96
CF-5	430	36.3	271.0	12.40	6.25	250	1500	361	500	425	236	1.79	1.56	0.59	-2.95	3.59
CF-6	562	57.5	262.0	10.00	6.25	250	1500	361	500	425	243	1.75	1.79	0.59	-3.19	4.05
CF-7	592	58.4	247.0	16.10	6.45	250	1500	361	500	425	234	1.82	1.89	0.80	-2.88	4.07
CF-8	1496	59.5	271.0	12.40	6.20	250	1500	361	250	175	238	0.74	2.80	-0.31	-2.95	4.09
CF-9	891	61.0	271.0	12.50	6.35	250	1500	361	500	375	238	1.58	2.29	0.65	-2.95	4.11
CF-11	1514	58.2	268.0	9.54	6.35	250	1250	375	208	133	241	0.55	2.82	-0.59	-3.23	4.08
CF-12	1544	58.6	268.0	9.54	6.35	250	1250	375	313	113	241	0.47	2.84	-0.78	-3.23	4.04
CF-13	712	56.0	268.0	9.54	6.35	250	1250	375	417	342	241	1.42	2.08	0.35	-3.23	4.02
CF-14	745	60.0	268.0	9.54	6.35	250	1250	375	417	342	241	1.42	2.11	0.35	-3.23	4.09

Regression Output:

Constant	0.184	variable constant
Std Err of Y Est	0.121	const. 1.20
R Squared	0.943	fc 0.82
No. of Observations	12	Ae/d 0.50
Degrees of Freedom	8	AV -0.84

$$V_u = \frac{1.20 p^{0.59} f_c^{0.97} b d}{(AV)^{0.84}}$$

X Coefficient(s)	-0.84	0.501	0.92
Std Err of Coef.	0.08	0.138	0.28

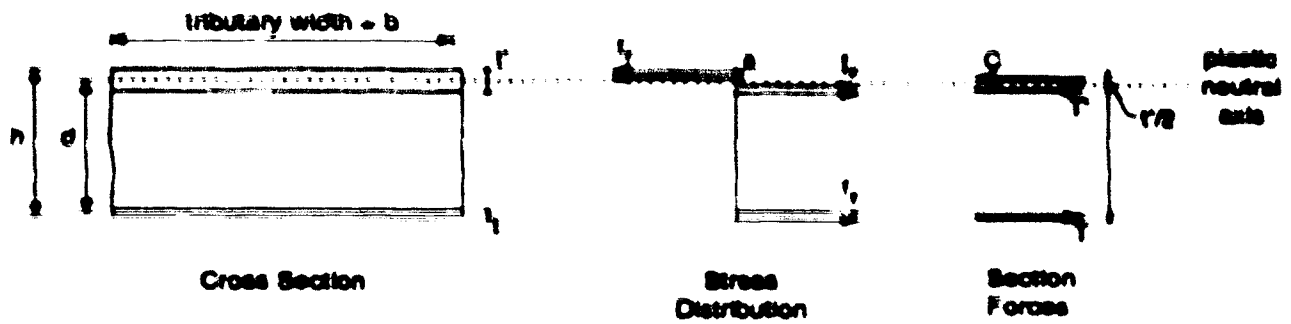
Table 5.3 Summary of Results and Failure Load Predictions

Specimen No.	Type of Failure	V_u (kN)	Predicted Shear Failure Loads (kN)			Ratio of Actual to Predicted		
			Empirical eqn. 5.13b	UBP eqn. 5.20 w=eqn. 5.26	UBP eqn. 5.20 u = 0.95	Empirical eqn. 5.13b	UBP eqn. 5.20 w=eqn. 5.26	UBP eqn. 5.20 u = 0.95
CF-1	shear	684	766	750	811	0.89	0.91	0.84
CF-2 ^a	flexure	817	820	784	834	0.78	0.81	0.74
CF-3	shear	717	721	693	759	0.99	1.04	0.94
CF-4	shear	661	608	668	640	0.91	0.97	1.02
CF-5	shear	430	410	387	398	1.05	1.11	1.17
CF-6	shear	552	591	597	606	0.93	0.92	0.91
CF-7	shear	882	737	886	856	0.80	1.01	1.08
CF-8	shear	1488	1388	1248	1188	1.10	1.20	1.28
CF-9	shear	891	766	724	688	1.16	1.23	1.29
CF-10 ^{***}	shear	1816	1099	1173	1115	1.65	1.58	1.63
CF-11	shear	1514	1482	1458	1385	1.04	1.04	1.09
CF-12	shear	1544	1625	1533	1458	0.95	1.01	1.08
CF-13	shear	712	680	709	705	1.08	1.00	1.01
CF-14	shear	745	707	734	755	1.05	1.02	0.99
SP-1	shear	1636	1801	1484	1409	0.91	1.10	1.18
S-1 ^{***}	punching	1250	1871	1915	2244	0.67	0.65	0.56
S-2	shear	2085	2521	2530	2555	0.83	0.82	0.82
B-1	shear	531	677	643	762	0.78	0.83	0.70
B-2	shear	525	655	634	753	0.79	0.83	0.70

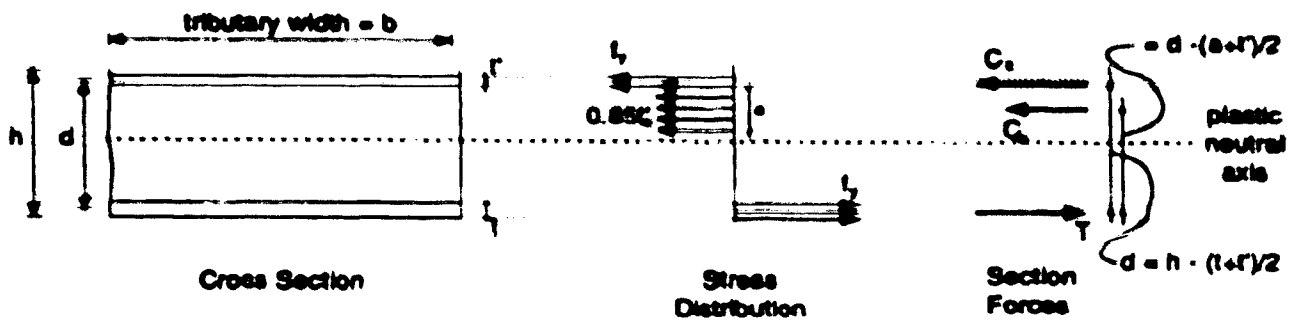
Mean (excluding CF-2, CF-10 & S-1) 0.95 1.00 1.00
 Standard Deviation (excluding CF-2, CF-10 & S-1) 0.12 0.12 0.18

- a - shear span
- d - specimen height, centre-to-centre of exterior plates
- V_u - shear force across critical shear crack, at ultimate load; calculated from statics, assuming that any loads between the shear crack and the support go directly to the support and therefore do not contribute to the shear force.

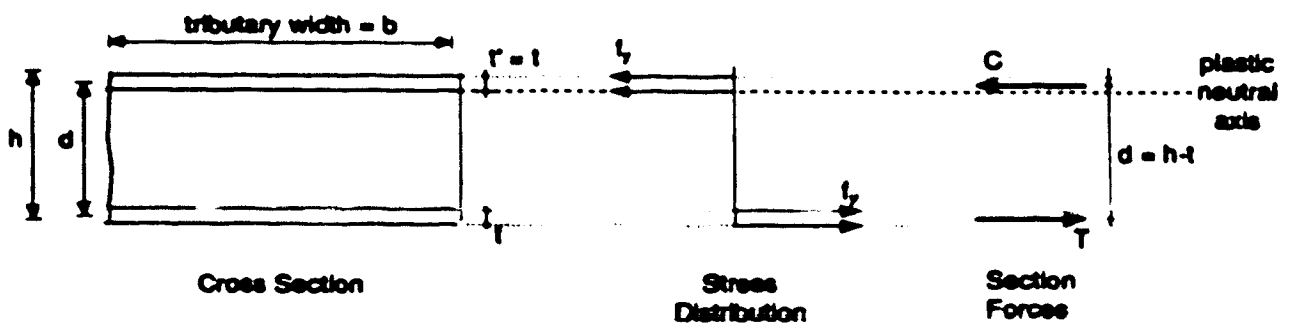
Notes: Specimens which were not used to determine mean and standard deviation:
 • CF-2 Failed in flexure.
 ** CF-10 shear equations contain terms for reinforcement crossing crack.
 *** S-1 failed in punching shear.



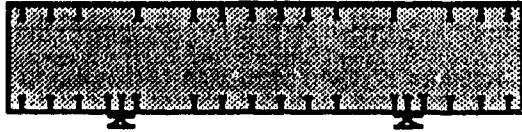
(a) Thicker top plate, $t' > t$



(b) Thicker bottom plate, $t' < t$



(c) Equal plate thickness, $t' = t$



Deep members ($L/d > 4$) with non-linear ϵ strain distributions



Members which allow slip (between diaphragm web plates) at the interface of the concrete core and exterior steel plates



Members which allow slip (between shear connectors) at the interface of the concrete core and exterior steel plate on one (or both) faces

(a) Examples of composite wall types where plane sections method may not be valid



Members with continuous overlapping shear connectors which provide compatibility between the concrete core and the steel plates



Members with continuous angle shear connectors which provide compatibility between the concrete core and the steel plates

(b) Examples of composite wall types where plane sections method may be valid

Figure 5.2 Applicability of Plane Sections Method

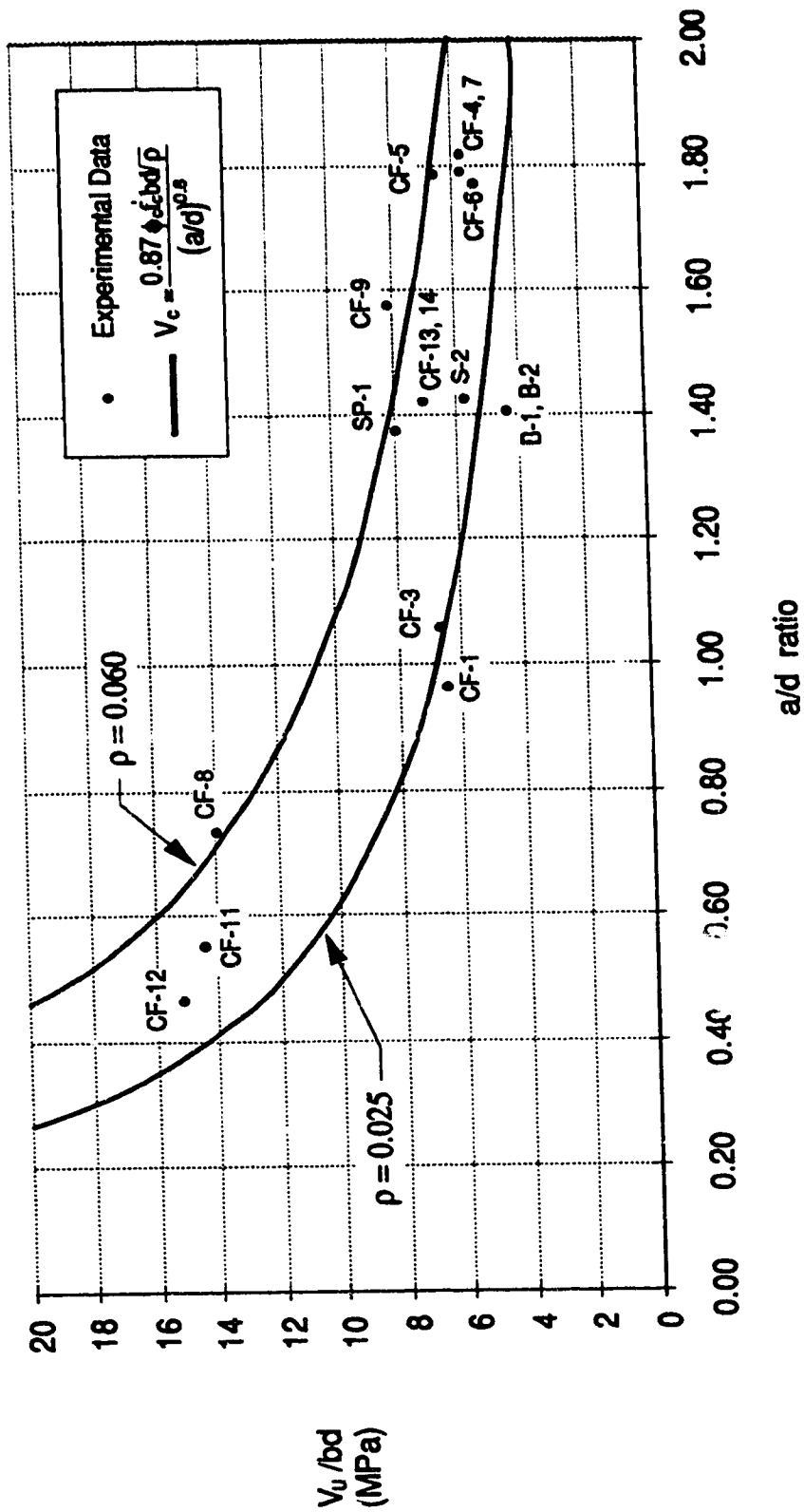


Figure 5.3 Empirical Equation for Shear Strength of Composite Wall; Eqn. 5.13b

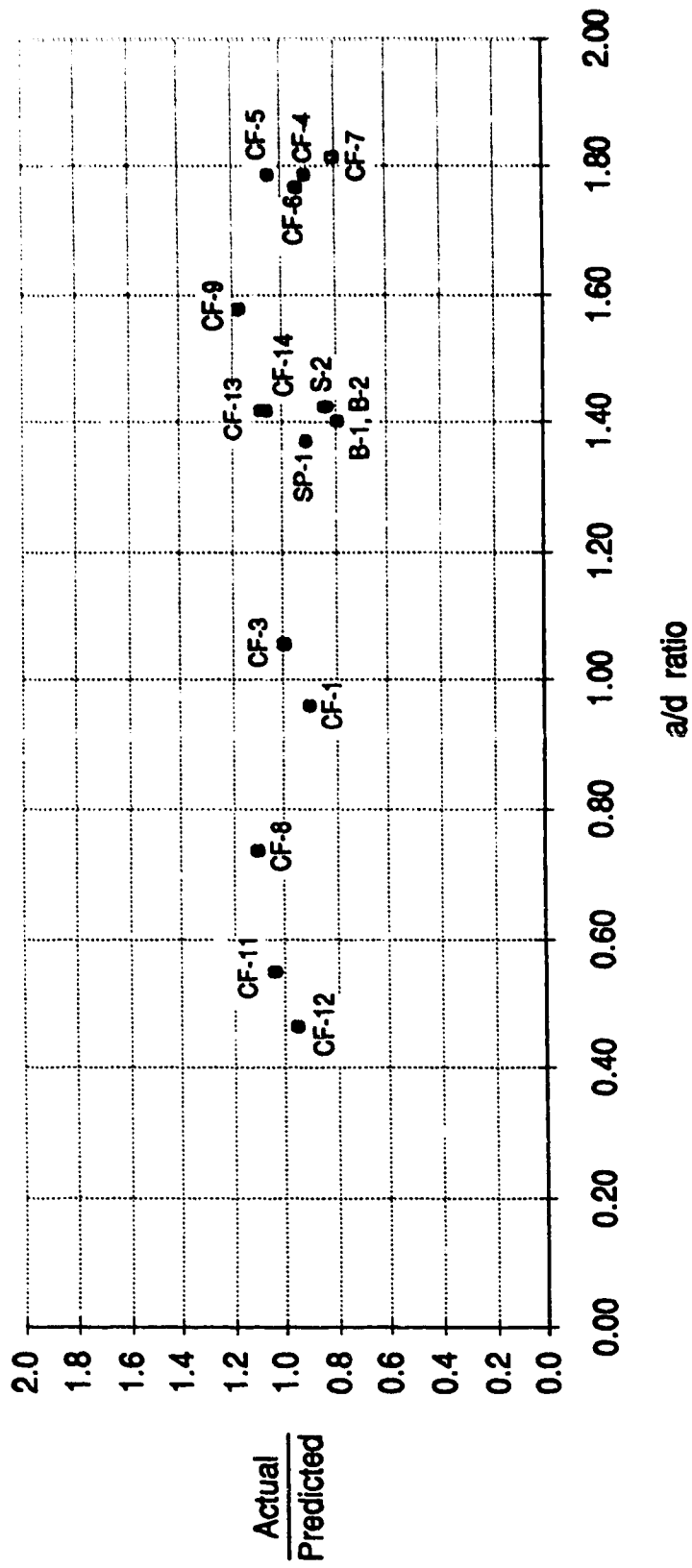


Figure 5.4 Accuracy of Empirical Equation for Shear Strength (Eqn. 5.13b)

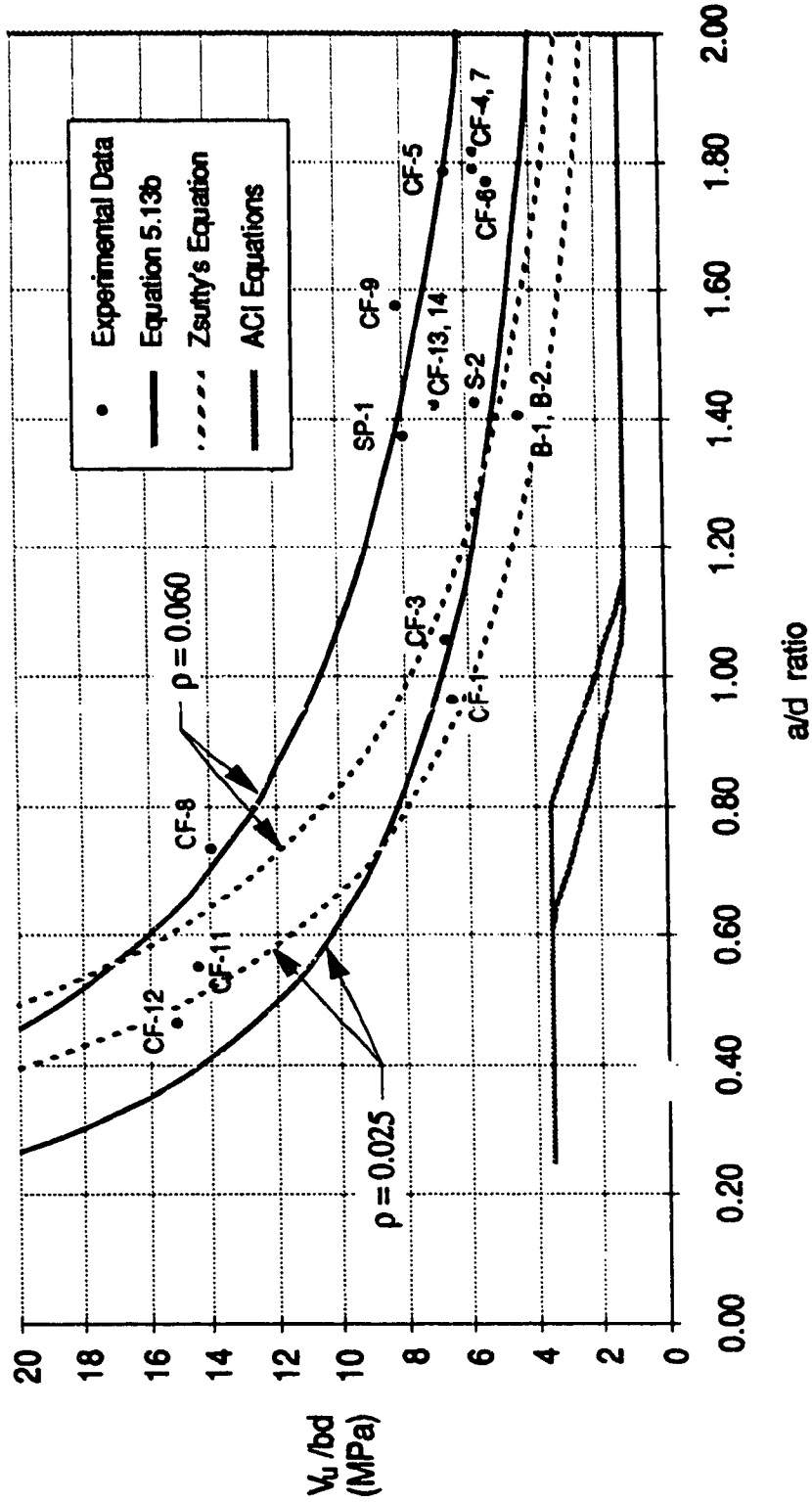


Figure 5.5 Comparison of Empirical Equations for Shear Strength

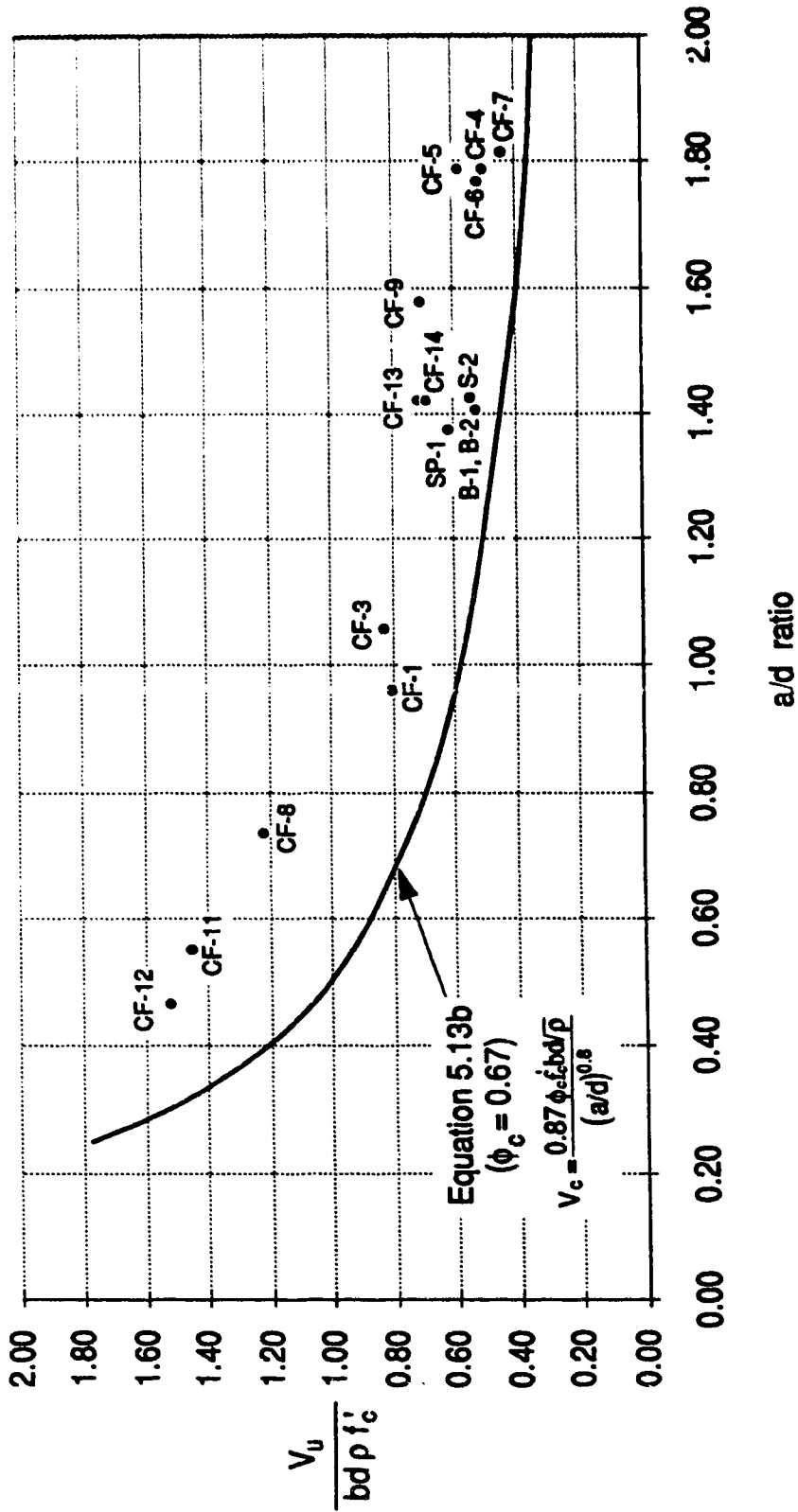


Figure 5.6 Empirical Shear Strength Equation Including Concrete Material Resistance Factor

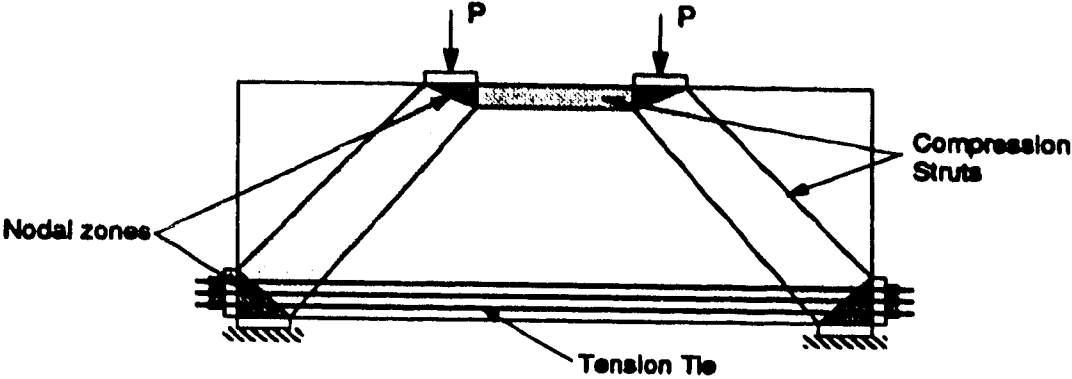


Figure 5.7 Lower Bound Truss Model for a Simply Supported R.C. Deep Beam

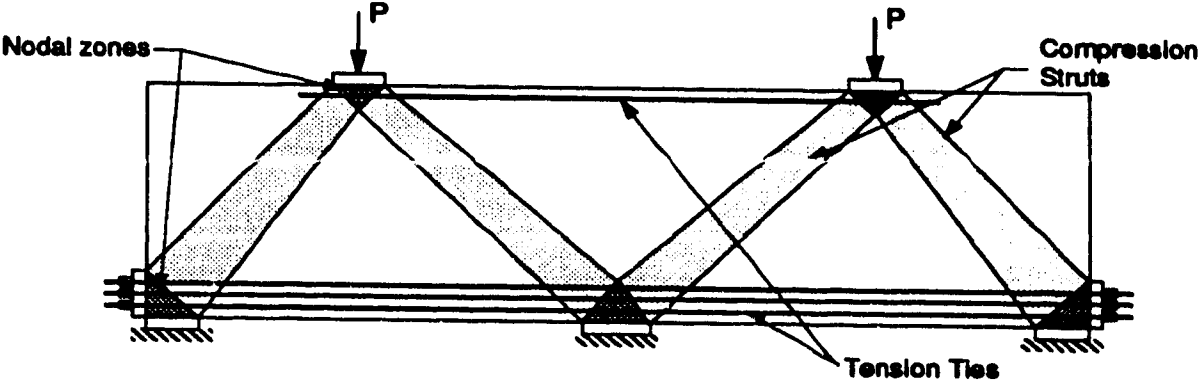


Figure 5.8 Lower Bound Truss Model for a Continuous R.C. Deep Beam

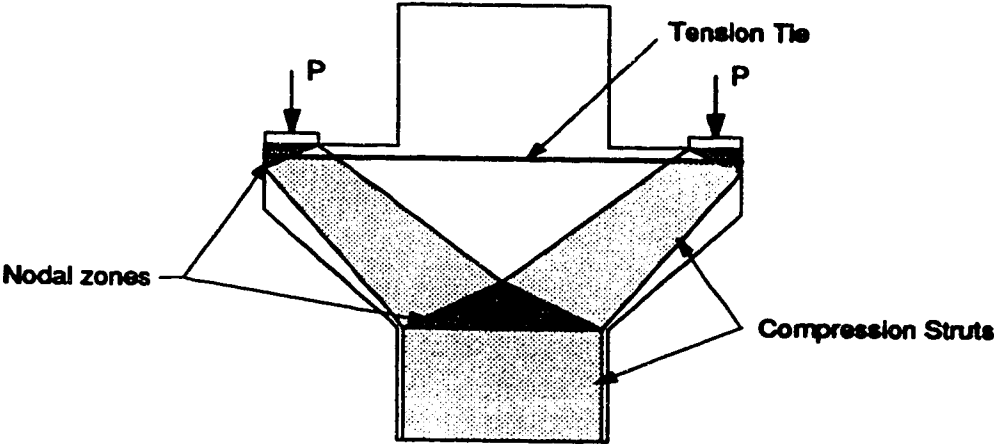
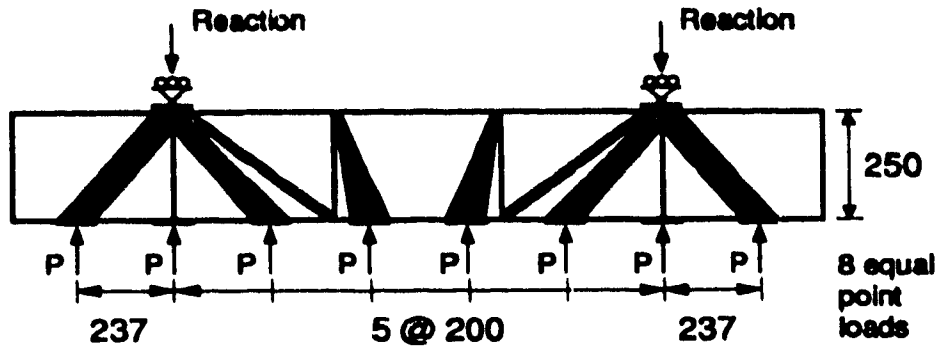
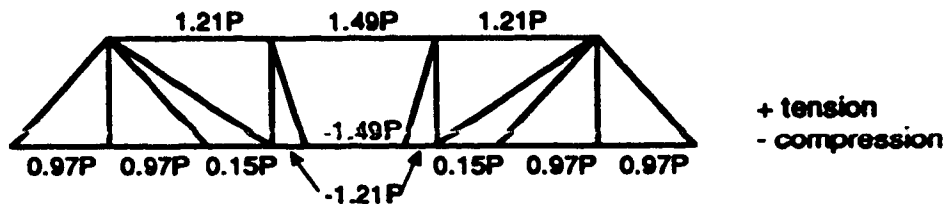


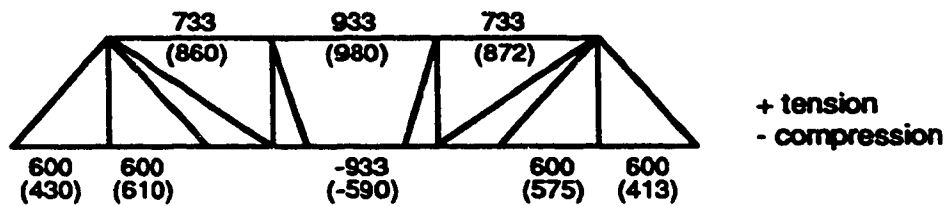
Figure 5.9 Lower Bound Plastic Truss Model for a R.C. Corbel



(a) Strut-and-tie model

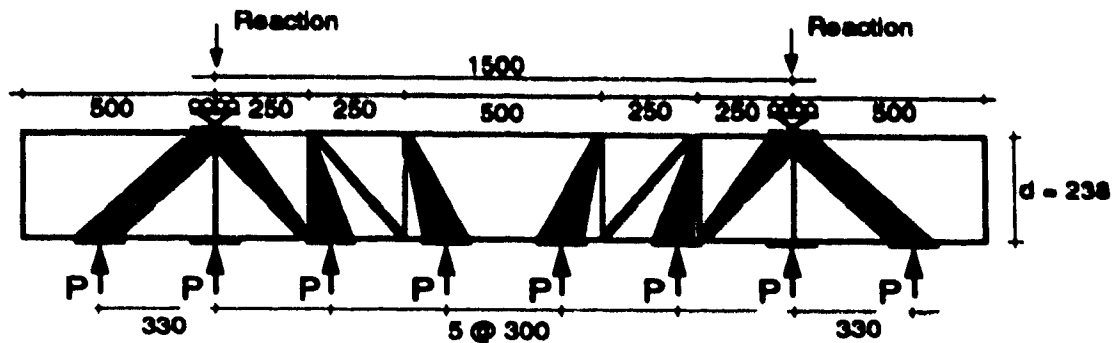


(b) Calculated forces in steel plates

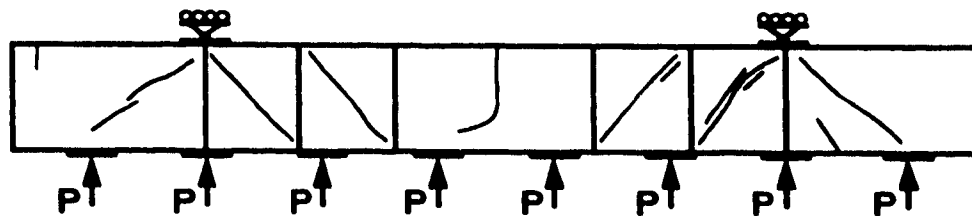


(c) Micro-strains ($\times 10^{-6}$) in steel plates
at $P = 4.0 \text{ MPa} (375\text{mm})(200\text{mm})/1000 = 300 \text{ kN}$
(measured strains in parentheses)

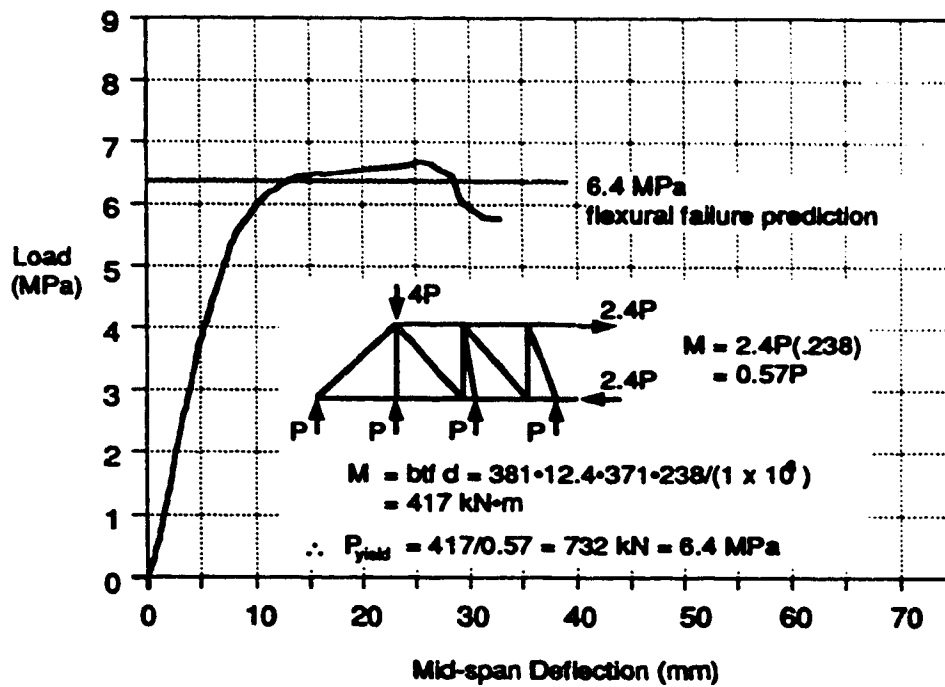
Figure 5.10 Lower Bound Plastic Truss Model for Specimen CF-2



(a) Strut-and-tie model

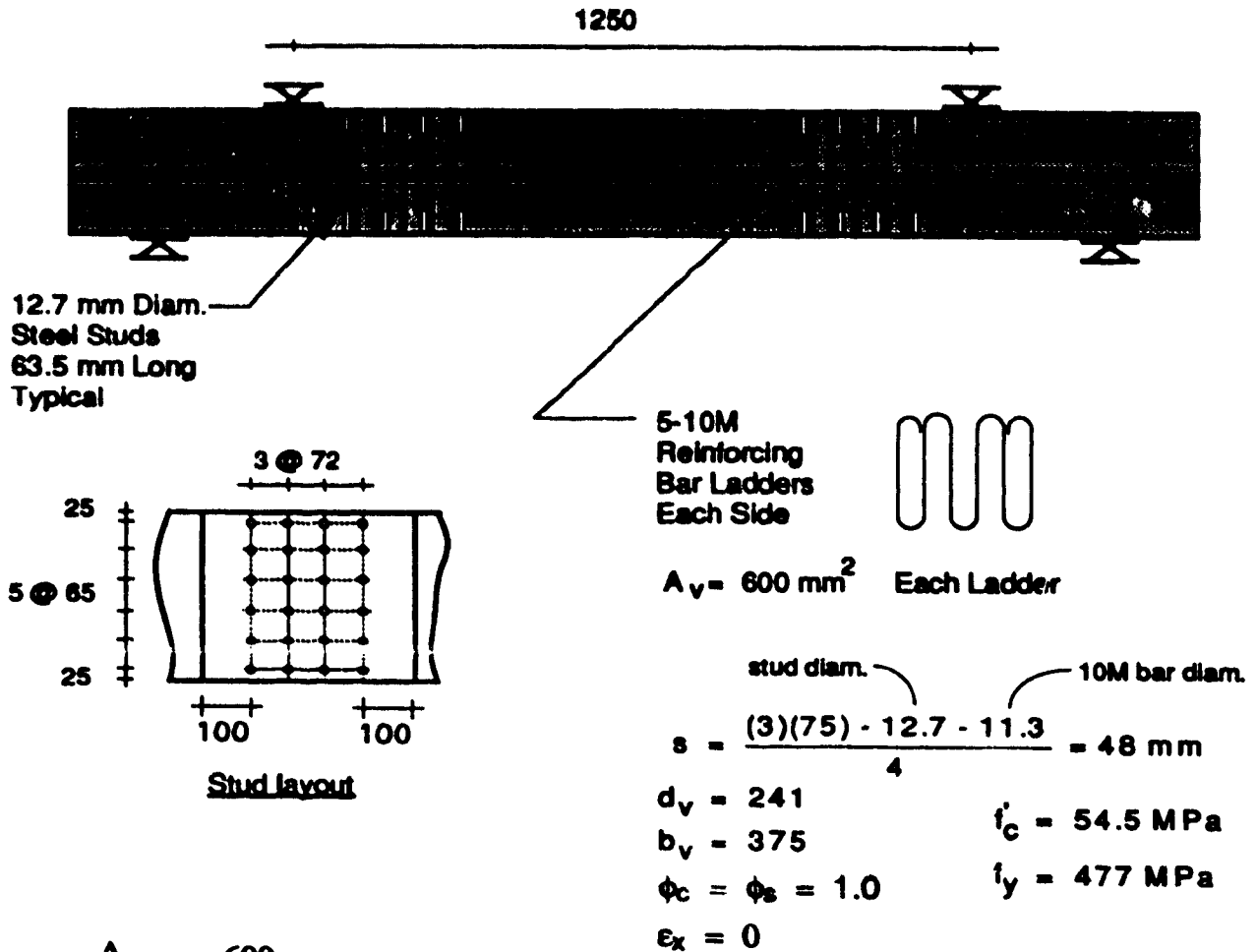


(b) Actual cracking pattern



(c) Strength prediction from truss model

Figure 5.11 Truss Model Analysis for Specimen CF-8



$$\rho_v = \frac{A_v}{sb} = \frac{600}{48(375)} = 0.033$$

$$\omega_v = \frac{\rho_v \phi_s f_y}{\phi_c f'_c} = \frac{0.033(477)}{54.5} = 0.292$$

$$V_r = b_v d_v \rho_v \phi_s f_y \sqrt{\frac{\sqrt{0.22 + \frac{1}{\omega_v} (680 \epsilon_x + 1.36)} - (1.14 + 340 \epsilon_x)}{340 (\epsilon_x + 0.002)}} = 1798 \text{ kN}$$

$V_{test} = 1816 \text{ kN}$ i.e. good agreement

Figure 5.12 Compression Field Method for Predicting Shear Capacity of Specimen CF-10

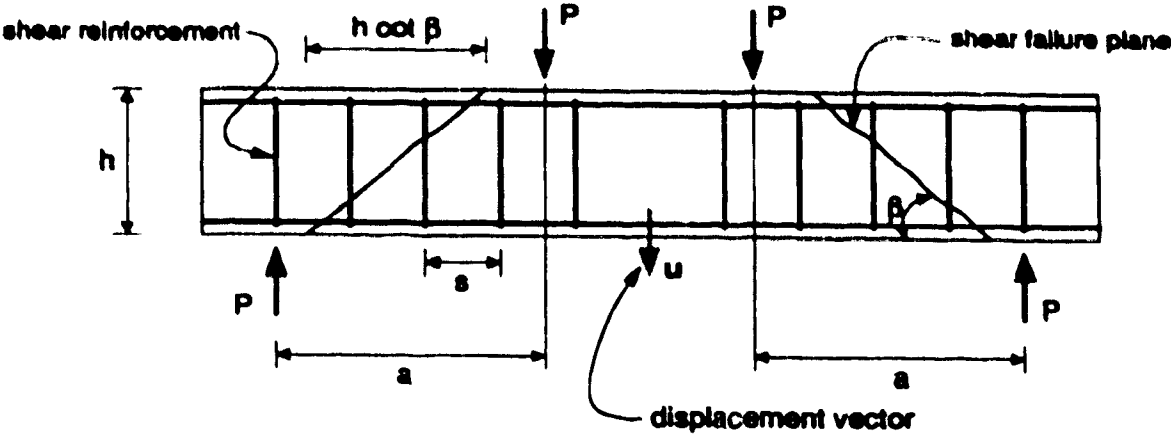


Figure 5.13 Upper Bound Failure Mechanism for a Reinforced Concrete Beam

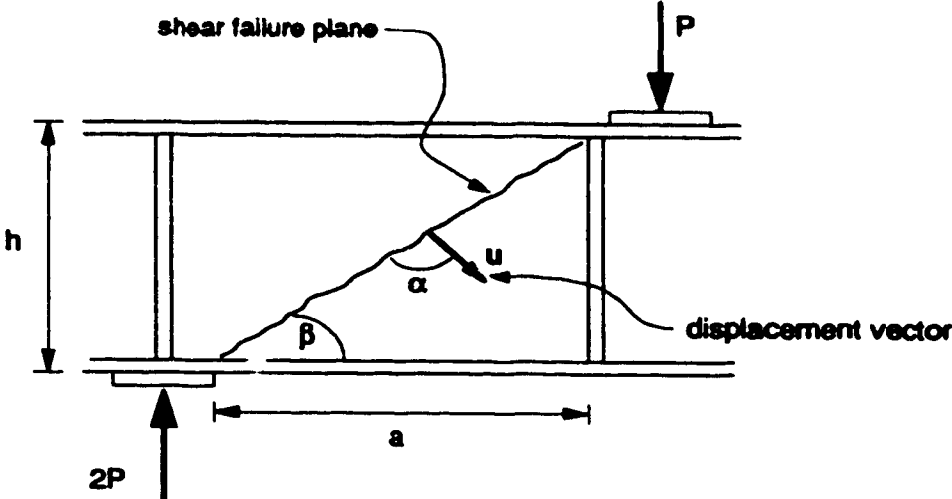


Figure 5.14 Upper Bound Failure Mechanism for a Composite Beam

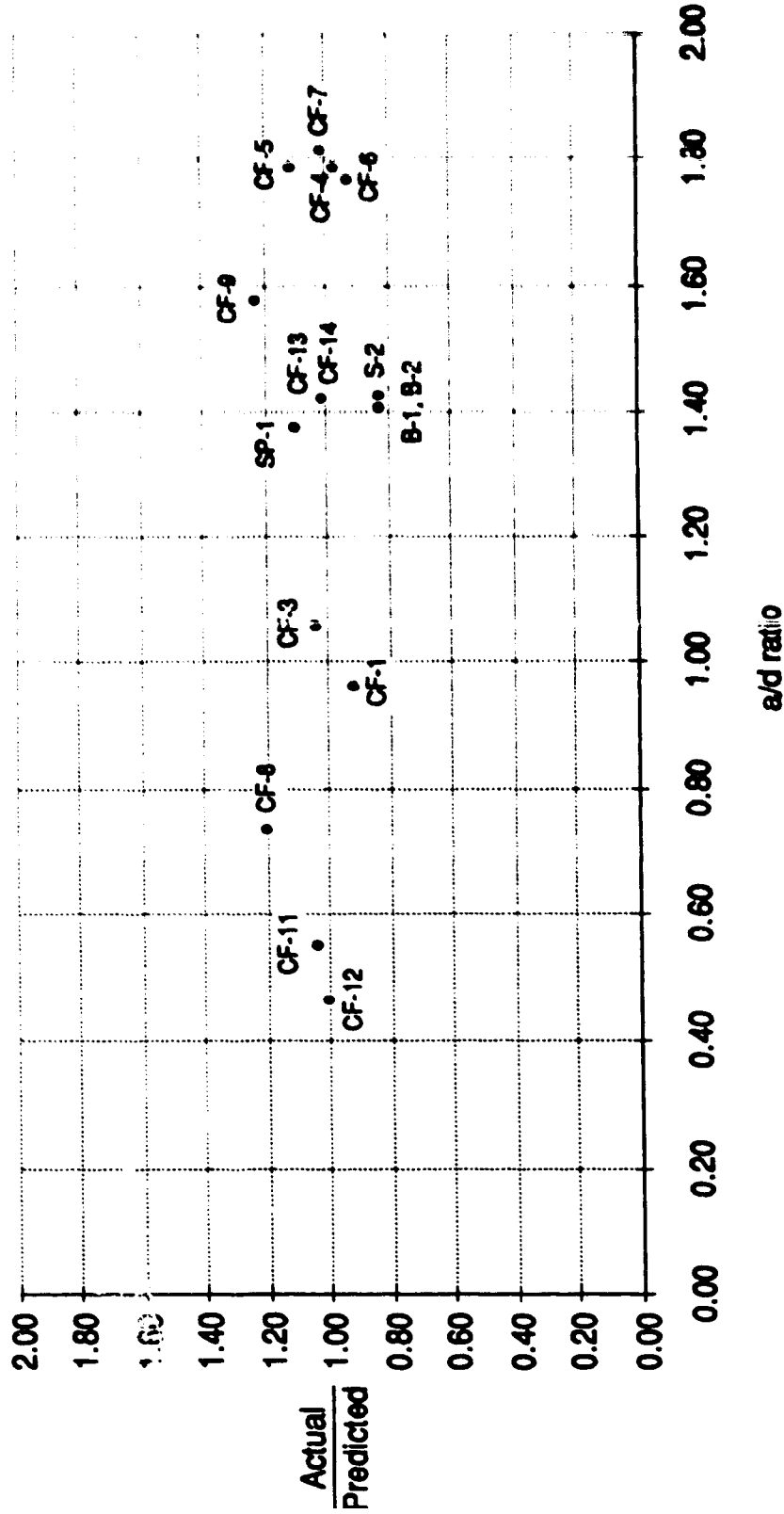


Figure 5.15 Accuracy of Upper Bound Shear Strength Equation (Eqns. 5.23 & 5.24)

6.0 DESIGN METHOD

This section presents the composite design method developed as part of this research work. It is suggested that this design method be restricted in application to the design of composite members only of the type considered herein: i.e. one-way composite members subjected to distributed lateral loads. Design guidelines pertaining to local punching shear considerations and the effects of in-plane loads on lateral load capacity are beyond the scope of this method. There are also many other aspects that enter into the design process (see Appendix D) which are not covered here.

6.1 Recommended Design Method

CSA Standard S473 Steel Structures, Part III-Code for the Design, Construction, and Installation of Fixed Offshore Structures is the first offshore structures code to provide design requirements for composite walls. API RP 2N currently cites several proprietary reports as references for composite wall design, but no actual design guidance or requirements are given. The code requirements contained in S473 are drafted in rather general terms thereby giving the designer considerable latitude in choosing both analysis and design methods. The design method proposed here for composite walls is consistent with, and satisfies the intent of, Clause 13 of CSA Standard S473.

The proposed design method is summarized in the flow charts shown in Figures 6.1 and 6.2. Figure 6.1 shows the overall logic of the design method; Figure 6.2 summarizes the equations to be used in this iterative design procedure.

Consistent with most modern and progressive structural design codes, the design method is based on a limit state design philosophy. It allows the full ultimate member capacity to be utilized, including the effects of inelastic deformations, provided that the member exhibits sufficient ductility to achieve the desired state. The design process is iterative; trial sections are evaluated for their ultimate flexure and shear capacities and revised as necessary until adequate strength is obtained.

6.1.1 Determine Ultimate Limit State Loads

The design of individual structural elements to resist forces caused by ice/structure interaction is generally based on local ice pressures which are associated with the crushing

strength of ice. The effective local ice failure pressures are primarily influenced by the mechanical properties of the ice, the size and shape of the loaded area, and the mode of ice/structure interaction. Existing data shows a trend of decreasing local ice pressure with increasing size of contact area. This variation in pressure intensity with loaded area (size effect) complicates the process of establishing governing load cases. In determining ice load patterns and intensities that control member design, the designer must make reasonable assumptions about the shape of the loaded area and must then consider load patterns in which both the size and location of the loaded area are varied. The choice of load factors and material resistance factors required to facilitate strength and serviceability calculations are left to the designer. For guidance in selecting appropriate factors the designer is directed to the appropriate clauses in CSA Standards S471 and S473.

In establishing maximum design moments it is important to note that peripheral composite wall elements designed to resist ice loads will be supported by bulkheads having a width which amounts to a significant fraction of the total span length. The effective span length will, therefore, be much closer to the clear span distance than to the centre-to-centre span distance. An efficient wall design should take into account the reduction in design moments resulting from the fact that the reaction force will be distributed over the support width.

No further discussion is provided here concerning these issues, as it is considered beyond the scope of this work.

6.1.2 Trial Sections: General Requirements

Since most of this research effort has been directed at the behaviour of beam-type elements, the proposed design method is restricted in application to walls which span primarily in one direction. This is consistent with the peripheral wall design concepts currently being considered for use in the Beaufort Sea.

The general requirements outlined here are intended to constrain member designs so as to ensure that geometric and material parameters fall within the range of values for the experimental test data for which the strength and ductility assumptions have been shown to be valid.

Trial sections should be chosen within the following limits:

1. $250 \text{ MPa} \leq f_y \leq 400$
2. $35 \text{ MPa} \leq f_c \leq 70$
3. $4 \leq L/h \leq 6$
4. $0.45 \leq a/d \leq 2.0$
5. $1.5\% \leq i/h \leq 6.5\%$
6. $w \leq t$
7. $t' = t = \text{constant for span}$

In addition, the wall configuration should be such that the face plates are interconnected by continuous transverse diaphragm web plates, designed to carry a minimum tensile force equal to the full transverse shear force acting at the diaphragm location. The welds connecting the diaphragm plates to the face plates should be sized to develop the full tensile capacity of the diaphragm plate.

6.1.3 Design for Flexure

Flexural capacity calculations are based on a lower bound plasticity approach using either a plane sections analysis method or a lower bound plastic truss method. The basic difference in the results of these two methods relates to the amount of tensile steel required at various sections in the span. However, since the proposed design method stipulates that a constant external plate thickness should be used across the span, and that the same plate thickness should be used top and bottom, the two methods end up being the same: i.e. equation 5.7 is used to determine the plate thickness required for the larger of the positive and negative moment.

The flexural strength formulae do not take into account the effects of passive in-plane restraint provided to the loaded spans by the surrounding structure. Assessment of the actual in-situ strength of continuous reinforced concrete bridge decks subject to local loads (Csagoly et al.1978) has shown that passive in-plane restraint can significantly enhance ultimate flexural capacity. Similar behaviour has been observed in tests of restrained composite wall specimens subject to distributed lateral patch loads (Gerwick 1987). In design situations where the extent of passive in-plane restraint can be accurately quantified, the additional flexural capacity attributed to the internal force couple generated

by boundary restraint may be taken into account in the evaluation of ultimate member strength.

6.1.4 Design for Shear

Shear strength calculations are made in two different ways, depending on member details and the presence or absence of additional shear reinforcing (in addition to that provided by the diaphragm plates). In regions where the shear stresses can be assumed to be evenly distributed over the member cross-section, the compression field theory method can be used. For other cases (deep members, or members that allow slip at the concrete-to-steel interface), the upper bound plasticity method is used.

6.1.5 Additional Considerations

Serviceability requirements are checked once the member configuration has been determined (based on ultimate strength criteria) and revisions made if necessary. For a composite ice-resisting wall, the serviceability check basically reduces to ensuring that yielding does not occur at service load levels. Crack widths in the concrete core are not a consideration, as the impervious, exterior steel plate prevents the ingress of water. Deflections are also not generally important, except perhaps as they effect the failure mechanism of the ice sheet (little is currently known about this phenomenon and whether it makes any difference). Lastly, it is recommended that due consideration be given to the need for an increase in exterior steel plate thickness to provide a corrosion allowance.

6.2 Design Example

Appendix D presents a conceptual design for a bottom-founded fixed offshore structure proposed for Gulf Canada's Amauligak field in the Beaufort Sea. Three structural schemes are presented for constructing the main drilling and production barges for that structure, each utilizing composite walls around their entire perimeter. This work was conducted by the author and Mr. Mark Stephens of C-FER as part of a proprietary contract project for Gulf Canada conducted by C-FER, in collaboration with Ben C. Gerwick Inc., San Francisco. The design work relied heavily on the research work conducted as part of this thesis and is the first use of the research results for the conceptual design of an actual planned structure.

In order to develop the conceptual designs for the three schemes, detailed preliminary design engineering had to be undertaken for those parts of the structure using new methods or details not previously considered, such as the exterior composite walls. The greatest design effort was aimed at the composite peripheral walls, as it was considered important to demonstrate that those walls would function adequately under all potential load combinations. Ice loads, foundation settlements and thermal gradients all had to be considered. Considerable effort was directed at determining the ice load effects: critical ice feature configurations; the determination of local ice pressure intensities and distributions; and the adjustments required to account for load spreading. Computer models were used to determine design forces and force influence lines were developed for the various trial configurations to establish critical ice load patterns.

It is beyond the scope of this document to reproduce the design calculations that went into that proprietary project. Many parts of that work are confidential and in addition, use was made of research work conducted at C-FER by Mark Stephens, which extended the authors work to cover composite walls subjected to combined axial load and bending. This consideration was important for the Gulf structure, since advantage was taken of the beneficial effects of axial compression in the peripheral wall (caused by the non-perpendicular interior bulkhead walls) on flexural and shear capacity.

In order to demonstrate the use of the design method developed by the author and presented in this document, a simplified example design is presented. It is given in Figure 6.3. The example considers ice forces as the only loading event, and does not consider all of the loading patterns which would need to be checked in practice. Nonetheless, Figure 6.3 demonstrates the feasibility and relative ease with which a composite ice-resisting wall design can be undertaken. Appendix D illustrates the end result of taking such a design to the detailed preliminary design stage.

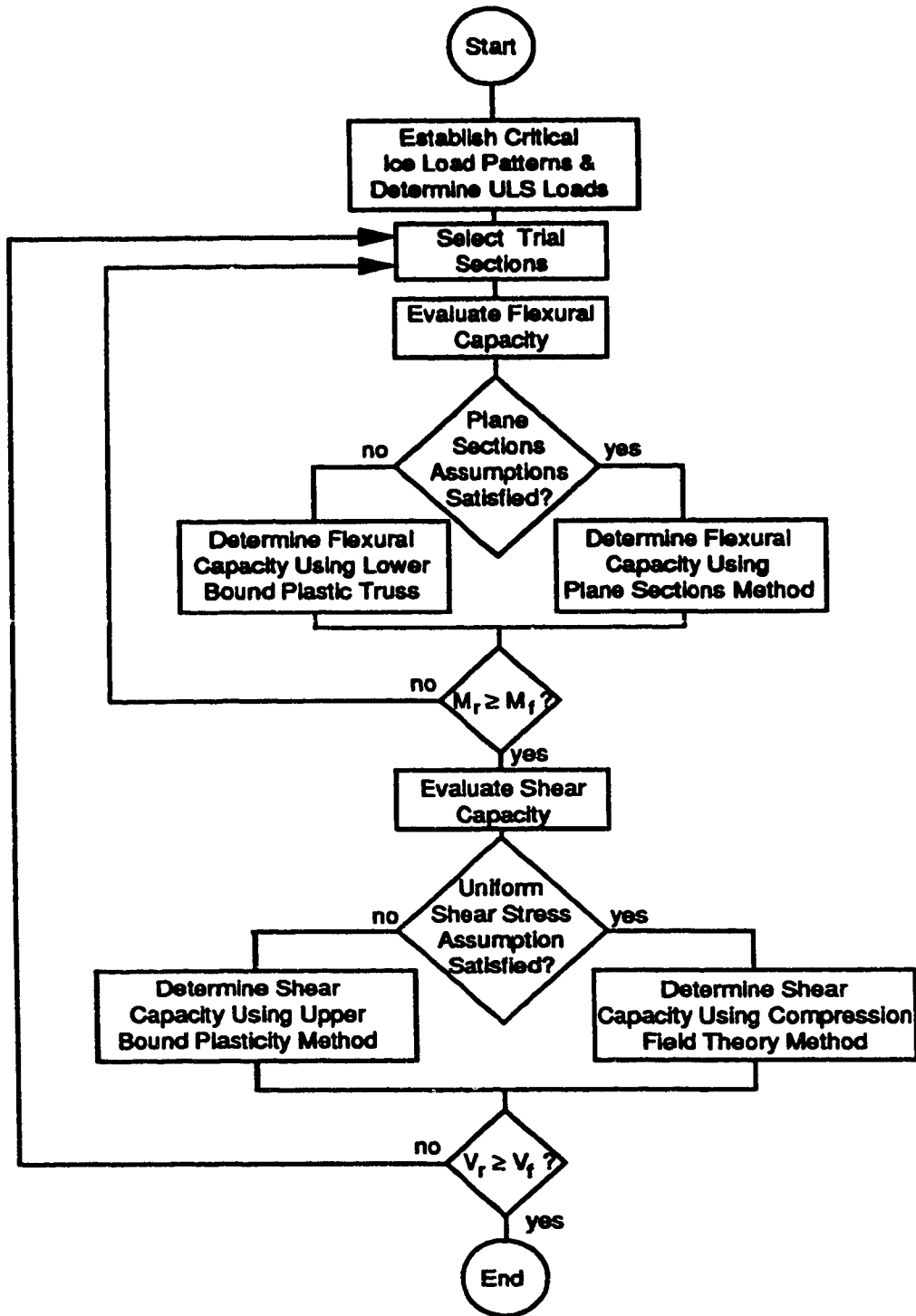
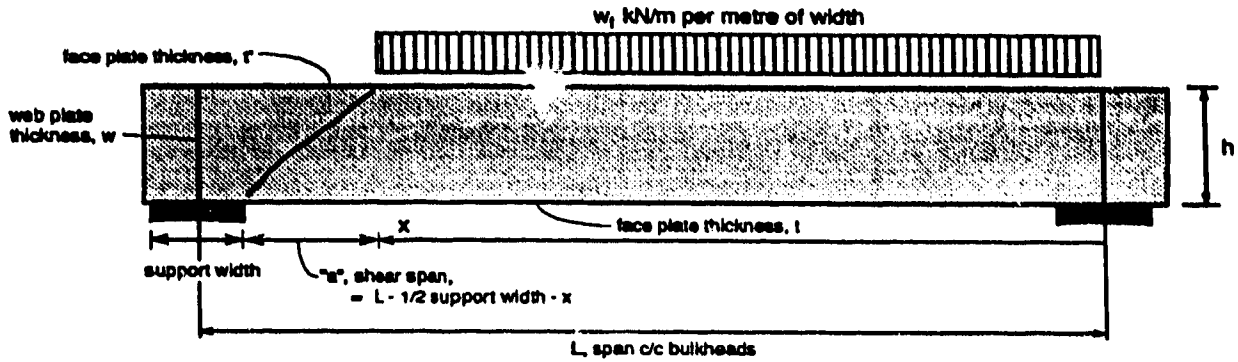


Figure 6.1 Composite Wall Design Flow Chart



Materials Properties Limits

$$35 \text{ MPa} \leq f_c \leq 70 \text{ MPa}$$

$$250 \text{ MPa} \leq f_y \leq 400 \text{ MPa}$$

Dimensions Limitations

$$L/h \geq 5.0f$$

$$0.45 \leq a/d \leq 2.0 \text{ where } d = h - t = \text{c/o of face plates}$$

$$1.5\% \leq t/h \leq 6.5$$

$$w \leq t$$

$$t = t' = \text{constant for span}$$

Design for Flexure

- design bending moment for three-hinge mechanism = $M_k = \frac{w_f L^2}{16}$
- bending capacity (Equation 5.7) = $M_u = A_s \phi_s f_y d$ (Eqn. 5.7)

Design for Shear

- determine design shear from static analysis, with load on part of span;
- for composite walls with diaphragm web plates and no additional shear reinforcement, evaluate shear capacity using one of two methods:

empirical equation (5.13b):
$$V_c = \frac{0.87 \phi_c f_c b d \sqrt{\rho}}{(a/d)^{0.8}}$$

upper bound plasticity equation (5.22 to 5.25):

$$V_r = \frac{b t w \phi_c f_c}{2} \left[\sqrt{\left(\frac{a}{h}\right)^2 + \frac{4\phi(\nu - \Phi)}{\nu^2}} - \frac{a}{h} \right] \text{ for } \Phi \leq \nu/2$$

$$V_r = \frac{b t w \phi_c f_c}{2} \left[\sqrt{\left(\frac{a}{h}\right)^2 + 1} - \frac{a}{h} \right] \text{ for } \Phi > \nu/2$$

where
$$\Phi = \frac{(A_s + A_s') \phi_s F_y}{b h \phi_c f_c}$$

$$\nu = 0.95$$

- for composite walls which meet the requirements of Section 5.2.1.3 and have additional shear reinforcement, evaluate shear capacity using:

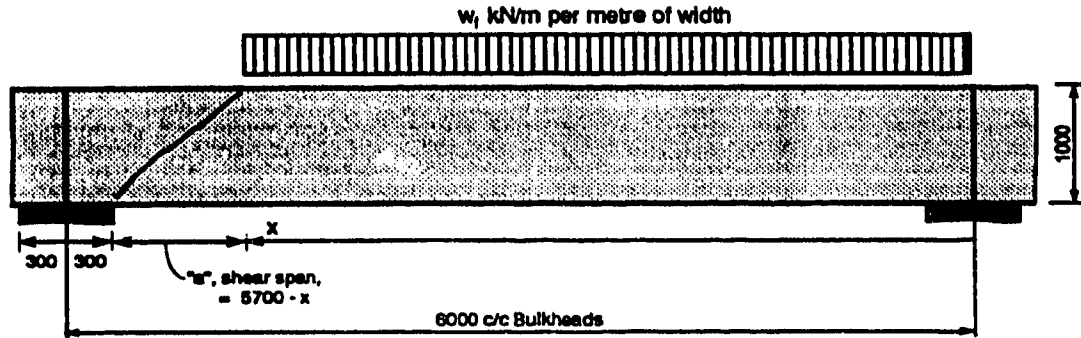
compression field theory equation (5.16 to 5.18):

$$\frac{V_r}{b h} \max = \rho_v \phi_s f_y \sqrt{\frac{\sqrt{0.22 + \frac{1}{\omega_v} (680 \epsilon_s + 1.36)} - (1.14 + 340 \epsilon_s)}{340 (\epsilon_s + 0.002)}}$$

where
$$\rho_v = \frac{A_v}{s b}$$

$$\omega_v = \frac{\rho_v \phi_s f_y}{\phi_c f_c}$$

Figure 6.2 Summary of Composite Wall Design Equations



Materials Properties

Concrete: $f_c = 60 \text{ MPa}; \phi_c = 0.67$
 Plate Steel: $f_y = 350 \text{ MPa (Grade EH36)}; \phi_s = 0.90$
 Stud Steel: $f_y = 350 \text{ MPa}; \phi_s = 0.90$

Dimensions of Trial Section

$h = 1000 \text{ mm}$
 $L = 6000 \text{ mm}$
 assume $d = 0.98h = 980 \text{ mm}$

Design Ice Load (as determined from Figure 3.2, assuming a 1:1 aspect ratio on the ice load patch)

loaded length, x (mm)	ice pressure (MPa)	w_i kN/m per metre of width
3600	2.6	2600
4800	2.5	2500
6000	2.4	2400

note: Load factor = 1.0, assuming a Safety Class 2 structure in accordance with CSA Standard S471-02.

Design for Flexure

- design bending moment for three-hinge mechanism = $M_f = \frac{w_i L^2}{16} = \frac{2600(6000)^2}{16 \times 10^6} = 5400 \text{ kN}\cdot\text{m}$
- bending capacity (Equation 5.7) = $M_u = A_s \phi_s f_y d$
 $\therefore t_{reqd} = \frac{5400(1 \times 10^6)}{1000(.9)(350)(980)} = 17.5 \text{ mm}$

\therefore use 18 mm plate ea. side

Design for Shear - use Eqn. 513b to determine shear capacity

x (mm)	a, shear span	w_i kN/m	Assume simple beam model is conservative	V_f	$V_r = \frac{0.87\phi_c f_c b d \sqrt{p}}{(a/d)^{0.8}}$
5100	600 mm	2500		5418 kN	> 6896 kN O.K.
4800	900 mm	2500		4800 kN	> 4986 kN O.K.
4500	1200 mm	2500		4219 kN	< 3960 kN N.G.

- \therefore place first diaphragm plates at $x = 4800$ (i.e. 1200 from centre of left support), and $x = 1200$.
- need at least two more diaphragm plates between these two in order to keep within limit $a/d \leq 2.0$ (Section 6.2.2) \therefore space diaphragms evenly at 1200 c/c.

Figure 6.3 Composite Wall Design Example

size diaphragm plates - design for full shear force of 4800 kN

$$\therefore w_{req'd} = \frac{V_f}{b\phi_s f_y} = \frac{4800 \times 10^3}{1000(0.9)(350)} = 15.2 \text{ mm}$$

\therefore use 16 mm plate for first diaphragm web at each end

at $x = 3600 \text{ mm}$, $V_f = 2808 \text{ kN}$, $\therefore w_{req'd} = 8.9 \text{ mm}$

but too thin to handle; say limit $KL/r = 200$

\therefore use $t = 12 \text{ mm}$ for two inner diaphragm web plates

Design Shear Connectors to Prevent Plate Buckling

• to determine spacing requirements, treat exterior plates like cover plates on built-up members as per CSA Standard S16.1, Clauses 11 and 18.

• parallel to span: max. spacing

• perpendicular to span: max. spacing
 $= \frac{300t}{\sqrt{f_y}} = \frac{300(18)}{\sqrt{350}} = 318 \text{ mm} \leq 300 \text{ mm}$

• size studs for 2% bracing force:
 $= \frac{525t}{\sqrt{f_y}} = \frac{525(18)}{\sqrt{350}} = 505 \text{ mm}$, say 500 mm

$$T_f = 0.02 (A_s f_y) = \frac{0.02(18)(500)(350)}{1000} = 63 \text{ kN}$$

$$T_r = \phi_{stud} A_{stud} f_y \therefore A_{stud req'd} = \frac{63,000}{0.85(350)} = 212 \text{ mm}^2 \quad \therefore \text{use 20 mm diam. studs x 150 long}$$

Composite Wall Details

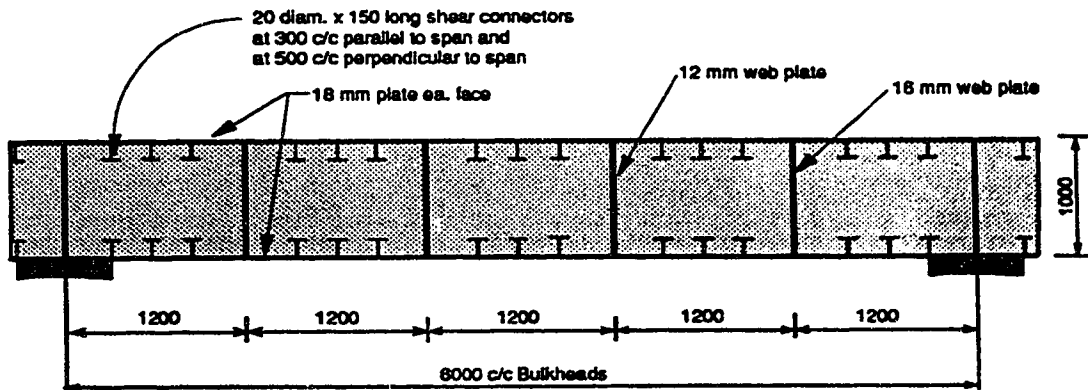


Figure 6.3 Composite Wall Design Example, continued

7.0 COMPARATIVE COST ANALYSIS

In order to determine the economic feasibility of using composite walls for an offshore structure, a cost comparison was made between three different construction types: reinforced concrete, all-steel and composite. The comparison is made for an individual exterior wall element subjected to some hypothetical ice load.

7.1 Isolated Peripheral Wall Element

In order to compare the various material types, a number of preliminary designs were carried out. Four alternatives were selected for the comparison work, including a composite scheme (Figure 7.1), a hybrid scheme (open-faced composite; Figure 7.2), a reinforced concrete scheme (Figure 7.3) and an all-steel scheme (Figure 7.4). All of these designs are technically feasible, the exercise is to determine if cost makes some more attractive than others.

The four basic peripheral wall alternatives are shown in Figures 7.1 to 7.4. All of these schemes are based on a bulkhead spacing of 6 m, which was chosen somewhat arbitrarily for the purpose of initial comparison. The basic layout of the structure assumed in this work is shown in Figure 7.5. The material properties used in the preliminary designs are shown on the design sketches; they are considered to be close to optimum and well within industry's capabilities.

The ice load assumed for the preliminary designs are those obtained from the ice load curve shown in Figure 3.2, with a load factor of 1.0 applied.

7.1.1 Composite Wall

Figure 7.1 shows the composite wall alternative. In this scheme, shear connectors have been included, sparsely distributed over both the outside and inside steel plates. Although the research presented here did not indicate a need for these shear connectors, they were included in response to concerns that in some instances the exterior steel plates could buckle in compression prior to the ultimate capacity of the wall being reached. The studs included are sufficient in number to prevent plate buckling, but are too few to provide complete compatibility between the concrete core and the steel plates. It was though

necessary to demonstrate that if the shear connectors were included as part of an actual design, the cost penalty would be small.

7.1.2 Open-faced Composite Wall

Figure 7.2 shows the "hybrid" scheme; a combination of a reinforced concrete wall and a composite wall. This alternative came about by recognizing the possible need for a steel wear plate on the outside of a reinforced concrete wall and attempting to take advantage of the situation by using the plate structurally. The outside plate is connected to the wall using large diameter, friction-welded studs. The scantlings indicated in the figure are required to support the outside steel plate during concrete placing operations. The friction-welded studs look very much like conventional headed studs; they consist of a circular steel bar shaft and a steel plate head (circular or square). However, the great length and large diameter of the shaft make them too large to be welded using conventional induction welding, hence the need for the friction welding technique. These studs have been developed through discussions with Metalock, of Norway, and use friction welding technology both for attaching the head to the stud and for attaching the stud to the plate. Although this is a less well known process than induction welding, it has been successfully used by Metalock in producing the T-headed stirrups (shear reinforcement) used by the Norwegian Contractors for the Gullfaks C and Oseberg A platforms in the North Sea. They have also been specified by Phillips (operator) for use on the Ekofisk peripheral barrier wall.

7.1.3 Reinforced Concrete Wall

Figure 7.3 shows the reinforced concrete scheme. This is a conventional type of wall, in most respects, except for the T-headed stirrups (manufactured by friction welding) which are used to provide all of the shear reinforcement. Stirrups of this type have shown their effectiveness during the construction of the Condeeps and are reportedly preferred to conventional shear reinforcement because of the ease with which they can be placed. Fairly high percentages of shear steel and transverse (vertical) steel have been provided in this design in order to prevent a brittle type of punching shear failure.

7.1.4 All-steel Wall

Figure 7.4 shows the last alternative: an all-steel design with a single outer face plate and heavy T-beam stiffeners. This scheme looks like a fairly conventional steel design and is not unlike that used on the SSDC Steel MAT. There is a significant difference however. The high local ice loads being considered (30 MPa on an area 0.4 m by 0.4 m) require that a membrane approach be taken in designing the outer steel face plate, in order to keep the plate at a reasonable thickness. Although a membrane plate design is non-conventional, there is precedence for its use on ship structures and on the steel CRI which was used by Esso in the Beaufort Sea. Membrane design is also allowed by CSA Preliminary Standard S473, although little guidance is given. The approach used for this membrane design is based on research work conducted at the University of Alberta by Ratslaff and Kennedy. The T-beam stiffeners are designed conventionally. Their size is governed by shear considerations; as bending members they do not operate outside of the elastic range.

It is interesting to note that the steel wall is remarkably insensitive to span; that is, the face plate and web plates change very little as the span increases. This is because the face plate is governed by the maximum local load (30 MPa), which is the same for all spans, and the web plates are governed by shear, which remains relatively constant since the increase in loaded area associated with increased span is offset by a proportional decrease in ice load intensity (resulting from the greater loaded area).

7.2 Cost Comparison

In order to obtain cost comparisons for the alternative wall designs, a number of fabricators and contractors in Vancouver, California, and Washington were contacted for unit cost information. From these sources, average unit costs for construction in Canada were adopted as follows:

Item	Unit Cost
Concrete	\$ 250/m ³
Formwork	\$ 135/m ²
Rebar (including splices)	\$1400/kg
T-headed stirrups, 25 dia.x 955	\$ 15/ea.
Studs, 25 dia.x 830 (friction welded)	\$ 15/ea.
Studs, 35 dia.x 1015 (friction welded)	\$ 22/ea.
Studs, 20 dia. 150 (regular Nelson)	\$ 2/ea
Steel Plate, composite walls (fab.shop)	\$2400/tonne
Steel Plate, all-steel walls (shipyard)	\$3500/tonne

The information supplied by Canron Ltd., Concrete Technology Corporation, Dillingham Construction Ltd., Kiewit Engineering Co. Ltd., Southwest Marine, Inc., and Vancouver Shipyards was used to determine these unit costs. These were then used to develop the total wall costs for each alternative.

The total wall cost developed for construction in Canada is as follows:

Company	Composite	Hybrid	Concrete	Steel
Cost per square meter	\$1350 - \$1400	\$1550 - \$1700	\$1400 - \$1600	\$2400 - \$2800

The cost comparisons obtained are illustrated in Figure 7.6. Ranges have been shown for the costs to reflect the differences in prices obtained from the various sources. All costs shown are in 1989 Canadian dollars and assume that construction will take place in the Vancouver area. The costs apply only to the 6 m span and do not include any component for constructing the bulkhead support walls.

In reviewing the cost comparisons the following is apparent:

- (a) The concrete, composite and hybrid schemes are all in the same general range;
- (b) The all-steel cost is much higher than all of the other schemes;

The high cost of the all-steel alternative and the competitive cost of the composite scheme are perhaps the two most important findings from this costing study. The high all-steel cost is not a surprise; it is consistent with the findings of others. The competitive cost of the composite alternative is also consistent with preliminary expectations. It means that the beneficial attributes of the composite scheme (such as abrasion resistance and ductile response at ultimate) can be taken advantage of without incurring a cost penalty.

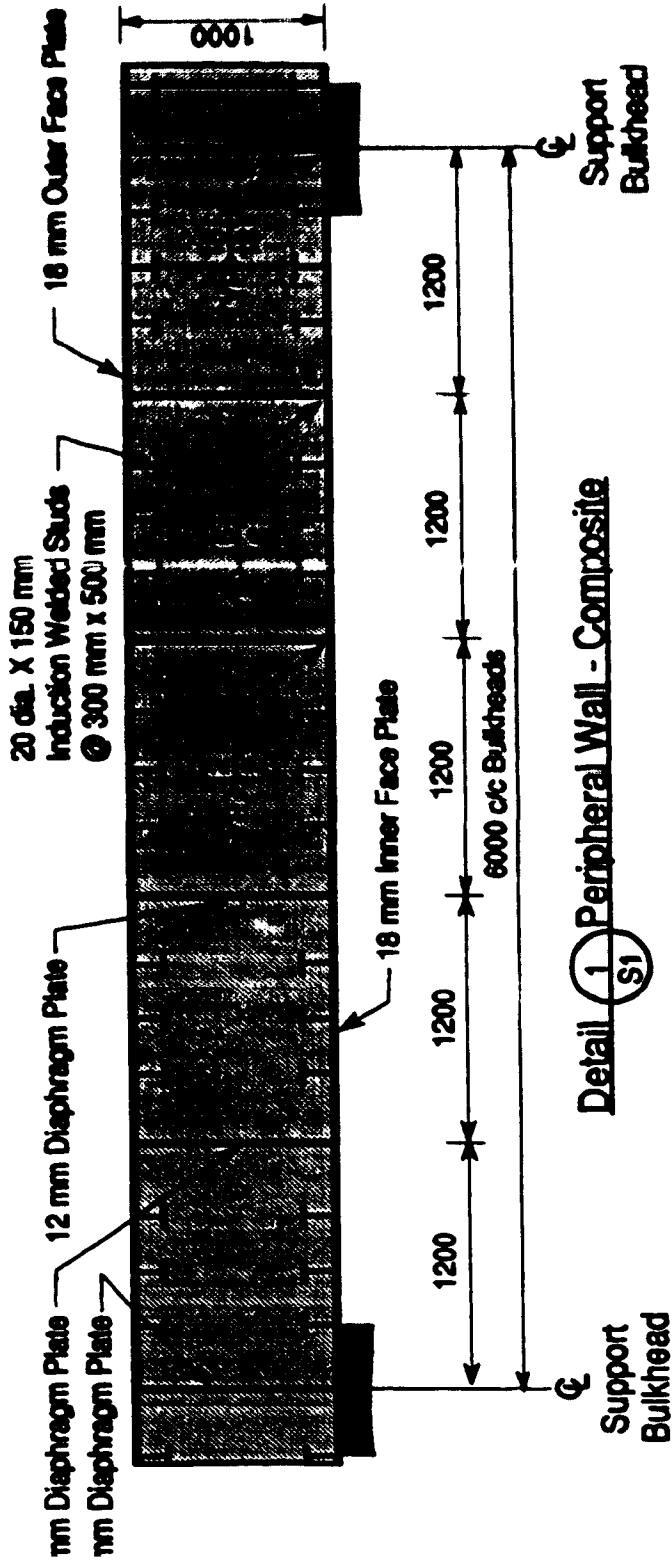
These cost comparisons were made assuming that the bulkhead support walls have no effect on the cost. However, one cannot truly evaluate the different types of structural systems based on their local structural capacity and cost alone. They are part of a structural system which includes diaphragms (support bulkheads), top deck and base slab. Therefore, a true cost comparison must look at the 3-D structure as a whole. Nonetheless, there is no doubt that the information generated by looking only at the outside wall is valuable in helping to determine which alternatives are the most attractive. The total structural cost however, is dependent on the cost of the bulkhead walls and particularly the connections between the exterior wall and the bulkhead walls.

7.3 Total Structural Cost

The major, over-riding, advantage to composite systems over reinforced concrete systems has to do with fabrication; since the steel shells can be fabricated and launched with minimum weight and draft, using a slipway, or shallow-draft basin, or even several barges temporarily fixed together. Such a system was used for the composite tunnel segments for the San Francisco BARTD Tube. Each segment was 90 m long; they were launched from a slipway into shallow water with all the reinforcing steel inside; then concreted afloat.

Appendix D presents a conceptual design for a bottom-founded fixed offshore structure which uses a composite wall of the type developed in this research work around its entire perimeter. The design concept was developed, in part, by the author for Gulf Canada Resources Ltd. as part of proprietary development studies for Gulf's Amaulikak field in the Beaufort Sea. Cost studies associated with that work revealed that the total cost of the composite perimeter wall is approximately 25% of the total cost of the structure; the supporting composite bulkhead walls make up an additional 17%.

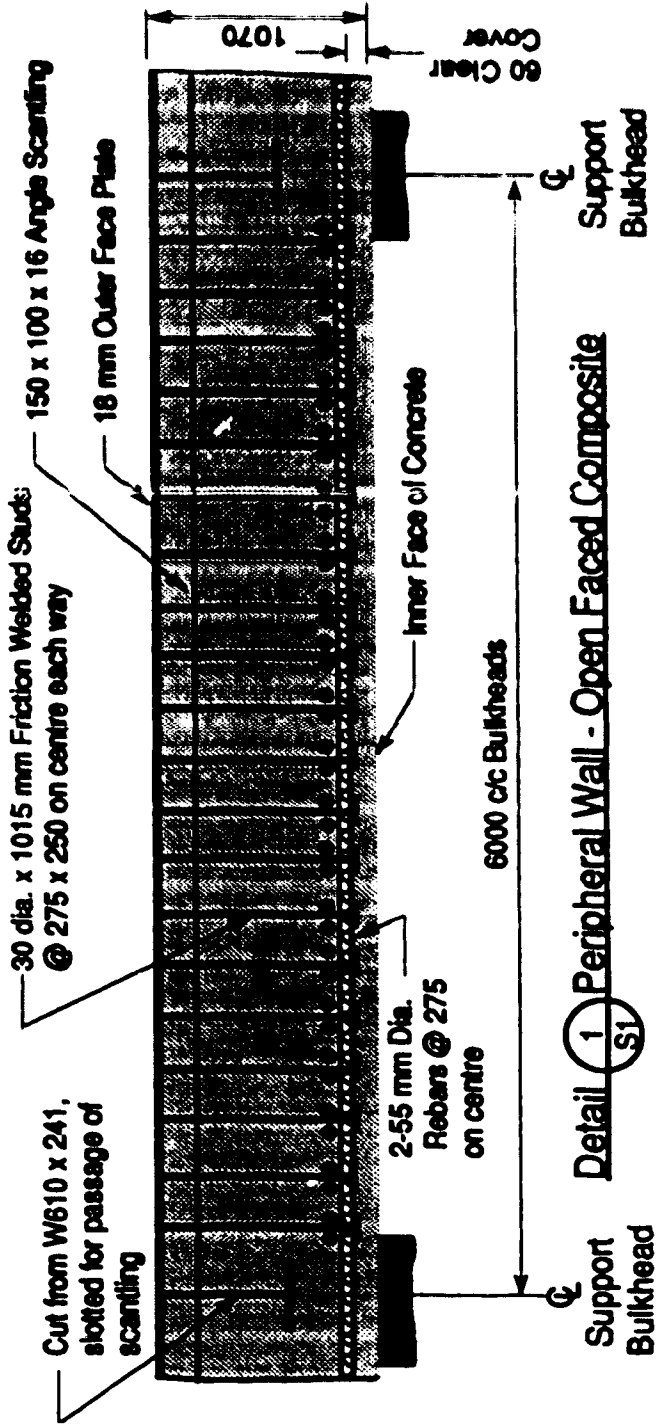
While the initial apparent cost savings of composite construction over reinforced concrete construction appears to be minimal, it does provide an additional viable alternative, with more options for construction location. This allows the owner of such a structure to be flexible in choosing a particular scheme to be used. Carrying this flexibility to the tendering stage will allow the marketplace to decide the most economical method of construction.



Material Requirements

- | | | |
|--------------------|--|------------------------|
| 1. Concrete : | compressive strength | 60 MPa |
| | density (semi-light) | 1850 kg/m ³ |
| 2. Reinforcement : | yield strength | 400 MPa |
| 3. Plate Steel : | yield strength
(Grade EH36) | 350 MPa |
| 4. Stud Steel : | yield strength
(studs longer than 200mm) | 470 MPa |
| | yield strength
(studs shorter than 200mm) | 350 MPa |

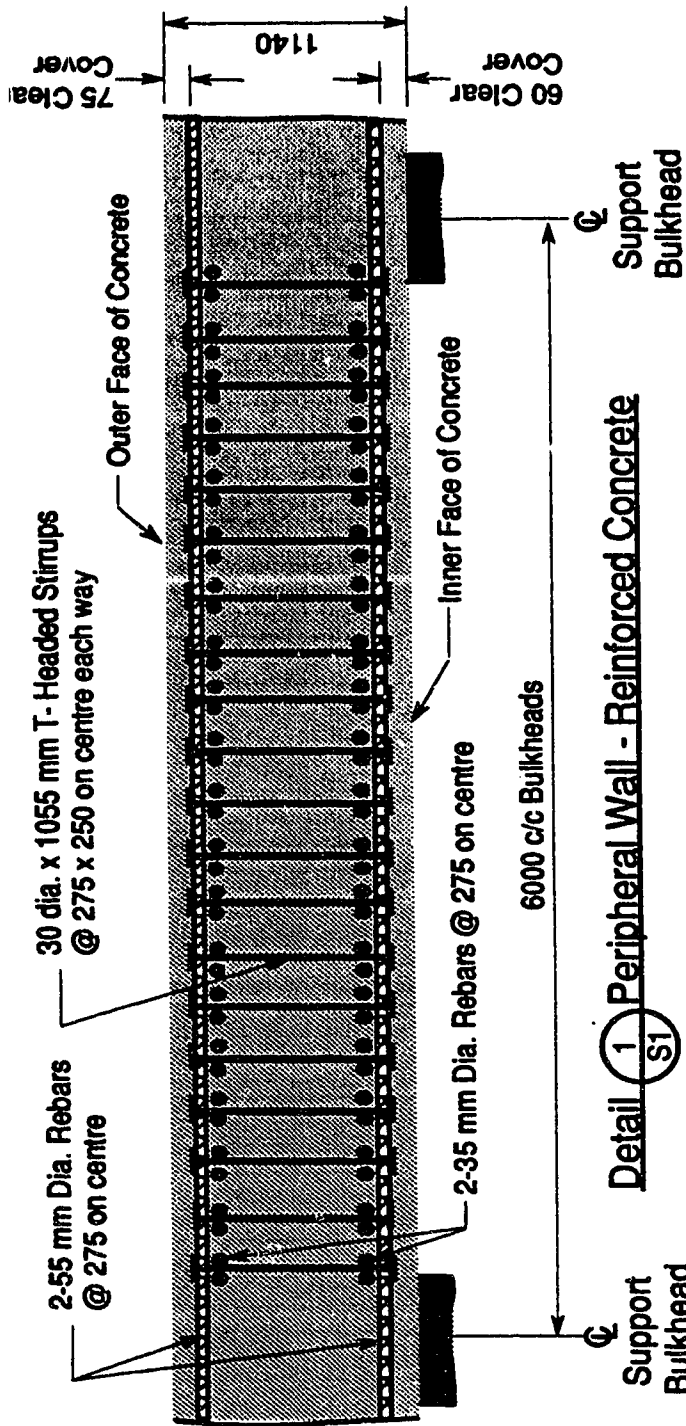
Figure 7.1 Composite Wall Alternative



Material Requirements

1. Concrete : compressive strength 60 MPa
density (semi-light) 1850 kg/m³
2. Reinforcement : yield strength 400 MPa
3. Plate Steel : yield strength 350 MPa
(Grade EH36)
4. Stud Steel : yield strength 470 MPa
(studs longer than 200mm)
yield strength 350 MPa
(studs shorter than 200mm)

Figure 7.2 Hybrid Wall Alternative



Material Requirements

1. Concrete : compressive strength 60 MPa_a
density (semi-light) 1850 kg/m³
2. Reinforcement : yield strength 400 MPa
3. Plate Steel : yield strength 350 MPa
(Grade EH36)
4. Stud Steel : yield strength 470 MPa
(studs longer than 200mm)
yield strength 350 MPa
(studs shorter than 200mm)

Figure 7.3 Reinforced Concrete Wall Alternative

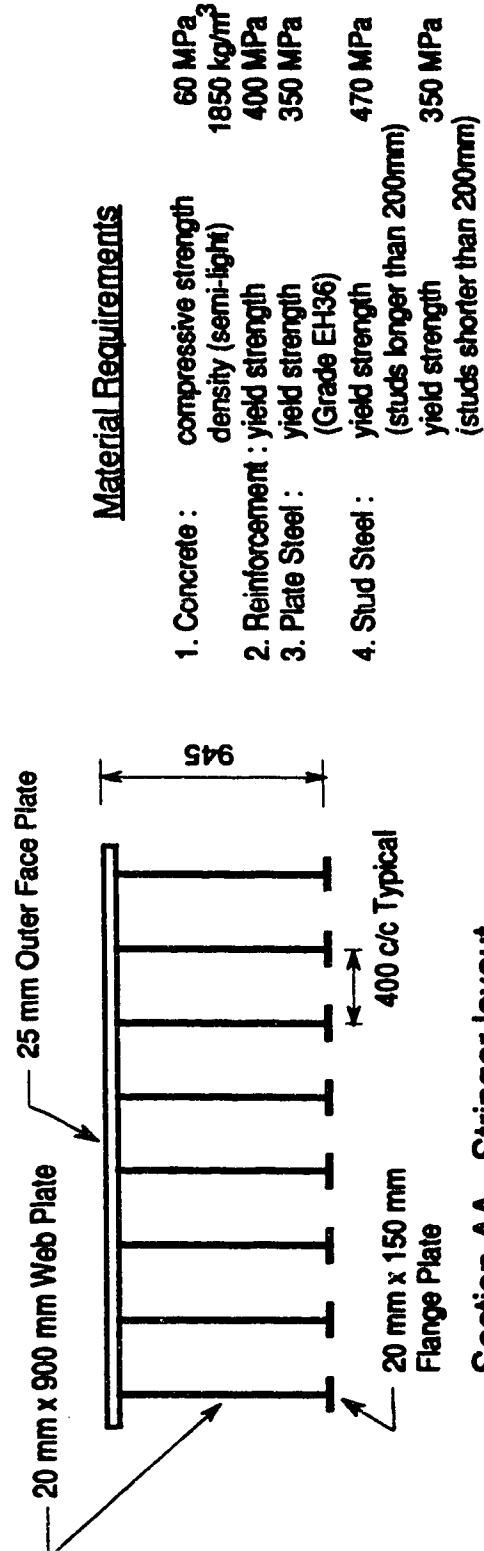
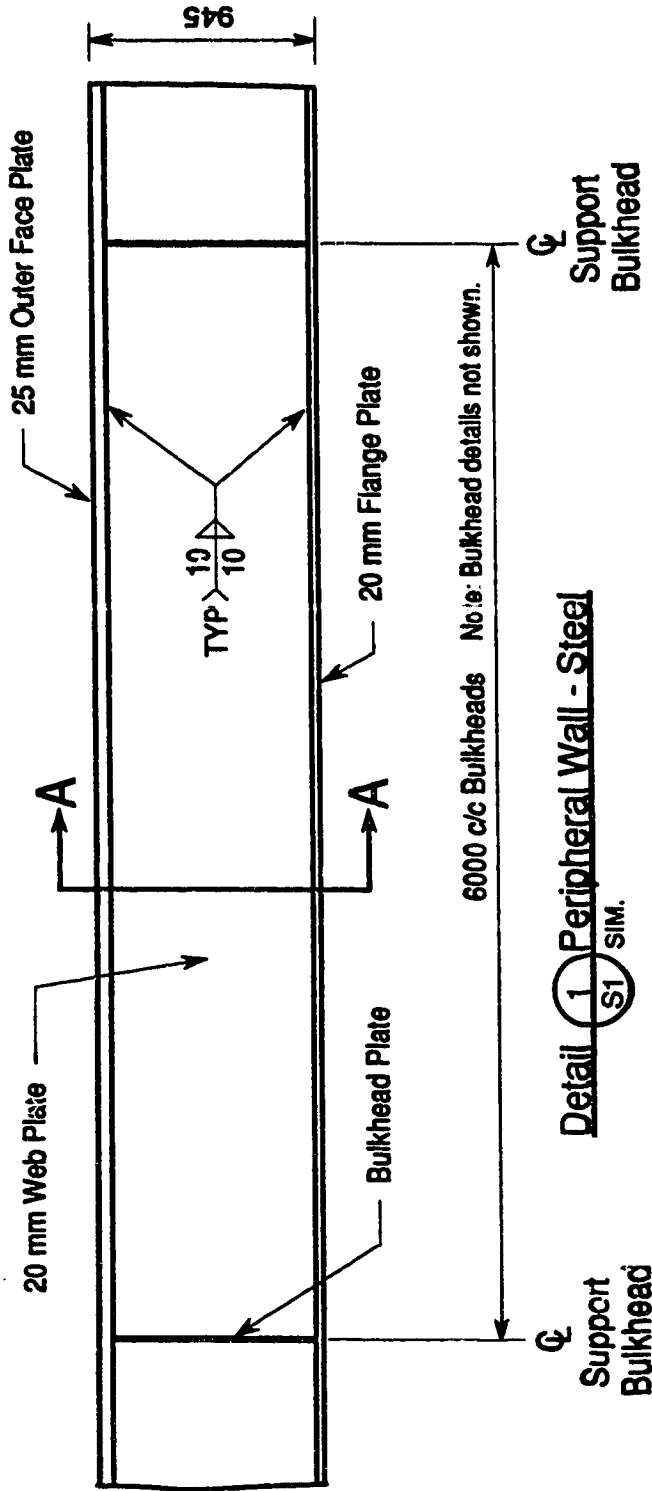


Figure 7.4 Structural Steel Wall Alternative

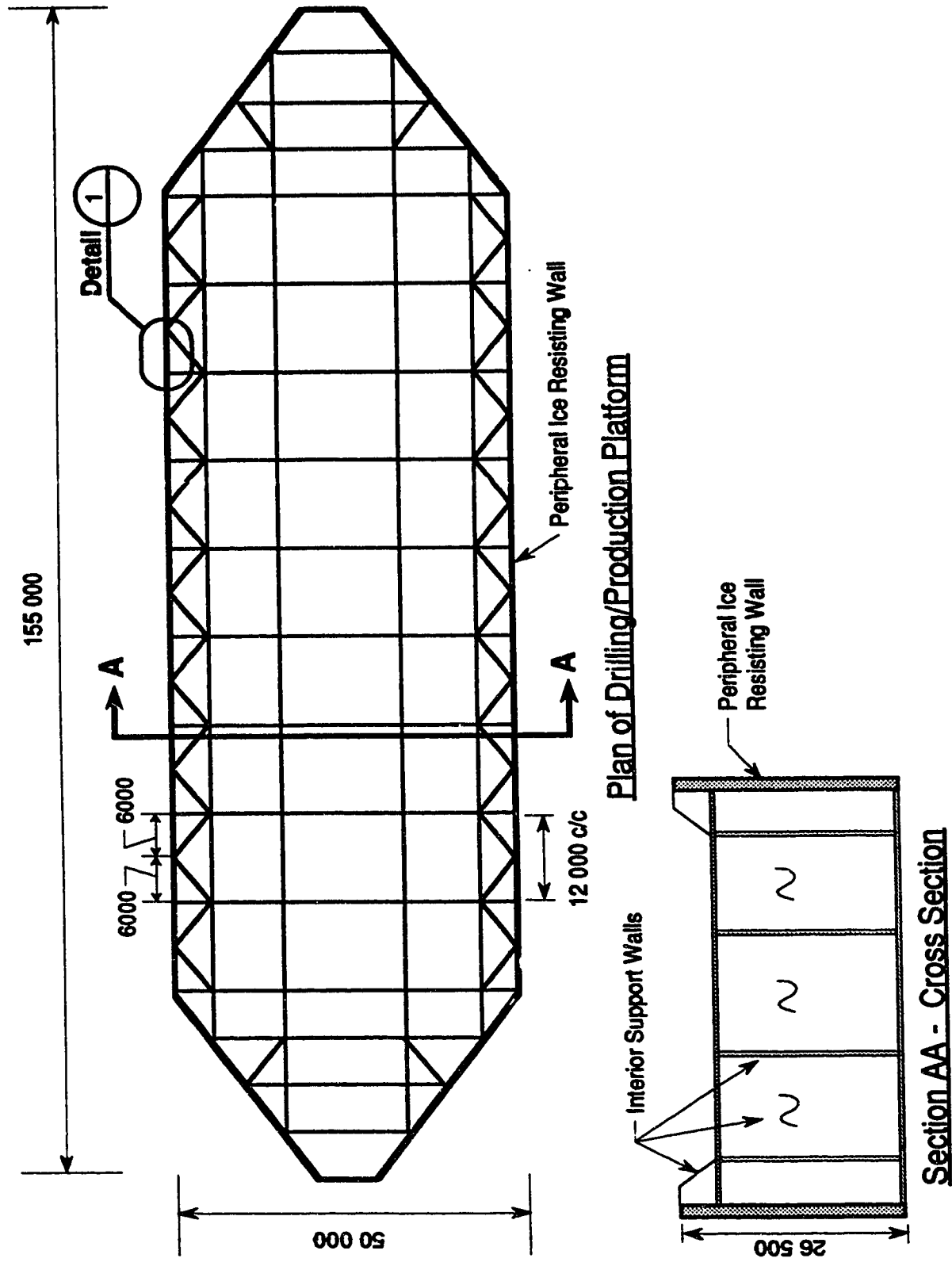


Figure 7.5 Vessel Schematic

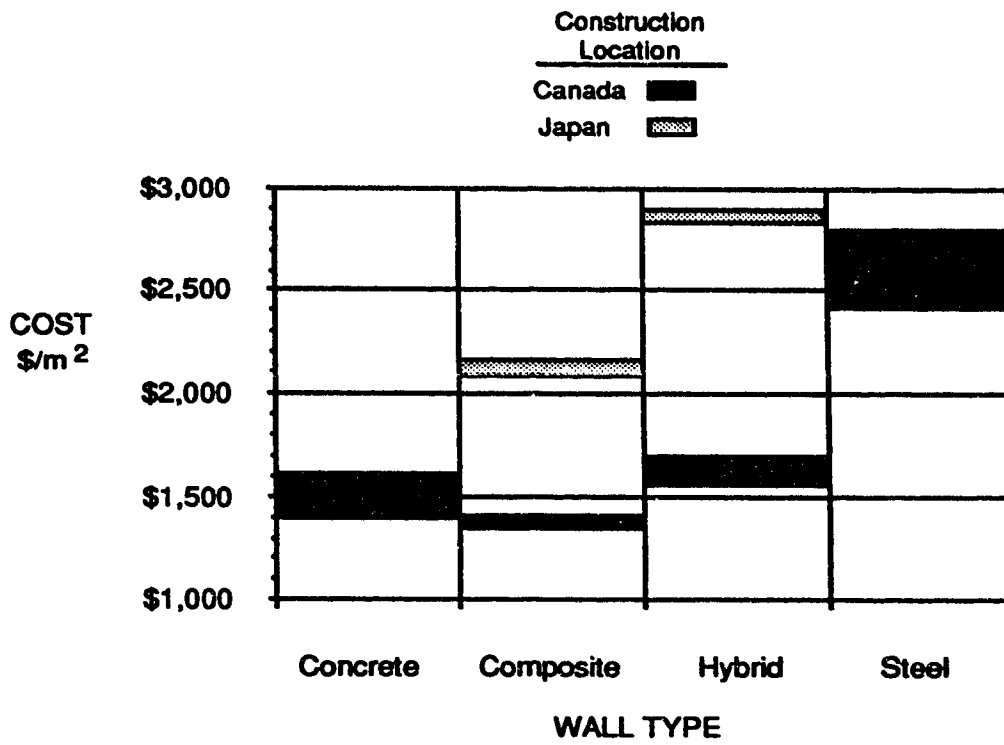


Figure 7.6 Cost Comparison for Peripheral Wall Alternatives

8.0 OTHER CONSIDERATIONS

8.1 Finite Element Method

The finite element work that has been conducted as part of this study was conducted under the indirect supervision of the author, but not by the author. The work was conducted by Dr. Rick Link, formerly a research engineer with C-FER. The work is only mentioned briefly here in order to illustrate the feasibility of doing finite element analysis (FEA) for composite walls and to direct the reader to other sources of information of a similar nature.

C-FER's FEA work is not the first such effort related to composite walls. A Japanese researcher, Mr. Matsuishi of the Hitachi Zosen Technical Research Laboratory, published FEA work in the 3rd report (Matsuishi, et.al., 1980a) on his composite wall research.

The work conducted at C-FER used the finite element program FEPARCS, written by Drs. Murray and Elwi of the University of Alberta's Civil Engineering Department. The program incorporates sophisticated models for both the steel and the concrete that enable the program to trace the load deformation behaviour to initial fracture and on to final collapse. In addition, the finite element model incorporates recently developed interface elements which simulate slippage at the steel-to-concrete boundaries. The basic finite element model used is shown in Figure 8.1. Load deflection curves for two of the specimens which were analysed (CF-2, flexural failure; and, CF-4, shear failure) are shown in Figures 8.2 and 8.3. Generally the test results are bounded by the two curves obtained from the FEA. One analysis assumed conditions of plane stress and the other, conditions of plane strain. As expected, the true behaviour falls somewhere in between. Work is continuing to improve the prediction.

The use of interface "slip" elements, combined with the ability to trace the "post-ultimate" response of a composite member which fails in shear, is a unique approach to the analysis of composite walls. It constitutes a significant step forward in the analytical study of the behaviour of this structural system.

8.2 Concrete Fatigue Due to Cyclic Loads

The concrete fatigue tests, which were conducted as an extension of this work, were planned and designed by the author and were conducted at the University of Alberta (U of A) and at the Technical Research Centre of Finland (VTT), in Helsinki. [This was possible because of a Joint Research Agreement which C-FER and VTT signed in 1987.] The U of A work was designed to consider the case of high-cycle, low-amplitude fatigue loading, while the VTT tests looked at low-cycled, high-amplitude fatigue.

8.2.1 Low-intensity, Long-term Fatigue

A single test was conducted at the U of A which was intended to simulate the cyclic load on an actual structure during 50 years of service, with 4 moderate ice events occurring per year of approximately 1000 cycles each. Gulf Canada's ice engineers have indicated that this is not unrealistic.

The specimen, shown in Figure 8.4, was loaded up to the point where well defined shear cracking occurred, at a total applied load of 1530 kN (5.7 MPa). The load was then lowered and cycled through 214,000 cycles between 500 kN and 1000 kN (1.9 and 3.8 MPa), 25% and 50% of the anticipated ultimate capacity of the specimen. This loading sequence represents the case in an actual structure where a one-time, large load cracks the wall, and the structure is then subject to more frequent cyclic loading of a lesser intensity for the remainder of its life.

The test turned out well; no visible deterioration took place during the load cycling. A small increase in permanent deflection did take place, however, this small amount of permanent deformation over the life of the structure is considered insignificant. On completion of the cyclic testing, the specimen was loaded to failure. Failure occurred at a load of 2050 kN (7.7 MPa), which compared well with the failure load of a control specimen (no fatigue cycles), which failed at 2090 kN (7.8 MPa). A load-deflection curve for the fatigue specimen is shown in Figure 8.5.

8.2.2 High-intensity, Single-event Fatigue

The tests conducted at VTT treated a different cyclic loading condition; low-cycle, high-amplitude fatigue loading. During a single large magnitude ice event, an ice load

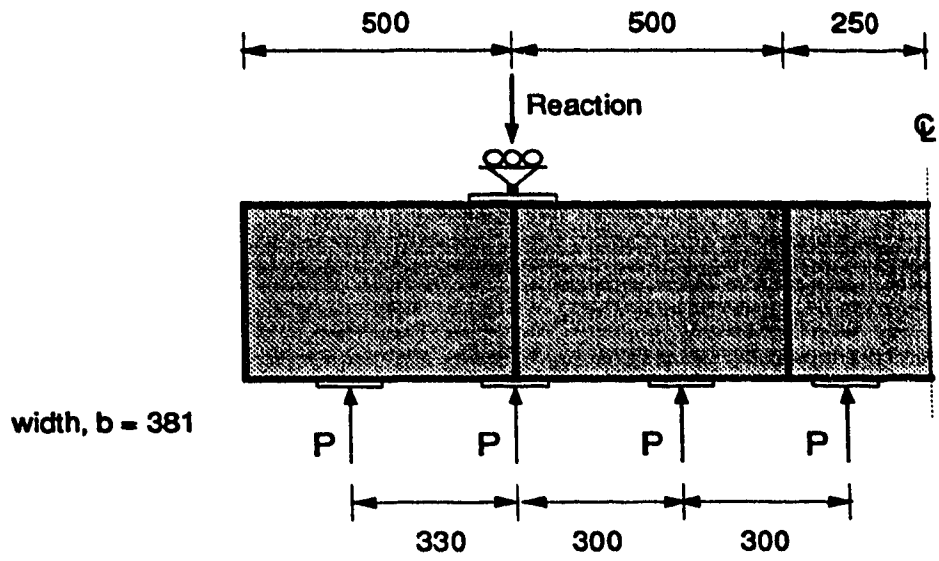
could occur which would repeatedly load a wall member into the plastic response range (close to ultimate capacity), resulting in the potential for a progressive collapse type of failure. This type of low-cycle fatigue load would be expected to occur very few times during the life of a structure, and is quite different in nature from the 200,000 cycle, lower-intensity fatigue load.

Two fatigue specimens were tested at VTT, giving similar results; only one test is presented here. The test set-up, which was similar to the U of A test, is shown in Figure 8.6. The specimen was loaded to 1700 kN in static load steps and was then cycled through 2000 cycles of load ranging between 900 kN and 1700 kN (46% and 86% of the ultimate capacity). Following the load cycling, the specimen was loaded to failure, which occurred at a load of 1962 kN. This can be compared to the statically loaded, control specimen, which failed at a load of 1866 kN (5% lower than the fatigue specimen).

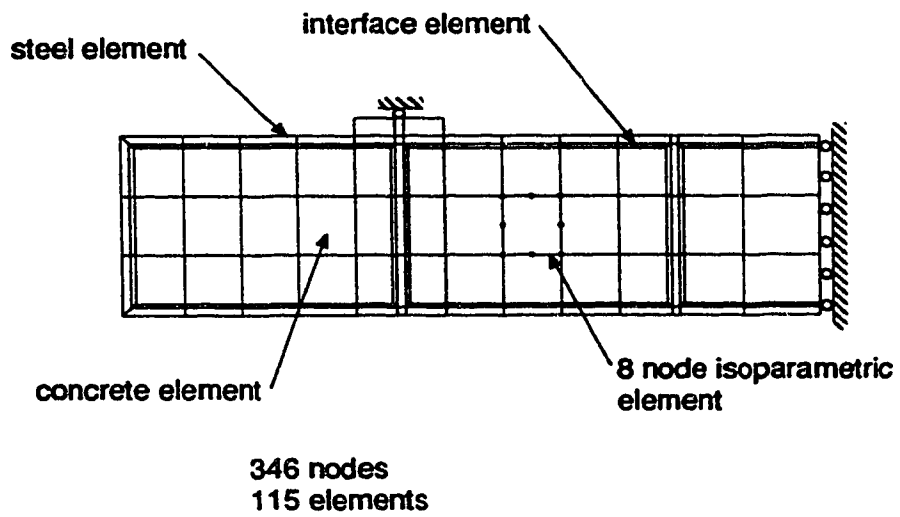
Again, no deterioration was evident as a result of the load cycling. As shown in the load-deflection curve in Figure 8.7, the increase in permanent deflection which occurred during load cycling was minor.

8.2.3 Summary of Fatigue Tests

The results of the two fatigue tests suggest that cyclic loading has no detrimental effect on the performance of this type of composite wall. While the results of only a few tests cannot be considered conclusive, they are certainly encouraging.



(a) Dimensions for Specimen CF-4



(b) Finite Element Mesh for Specimen CF-4

Figure 8.1 Composite Beam Finite Element Model

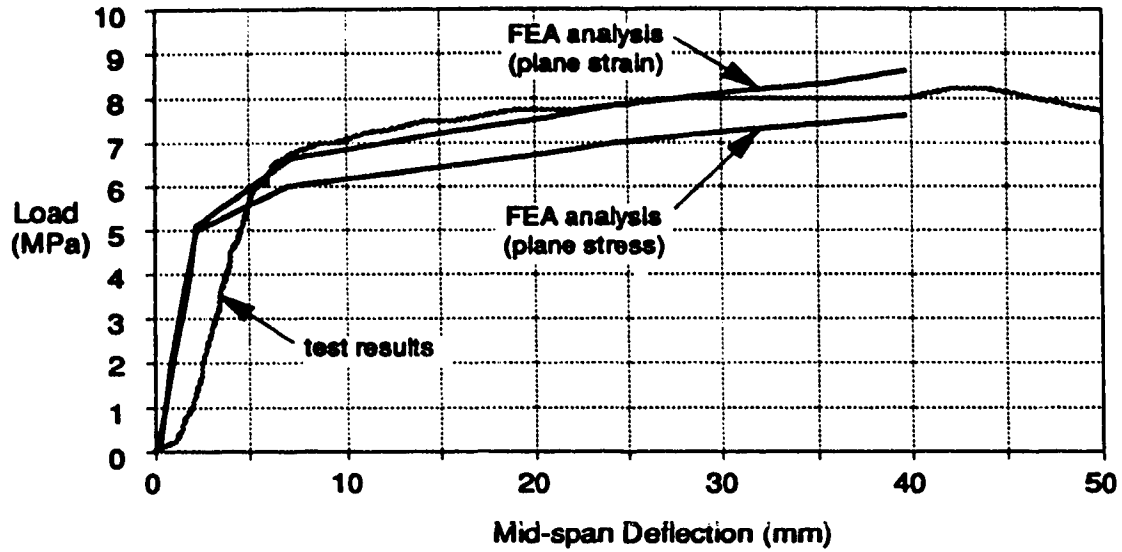


Figure 8.2 Load-deflection Plot for Specimen CF-2 (flexural failure)

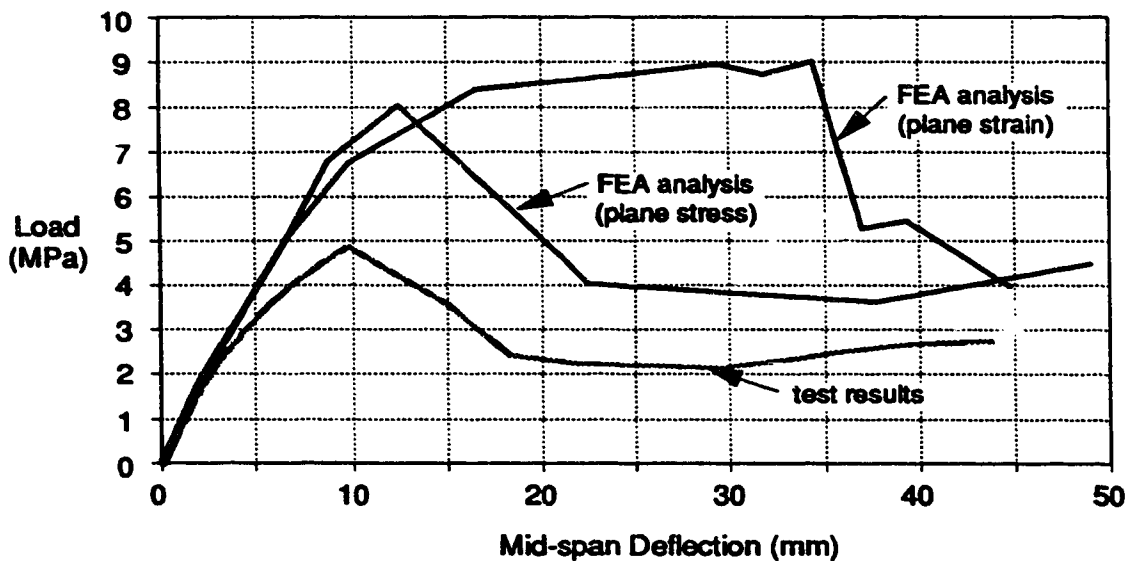


Figure 8.3 Load-deflection Plot for Specimen CF-4 (shear failure)

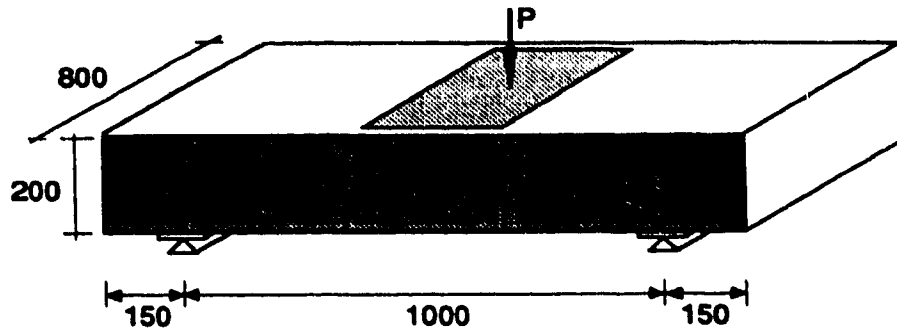


Figure 8.4 High-cycle Low-amplitude Fatigue Specimen (tested at University of Alberta)

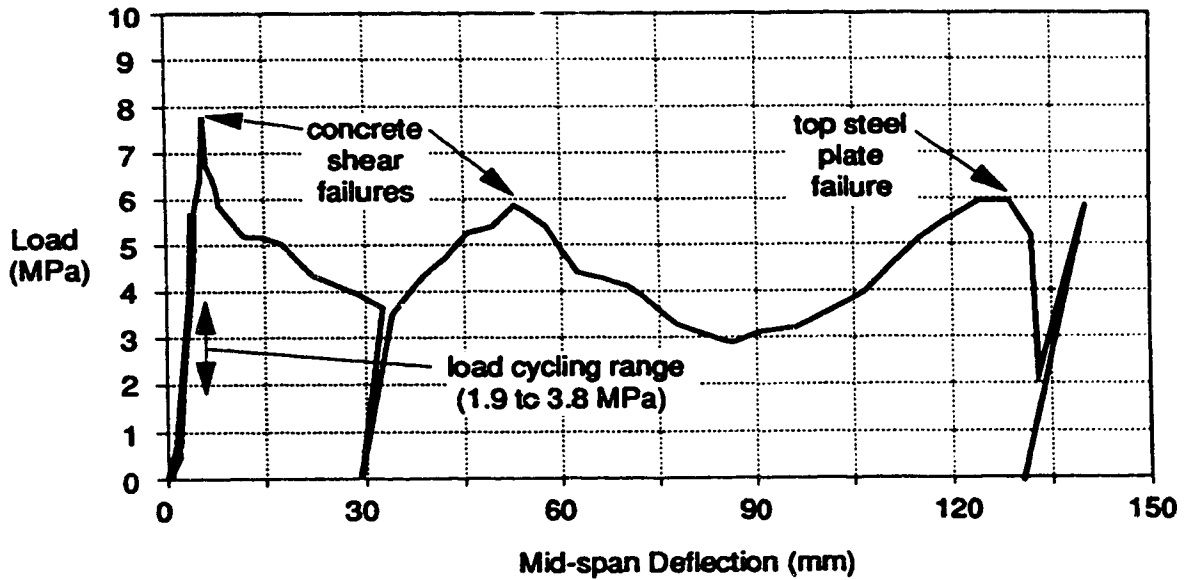


Figure 8.5 Load-deflection Plot for High-cycle Low-amplitude Fatigue Specimen

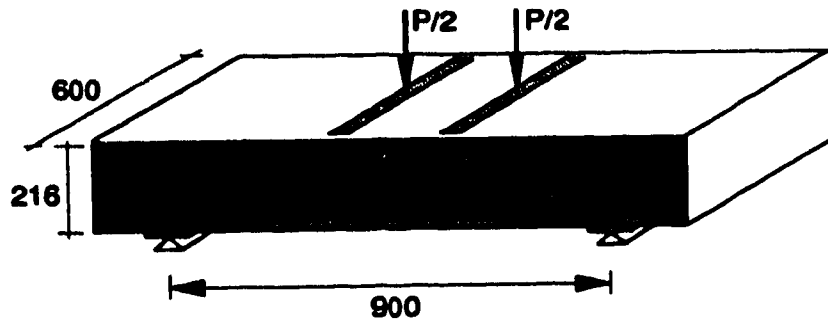


Figure 8.6 Low-cycle High-amplitude Fatigue Specimen (tested at Technical Research Centre of Finland)

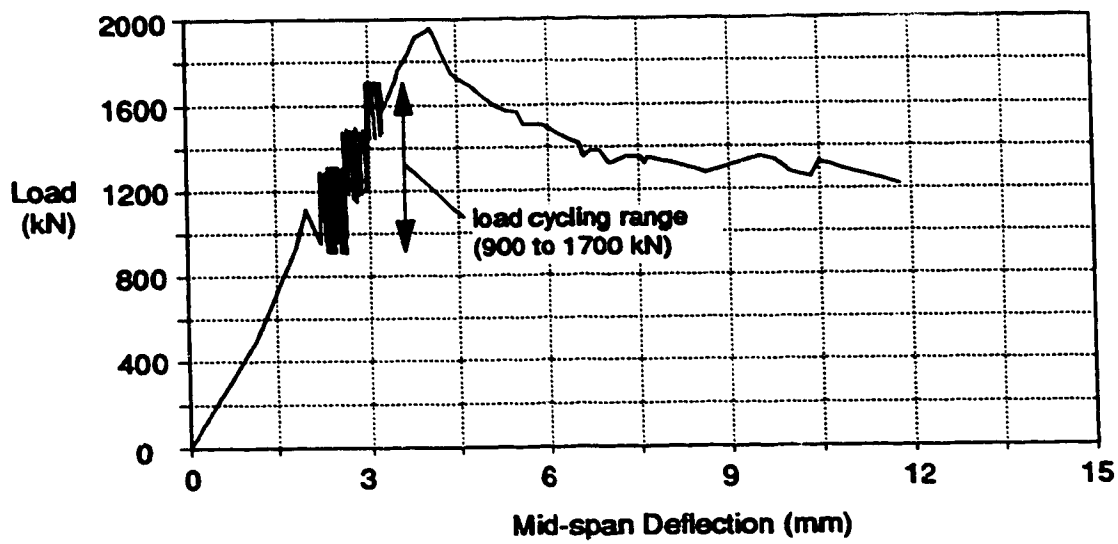


Figure 8.7 Load-deflection Plot for Low-cycle High-amplitude Fatigue Specimen

9.0 CONCLUSIONS

This research work has shown that a composite ice-resisting wall can be constructed which is simple from a fabrication and construction point of view and which also satisfies the high strength and ductility requirements for a structure of this type.

The most notable feature of the wall is its simplicity. The outer and inner steel plates are fastened together with continuous, vertical steel diaphragms which are at a relatively wide spacing. There are no other welded details in the wall. This results in a significant reduction in labour-intensive welding, compared to a conventional, all-steel wall. The steel frame is self-supporting and therefore requires no additional formwork when concrete is poured. There is no additional reinforcing steel required, beyond that provided by the external steel plates and the diaphragm plates.

Tests have shown the wall to possess high strength in both flexure, shear and "punching" shear and to exhibit a very ductile mode of failure when the ultimate capacity of the wall is exceeded. Further, the tests have shown that the wall can develop this ductile mode of failure in shear, as well as in flexure. The typical mode of shear failure initially involved crushing of the concrete core at either end of a major diagonal shear crack extending from one side of the wall to the other between diaphragm plates. The post-failure response depended on the diaphragm plate spacing and exterior plate thickness. It was often ductile due to the confining effect of the steel shell on the concrete core, as well as catenary action in the steel plates, both of which allowed load to continue to be carried to the supports across the zones of crushed concrete.

A design approach has been presented which is consistent with the generally accepted engineering principles used in reinforced concrete design, utilizing empirical equations, lower bound plasticity methods and upper bound energy methods. The methods showed good agreement with test results and are also consistent with the provisions contained in the new CSA Preliminary Standard for the Design, Construction and Installation of Fixed Offshore Structures.

The main conclusion of this work is that a steel-concrete composite sandwich wall is a viable concept, both technically and economically, which provides an alternative to

Conclusions

132

reinforce concrete or structural steel for constructing the peripheral, ice-resisting wall of an Arctic offshore structure.

10.0 REFERENCES

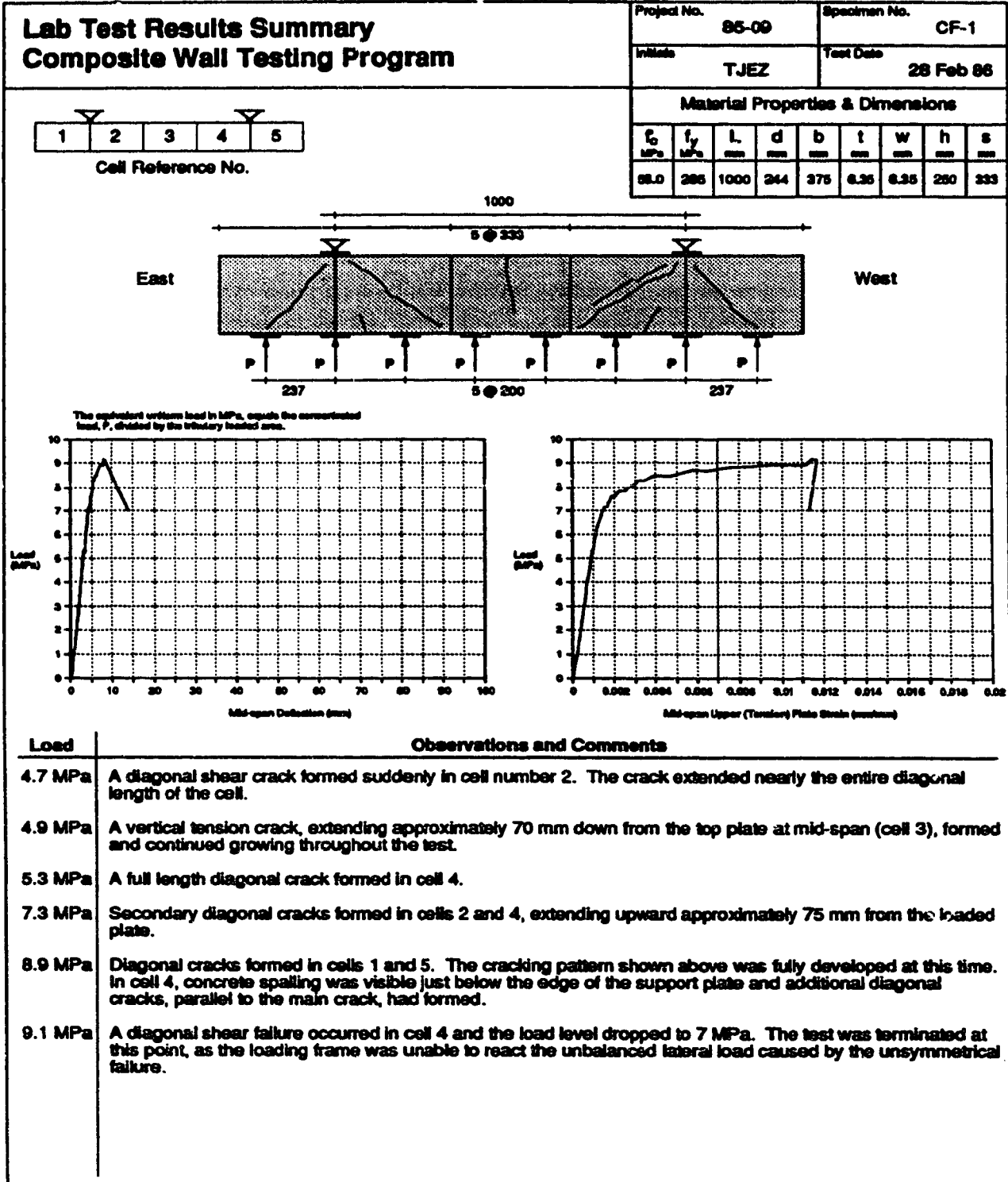
- Adams, P.F., Zimmerman, T.J.E. and MacGregor, J.G. 1988. **Design and Behaviour of Ice-Resisting Walls.** ACI Second International Conference on Performance of Concrete in Marine Environment, St. Andrew by-the-Sea, New Brunswick, Canada.
- Adams, P.F., Zimmerman, T.J.E. and MacGregor, J.G. 1987. **Design and Behaviour of Composite Ice-Resisting Walls.** C-FER Special Publication No. 1, Steel/Concrete Composite Structural Systems, C-FER, Edmonton.
- ACI Standard 318-83. 1983. **Building Code Requirements for Reinforced Concrete.** American Concrete Institute, Detroit, Michigan.
- ACI-ASCE Committee 426. 1973. **The Shear Strength of Reinforced Concrete Members - Chapters 1-4.** Proceedings ASCE, Journal of the Structural Division, Vol. 99, No. ST6, June.
- Allyn, N.F.B. 1986. **Global and Local Ice Loads Including Dynamic Effects.** Canada Oil and Gas Lands Administration, Ice/Structure Interaction, PERD Task 6.2, Program Evaluation Workshops Proceedings, May-June, Calgary, Alberta, Canada.
- Bruce, J.C. and Roggensack, W.D. 1984. **Second Generation Arctic Platforms; Lessons from First Generation Design Experience.** OTC Paper 4798, Offshore Technology Conference, Houston.
- Canadian Standards Association. 1977. **Standard CAN3-A23.3-M77. Design of Concrete Structures for Buildings.** Canadian Standards Association, Rexdale, Ontario.
- Canadian Standards Association. 1984. **Standard CAN3-A23.3-M84. Design of Concrete Structures for Buildings.** Canadian Standards Association, Rexdale, Ontario.
- Canadian Standards Association. 1992. **CAN/CSA-S474-92, Concrete Structures, part of the Code for the Design, Construction and Installation of Fixed Offshore Structures.** Canadian Standards Association, Rexdale, Ontario.
- Canadian Standards Association. 1992. **CAN/CSA-S473-92, Steel Structures, part of the Code for the Design, Construction and Installation of Fixed Offshore Structures.** Canadian Standards Association, Rexdale, Ontario.
- CEB-FIP. 1978. **Model Code for Concrete Structures.** CEB-FIP International Recommendations, Third Edition, Paris, France.
- Chen, W.F. 1982. **Plasticity in Reinforced Concrete.** McGraw-Hill Book Company, New York.

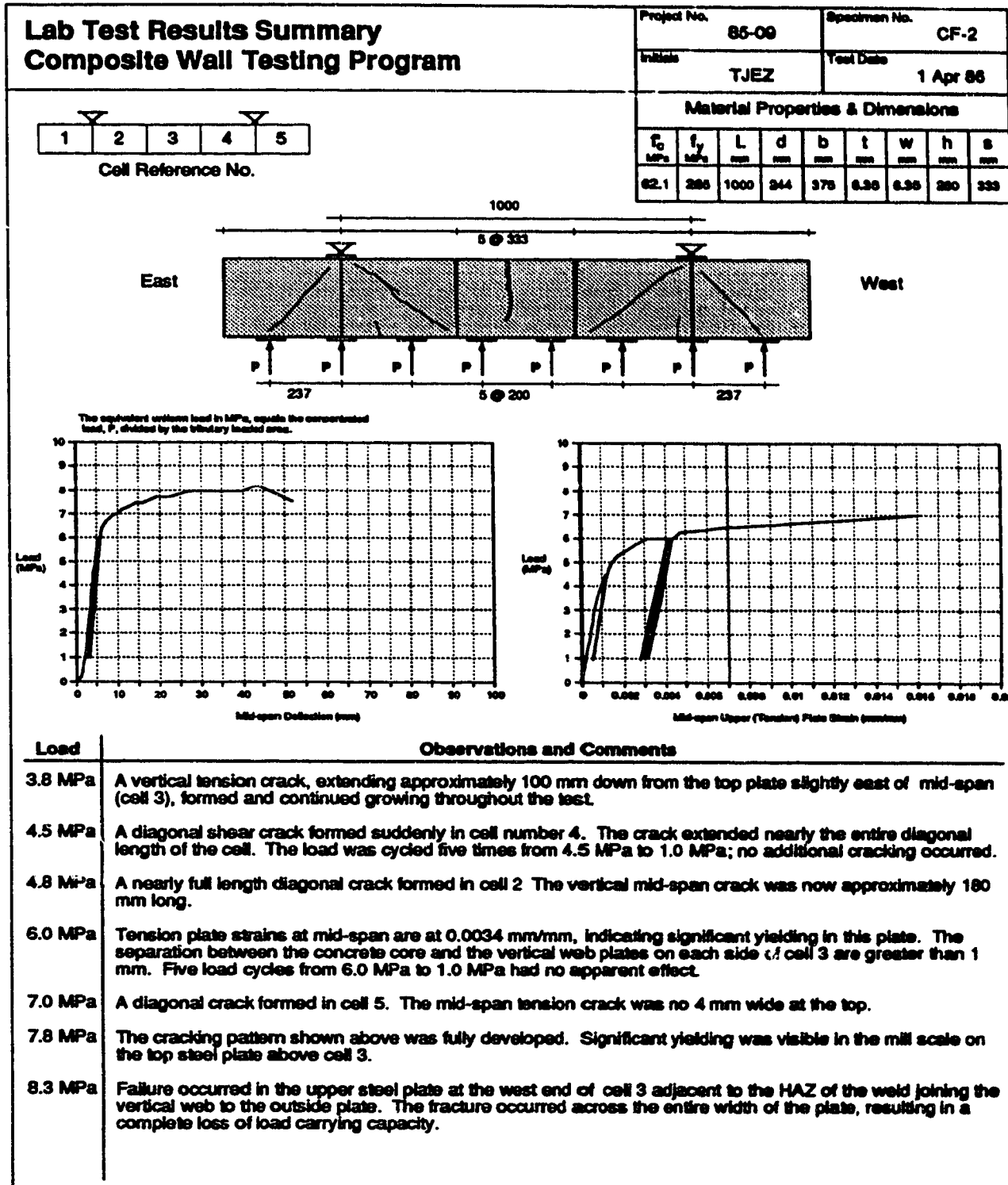
- Collins, M.P. and Mitchell, D. 1980. Shear and Torsion Design of Prestressed and Non-Prestressed Concrete Beams. *Journal of the Prestressed Concrete Institute*, January/February, Vol. 21, No. 1, Chicago, Illinois.
- Csagoly, P.F., Holowka, M., and Dorton, R. 1978. The True Behaviour of Thin Concrete Slabs. TRR664, Transportation Research Board, Washington, D.C., September.
- Croasdale, K.R. 1984. Sea Ice Mechanics: A General Overview. *Marine Technology Society Journal*, Vol. 18.
- Fitzpatrick, J. 1983. The Single Steel Drilling Caisson - A Novel Approach to Bottom Founded Structures in Arctic Waters. Society Petroleum Engineers, 53 Annual Technical Conference, San Francisco.
- Gerwick, B.C. and Berner, D. 1987. Utilization of Composite Design in the Arctic and Sub-Arctic. C-FER Special Publication No. 1, Steel/Concrete Composite Structural Systems.
- Gerwick, B.C. 1985. Lessons from an Exciting Decade of Concrete Sea Structures. *Concrete International: Design and Construction*, August.
- Hattori, Y., Ishihama, T., Yamamoto, T., Matsuishi, M. and Iwata, S. 1985. On the Ultimate Strength of Composite Steel-Concrete Structures. POAC 85, 8th International Conference on Port and Ocean Engineering Under Arctic Conditions, Proceedings, Narssarssuaq, Greenland.
- Leonhardt, F. and Walther, R. 1964. The Stuttgart Shear Tests, 1961. Translation No. 111, Cement and Concrete Association, London.
- Marcellus, R.W., Morrison, T.B., Allyn, N.F.B., Croasdale, K.R., Iyer, H.S. and Tseng, J. 1988. Ice Forces on Marine Structures, Volume 2, Discussions. Publication No. W62-11/88-5-2E, Public Works Canada, Ottawa, Ontario.
- Marti, P. 1985. Basic Tools of Reinforced Concrete Beam Design. *ACI Journal*, January-February.
- Matsuishi, M., Takeshita, H., Suhara, T., Nishimaki, K. and Iwata, S. 1977a. On Strength of New Composite Steel-Concrete Material for Offshore Structure. OTC Paper 2804, Offshore Technology Conference, Houston.
- Matsuishi, M., Takeshita, H., Suhara, T., Nishimaki, K. and Iwata, S. 1977b. On the Strength of Composite Steel-Concrete Structure of a Sandwich System (1st Report). *Hitachi Zosen Technical Review*, Vol. 38. Sept.
- Matsuishi, M., Takeshita, H., Suhara, T., Nishimaki, K. and Iwata, S. 1978. On the Strength of Composite Steel-Concrete Structure of a Sandwich System (2nd Report). *Hitachi Zosen Technical Review*, Vol. 39, March.

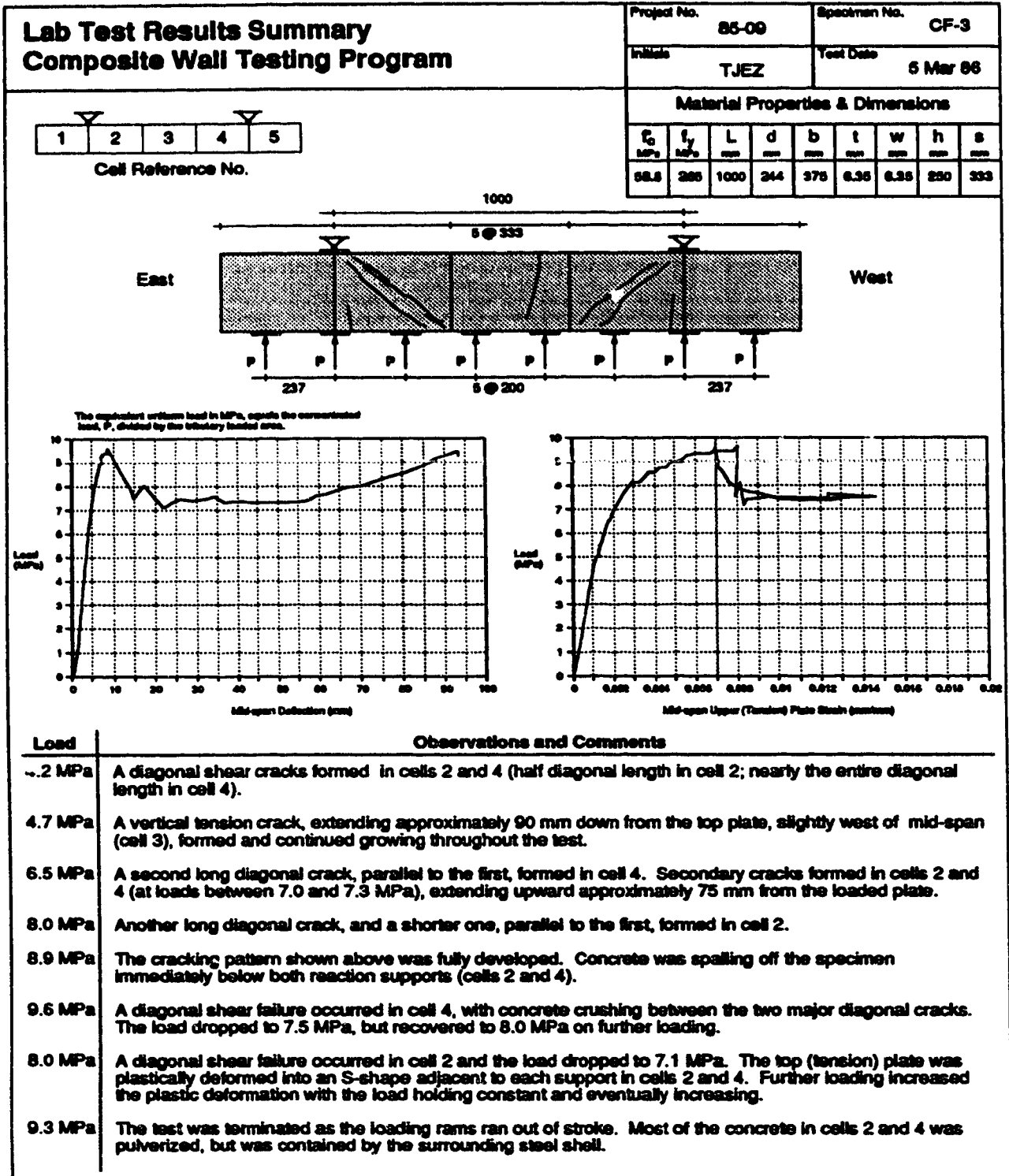
- Matsuishi, M., Nishimaki, K., Iwata, S., and Suhara, T. 1980a. On the Strength of Composite Steel-Concrete Structure of a Sandwich System (3rd Report). Hitachi Zosen Technical Review, Vol. 40, March.
- Matsuishi, M., Nishimaki, K., Iwata, S., and Suhara, T. 1980b. On the Strength of Composite Steel-Concrete Structure of a Sandwich System (4th Report). Hitachi Zosen Technical Review, Vol. 41, December.
- Matsuishi, M. and Iwata, S. 1987. Strength of Composite Sandwich System Ice-Resisting Structures. C-FER Special Publication No. 1, Steel/Concrete Composite Structural Systems.
- Morrison, T.B., Marcellus, R.W., Allyn, N.F.B. and Tseng, J. 1988. Ice Forces on Marine Structures, Volume 1, Calculations. Publication No. W62-11/88-5-1E, Public Works Canada, Ottawa, Ontario.
- Nessim, M.A., Hong, H.P., Zimmerman, T.J.E. and DeGeer, D.D. 1990. Calibration of Material Resistance Factors in CSA S474-M1989. C-FER Report, Project No. 89-25, December.
- Nielsen, M.P. 1984. Limit Analysis and Concrete Plasticity. Prentice-Hall, Inc., Englewood Cliffs, New Jersey.
- Nielsen and Braestrup. 1978. Shear Strength of Prestressed Concrete Beams Without Web Reinforcement. Magazine of Concrete Research, Vol. 30, No. 104. September.
- Niwa, J. 1984. Equation for Shear Strength of Reinforced Concrete Deep Beams Based on FEM Analysis. Concrete Library International of Japan Society of Civil Engineers, No. 4, December.
- Nojiri, Y. and Koseki, K. 1986. Structural Behavior and Design Method of Steel/Concrete Composite Ice Walls for Arctic Offshore Structures. OTC Paper 5292, Offshore Technology Conference, Houston, Texas.
- O'Flynn, B. 1987. Composite Ice-Resisting Walls. Ph.D. Thesis, University of Alberta, Edmonton, Alberta
- O'Flynn, B. and MacGregor, J.G. 1987. Tests on Composite Ice-Resisting Walls. C-FER Special Publication No. 1, Steel/Concrete Composite Structural Systems.
- Ohno, F., Shioya, T., Nagasawa, Y., Matsumoto, G., Okada, T. and Ota, T. 1987. Experimental Studies on Composite Members for Arctic Offshore Structures. C-FER Special Publication No. 1, Steel/Concrete Composite Structural Systems.
- Rogowski, D.M. 1983. Shear Strength of Deep Reinforced Continuous Beams. Ph.D. Thesis, University of Alberta, Edmonton, Alberta.

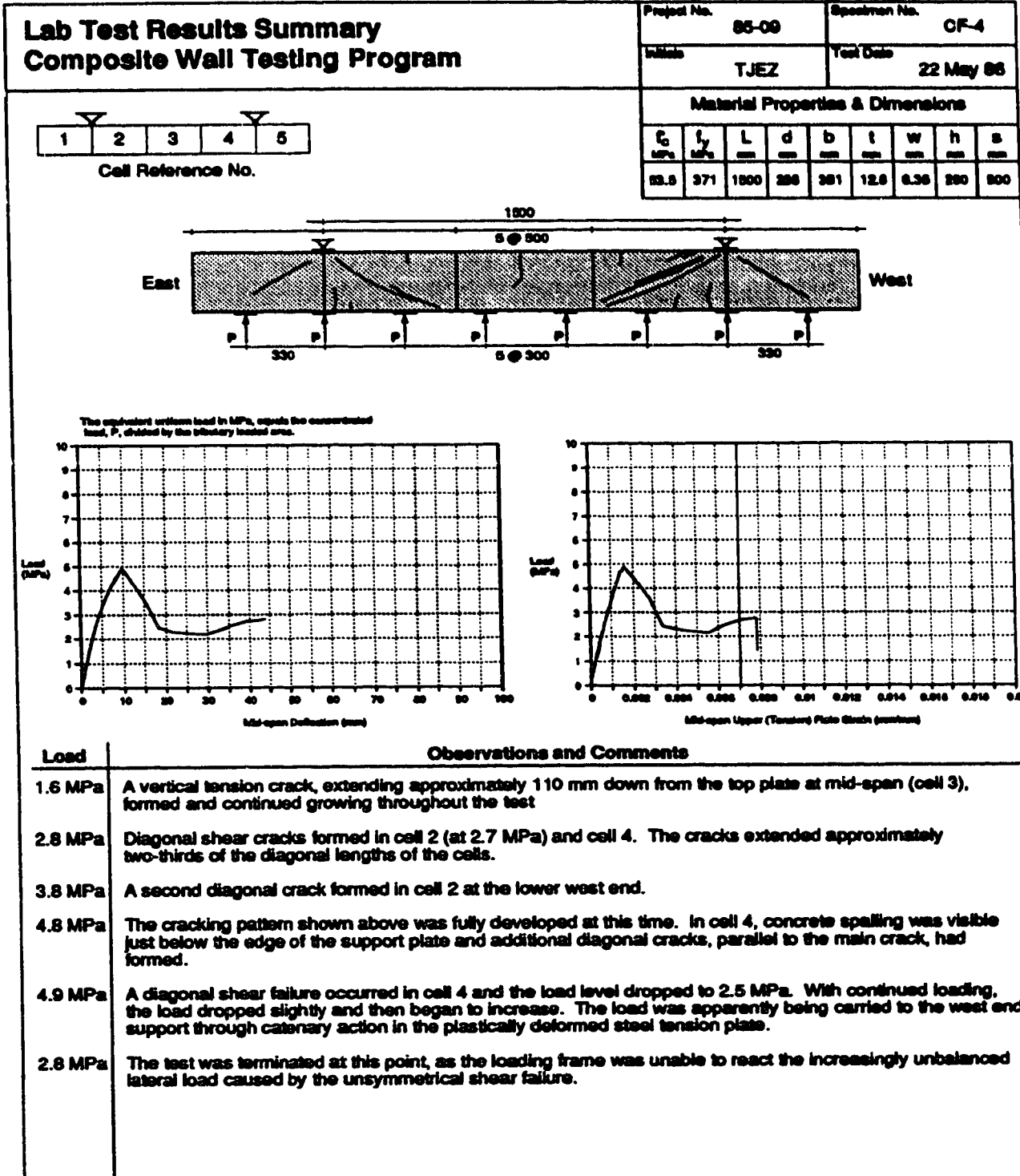
- Rogowski, D.M. and MacGregor, J.G. 1986. Design of Reinforced Concrete Deep Beams. *Concrete International: Design and Construction*, Vol. 8, No. 8, August.
- Rojansky, M. and Hsu, Y. 1985. An Icy Challenge. *Concrete International*, August.
- Sanderson, T.J.O. 1988. *Ice Mechanics: Risks to Offshore Structures*. Graham and Trotman Ltd., London.
- Schlaich, J., Schafer, K., and Jennewein, M. 1987. Toward a Consistent Design of Structural Concrete. *Journal of the Prestressed Concrete Institute*, Vol. 32, No. 3, May/June, Chicago, Illinois.
- Shioya, T., Matsumoto, G., Okada, T. and Ota, T. 1986. Development of Composite Members for Arctic Offshore Structures. POLARTECH '86, VTT Symposium 71, Helsinki, Finland.
- Smith J.R. and McLeish, A. 1987. Resistance of Composite Steel/Concrete Structures to Localized Loading. C-FER Special Publication No. 1, Steel/Concrete Composite Structural Systems.
- Zinserling, W. and Cichanski, W. 1986. Economical Arctic Structures Using Concrete. OMAE, Fifth International Offshore Mechanics and Arctic Engineering Symposium, Tokyo, Japan.
- Zsutty, T. 1968. Beam Shear Strength Prediction by Analysis of Existing Data. *American Concrete Institute Journal*, Vol. 65, November.

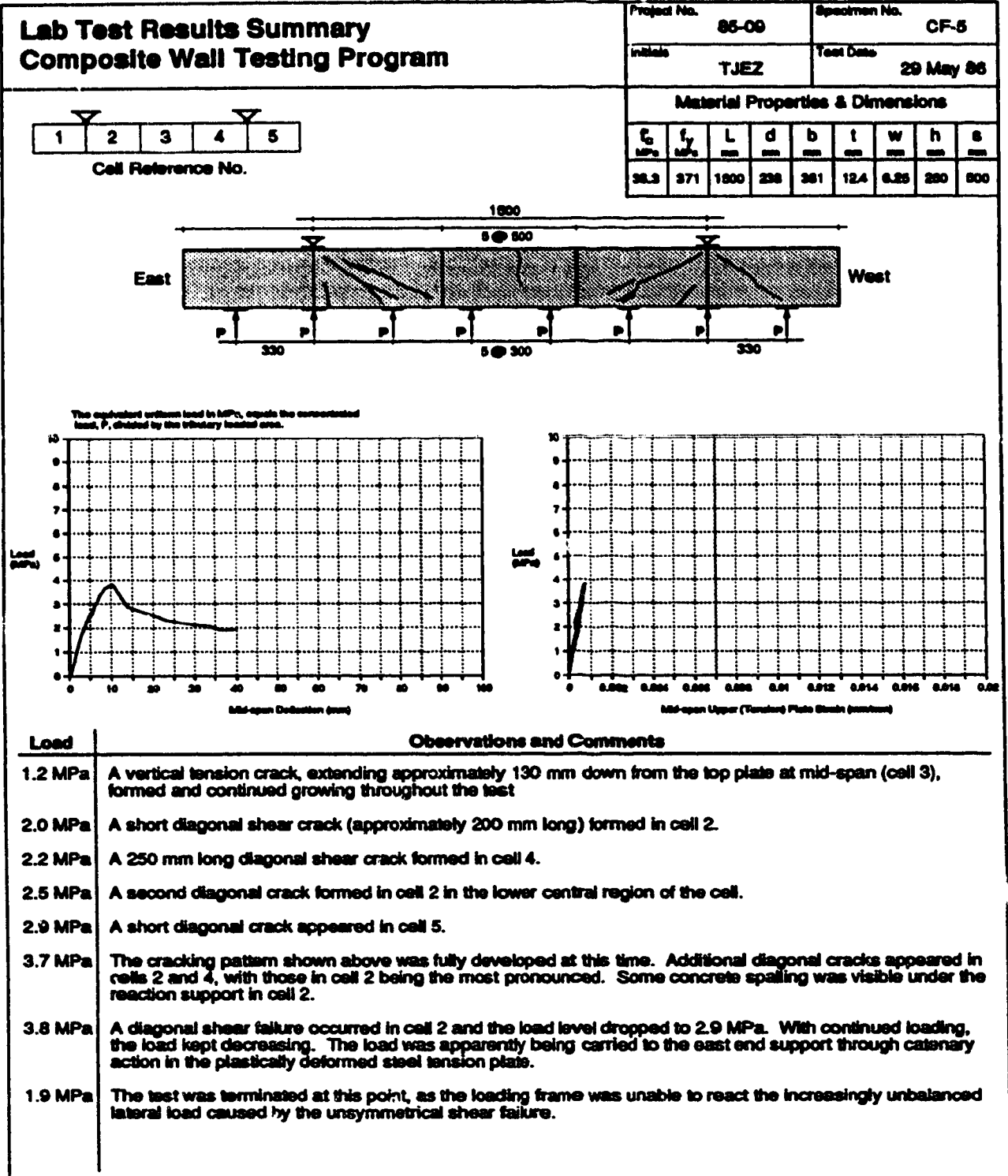
APPENDIX A - DETAILED RESULTS

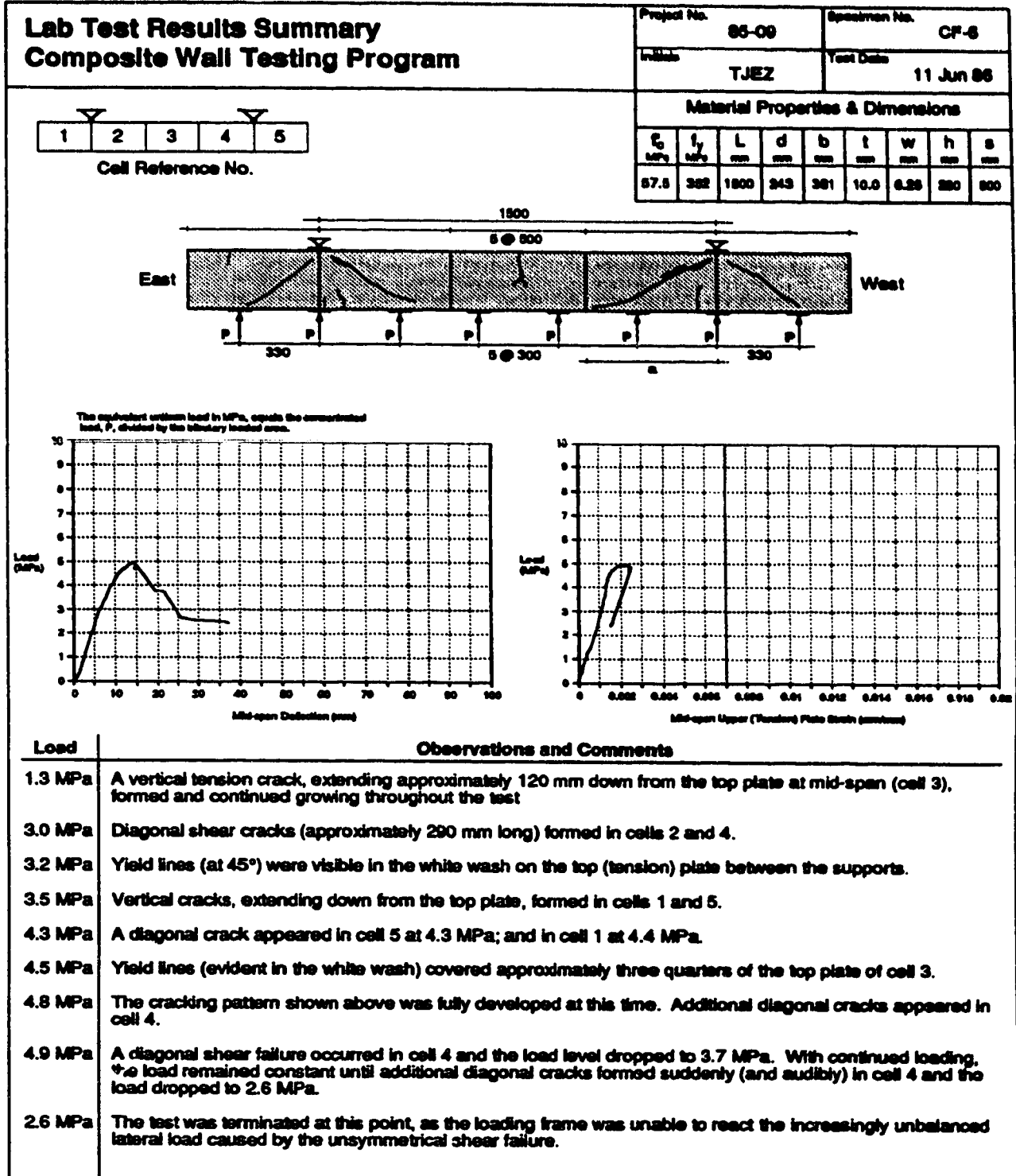


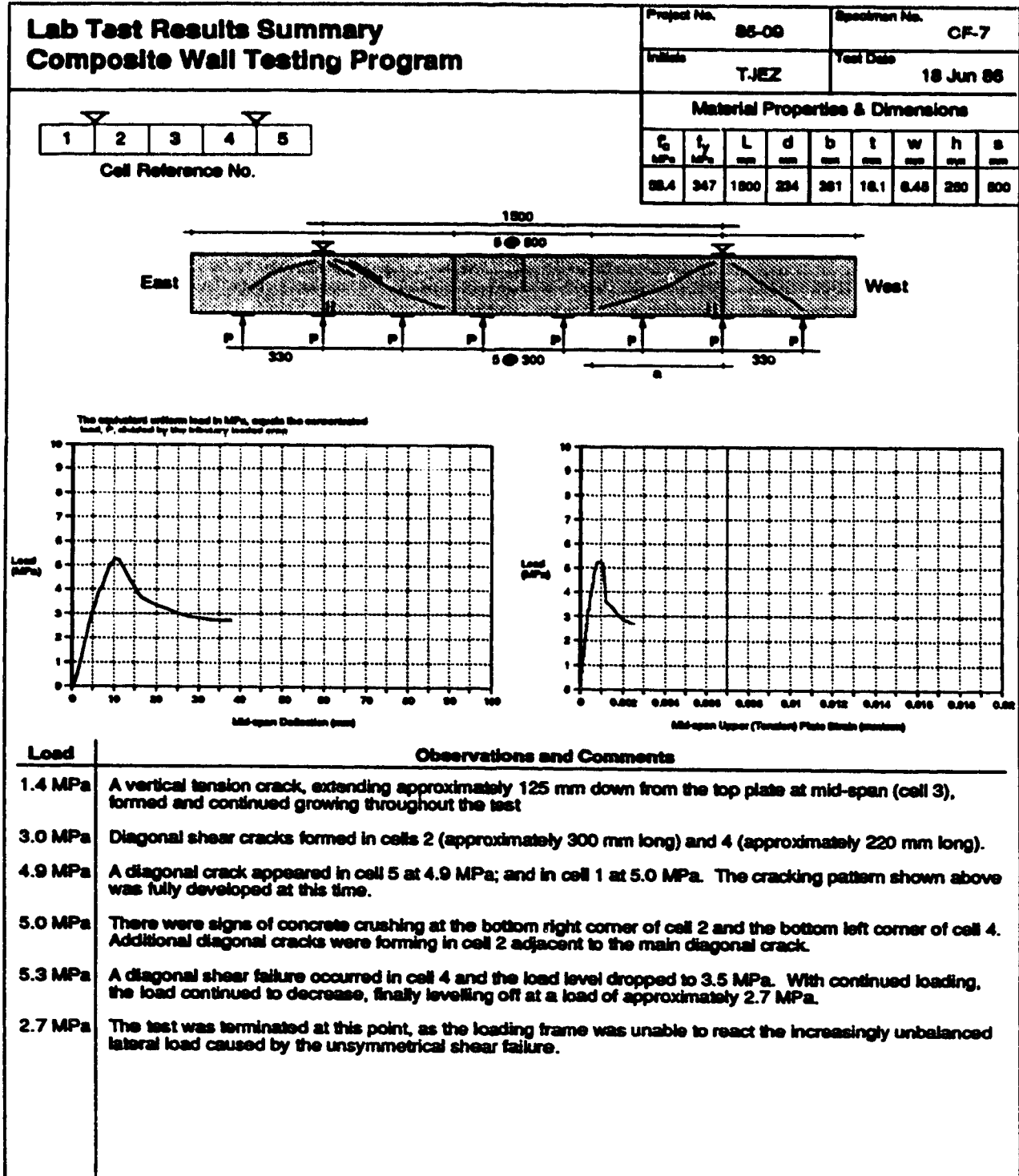


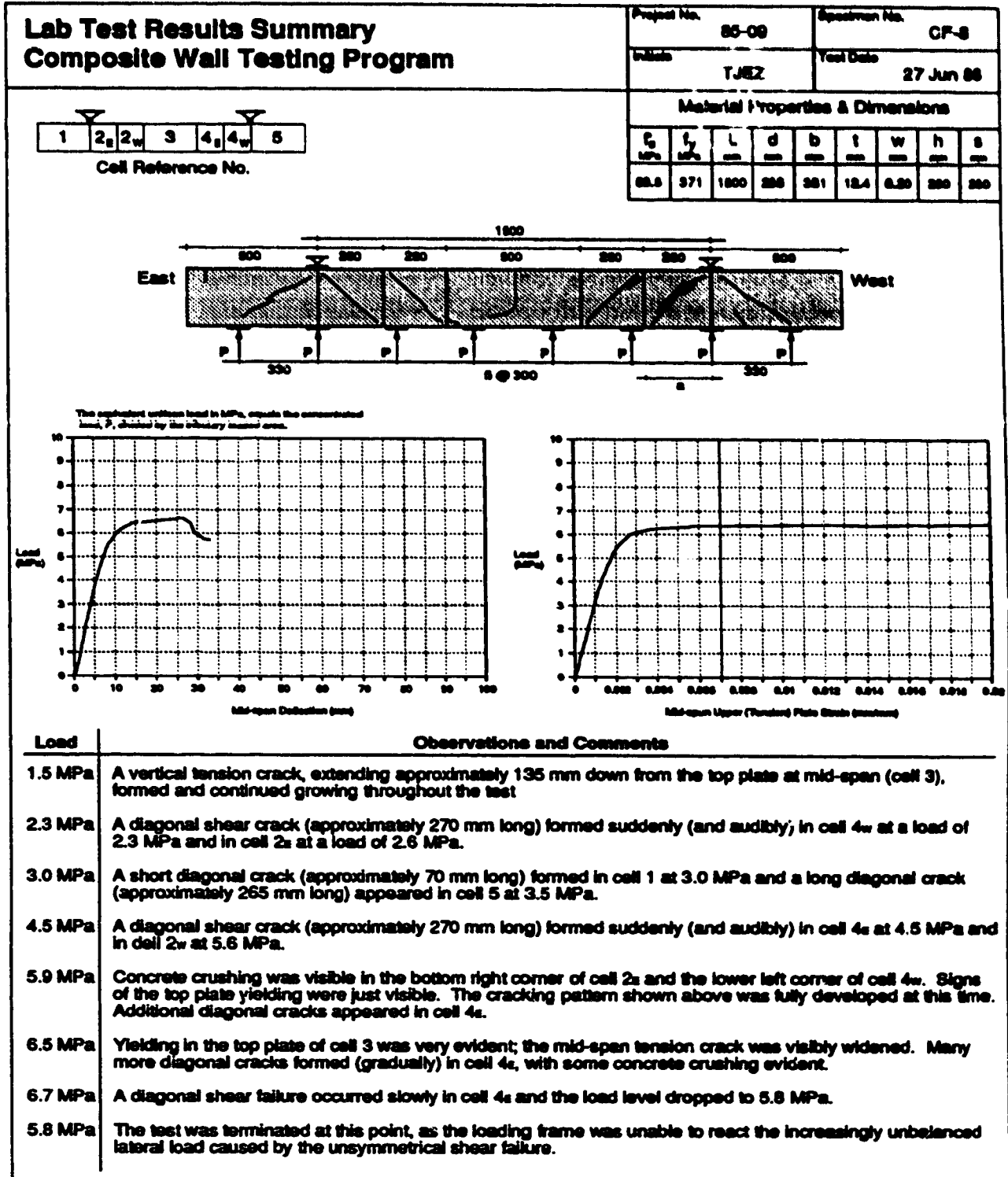


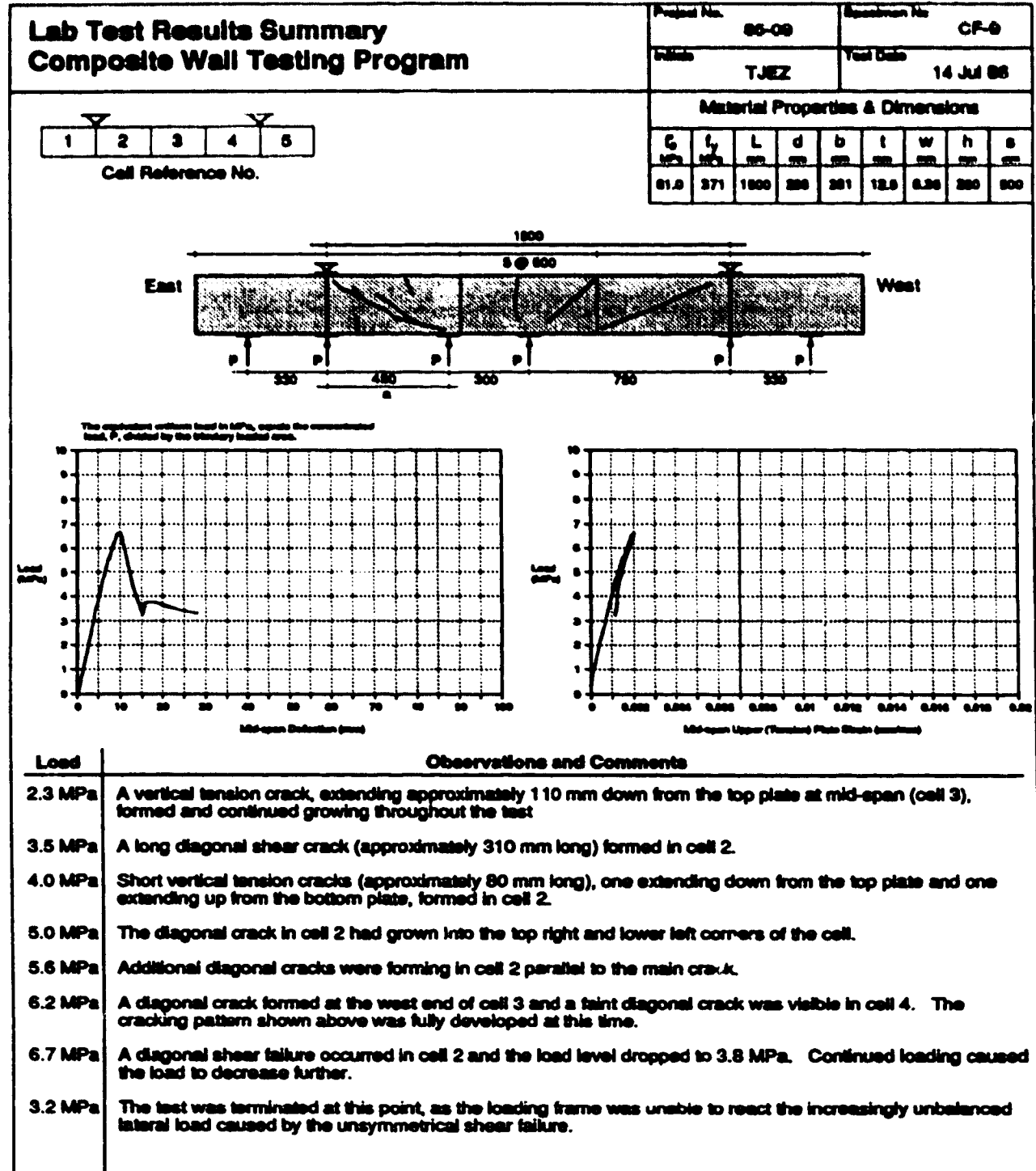


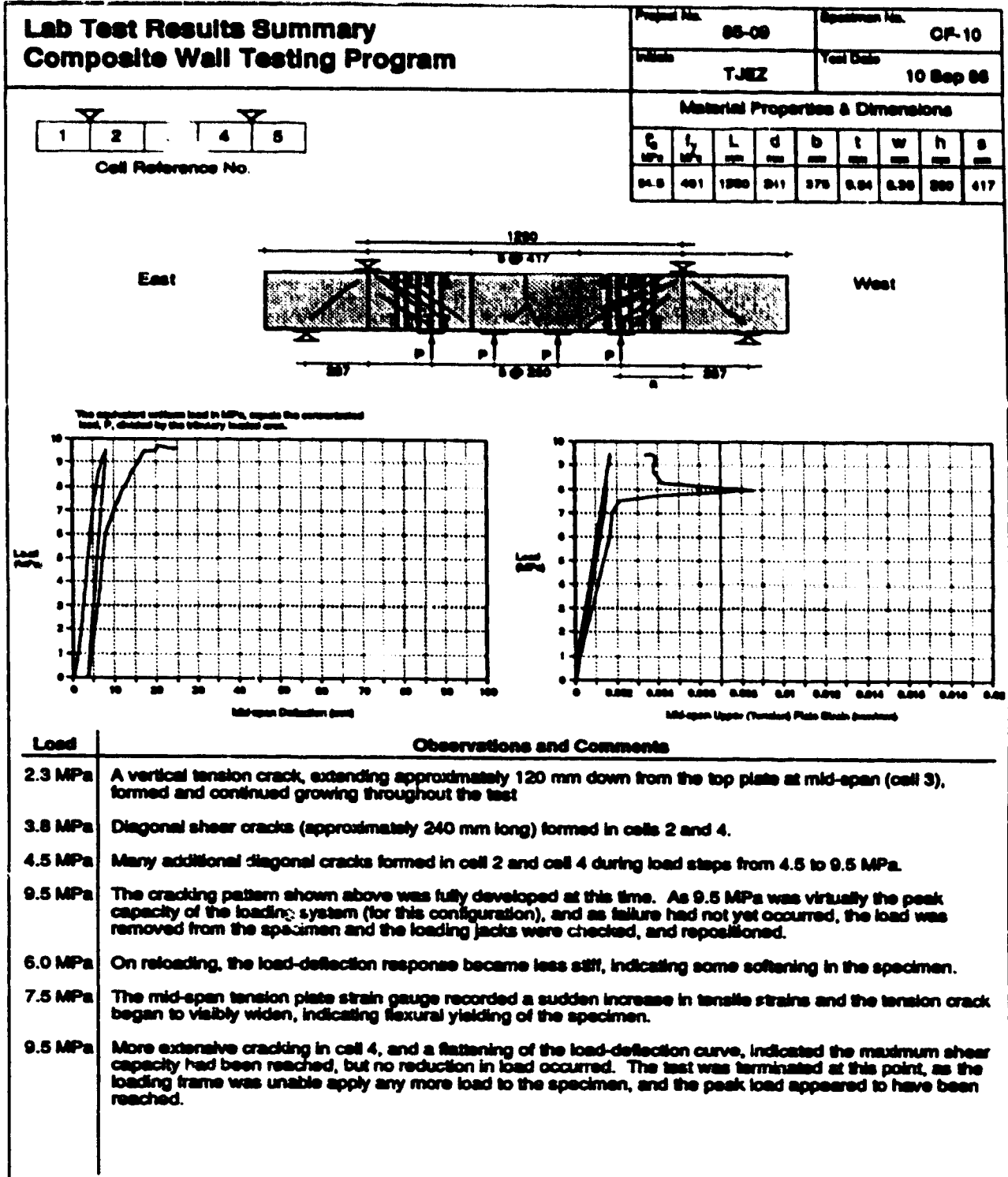


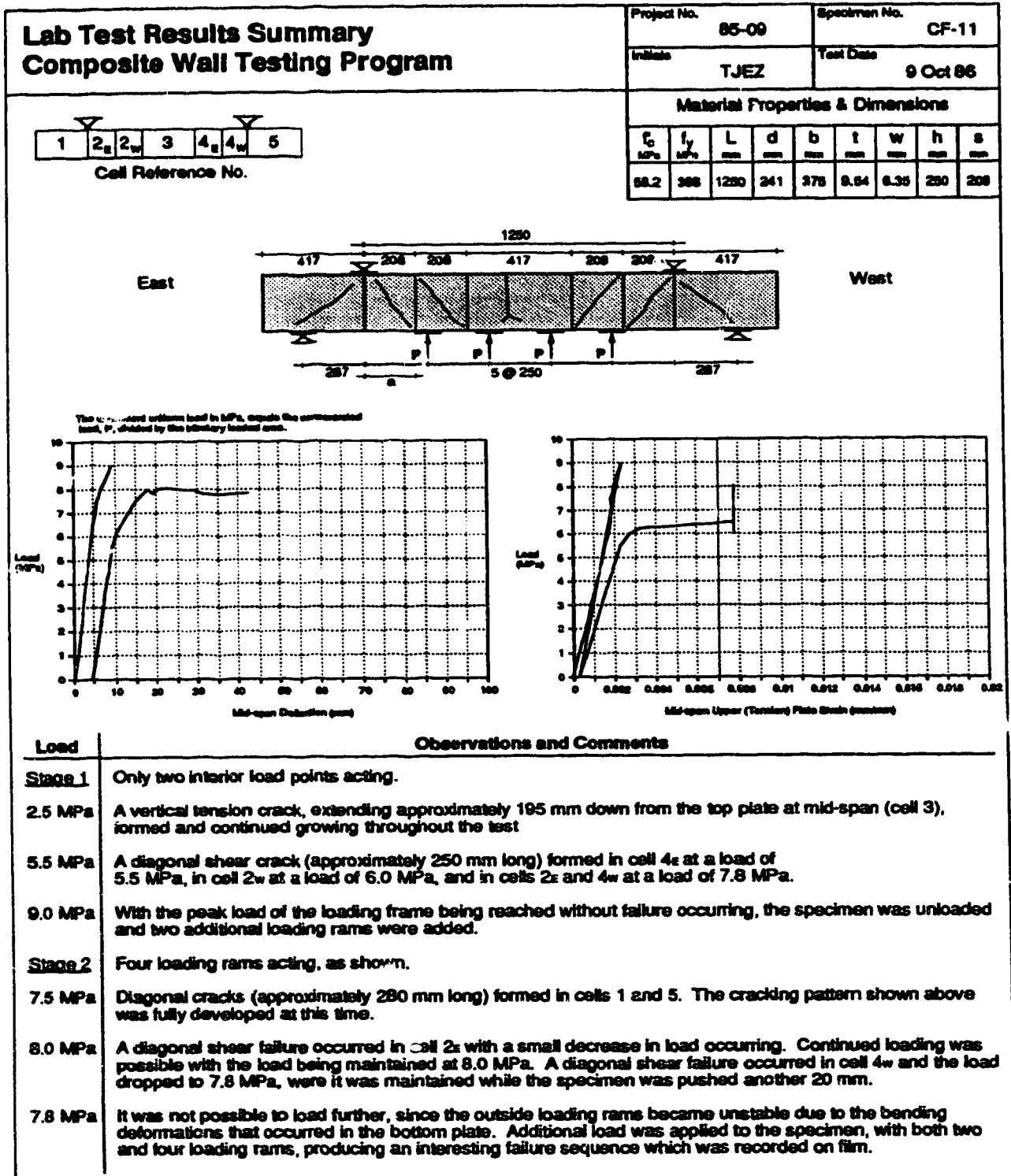


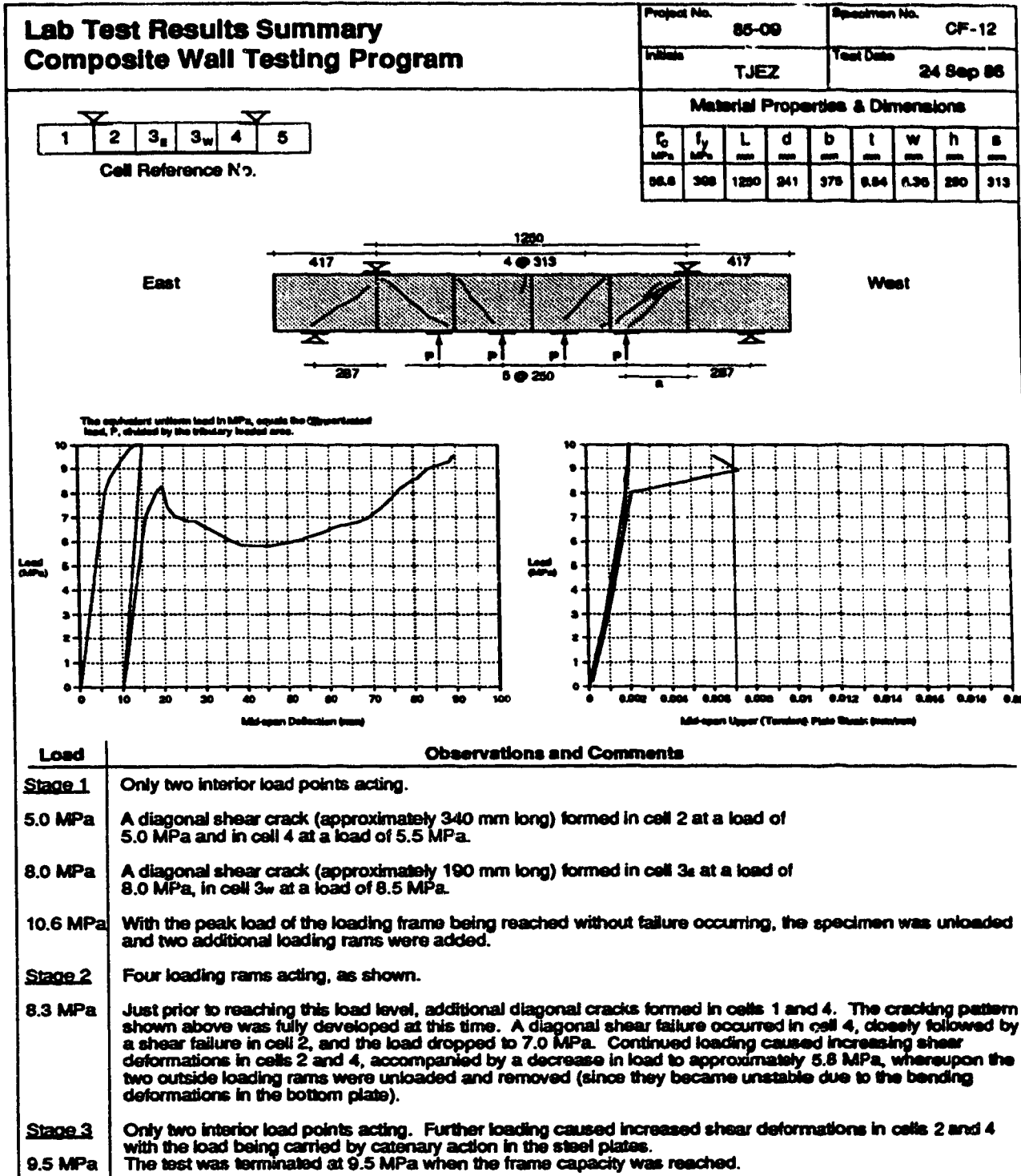


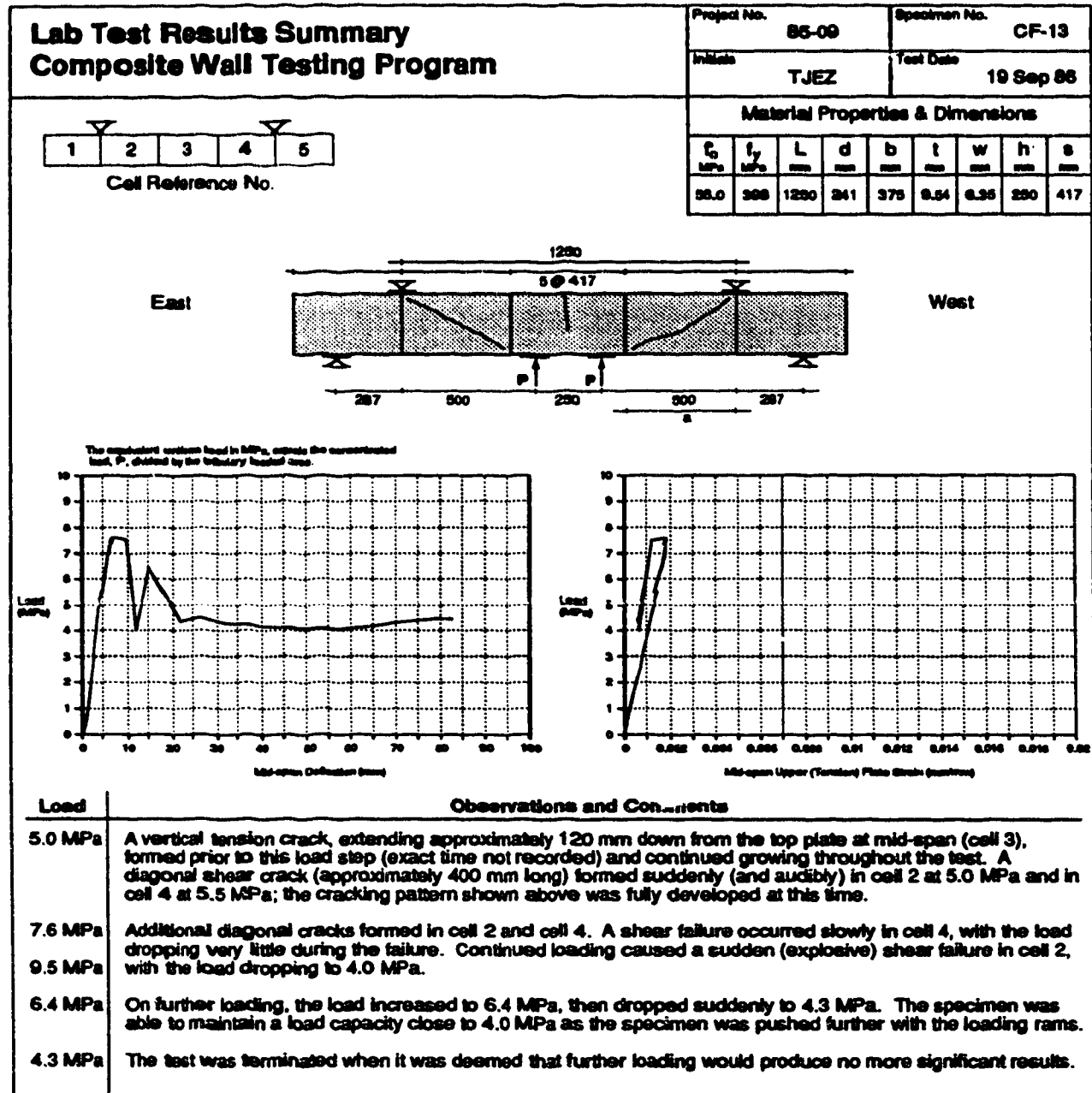


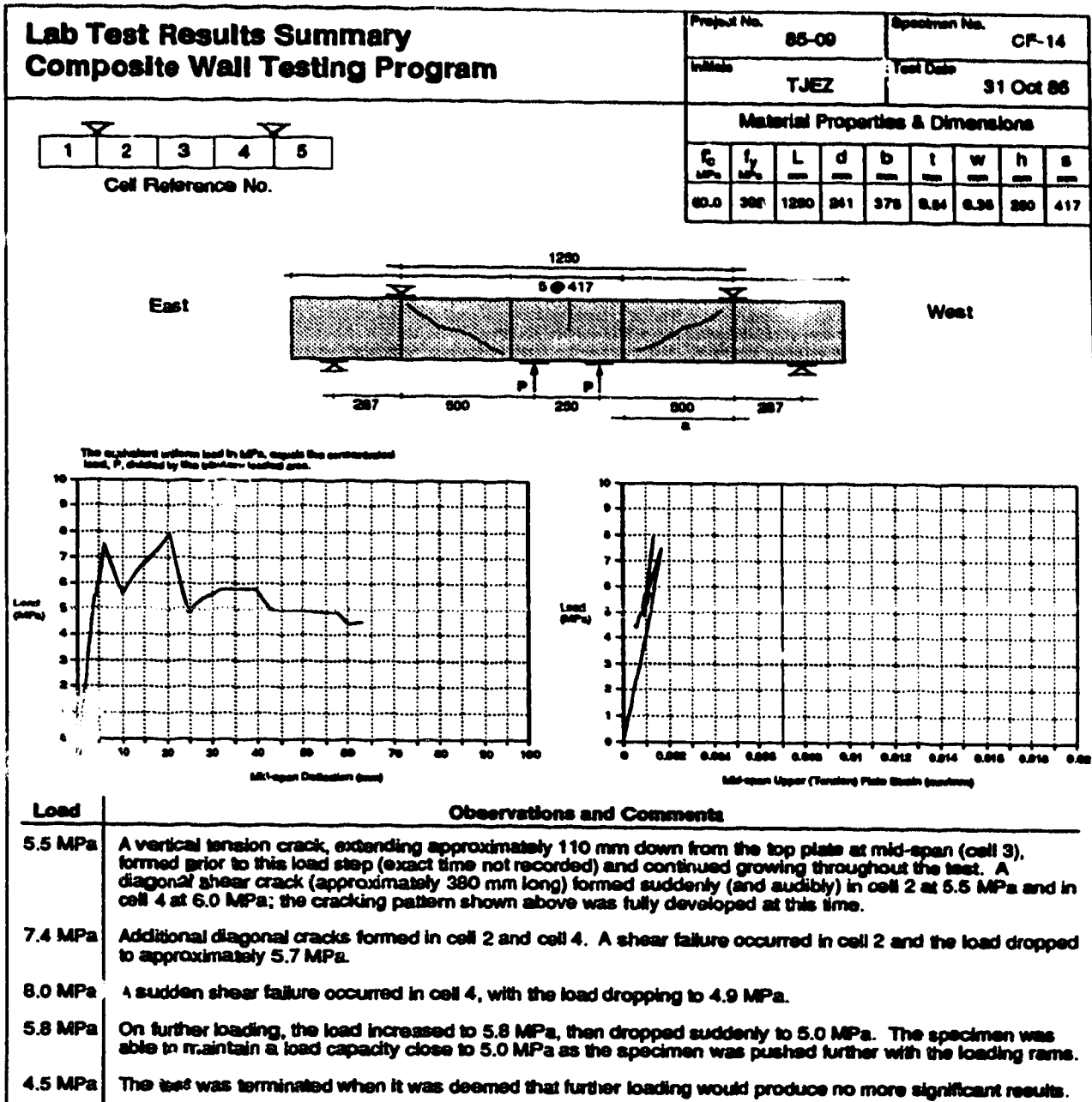



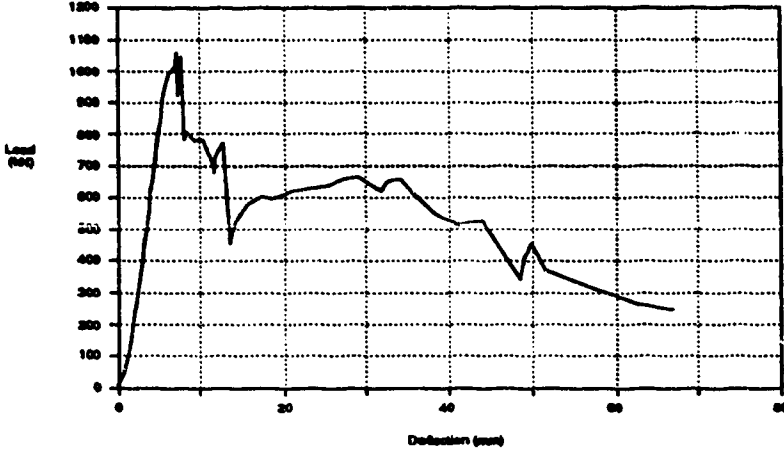


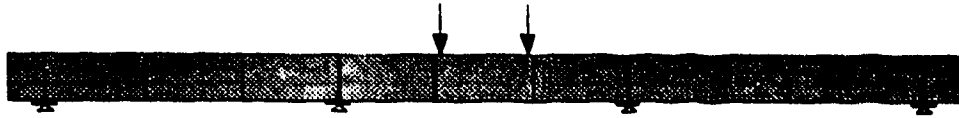
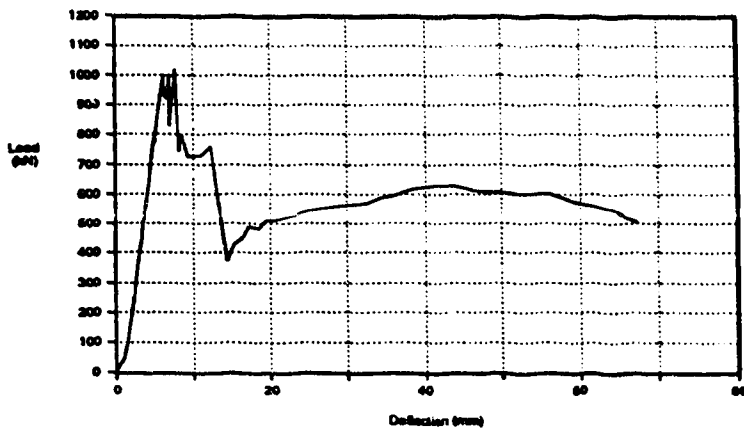


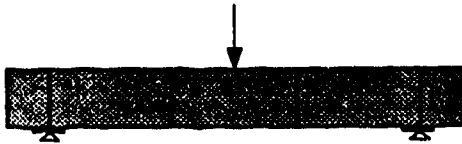
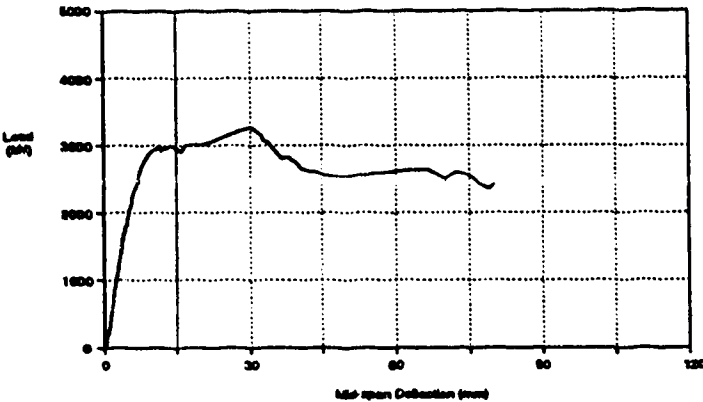







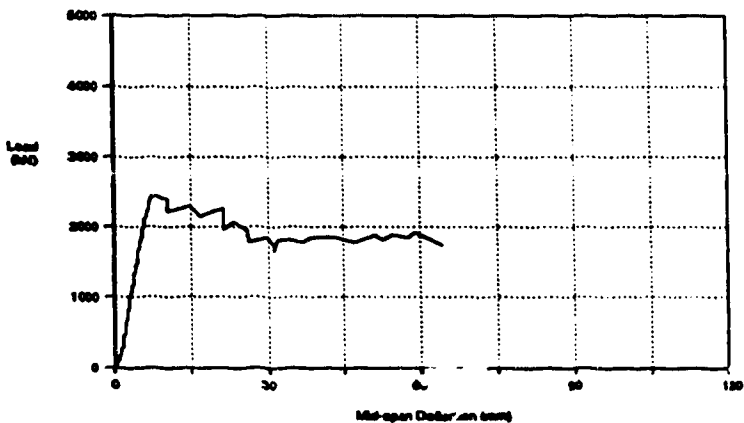
Lab Test Results Summary Composite Wall Testing Program		Project No. 85-09	Specimen No. B-1					
		Initials TJEZ	Test Date 26 Mar 87					
Material Properties & Dimensions								
f_c MPa	f_y MPa	L mm	d mm	b mm	t mm	w mm	h mm	s mm
66.5	340	1290	243	375	6.91	6.80	250	417
								
Load	Observations and Comments							
	Not available.							

Lab Test Results Summary Composite Wall Testing Program		Project No. 85-00	Specimen No. B-2					
		Initials TJEZ	Test Date 24 Mar 87					
Material Properties & Dimensions								
E_c MPa	f_y MPa	L mm	d mm	b mm	t mm	w mm	h mm	s mm
88.9	340	1200	243	375	6.75	4.90	280	417
								
Load	Observations and Comments							
	Not available.							


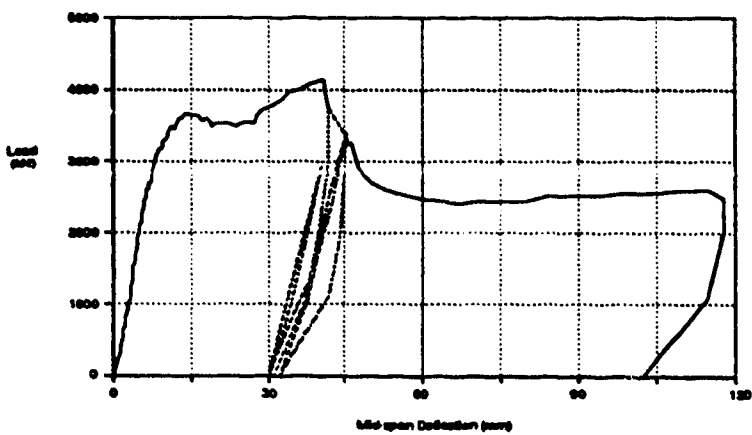
Lab Test Results Summary Composite Wall Testing Program		Project No.	85-09	Specimen No.	SP-1			
		Initiate	TJEZ	Test Date	9 Jan 87			
Material Properties & Dimensions								
f_c	f_y	L	d	b	t	w	h	s
MPa	MPa	mm	mm	mm	mm	mm	mm	mm
46.0	340	1000	188	1200	12.5	6.35	200	333
								
								
Load	Observations and Comments							
2.80 MN	Diagonal shear cracks formed in the cells on either side of centre. Punching shear failure beginning to occur (bottom plate is bulging).							
3.18 MN	Shear failures occurring on both sides. Load dropping slowly (load control on MTS machine). The specimen was able to maintain a load capacity close to 2.6 MN as the specimen was pushed further with the MTS ram.							
2.50 MN	The test was terminated when it was deemed that further loading would produce no more significant results.							

Lab Test Results Summary Composite Wall Testing Program		Project No.	85-09	Specimen No.	S-1			
		Initials	TJEZ	Test Date	4 Mar 87			
Material Properties & Dimensions								
f_c MPa	f_y MPa	L mm	d mm	b mm	t mm	w mm	h mm	s mm
58.5	340	1280	343	1200	6.66	6.36	280	417





Load	Observations and Comments
2.50 MN	A vertical tension crack formed at mid-span extending approximately 90 mm down from the top plate. Can't hold the load; a punching shear failure is occurring. Loading dropping steadily.
1.86 MN	Load drops suddenly to zero; a shear failure in the top steel plate occurred.

Lab Test Results Summary Composite Wall Testing Program		Project No.	85-09	Specimen No.	S-2			
		Initials	TJEZ	Test Date	16 Mar 87			
Material Properties & Dimensions								
f_c	f_y	L	d	b	t	w	h	s
MPa	MPa	mm	mm	mm	mm	mm	mm	mm
64.3	430	1250	240	1200	10.4	6.35	250	417
								
								
Load	Observations and Comments							
2.83 MN	Diagonal shear crack formed in cell 1.							
3.16 MN	Shear crack in cell 3. Load leveling off. Denting around the loading point is noticeable.							
7 MN	Shear failure in concrete beginning in cell 1. Load dropping quickly.							
3.7 MN	Unload to reset data acquisition equipment.							
3.0 MN	Shear failure occurring in cell 3. Load drops then levels off and maintains at approx. 2.5 MN.							
2.5 MN	The test was terminated when it was deemed that further loading would produce no more significant results.							

APPENDIX B - COMPRESSION FIELD METHOD FOR SHEAR

B1.0 General Method for Shear Design According to CSA Standard A23.3-M84

The general method for shear design of reinforced concrete beams given in Clause 11.4 in CSA Standard A23.3-M84 (CSA 1984) is based on the lower bound theory of plasticity. This method of design determines the resistance of members in shear "by satisfying applicable conditions of equilibrium and compatibility of strains and by using appropriate stress-strain relations for reinforcement and for diagonally cracked concrete". For a given concrete strength, cross sectional dimensions are chosen to ensure that the diagonally cracked concrete has sufficient capacity to resist the inclined compressive stresses. Areas of longitudinal and transverse reinforcement are chosen which are capable of equilibrating this field of diagonal compression.

The method assumes that shear stresses are uniformly distributed over an area b_v wide and d_v deep and that the direction of the principal compressive stresses (defined by the angle θ) remains constant over d_v (Figure B.1). Tensile stresses in the cracked concrete are ignored.

B1.1 Shear Capacity Based on Diagonal Crushing Strength

Clause 11.4.2 gives expressions for the diagonal compressive stresses in the concrete (f_2), as a function of the strut angle θ , and the diagonal crushing strength of concrete (f_{2max}), as functions of the principal tensile strain (ϵ_1) and θ .

$$f_2 = \left(\tan \theta + \frac{1}{\tan \theta} \right) \left(\frac{V_f}{b d_v} \right) \quad [1]$$

$$f_{2max} = \frac{\lambda \phi f'_c}{(0.8 + 170\epsilon_1)} \quad [2]$$

It then gives an expression for ϵ_1 as a function of ϵ_x , the longitudinal strain at the mid-depth of the member. A plane sections analysis can be used to determine ϵ_x , or it may conservatively be taken as 0.002.

$$\epsilon_1 = \epsilon_x + \frac{\epsilon_x + 0.002}{\tan^2 \theta} \quad [3]$$

Setting f_2 equal to f_{2max} , equations [1] and [2] can be used to write an equation for the shear capacity of a beam based on the diagonal crushing strength of the concrete.

$$\frac{V_r}{bd_v} = \frac{\lambda \phi_c f'_c}{0.8 + 170\epsilon_1} \left[\frac{1}{\tan \theta + \frac{1}{\tan \theta}} \right] \quad [4]$$

For given values of λ , ϕ_c , f'_c , b_v , d_v and ϵ_1 , Equation [4] becomes an equation for shear capacity as a function of the angle θ . The equation is shown graphically in Figure B.2. This figure is similar to Figure 4.7, in Part II of the CPCA Concrete Design Handbook (1985).

At all points along this curve, it is assumed that the diagonal compression struts are crushing at a principal compressive strain of -0.002. The state of strain at the mid-depth of the web is therefore as shown in Figure B.3 (Figure N11.5 in the CPCA Handbook).

From Figure B.3 an expression for the strain in the transverse reinforcement can be written.

$$\epsilon_t = \epsilon_1 - \epsilon_x - 0.002 \quad [5]$$

In order to ensure that the transverse reinforcement is yielding when the concrete crushes, Clause 11.4.3 requires that

$$\epsilon_t > f_y/E_s \quad [6]$$

This effectively puts an upper limit on the curve shown in Figure B.2. For f_y equal to 400 MPa, equations [5] and [6] require that $\epsilon_1 - \epsilon_x$ be greater than 0.004. The θ angle at which the upper limit occurs can then be determined from equation [3].

$$\theta = \tan^{-1} \sqrt{\frac{\epsilon_x + 0.002}{0.004}} \quad [7]$$

For an assumed value of $\epsilon_x = 0.002$, the limit occurs at $\theta = 45^\circ$. Beyond this point, diagonal crushing will occur without the transverse steel yielding.

B1.2 Shear Capacity of Transverse Reinforcement

Clause 11.4 requires that transverse reinforcement be provided to equilibrate the outwards thrust of the diagonal compressive stresses in the concrete. Thus, the shear resistance is governed by the amount of transverse reinforcement, provided that the θ angle assumed is greater than that for which diagonal crushing occurs. An expression for the factored shear resistance is given in Clause 11.4.4; for non-prestressed members the equation can be written

$$\frac{V_r}{b_s d_v} = \frac{\phi_s A_s f_y}{s b_s \tan \phi} \quad [8]$$

For given values of A_s , $\phi_s f_y$, s , b_s and d_v , Equation [4] becomes an equation for shear capacity as a function of the angle θ . This equation is shown graphically in Figure B.4.

In order to determine the factored shear resistance of a member with given dimensions and material properties, the designer is allowed to choose a value of θ between 15° and 75° (Clause 11.4.2.6), provided the same angle is used in satisfying other requirements (i.e. flexure) at that section. However, an additional restriction on the choice of θ results from the requirement that the shear capacity be governed by yielding of the transverse reinforcement and not diagonal crushing. This puts a lower limit on θ at the point where the curves shown in Figures B.2 and B.4 intersect. This is shown in Figure B.5, where the minimum θ angle is shown as θ_{\min} . The designer has the option of choosing a θ angle anywhere between θ_{\min} and 75° , although normally the maximum shear resistance, which occurs at θ_{\min} , is desired for design.

B1.3 Equation for Ultimate Shear Capacity

The highest shear capacity available for a given amount of shear reinforcement is at the point of intersection of the two curves shown in Figure B.5. The intersection point can be found graphically or it can be determined by solving equations [4] and [8] simultaneously. This results in a fourth order quadratic equation for $V_r/b_s d_v$.

$$\begin{aligned}
& \left[\frac{170(\epsilon_r + 0.002)}{(\phi \rho f_y)^2} \right] (V_d / b_v d_v)^2 \\
& + [0.8 + 170\epsilon_r + 170(\epsilon_r + 0.002)] (V_d / b_v d_v)^2 \\
& + \left[\left(0.8 + 170\epsilon_r - \frac{\phi f_c'}{\phi \rho f_y} \right) (\phi \rho f_y)^2 \right] = 0
\end{aligned} \tag{9}$$

Solution of this quadratic equation gives a single equation for the maximum factored shear capacity of a non-prestressed beam of given dimensions and material properties.

$$\frac{V_r}{b d_v} = \rho \phi f_y \sqrt{\frac{0.22 + \frac{1}{\omega_v} (680\epsilon_r + 1.36) - (1.14 + 340\epsilon_r)}{340(\epsilon_r + 0.002)}} \tag{10}$$

where

$$\rho_v = \frac{A_v}{s b_v} \tag{11}$$

and
$$\omega_v = \frac{\rho \phi f_y}{\phi f_c'} \tag{12}$$

The θ angle associated with this shear capacity is:

$$\theta_{min} = \tan^{-1} \left(\frac{\rho_v \phi f_y}{V_d / b_v d_v} \right) \tag{13}$$

Equation [10] can be used directly for design, in which case the designer uses the θ angle given by equation [13] for designing the flexural reinforcement (i.e. determining the bar cut-off locations). Alternatively, a higher θ angle can be used, which results in a lower shear resistance as given by Equation [8].

These same equations can also be used for composite wall members, where width b is used in place of b_v and where depth h is used instead of d_v .

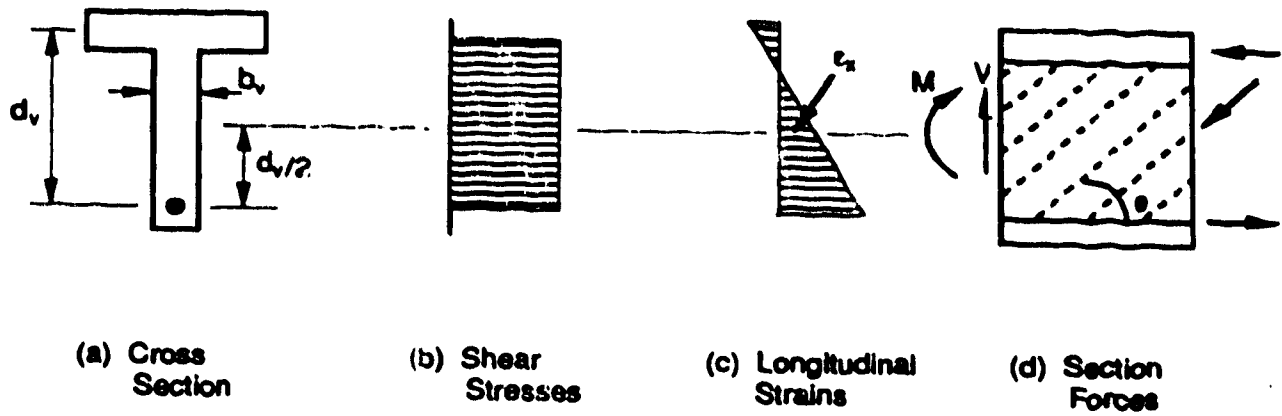


Figure B.1 Compression Field for Beam in Shear

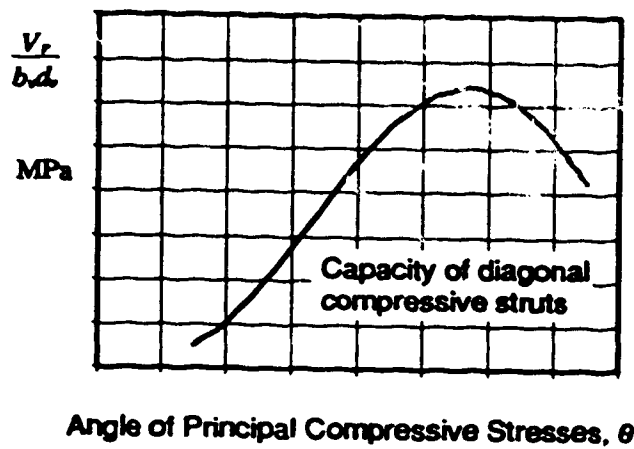


Figure B.2 Shear Resistance Based on Diagonal Crushing Strength

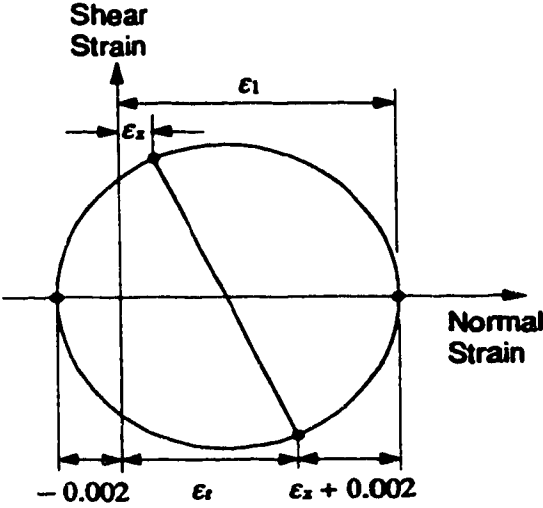


Figure B.3 Strains at Mid-Depth of Web

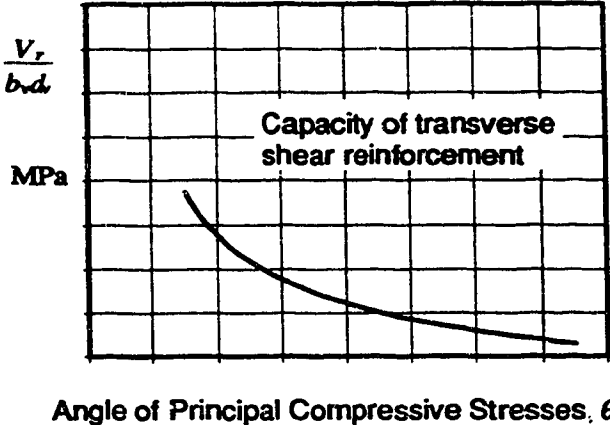


Figure B.4 Shear Strength Based on Stirrups Yielding

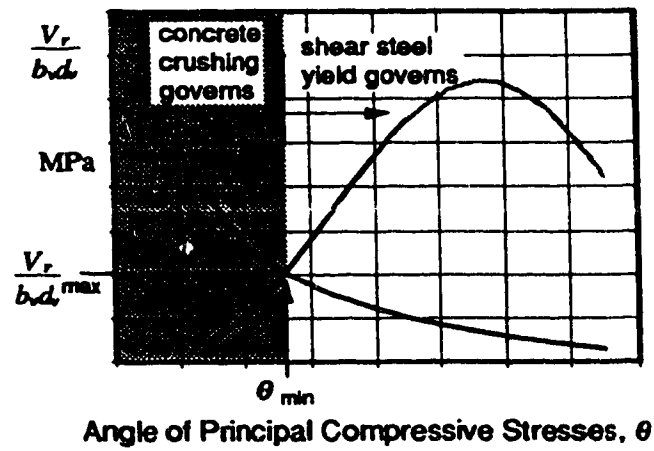


Figure B.5 Shear Design Diagram

APPENDIX C - UPPER BOUND PLASTICITY METHOD FOR SHEAR

C1.0 The Upper Bound Plasticity Concept

“Limit-analysis” techniques, based on the upper and lower bound theorems of plasticity, have been used successfully for a great number of years in the analysis and design of structural steel and reinforced concrete members. The basic tenets of plastic theory, including the upper and lower bound theorems, are given in detail in a number of references (Chen 1982, Nielsen 1984). They were described in simple terms at the beginning of Chapter 5 as follows:

Lower Bound Plasticity Methods:

Those plasticity methods which do not require strain compatibility, but which do require the maintenance of equilibrium by assuming some statically admissible stress distribution within the member which nowhere exceeds the strength of the material and which assumes sufficient material ductility such that the assumed stress field can be achieved.

Upper Bound Plasticity Methods:

Those plasticity methods which do not require strain compatibility, but which do require the maintenance of equilibrium during failure by some kinematically admissible failure mechanism, and which assume that the external work done during failure equals the internal work expended, as calculated by a plastic failure theory.

Nielsen (1984) points out that in reinforced concrete beams and slabs, plastic behaviour is largely the result of the reinforcement, since it is a material that “yields” (i.e. it can sustain a high percentage of its failure stress through large deformations). However, in situations where the properties of concrete are more important in determining structural capacity (such as crushing or shear in plain concrete or over-reinforced concrete members), it is less clear how plastic theory applies, since concrete is a brittle material, which exhibits significant strain softening. For these situations, there are problems applying either upper or lower bound plasticity methods.

The problem with lower bound techniques is that the statically admissible stress distribution might never be achieved. A caveat is therefore put on the use of these methods

requiring that there be sufficient ductility for the failure mode being considered, such that the section can reach the assumed distribution of stress.

For upper bound plasticity methods, the problem is somewhat more fundamental; the kinematically admissible failure mechanism involves yielding, which is not a property exhibited by plain concrete. None-the-less, a research group at The Technical University of Denmark, lead by M.P. Nielsen, has been successful in applying upper bound techniques to shear in plain and reinforced concrete. There has not yet been general acceptance of these methods, however, mainly because the theoretical results have to be modified in an empirical manner in order to make them work. In the author's opinion, this does not detract from their usefulness, for two reasons: firstly, the design methods are far less empirical in nature than those used to date; and secondly, they can increase one's understanding of structural behaviour by forcing the designer to focus on the actual modes of failure.

In this section of the thesis, a review is provided of the upper bound plasticity methods developed by Nielsen for shear in reinforced concrete members. This same basic method is then adapted for use in determining the shear capacity of composite members.

C2.0 Energy Dissipation in Plain Concrete

In order to develop an upper bound approach for shear in reinforced concrete, it is first necessary to derive expressions for the energy which is dissipated along a shear failure plane in plain concrete.

Nielsen (1984) has derived expressions for energy dissipation in plain concrete per unit length of a yield line, where the concrete is considered as a modified Coulomb material with a zero tension cut-off (see Figures C.1 and C.2). Referring to Figure C.3, we shall consider the rate of internal work dissipated per unit area in the kinematic discontinuity (or yield line) between the two rigid parts A and B, where B is moving with velocity vector u with respect to A. The dissipation formula developed by Nielsen for both plane stress and plane strain is as follows:

$$W_L = \frac{1}{2} f'_{cub} (1 - \sin \alpha) \quad [C1]$$

- where
- W_{Ic} = internal work dissipated per unit length
 - f_c' = uniaxial compressive strength of concrete = $k\sigma_1 - \sigma_2$,
which is the Coulomb failure criteria
 - u = displacement of one side of the yield line with respect to
the other
 - b = thickness of the element
 - k = $(\tan \phi + \sqrt{1 + \tan^2 \phi})^2$; where ϕ is defined in figure C.1
 - α = angle between the yield line and the displacement vector
 - σ_1 = major principal stress
 - σ_2 = minor principal stress

Nielsen goes on to state that good correlation with test results is only achieved if an "efficiency" factor, ν , is used to modify the concrete strength, f_c' . The modified concrete strength, $\nu f_c'$, is referred to as the effective concrete strength or the plastic concrete strength. Concrete efficiency factors are given for a variety of cases, including shear in reinforced concrete (Figure C.4); the factors typically range from as high as 1.0, to as low as 0.3. Including the effective strength of concrete, the equation for energy dissipation across a yield line becomes:

$$W_{Ic} = \frac{1}{2} \nu f_c' u b (1 - \sin \alpha) \quad [C2]$$

C3.0 Energy Dissipation in Reinforcing Steel

In a reinforced concrete member containing shear reinforcement, account needs to be taken of the energy dissipated in the steel reinforcing bars that cross a failure surface. Two well established failure theories which have been shown to be applicable for steel are the von Mises and the Tresca theories of failure. Figure C.5 shows these two criteria plotted in principal stress space.

Several reasonable assumptions are made concerning the reinforcing bars. Firstly, the bars are assumed to be straight; secondly, the material is assumed to be rigid-plastic, with a stress-strain curve as shown in Figure C.6; and finally, the bars are assumed to be capable of carrying axial tensile and compressive stress only. Shear and bending stress are

not allowed. This means that there is a stress state of uniaxial tension or compression; i.e. in Figure C.5, the stress state is constrained to stay on the σ_1 axis ($\sigma_2=0$). Regardless then, of whether a von Mises or Tresca failure theory is used, the material is assumed to yield when the axial stress reaches f_y , the yield stress from a uniaxial tensile test.

Using these assumptions, the energy dissipation in a reinforcing bar crossing a yield line in the concrete can be expressed as follows (refer to Figure C.7).

$$W_L = A_s f_y u \cos \theta \quad [C3]$$

or

$$W_L = -A_s f_y u \cos (\alpha + \beta) \quad [C4]$$

(since $\theta = 180 - (\alpha + \beta)$; therefore $\cos \theta = -\cos (\alpha + \beta)$)

where

W_{Is} = internal work dissipated in the reinforcing steel bar

A_s = area of reinforcing steel bar

f_y = yield strength of steel

u = displacement of one side of the yield line with respect to the other

α = angle between the yield line and the displacement vector

β = angle between the yield line and the reinforcing bar

θ = angle between the displacement vector and the reinforcing bar

C4.0 Upper Bound Solution for Shear in a Reinforced Concrete Beam Without Web Reinforcement

The upper bound energy method has been used to derive solutions for determining the shear capacity of reinforced concrete beams without shear reinforcement (Nielsen and Bræstrup, 1978). Figure C.8 shows one shear span of a beam, with top and bottom longitudinal reinforcement, subjected to a single point load, V . The upper bound failure mechanism consists of a yield line, inclined at an angle β to the horizontal and extending from the edge of the loading plate to the edge of the support plate. The right-hand side of

the beam is assumed to be moving downward and to the right with a displacement u , while the right end of the beam is not moving. The displacement vector, u , is inclined at an angle, α , to the yield line. The shear span, a , is the horizontal clear distance between the edges of the loading and support plates.

The internal work dissipated during this kinematically admissible failure mechanism is:

$$W_I = \frac{1}{2} u f'_c u b (1 - \sin \alpha) \frac{h}{\sin \beta} - (A_s + A'_s) F_y u \cos (\alpha + \beta) \tag{C5}$$

where W_I = internal work dissipated
 A_s = total area of top steel
 A'_s = total area of bottom steel
 $\frac{h}{\sin \beta}$ = the length of the yield line

and other terms are as previously defined.

The first term in Equation C5 is the energy dissipated in the concrete; the second term, the energy dissipated in the reinforcing steel.

If we now define the mechanical degree of longitudinal reinforcement, Φ , as:

$$\Phi = \frac{(A_s + A'_s) F_y}{bh f'_c} \tag{C6}$$

Equation C5 becomes:

$$W_I = \frac{1}{2} u f'_c u b (1 - \sin \alpha) \frac{h}{\sin \beta} - bh f'_c \Phi u \cos (\alpha + \beta) \tag{C7}$$

The external work done during this mechanism is:

$$W_E = Vu \sin (\alpha + \beta) \tag{C8}$$

Equating external work to internal energy dissipated on the yield line results in the following work equation.

$$V \sin(\alpha + \beta) = bhf'_c \left[\frac{v(1 - \sin \alpha)}{2 \sin \beta} - \Phi \cos(\alpha + \beta) \right] \quad [C9]$$

which reduces to:

$$V = bhf'_c \left[\frac{v(1 - \sin \alpha) - 2\Phi \sin \beta \cos(\alpha + \beta)}{2 \sin \beta \sin(\alpha + \beta)} \right] \quad [C10]$$

To find the lowest upper bound, Equation C10 is minimized with respect to the variable angle α . Solving for $\frac{dV}{d\alpha} = 0$ results in the minimum value for V :

$$V = \frac{bhvf'_c}{2} \left[\sqrt{\left(\frac{a}{h}\right)^2 + \frac{4\Phi \sin \beta}{v}} - \frac{a}{h} \right] \quad [C11]$$

Equation C11 is valid for $\Phi \leq v/2$. For larger values of Φ , the minimum is obtained for $\alpha + \beta < \pi/2$; i.e. for a condition where the right side of the beam in Figure C.8 moves toward the left, putting the reinforcement in compression. For this case, the lowest upper bound is obtained for $\alpha + \beta = \pi/2$; i.e. the right side of the beam in Figure C.8 moves vertically downward. Inserting $\Phi = v/2$ into Equation C11 results in an equation for the minimum shear capacity when $\Phi > v/2$:

$$V = \frac{bhvf'_c}{2} \left[\sqrt{\left(\frac{a}{h}\right)^2 + 1} - \frac{a}{h} \right] \quad [C12]$$

Equations C11 and C12 are both given by Nielsen and Bræstrup (1978), and are shown to give reasonably accurate results when verified against experimental results for reinforced concrete beams without web reinforcement.

C5.0 Upper Bound Solution for Shear in a Reinforced Concrete Beam With Web Reinforcement

Nielsen has also used the upper bound energy method to derive solution for determining the shear capacity of reinforced concrete beams with web reinforcement. The beam in Figure C.9 has top and bottom longitudinal reinforcement and uniformly distributed shear reinforcement. It is loaded with two symmetrically placed point loads V . The upper bound failure mechanism consists of two symmetric yield lines, inclined at an angle β to the horizontal and extending from the bottom face of the beam to the top. In this

case, the yield line will not necessarily run from the edge of the loading plate to the edge of the support plate. The presence of the shear reinforcement will tend to cause the shear crack to be inclined at a steeper angle, since fewer lines of vertical shear reinforcement will then be crossed. To facilitate a solution in this case, the central part of the beam is assumed to be moving vertically downward with a displacement u , while the ends of the beam are not moving. A work equation is then written and minimized with respect to the crack angle β to determine the angle at which failure occurs.

Equating external work to internal energy dissipated on the yield line results in the following work equation:

$$V \cdot u = \rho_v f_y b h \cot \beta \cdot u + \frac{1}{2} \nu f'_c b (1 - \cos \beta) \frac{h}{\sin \beta} \cdot u \quad [C13]$$

where $\rho_v = A_v/sb =$ shear reinforcement ratio
 $f_y =$ yield strength of the shear reinforcement

The first term on the right-hand side of the equation is the energy dissipation in the stirrups which cross the yield line; the second term is the energy dissipation in the concrete (note that $(1 - \cos \beta) = (1 - \sin \alpha)$). Since the movement is vertical, the longitudinal reinforcement is assumed to do no work (the reinforcing steel is assumed to have no bending or shear capacity).

If the degree of shear reinforcement is defined as :

$$\psi = \rho_v \frac{f_y}{\nu f'_c} \quad [C14]$$

then Equation C15 results in the upper bound solution:

$$V = \nu f'_c b h \left[\psi \cot \beta + \frac{1}{2} (1 - \cos \beta) \frac{1}{\sin \beta} \right] \quad [C15]$$

Minimizing Equation C15 with respect to the angle β provides the lowest upper bound solution:

$$\frac{dV}{d\beta} = \psi f'_c b h \left[-\psi \csc^2 \beta - \frac{\csc \beta \cot \beta}{2} + \frac{\csc^2 \beta}{2} \right] = 0 \quad [C16]$$

solving this results in the following:

$$1 - 2\psi = \cos \beta \quad [C17]$$

Referring to Figure C.10, the angle β is found to be:

$$\tan \beta = \frac{2\sqrt{\psi(1-\psi)}}{1-2\psi} \quad [C18]$$

The limits of the angle β are: $\tan \beta = \infty$, a vertical shear crack; and $\tan \beta = h/a$, the case where the crack runs from the edge of the support plate to the edge of the loading plate.

For the special case where $\tan \beta = h/a$, the lower bound solution, Equation C15, becomes:

$$V = \frac{bh\psi f'_c}{2} \left[\sqrt{\left(\frac{a}{h}\right)^2 + 1} - \frac{a}{h} \right] + \psi \frac{a}{h} bh\psi f'_c \quad [C19]$$

This can be compared to Equation C12, the upper bound solution for a beam without shear reinforcement. The only difference is the additional second term on the right side of the equation; the term which accounts for the contribution of the shear reinforcement.

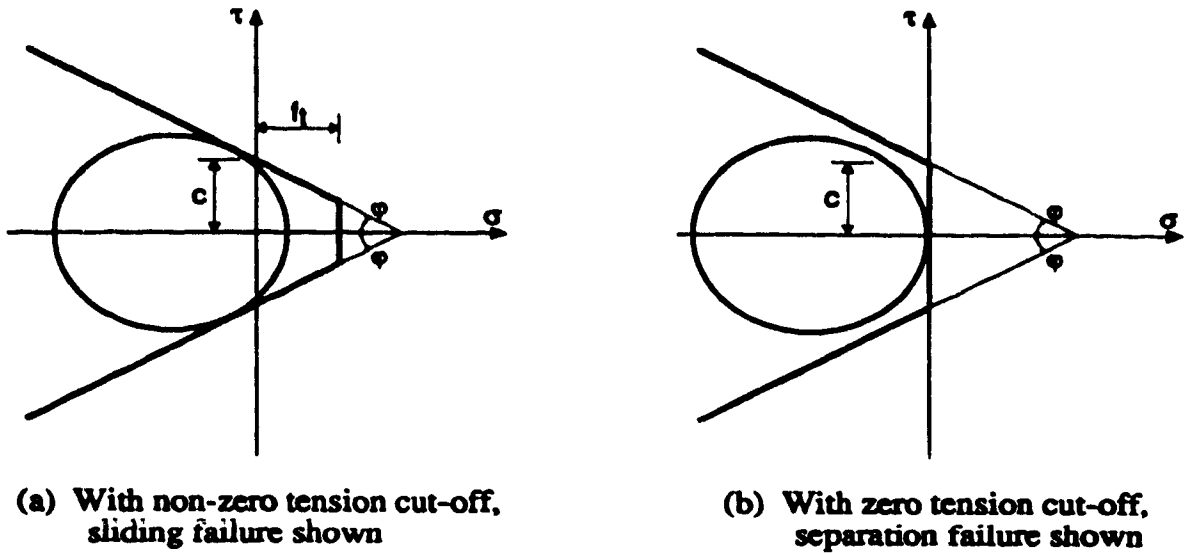


Figure C.1 Failure Criteria for Modified Coulomb Materials

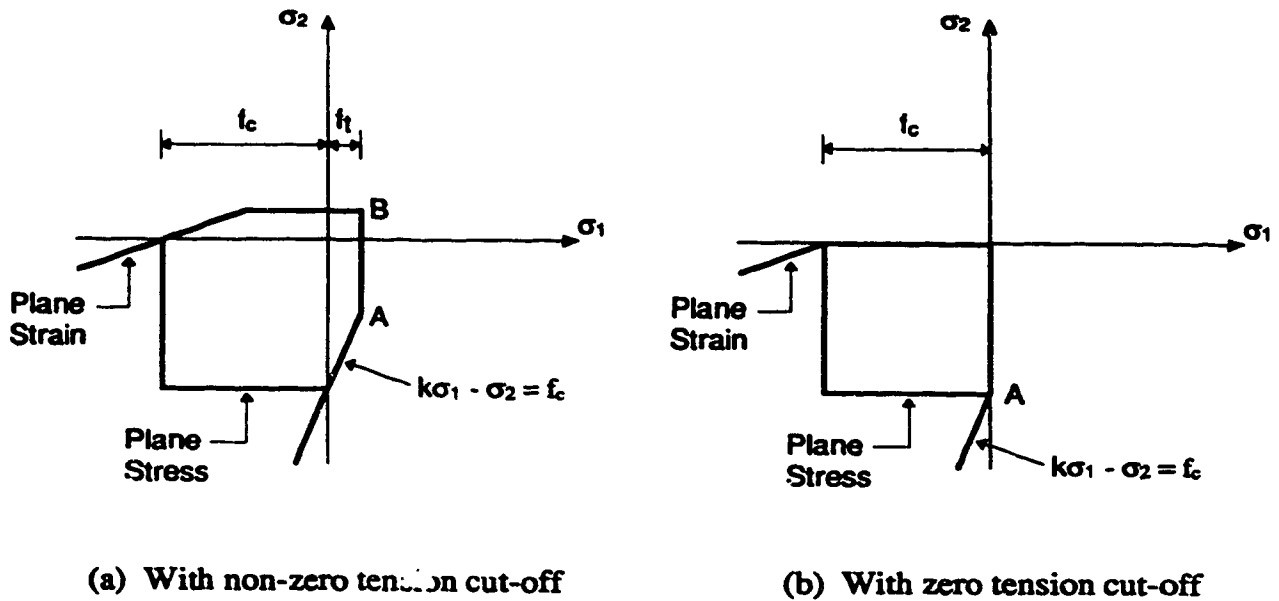


Figure C.2 Failure Criteria for Modified Coulomb Materials In Principal Stress Space

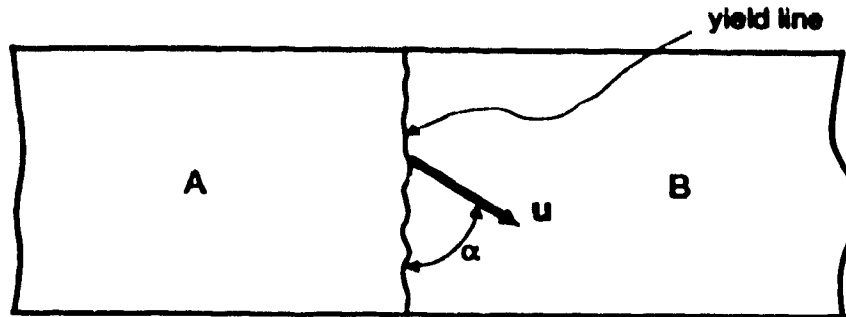


Figure C.3 Displacement in a Yield Line

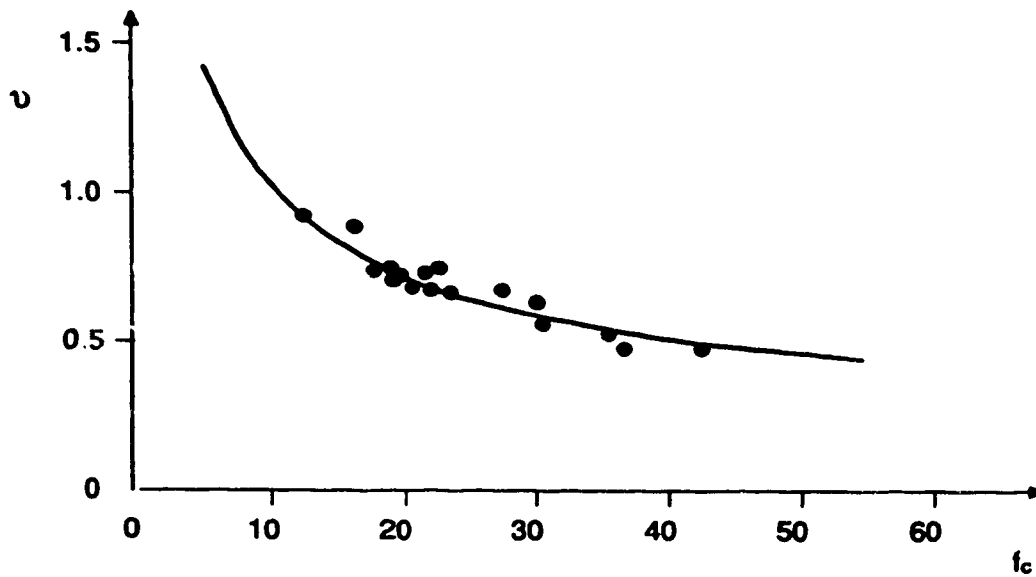


Figure C.4 Effectiveness Factor, ν , for Reinforced Concrete Members in Shear (adapted from Nielsen 1984)

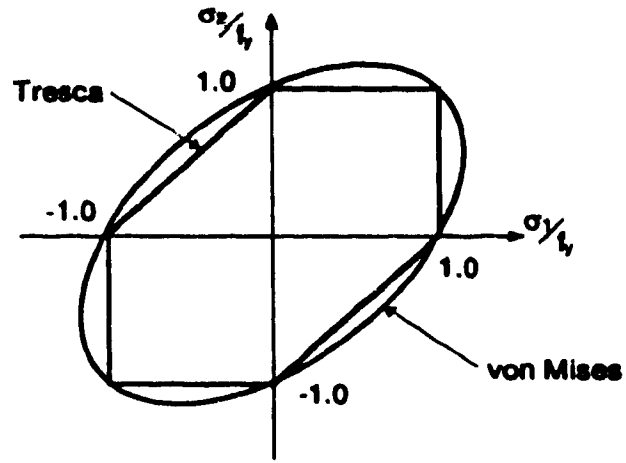


Figure C.5 Tresca and von Mises Yield Criteria

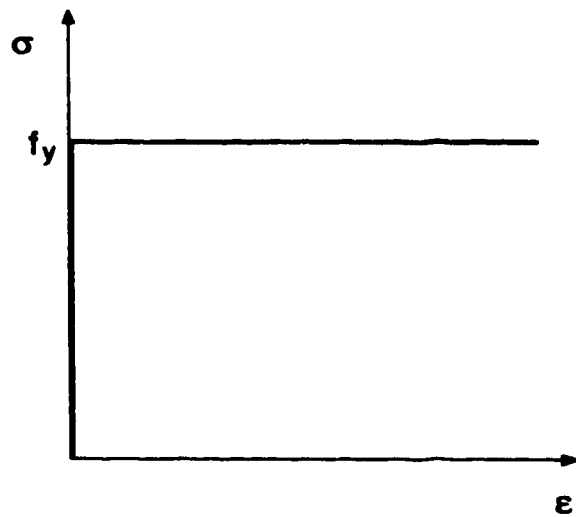


Figure C.6 Rigid-Plastic Stress-Strain Curve for Reinforcing Steel

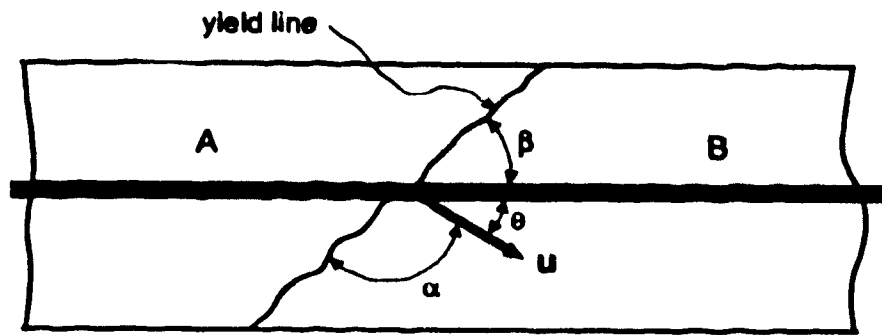


Figure C.7 Displacement in a Yield Line Crossing a Reinforcing Bar

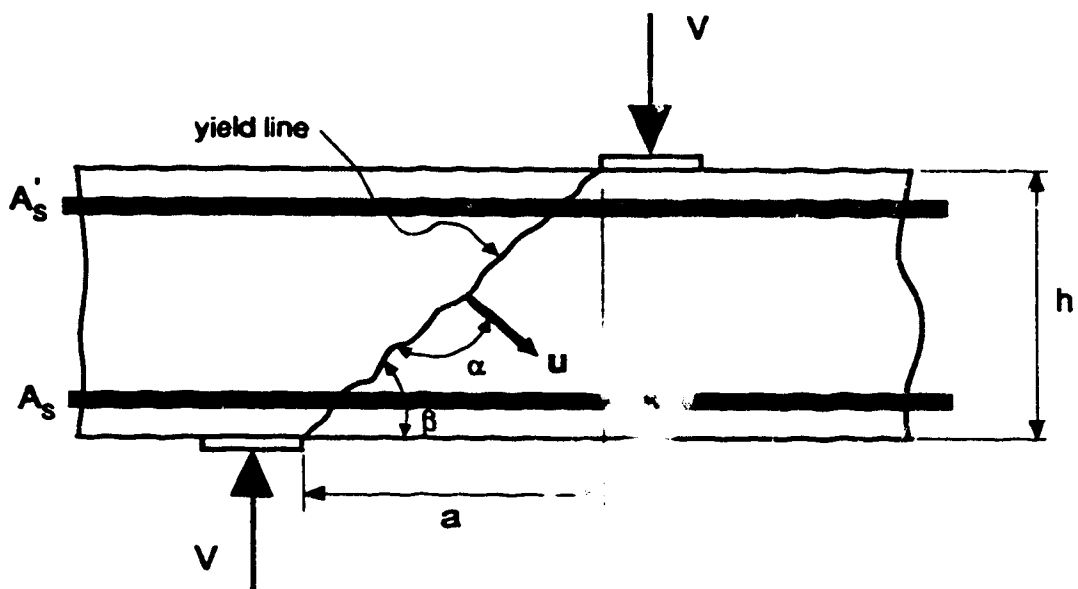


Figure C.8 Shear Failure Mechanism for Reinforced Concrete Beam

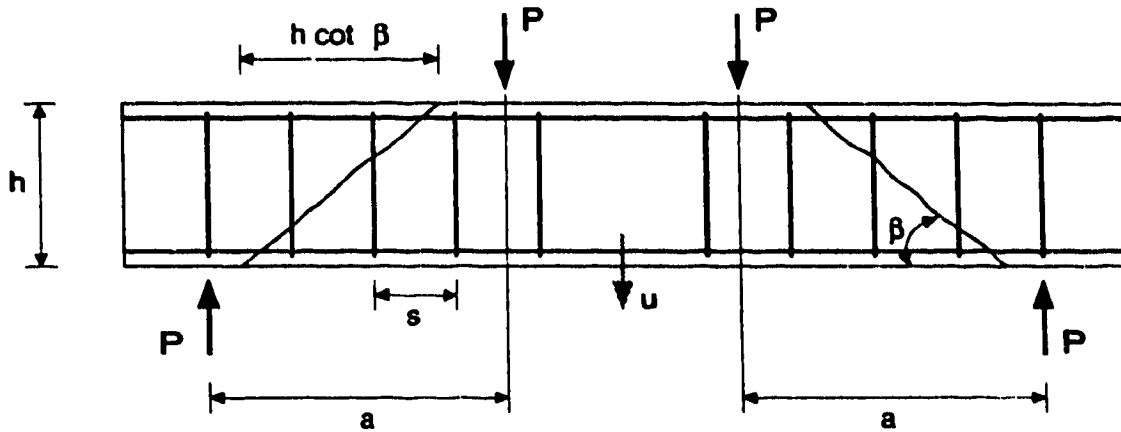


Figure C.9 Shear Failure Mechanism for Reinforced Concrete Beam with Shear Reinforcement

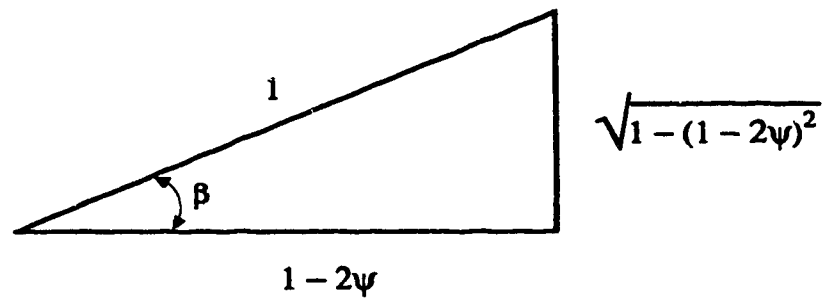


Figure C.10 Geometric Relationship for β

APPENDIX D OFFSHORE STRUCTURE CONCEPTUAL DESIGN

This section presents three structural schemes, each utilizing composite walls, for constructing the main barges for the drilling and production structure proposed for Gulf Canada's Amauligak field in the Beaufort Sea. This work was conducted by the author, and Mr. Mark Stephens of C-FER, as part of a proprietary contract project for Gulf Canada conducted by C-FER, in collaboration with Ben C. Gerwick Inc., San Francisco. The design work relied heavily on the research work conducted as part of this thesis, and is the first use of these research results for the conceptual design of an actual planned structure. The downturn in Beaufort Sea activities due to poor oil prices has prevented the Amauligak field from being developed; as a result, these structures have never been built. If the economic situation changes in future, it is expected that these schemes will be given serious consideration as alternatives to a design composed entirely of reinforced concrete.

D1.0 Rationale for Structural Configurations

Each of the three schemes is appropriate for several different types of construction site. The barges in Scheme 1 can be constructed in an 11.1 m deep graving dock (elev. -5.1 m) or on large steel deck-barges, linked together for that purpose. Scheme 2, which requires most of the concrete to be cast after float out, is appropriate for construction either in a 5.3 m deep graving dock (elev. +0.7 m) or on steel deck-barges. Scheme 3, which has all of the concrete cast after float out, can be constructed in a 4.2 m deep graving dock (elev. +1.8 m), on a skidway, or on steel deck-barges.

Although each of the three schemes has a different construction sequence and somewhat different details, the finished product in all three cases is very much the same. Each scheme has exactly the same plan layout of walls; each has composite walls around the entire perimeter, including the immediately adjacent bulkhead walls; each has reinforced concrete interior bulkhead walls, although two schemes have a steel frame embedded in these walls; and, each has a reinforced concrete +5 m deck, either formed conventionally or cast on a stay-in-place steel deck. The total barge weight of each scheme is also virtually the same: 54,100 tonnes, 54,700 tonnes and 55,000 tonnes for Schemes 1, 2 and 3 respectively. In all of the schemes, approximately 80% of the weight is concrete, either in reinforced concrete members or in composite members.

The major difference between the three schemes is the sequence in which they are put together. Each is designed to have a different total weight at float-out: Scheme 1 weighing approximately 54,000 tonnes, Scheme 2 weighing approximately 15,000 tonnes and Scheme 3 weighing approximately 5,000 tonnes. It is the weight difference at float-out that allows for the different types of construction site. Scheme 1 is heavy enough that it requires either a relatively deep graving dock. Scheme 2 is lighter, and can therefore be floated out of a less deep graving dock, or be launched from steel deck-barges after a shorter construction period. Scheme 3, which is the lightest, requires no graving dock at all, and can be launched from a shallow graving dock or a timber skidway.

For all of the schemes, it is assumed that the interior bulkheads will be either jump-formed or slip-formed. Twenty (20) meters is near the break even point for conventional slip-forming, and using the slipforms four times by slip-forming one-half of the bulkheads at a time will help reduce their costs. One major advantage of slip-forming is its speed.

Also for all schemes, it is recommended that a low head of fresh concrete be maintained within the steel shell of the sandwich composite walls, in order to minimize the outward pressure from the concrete, which tends to bow out the plate steel between diaphragms. This can readily be accomplished by placing concrete over large areas of the composite walls, thus limiting the head of fresh concrete to a level similar to that in slip-forming.

The structural configuration and construction sequence for each of the three schemes is given in Sections D3.1 to D3.3.

D2.0 Design Calculations and Assumptions

In order to develop the the conceptual designs for the three schemes, detailed preliminary design engineering had to be undertaken for those parts of the structure using new methods or details not previously considered. For example, exterior composite walls of the type shown in this thesis have not been designed before, and therefore required a considerable design effort, to ensure that the designs were accurate to the same level of detail as other parts of the structure. Wherever possible, advantage was taken of designs presented in previous reports produced for Gulf Canada, for those elements that were the same.

Those parts of the structure for which no design calculations were conducted include the reinforced concrete base slab, the reinforced concrete interior walls and the reinforced concrete +5 m deck slab. The designs for these elements (thickness and reinforcing) were taken from a report by Swan Wooster Engineering Ltd., Vancouver (1985).

The largest preliminary design effort was aimed at the composite peripheral walls. It was considered essential to demonstrate that these walls would function adequately under all potential load combinations. Naturally the most significant load effect was that due to ice loads, however, deformation induced loads, caused by berm settlements and thermal gradients, were found to be significant and therefore had to be considered.

The stresses induced in the peripheral wall due to differential settlement of the berm were assessed using the settlement calculations reported by O'Connor Associates Geotechnical Inc., in their report dated August 1989.

Thermal gradient induced stresses were calculated assuming a linear temperature gradient through the thickness of the peripheral wall above the waterline and a constant peripheral wall temperature below the water line. The calculations further assumed that an insulation layer would be located at the inner face of the peripheral wall system.

Considerable effort was directed at determining the ice load effects: critical ice feature configurations; the determination of local ice pressure intensities and distributions; and the adjustments required to account for load spreading. Computer models were used to determine design forces and force influence lines were developed for the various trial configurations to establish critical ice load patterns.

D3.0 Structural Schemes

D3.1 Scheme 1: Float-out Weight, 54,000 tonnes

Drawings of the barge for Scheme 1 are shown in Figures D-1.1 to D-1.3. This configuration is essentially identical to the "base case" concrete barge designed by Sandwell Swan Wooster, except for the composite walls used around the perimeter and for the immediately adjacent bulkhead walls.

The composite perimeter walls are 900 mm thick, with 16 mm face plates, excluding a corrosion allowance. The delta bulkhead walls, which support the peripheral ice wall, are 600 mm thick, with 12 mm face plates. The straight bulkhead walls, which support the core peripheral wall, are 500 mm thick, with 8 mm face plates.

Designs for the reinforced concrete base slab, +5 m deck slab and interior walls were extracted from the 1985 Swan Wooster report. These members are: a 600 mm base slab, a 265 mm +5 m deck slab and 350 mm thick interior walls.

The construction sequence for Scheme 1 is as follows:

- (a) Cast the reinforced concrete base slab.
- (b) Erect the steel shells for the peripheral composite walls and the composite bulkhead walls.
- (c) Cast the interior reinforced concrete walls, making the connections to the composite bulkhead walls with dowels and embedded steel studs, as shown in Figures D-1.2 and D-1.3.
- (d) Cast the infill concrete for the composite peripheral and bulkhead walls.
- (e) Cast the reinforced concrete +5 m deck.
- (f) Float out of the graving dock and tow to the topsides outfitting dock.

D3.2 Scheme 2: Float-out Weight, 15,000 tonnes

Drawings of the barge for Scheme 2 are shown in Figures D-2.1 to D-2.4. The main difference between this scheme and Scheme 1, is that most of the concrete in the barge (82%) is not cast until after the barge is afloat. Only the reinforced concrete base slab, 1.2 m high stub walls and 1.2 m in the base of the composite peripheral walls are cast prior to float-out. The stub walls are required to provide support to the base slab for the hydrostatic pressures exerted on the base during float-out and while moored for the

remaining construction. The partial in-fill in the base of the composite walls is required to encase the rebar dowels which make the connection to the base slab.

The empty steel shells for the peripheral composite walls are water tight, and can easily resist the required hydrostatic pressures. These walls, however, require lateral support during float-out, as neither the interior walls nor the +5 m deck slab are yet in place. To provide this support, a steel interior erection frame and steel +5 m deck framing (elevation +5 m) are provided.

The interior erection frame consists of Hollow Structural Section (HSS) columns on a 10 m grid, with horizontal and diagonal bracing in both directions between each column. This provides lines of bracing along each grid line marking the locations of the interior bulkhead walls, with an HSS column at the intersection of each grid line. The columns and bracing are shown on the barge sections in Figure D-2.1.

The +5 m deck framing consists of Wide-flange shape (W-shape) beams and channels, spaced at 2 m centre-to-centre, supporting a light-gauge steel deck (50 mm flute depth), which will act as a stay-in-place form for casting the +5 m deck slab. The deck framing shown on the drawings is sufficient to carry the weight of the +5 m deck slab while it is being cast. The slab itself is assumed to carry the loads on the +5 m deck.

Once the barge has been floated out, the interior reinforced concrete walls will be constructed around the interior steel frame, embedding the entire frame inside these walls. The interior framing members have been chosen to allow them to fit between the two layers of reinforcing bars in the wall, assuming an interior wall thickness of 350 mm. Once the interior steel frame has been embedded, it has no further use. It is thus called an "erection" frame, as its sole purpose is to facilitate construction, by providing the required temporary support. Use of a such a steel erection frame, as part of a composite building frame, is common in the construction of high-rise buildings in the United States, where the primary impetus is to speed construction. The steel shell can be erected quickly, and the concrete work proceeds at its own pace.

The composite perimeter walls and immediately adjacent bulkhead walls are the same as those used in Scheme 1. Almost the same are the reinforced concrete base slab, +5 m deck slab and interior walls, except that the +5 m deck slab is cast on a steel deck and the

interior walls are cast around a steel frame (i.e. the thickness and reinforcing are generally the same, with some different connection details).

The construction sequence for Scheme 2 is as follows:

- (a) Cast the reinforced concrete base slab and stub walls.
- (b) Erect the interior steel erection frame.
- (c) Erect the steel shells for the peripheral composite walls and the composite bulkhead walls, fastening them to the erection frame.
- (d) Cast the partial infill concrete in the base of the peripheral composite walls.
- (e) Place the steel deck for the +5 m deck slab (elevation +5 m).
- (f) Float out of the graving dock, or launch from the steel deck-barges, and tow to topsides outfitting dock for construction completion.
- (g) Cast the interior reinforced concrete walls, encasing the interior steel erection frame.
- (h) Cast the infill concrete for the composite peripheral and bulkhead walls.
- (i) Cast the reinforced concrete +5 m deck slab on the steel deck.

D3.3 Scheme 3 Float-out Weight, 5,000 tonnes

Drawings of the barge for Scheme 3 are shown in Figures D-3.1 to D-3.4. The major difference between this scheme and Scheme 2, is that none of the concrete is cast until the barge is afloat. In this scheme, the reinforced concrete base slab and stub walls are omitted, in favour of an open-faced composite base slab, the concrete for which is cast after launching.

The steel shell for the composite base slab is of light, welded plate construction (see Figure D-3.1), designed to resist the hydrostatic pressures exerted on the base during

launching and while moored for concreting. The base plate is 12.7 mm thick (0.5 in.), excluding a corrosion allowance. Angle scantlings (150x150), spaced at 1 m on centre, support the base plate and span 5 m to 500 mm deep transverse T-beams. The T-beams, spaced at 5 m on centre, span 10 m to 1000 mm deep longitudinal T-girders.

After float-out, reinforcing bars are placed to provide top reinforcing for the base slab (the bottom reinforcing being provided by the steel base plate), and all of the steel base framing is then encased in concrete. The angle scantlings provide shear transfer between the steel base plate and the concrete allowing composite action to occur. The height of the transverse T-beams is chosen to allow the reinforcing in the top of the base slab to be continuous over top of the T-beams. Steel studs are detailed on the tops of the longitudinal girders, to facilitate shear transfer between the interior bulkhead walls and the base slab (see Detail E on Figure D-3.4).

Steel studs are also detailed on the underside of the steel base shell. These studs may be required to enhance the shear-friction connection between the base steel and the under-slab grout. They have been designed to ensure that a greater shear-friction coefficient exists at the steel-to-grout interface than that which will exist at the grout-to-sand-berm interface. It is possible that a detailed engineering analysis of global sliding resistance will indicate that the shear-friction coefficient without studs will be adequate; if so, the studs may be omitted (e.g. the SSDC MAT has no such studs). In any case, the cost of the headed studs is small.

For this scheme, the perimeter, 0.5 m deep grout curb is formed by extending the outside plate on the peripheral composite wall and stiffening it with steel gusset plates.

The rest of the structure (composite walls, interior erection frame and +5 m deck framing) is the same as that described for Scheme 2.

This option assumes that a concrete batch plant is set up at the topsides outfitting dock, and that the floating steel shell is towed there for concrete placement. Concrete would be first placed for the base slab. The concrete would be placed by pumping or by bucket passing through the construction beams of the +5 m deck slab, if the steel stay-in-place deck is installed later (small amounts of additional steel bracing would be required in the plane of the +5 m deck slab to replace the steel deck diaphragm). The cells away from

the peripheral wall would be cast first, in order to trim the structure. Assuming, that a concrete batch plant with a capacity of 75 m³/hr were available it would take approximately 9 hours of continuous operation to place the entire base slab, and the draft would increase. The scantlings are designed to resist the extra water head due to this increased draft.

The construction sequence for Scheme 3 is as follows:

- (a) Erect the welded steel base framing.
- (b) Erect the interior steel erection frame.
- (c) Erect the steel shells for the peripheral composite walls and the composite bulkhead walls, fastening them to the erection frame.
- (d) Place the steel deck for the +5 m deck slab (elevation +5 m).
- (e) Float out of the graving dock, or launch from the skidway or from the steel deck-barges, and tow to topsides outfitting dock for construction completion.
- (f) Cast the infill concrete for the composite base slab.
- (g) Cast the interior reinforce concrete walls, encasing the interior steel erection frame.
- (h) Cast the infill concrete for the composite peripheral and bulkhead walls.
- (i) Cast the reinforced concrete +5 m deck slab on the steel deck.

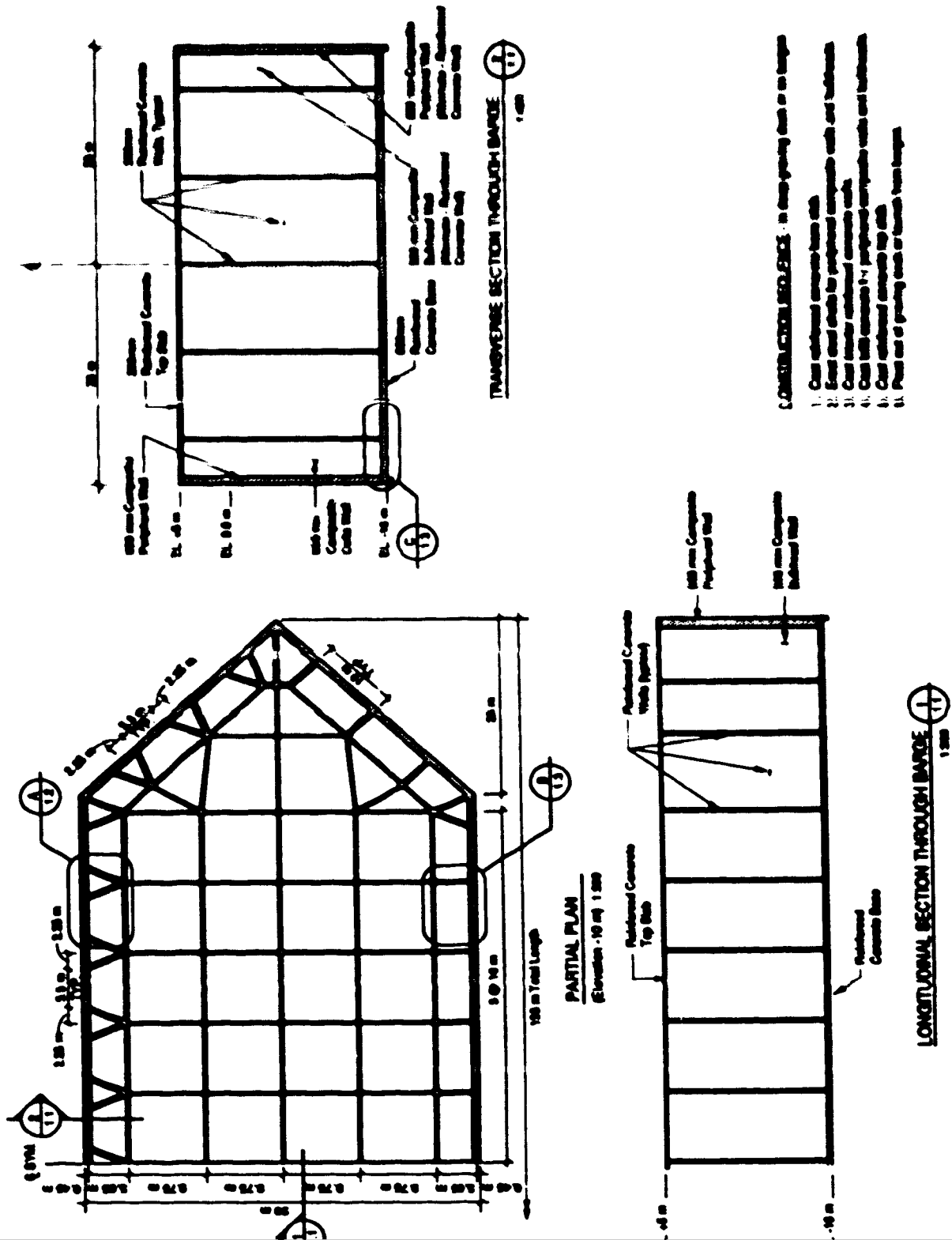


Figure D-1.1 Scheme 1, Plans and Sections

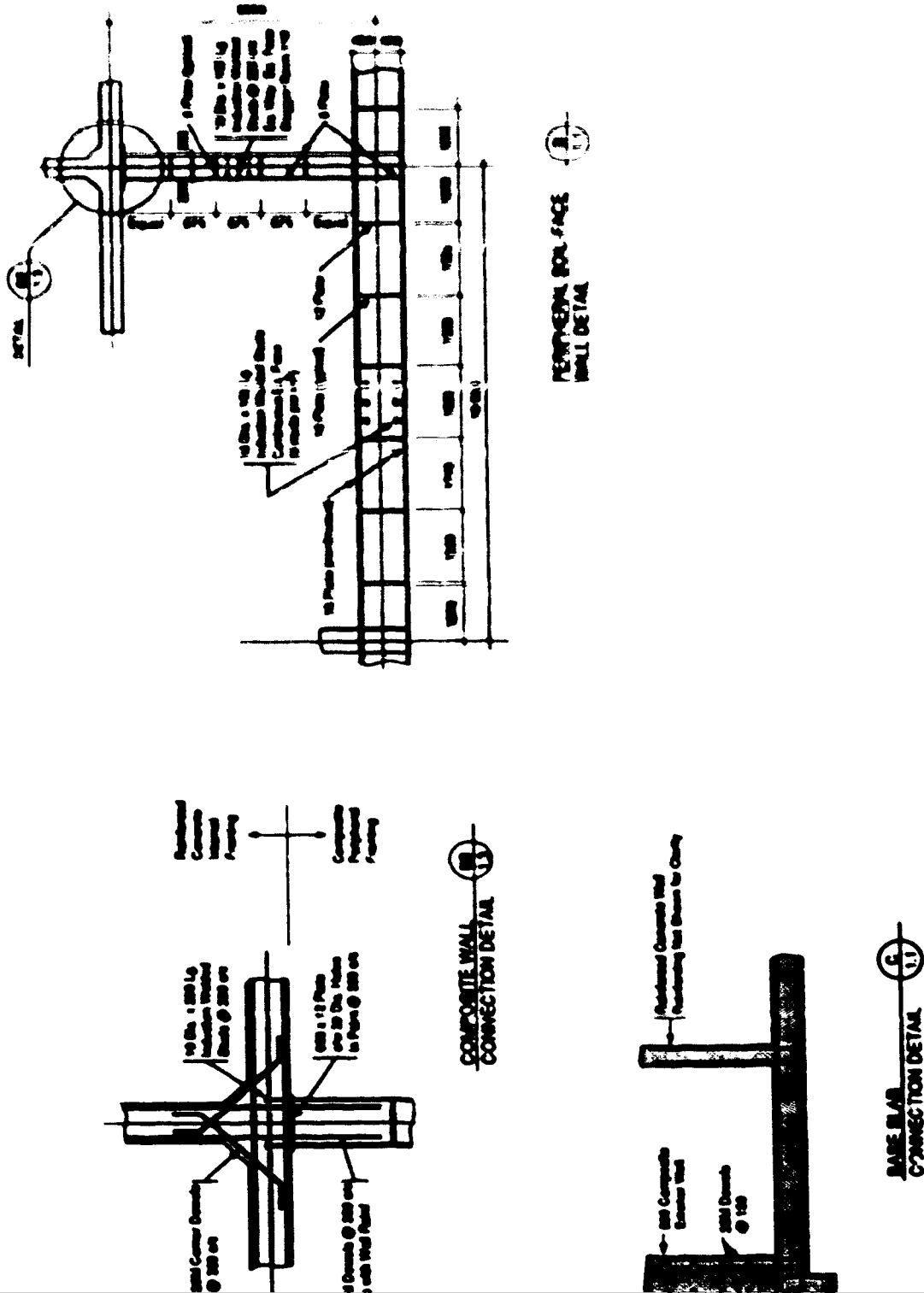


Figure D-1.3 Scheme 1, Details

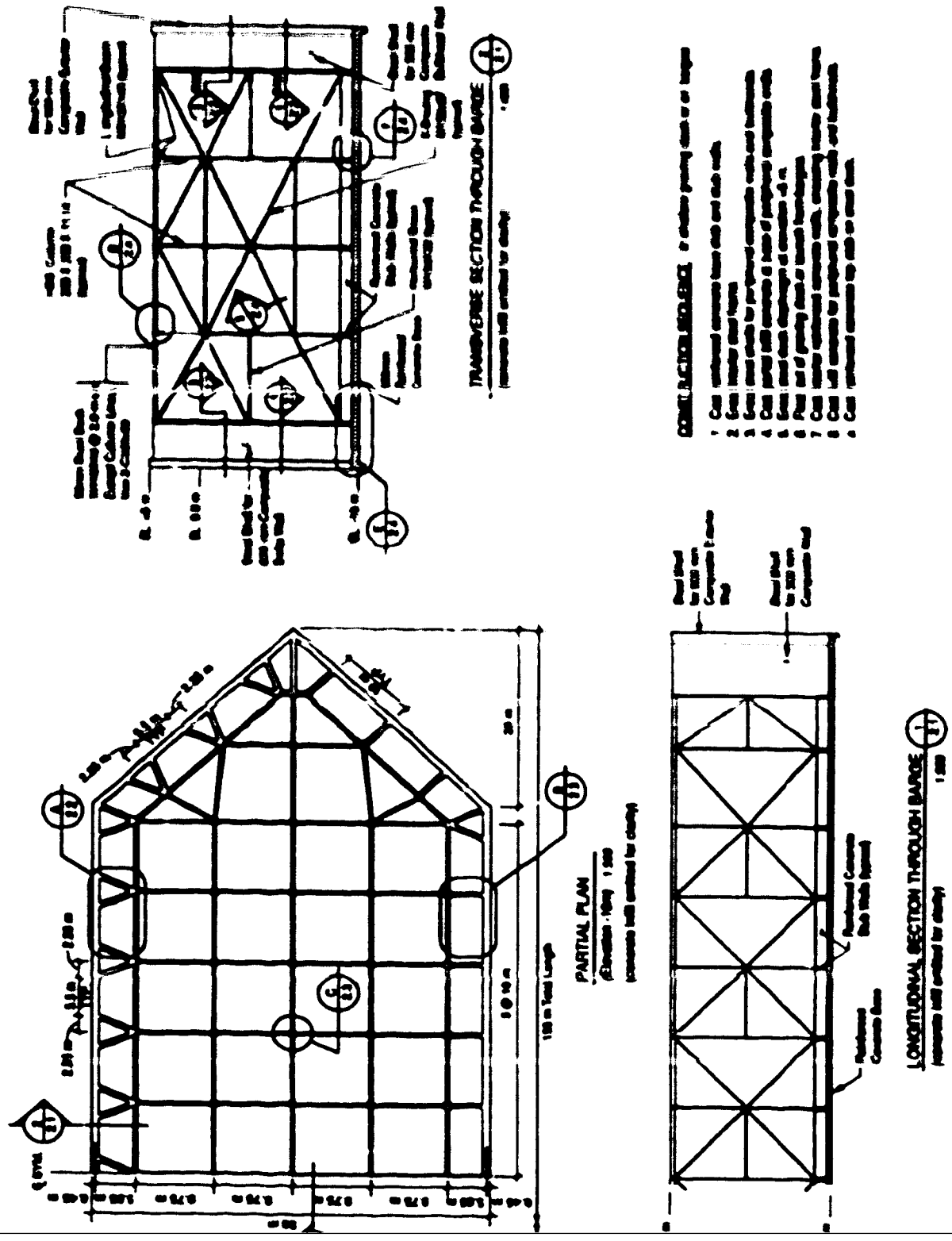
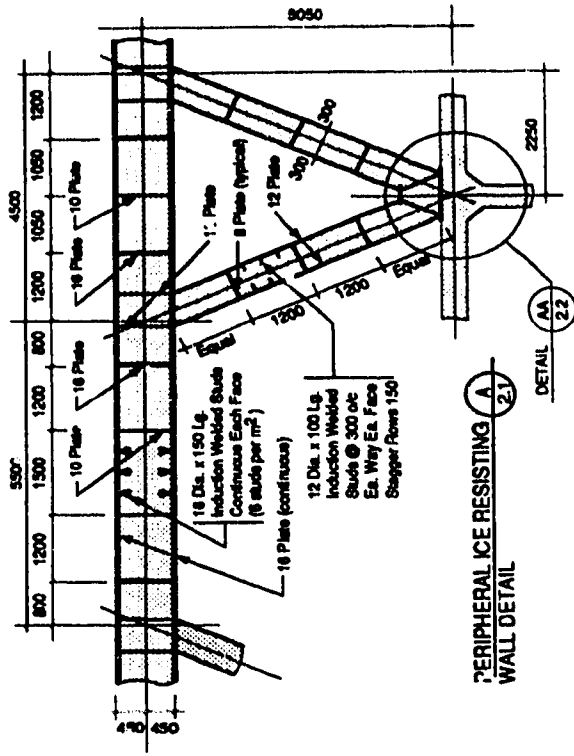
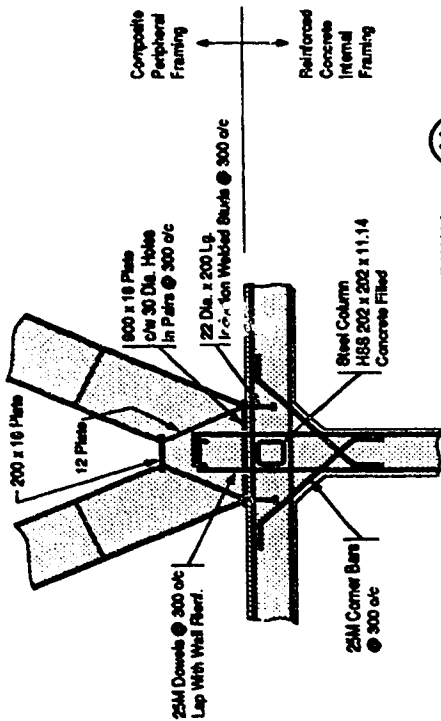


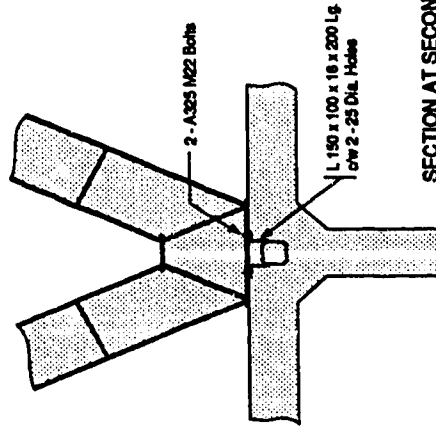
Figure D-2.1 Scheme 2, Plans and Sections



PERIPHERAL ICE RESISTING WALL DETAIL
DETAIL AA 2.2

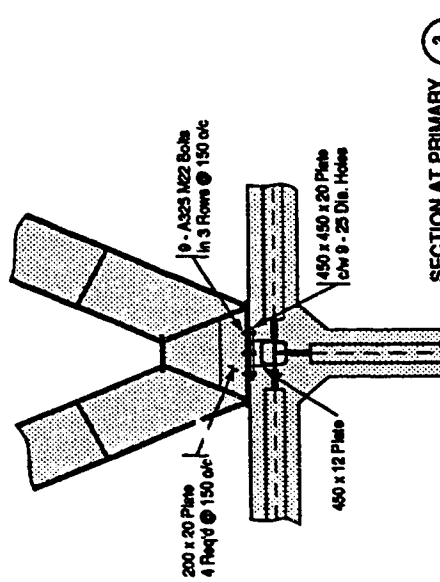


COMPOSITE WALL CONNECTION DETAIL 2.2
AA 2.2



SECTION AT SECONDARY STEEL CONNECTION 2.1

Note: secondary connections to internal steel framing at elevations +2.5m, 0m, -2.5m, -7.5m, -10m, and -12.5m.



SECTION AT PRIMARY STEEL CONNECTION 2.1

Note: primary connections to internal steel framing at elevations +5m, -5m and -15m.

Figure D-2.2 Scheme 2, Details

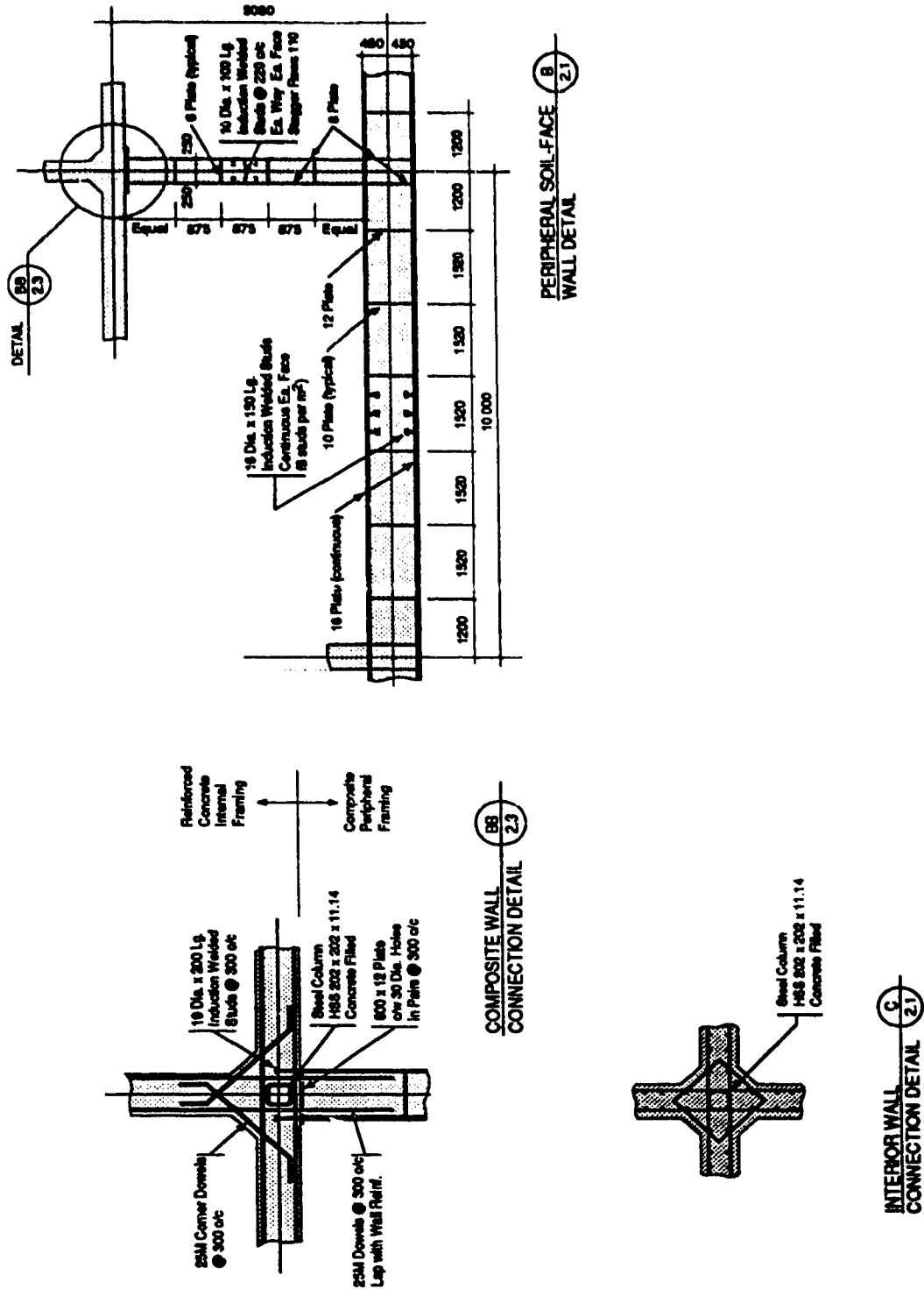


Figure D-2.3 Scheme 2, Details

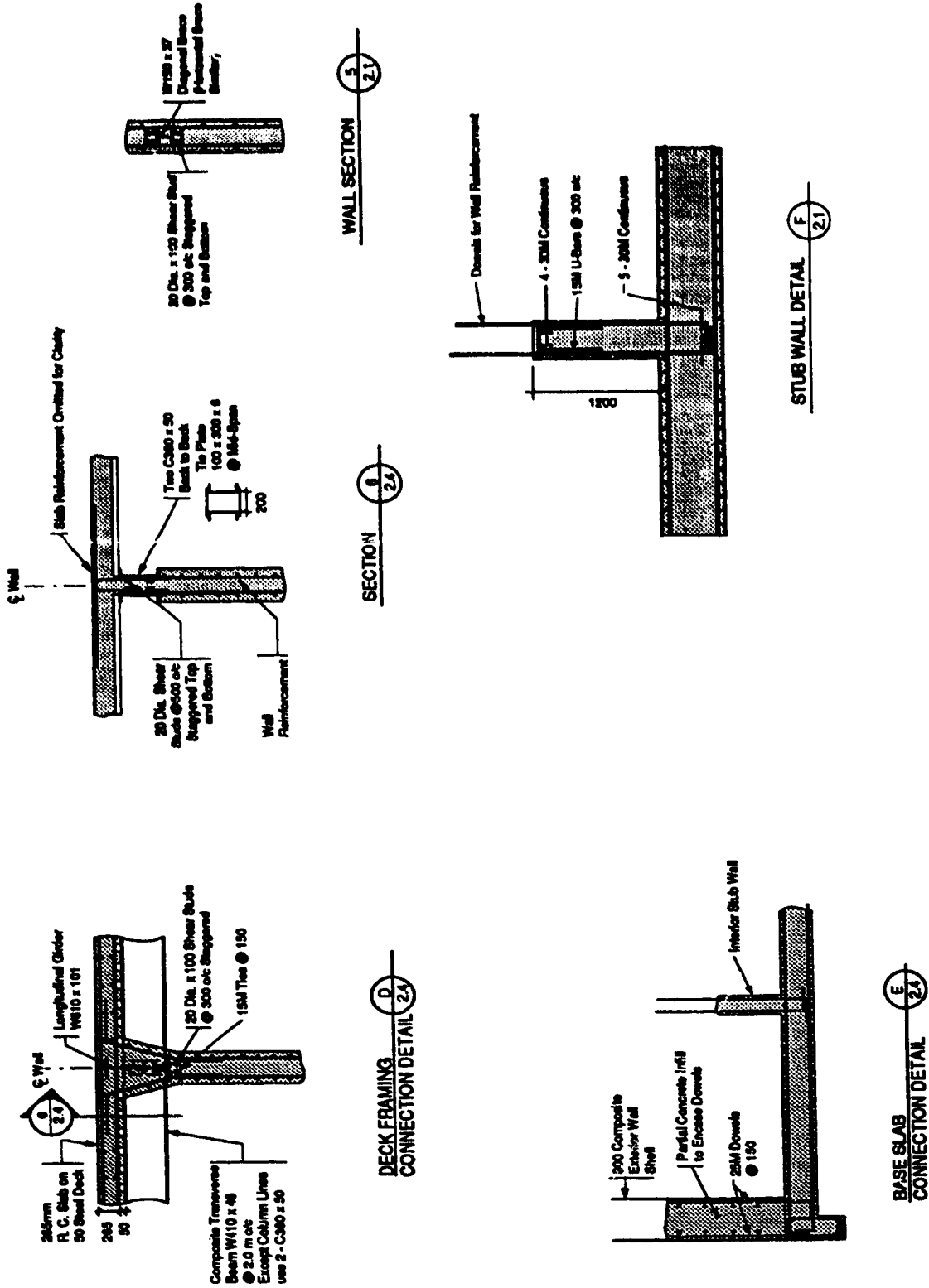


Figure D-2.4 Scheme 2, Details

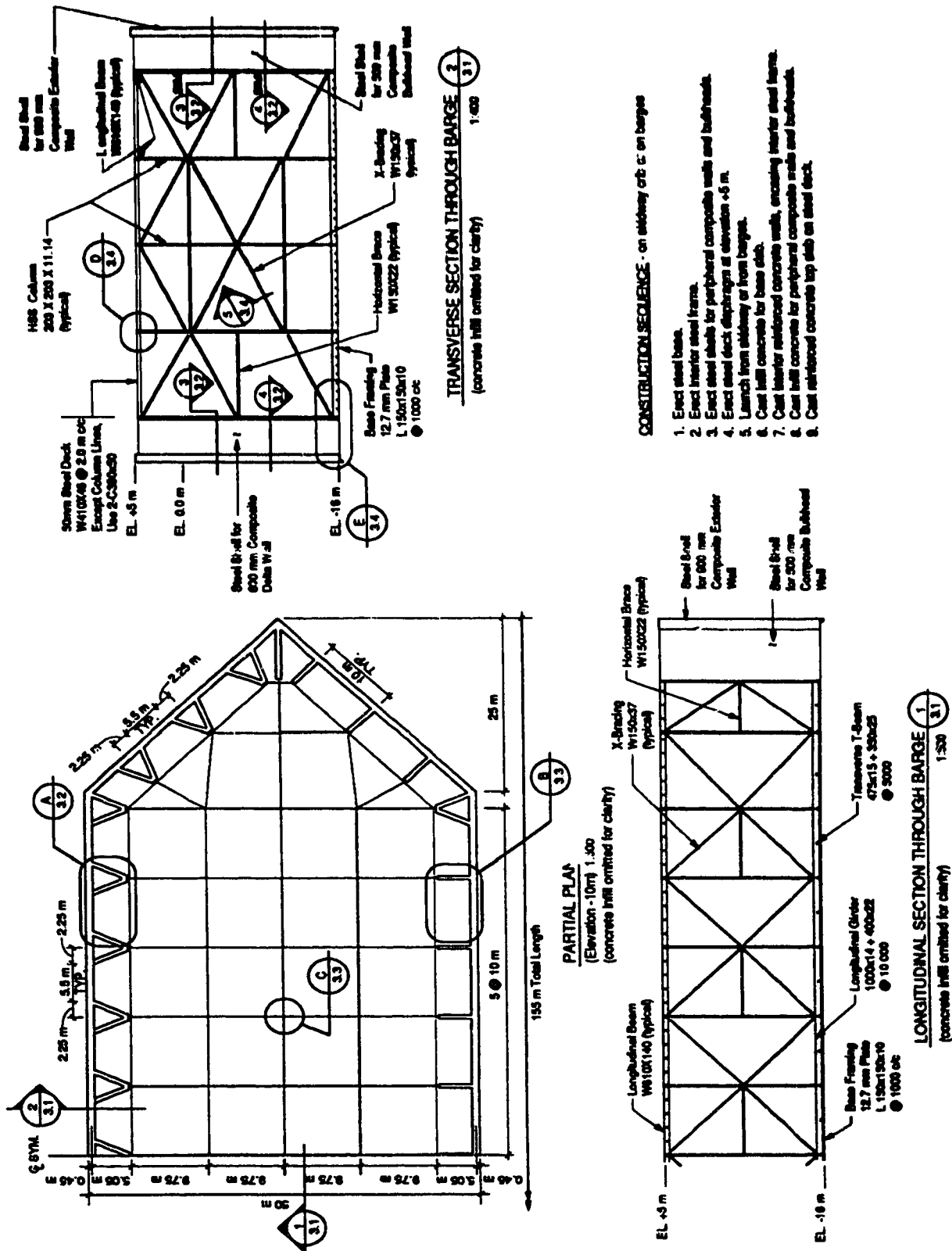
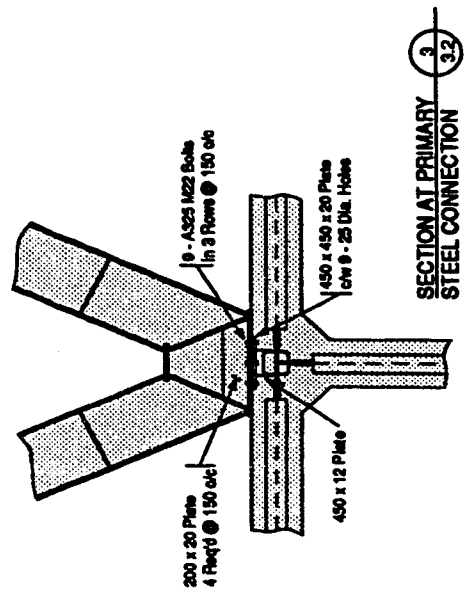
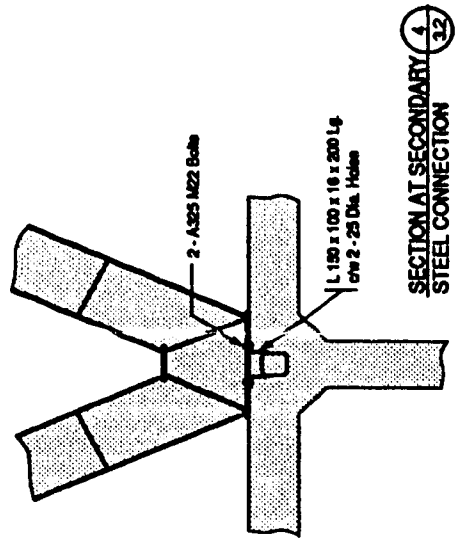
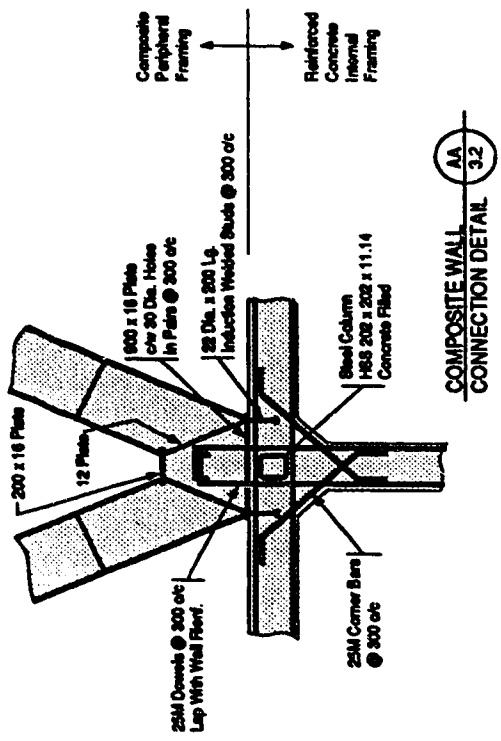
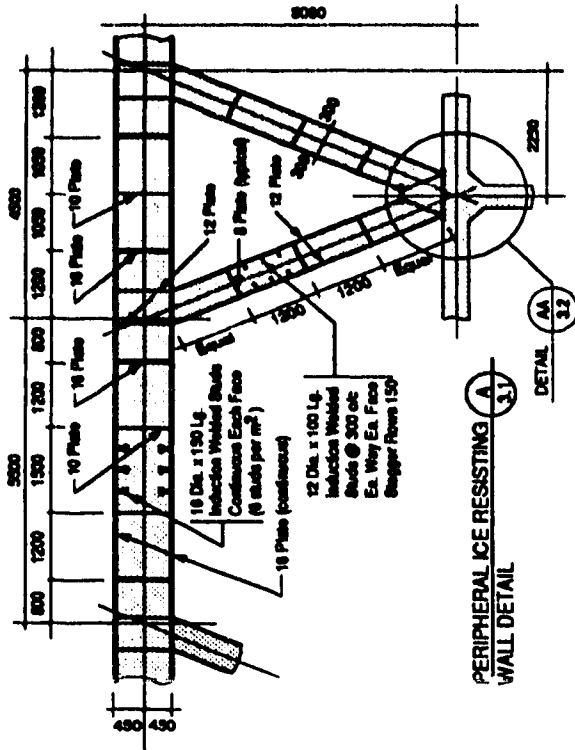


Figure D-3.1 Scheme 3, Plans and Sections



Note: secondary connections to internal steel framing at elevations +2.5m, 0m, -2.5m, -7.5m, -10m, and -12.5m.

Note: primary connections to internal steel framing at elevations +5m, -6m and -15m.

Figure D-3.2 Scheme 3, Details

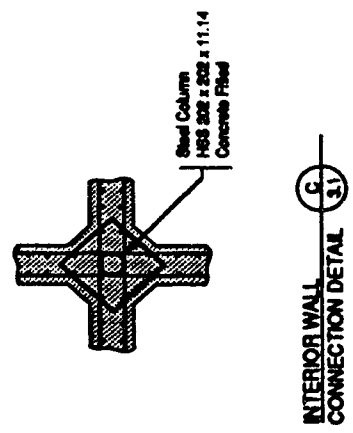
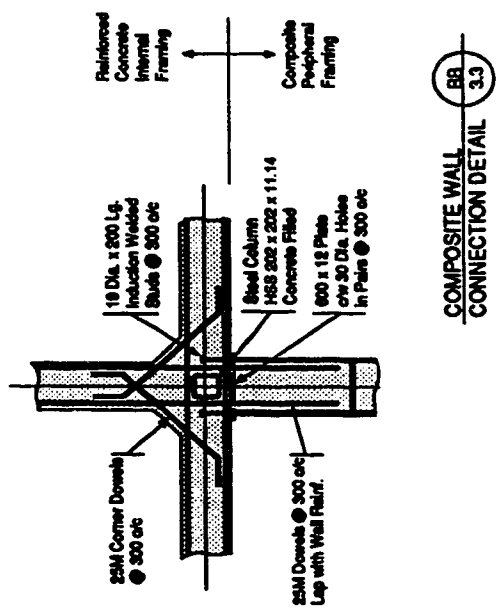
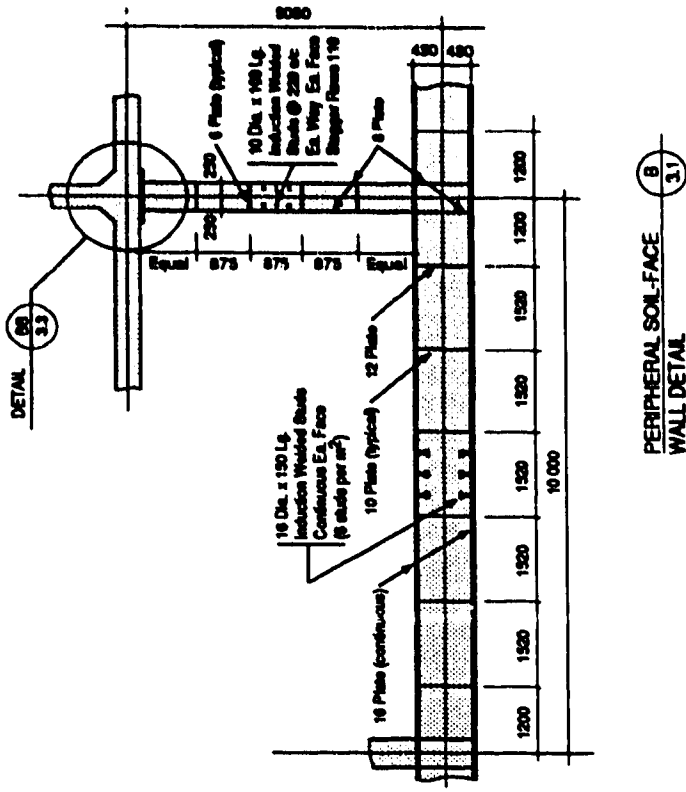


Figure D-3.3 Scheme 3, Details

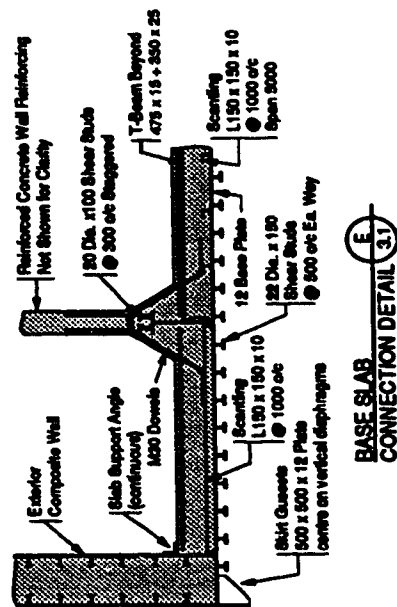
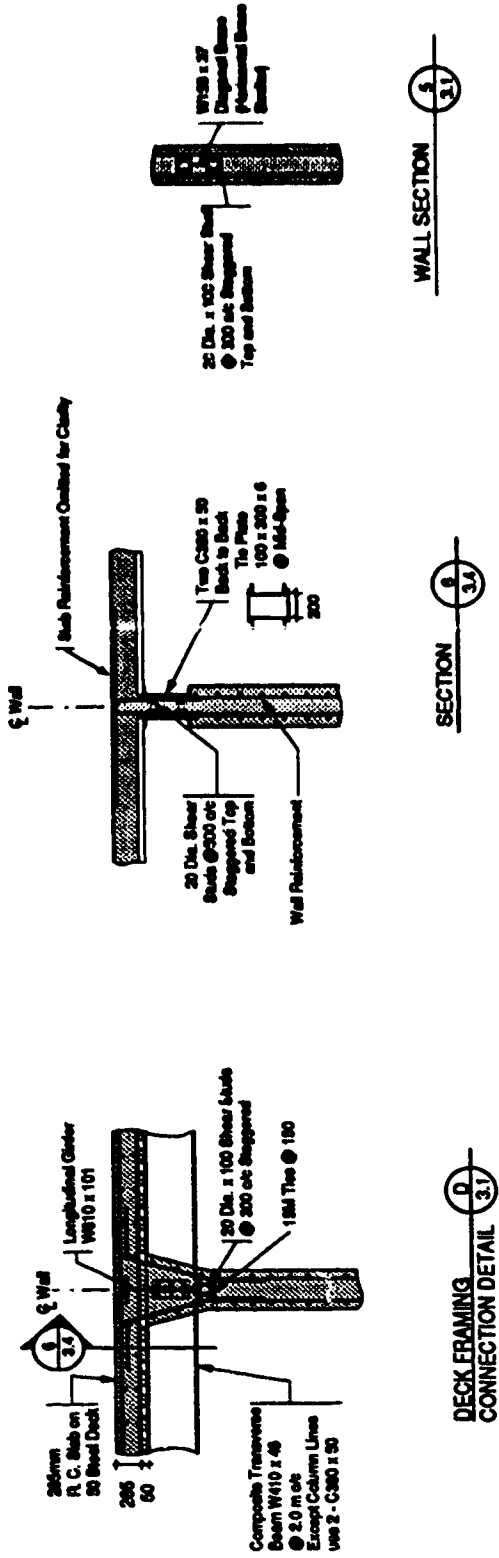


Figure D-3.4 Scheme 3, Details